Université catholique de Louvain
Faculté de Médecine

Laboratoire de Gastro-entérologie

Role of the cascade PPARγ–adiponectin–AMPK in the control of hepatic fibrogenesis and steatohepatitis

Alain da Silva Morais

Promotrice : Professeur Isabelle Leclercq

Thèse présentée en vue de l'obtention du grade de Docteur en Sciences biomédicales et pharmaceutiques (orientation : hépatologie)

J'aimerais tout d'abord remercier

MERCI à tous!

« Ne crains pas d'avancer lentement, crains seulement de t'arrêter »

Proverbe chinois

Contents

Résumé

Plusieurs études ont démontré que les agonistes du PPARγ, dont la pioglitazone (PGZ), améliorent les paramètres métaboliques et histologiques de la stéatohépatite non-alcoolique (NASH) chez l'homme et la souris, et qu'ils ont des effets bénéfiques sur la fibrose hépatique chez le rat. Les mécanismes d'action sont mal connus. La NASH, caractérisée par de la stéatose, des lésions hépatocytaires, de l'inflammation et une fibrose variable, est considérée comme une complication hépatique du syndrome métabolique. L'obésité, un des facteurs de risque pour le développement de la NASH, est caractérisée par de faibles taux d'adiponectine sérique. Cette adipocytokine, dont l'expression génique est régulée par le PPARγ, possède des propriétés anti-stéatosique et anti-fibrotique chez la souris. L'activité intracellulaire de l'adiponectine est médiée via ses récepteurs spécifiques qui activent la protéine kinase AMPK et/ou le PPARα. Une fois activée, l'AMPK induit les voies cataboliques de production d'énergie (telles que l'oxydation des acide gras) et inhibe les voies consommant de l'ATP (telles que la lipogenèse). L'activation du PPARα augmente l'oxydation des acides gras et inhibe la réponse inflammatoire.

Le but de notre travail est d'évaluer l'implication de la voie PGZ–adiponectine–AMPK et/ou PPARα dans la prévention de la NASH et de la fibrose hépatique.

Nous avons tout d'abord évalué l'effet de la PGZ sur la fibrose hépatique chez la souris. Nos observations montrent que, contrairement aux résultats observés chez le rat, la PGZ n'inhibe pas le développement de la fibrose hépatique chez la souris *in vivo*. Ces résultats ont été confirmés par des études sur les cellules stellaires hépatiques (HSCs), les cellules effectrices de la fibrose, *in vitro*. Dans une seconde étude, nous avons évalué l'impact de l'AMPK sur la fibrose hépatique *in vivo* et sur l'activation des HSCs *in vitro*. Nous avons constaté que l'AMPK jouait un rôle dans le contrôle de la trans-différentiation des HSCs *in vitro* mais pas dans le développement de la fibrose hépatique chez la souris *in vivo*. Finalement, nous avons évalué l'hypothèse que l'effet bénéfique de la PGZ sur la NASH résulte de la stimulation de l'AMPK et/ou du PPARα par l'adiponectine. Nos résultats ont montrés que cet effet de la PGZ était strictement dépendant de l'adiponectine mais ne semblait pas impliquer l'AMPK ni le PPARα. Nous avons également identifié SREBP-1c, régulant la lipogenèse *de novo*, comme cible thérapeutique potentielle pour le développement de la NASH.

Les résultats obtenus dans le cadre de ce travail de thèse fournissent une meilleure compréhension de l'axe PPARγ–adiponectine–AMPK dans le contrôle du développement de la NASH et de la fibrose hépatique chez la souris.

Summary

Several studies have demonstrated that peroxisome proliferator-activated receptor gamma (PPARγ) agonists, such as pioglitazone (PGZ), improve metabolic parameters and histology of nonalcoholic steatohepatitis (NASH) development in humans and mice, and have beneficial effects on liver fibrosis in rats. NASH, characterized by steatosis, hepatocellular damage, inflammation and variable fibrosis, is recognised as the hepatic complication of the metabolic syndrome. Obesity, one of the risk factors for NASH development, is characterized by low serum adiponectin levels. This adipocytokine, of which gene expression is regulated by PPARγ, demonstrates anti-steatotic and anti-fibrotic properties in mice. Intracellular activity of adiponectin is mediated through its specific receptors which activate AMP-activated protein kinase (AMPK) and PPARα. Once activated, AMPK switches on catabolic pathways (such as fatty acid oxidation and glycolysis) and switches off ATP-consuming pathways (such as lipogenesis). Activation of PPARα increases fatty acid oxidation and reduces inflammatory reaction.

The aim of the present work is to analyse the activation of the axis PGZ-adiponectin-AMPK and/or PPARα as a way to control NASH and hepatic fibrosis development.

We first evaluated the effect of PGZ on hepatic fibrosis in mice. We observed that, by contrast with results in rats, PGZ did not prevent hepatic fibrosis development *in vivo* in mice. These results were confirmed by *in vitro* studies on the key effector cells of fibrogenesis, the hepatic stellate cells (HSCs). We then assessed the impact of AMPK on hepatic fibrosis *in vivo* and on HSC trans-differentiation/activation phenomenon *in vitro*. We found that AMPK played a role in the control of HSC trans-differentiation *in vitro* but was not implicated in the wound-healing fibrosis *in vivo* in mice. Finally, we tested the hypothesis that the beneficial effect of PGZ on steatohepatitis results from the adiponectin-dependent stimulation of AMPK and/or PPARα. We found that this preventive effect was clearly dependent of adiponectin but did not involve AMPK or PPARα activation. We have also identified SREBP-1c, implicated in the regulation of *de novo* lipogenesis, as a potential therapeutic target for the control of the development of NASH.

The present thesis provides a better understanding of the axis PPARγ–adiponectin–AMPK in the control of NASH and hepatic fibrosis development in mouse.

List of figures

List of tables

Abbreviations

α-SMA	alpha smooth muscle actin
ACC	acetyl-CoA carboxylase
ACO	acyl CoA oxidase
ALT	alanine aminotransferase
AMP	adenosine 5'-monophosphate
AMPK	AMP-activated protein kinase
AST	aspartate aminotransferase
ATP	adenosine 5'-triphosphate
BDL	bile duct ligation
BMI	body mass index
CCl_4	carbon tetrachloride
cDNA	complementary DNA
ChREBP	carbohydrate response element binding protein
Col-α1	collagen-alpha1
CPT-1	carnitine palmitoyltransferase I
CXCR3	chemokine (C-X-C motif) receptor 3
DBD	DNA-binding domain
DEN	diethyl nitrosamine
DNA	deoxyribonucleic acid
DR1	direct repeat 1
ECM	extracellular matrix
ET-1	endothelin-1
FAS	fatty acid synthase
FFA	free fatty acids
GLUT	glucose transporter
HSC	hepatic stellate cell
IGF	insulin-like growth factor
Il	interleukin
JNK	c-jun terminal kinase
KC	Kupffer cell
KLF6	Kruppel-like factor 6
KO	knockout
LBD	ligand-binding domain
LFABP;	liver fatty acid binding protein
LPL	lipoprotein lipase
LPS	lipopolysaccharide
MAPK	mitogen-activated protein kinases
MCD	methionine and choline deficient
MCP-1	monocyte chemotactic protein-1
MMP	matrix metalloproteinase
mRNA	messenger ribonucleic acid
MUFA	mono-unsaturated fatty acids
NAFLD	non-alcoholic fatty liver disease
NASH	non-alcoholic steatohepatitis
NEFA;	nonesterified free fatty acids
NFκB	nuclear factor kappa B
NKT	natural killer T
NOS	nitric oxide synthase

PDGF	platelet-derived growth factor
PEPCK	phosphoenolpyruvate carboxykinase
PGZ	pioglitazone
PKA	cAMP-dependent protein kinase
PPAR	peroxisome proliferator-activated receptor
PPRE	PPAR response element
PUFA	poly-unsaturated fatty acids
RGZ	rosiglitazone
ROC	receive operating curve
ROS	reactive oxygen species
RXR	retinoid X receptor
SC	subcutaneous
SREBP-1c	sterol regulatory element-binding protein 1
T2DM	type 2 diabetes mellitus
TAA	thioacetamide
TG	triglyceride
TGF	transforming growth factor
TIMP	tissue inhibitors of MMPs
TNF	tumor necrosis factor
TRAIL	TNF-related apoptosis-inducing ligand
TZD	thiazolidinedione
UCP	uncoupling protein
VLDL	very low density lipoprotein
Wt	wild type

I. INTRODUCTION

1. The liver

The liver is the largest solid organ of the body and plays a central role in the maintenance of metabolic homeostasis and the biotransformation and elimination of xenobiotic substances from the body, associated with endocrine and exocrine activities.

a. Parenchymal liver cells

The hepatocyte, or parenchymal liver cell, makes up to 70-80% of the hepatic mass and is the main functional unit of the liver. The average life span of the hepatocyte is 5 months. Hepatic mass is maintained constant by self-renewal of mature hepatocytes through cell proliferation (1). These cells are insulin responsive (2) and involved in protein synthesis and storage, transformation of carbohydrates, synthesis and storage of lipids (triglycerides), synthesis of cholesterol, bile salts and phospholipids, as well as detoxification, modification and excretion of exogenous and endogenous substances. The hepatocyte also initiates the formation and secretion of bile (1). These processes depend on a complex, yet highly organized, vesicle trafficking machinery that requires the coordinated synergistic action of various enzymes, cytoskeletal proteins, molecular motors, and coat proteins. The hepatocytes are also able to synthesize hormones, like insulin-like-growth-factor IGF-I, thrombopoietin, erythropoietin, cytokines like interleukin (IL)-8 and respond to acute phase mediators like IL-6 (1).

b. Non-parenchymal liver cells

Non-parenchymal liver cells comprise sinusoidal endothelial cells, Kupffer cells, pit cells and hepatic stellate cells.

i. Sinusoidal endothelial cells

The liver receives a dual blood supply: the portal circulation which brings partially oxygenated blood from the gut, rich in compounds absorbed following digestion, and, the arterial circulation accounting for 30% of the hepatic blood flow. The two blood supplies get mixed at the edge of the portal tracts where the liver sinusoids are found. These, in essence, are the liver's capillaries and are lined by specialized fenestrated endothelial cells, controlling the flow of materials to and from the space between hepatocytes and endothelial cells (3).

Similar to vascular endothelial cells in general, sinusoidal endothelial cells (SECs) were found to have numerous functions in various biologic reactions, including active transport, coagulation, fibrinolysis, inflammation, immune response, regulation of blood pressure, angiogenesis, lipid metabolism and synthesis of stromal components. Nevertheless, liver SECs differ from vascular endothelial cells (e.g. portal vein, central vein) in different aspects but essentially in their fenestrations allowing a direct physical contact between intravascular lumen and Disse's space (4) (Figure 1).

ii. Kupffer cells

Kupffer cells are the tissue resident macrophages, representing 5% of the non-parenchymal cell population, scattered within the liver sinusoids and are the major part of the reticulo-endothelial system (5). Their development begins in the bone marrow with genesis of promonocytes and monoblasts into monocytes and then on to peripheral blood monocytes completing their differentiation into Kupffer cells (1). They function as a waste reservoir for all kinds of old, unnecessary, damaged, altered, or foreign material. Upon activation they secrete a number of products with potent biologic effects, including proteases and cytokines with influence on parenchymal and other sinusoidal lining cells (Figure 1).

iii. Pit cells

Pit cells correspond to large granular lymphocytes with natural killer (NK) activity and their number in the liver constitutes about 1% of the non-parenchymal cell population (1). They are well placed to play defensive roles against viral infection and tumor metastasis. The liver contains several unusual subtypes of T lymphocytes and NK-T cells, rendering the liver an unique immunologic environment and a tolerogenic organ where peripheral deletion of T lymphocytes occurs (6).

iv. Hepatic stellate cells

In healthy livers, hepatic stellate cells (HSCs) represent approximately 8% of total number of liver cells. These cells, presumably of mesenchymal origin, are localized in the space of Disse and are in close proximity to hepatocytes and hepatic sinusoidal endothelial cells (7) (Figure 1). The major functions that HSCs perform in healthy livers are related to retinol (vitamin A) metabolism and storage, regulation of sinusoidal blood flow by influencing the vascular tone, and regulation of the extracellular matrix (ECM) composition

in the space of Disse (8). With respect to retinol metabolism, HSCs are responsible for storage of the largest fraction of vitamin A in the body. Of all dietary retinol, 90% is stored in the liver and 75% of this amount is confined within HSCs. We take advantage of the high vitamin A content of HSCs, compared to other liver cells, conferring lower density for the isolation of primary HSCs by density-gradient-based centrifugation (see Annexe) (9, 10). The close proximity of HSCs to sinusoidal endothelial cells, and the presence of long cytoplasmic extensions which surround the endothelial cells, are analogous to that of vascular pericytes. Pericytes are responsible for the regulation of vascular tone in other organs and various studies confirm a similar role for HSCs in the liver (11). A third function of HSCs in the healthy liver is the maintenance of a correct composition of ECM in the space of Disse, mainly comprising collagen type I, III, IV, VI and XVIII, decorin, fibronectin and heparansulphate proteoglycan (Figure 1).

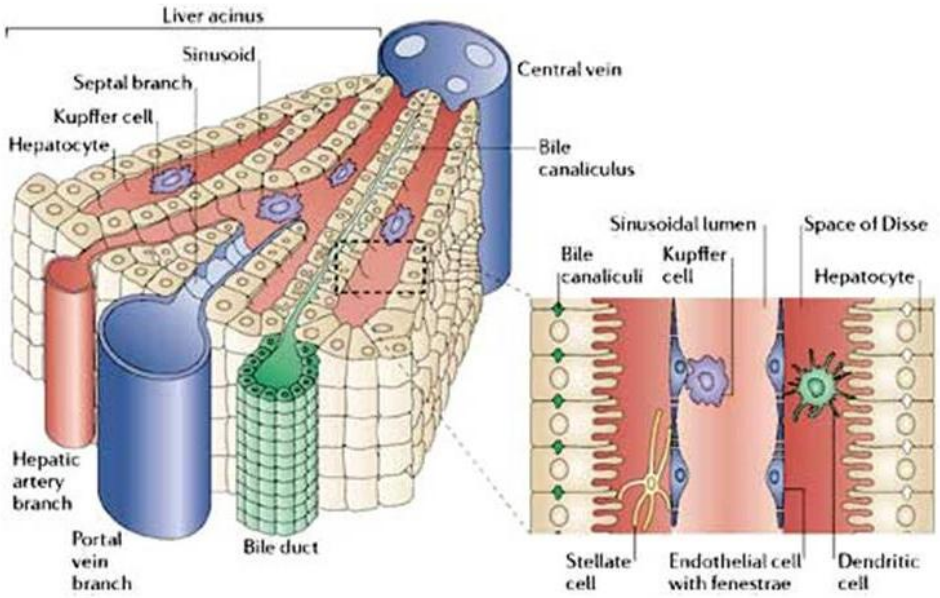

Figure 1: Three-dimensional structure of a liver lobule

The liver receives blood supply from the portal vein and the hepatic artery, and both terminate in the intrahepatic portal tracts, which contain bile ducts that transport bile from the canaliculus to the gut. The terminal portal veins give rise to septal branches that drain blood into the sinusoids that make up the distributing system. The hepatic artery terminates in axial branches that run parallel to the portal vein and terminate in the sinusoids. The sinusoids are lined by morphologically and phenotypically unique endothelial cells (see inset) that are characterized by the absence of tight junctions and the presence of fenestrations. The sinusoidal endothelium is interspersed with Kupffer cells and overlies the space of Disse, which contains the hepatic stellate cells. (Figure from Adams et al. Nature Reviews Immunology 2006) (12)

2. Hepatic fibrosis

a. What is liver fibrosis?

Fibrosis can be classified as a wound-healing response to chronic insult, such as viral hepatitis, alcohol abuse, and autoimmune diseases, to the liver (13, 14). It is characterized by excessive deposition of extracellular matrix (ECM), which includes three large families of proteins – glycoproteins, collagens, and proteoglycans. Pathological accumulation of ECM impairs hepatic functions by disruption of the organ structure and perturbation of the interactions between resident cells. Fibrosis may continue to progress into a severe condition called cirrhosis, which is characterized by the dissection of the hepatic lobule by fibrotic septa, encapsulating islets of hepatic cells (regenerative lobules) and associates portal hypertension and hepatocellular dysfunction (14). The poor prognosis of cirrhosis is aggravated by the frequent occurrence of hepatocellular carcinoma, which may also develop, albeit much more rarely, in normal livers.

Although the number of different collagens identified in the liver continues to increase, the two most commonly associated collagens, and the two that are increased to the greatest extent in fibrosis, are type I and III collagens. During liver fibrosis, altered collagen synthesis at both mRNA and protein levels is observed, with a dramatic increase in type I collagen along with smaller, but significant, increases in type III collagen (15). Although initially increased synthesis of ECM serves as a repair mechanism to allow healing of the injured organ, liver fibrosis can be viewed upon as a derailed healing response, in which the deposition of ECM is excessive, disproportionate to the extent of tissue injury, and eventually deleterious to tissue structure and function.

Several experimental animal models of liver disease support the role of the hepatic stellate cell (HSC) as the main cell type responsible for excess collagen production during fibrogenesis (16, 17). HSC activation is also associated with an increase in cell contractility, where endothelin-1 (ET-1) acts as a major contractile stimulus for HSCs (18). This process, leading to sinusoidal vasoconstriction, participates to portal hypertension associated with severe fibrosis/cirrhosis (19).

b. Mechanism of hepatic fibrosis

Fibrosis, or scarring of the liver, is thus a wound-healing response that engages a range of cell types and mediators to encapsulate injury. Acute injury activates mechanisms of fibrogenesis but fibrosis will be eventually resorbed and liver architecture restituted *ad*

integro. Sustained signals associated with chronic liver disease elicit several rounds or chronic stimulation of wound healing response resulting in matrix deposition not compensated for by its degradation. This consequently leads to liver fibrosis (Figure 2).

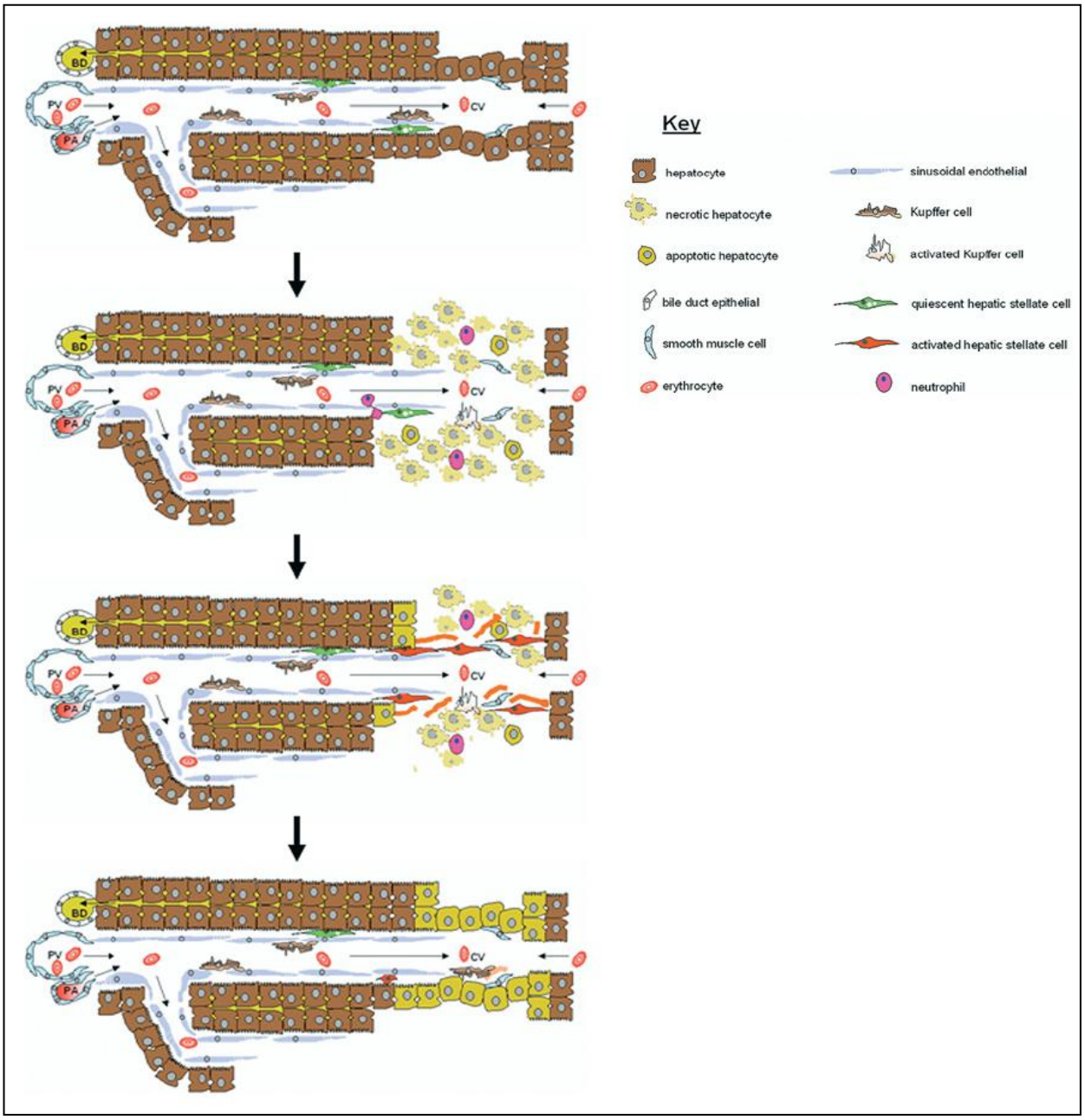

Figure 2: Schematic diagram of the events that occur in the liver in response to acute liver damage

Top to bottom: sequential events from normal structure, localized cell death, inflammation and regeneration (BD, bile duct; CV, central vein; PA, periportal arteriole; PV, periportal venule). (Figure from Wallace K et al. Biochem J. 2008) (3)

i. ECM accumulation: a dynamic balance

When fibrotic stimulus disappears, there is a window of opportunities for a tilt in the balance between fibrogenesis and fibrolysis allowing the progressive degradation of the scar. Indeed, although traditionally seen as an irreversible process, advanced fibrosis, even at the cirrhotic stage, may regress following control of the noxious stimulus (20).

1. ECM synthesis

The ECM is a network of proteins and molecules that serve specific functions in regulating and maintaining proper biological activity. The best-recognized role of the ECM is the ability of the collagens to polymerize and provide structural support to connective tissue, vasculature, and to generate the basement membrane (21). Also the ECM serves as a storage source for a variety of growth factors, including transforming growth factor (TGF)-β, platelet-derived growth factor (PDGF), tumor necrosis factor (TNF)-α, hepatocyte growth factor (HGF) and vascular endothelial growth factor (VEGF) (21). For the most part, the ECM is localized around portal tracts, sinusoid walls, and central veins, and serves to provide mechanical coherence and resistance of the organ (21).

The hepatic stellate cell (HSC) is the primary cell type in the liver responsible for excess collagen synthesis during hepatic fibrosis (22). Activated HSCs also dramatically increase the expression and secretion of the tissue inhibitors of matrix metalloproteinases (TIMP)-1 and -2, proteins inhibiting matrix degradation enzymes resulting in the persistence and stability of deposited matrix (21). The net effect of a rapid increase in ECM synthesis, in combination with increased TIMP activity, contributes to the formation of a fibrotic scar.

2. ECM degradation

The accumulation of the ECM is tightly regulated by matrix metalloproteinase (MMP)-mediated turnover of ECM proteins. During activation, HSCs express several MMPs, insuring a constant remodelling of the matrix (23). Matrix degradation represents a strong stimulus for HSC activation, as, during this process, cytokines and growth factors, sequestered in the matrix are released.

MMP-2 plays a particularly important role in matrix remodelling. Increased MMP-2 gelatinase activity is believed to be associated with enhanced destruction of the matrix, representing a perpetuated stimulus for HSC activation (21). Moreover, MMP-2 can induce

HSC migration and proliferation through PDGF, TGF-β, and oxidative stress–mediated signalling pathways, further promoting the fibrotic process (21).

As fibrotic stimulus become chronic, expression of ECM proteins such as type I collagen keep increasing while, except for MMP-2, the expression of most MMPs remains stable (21). This creates an unbalance between matrix production and its degradation in favour of matrix accumulation. Activation of MMPs at the wrong place and time can lead to removal of the regular, differentiation-inducing ECM, with subsequent unfavourable tissue remodelling, architectural distortion and a fibrogenic response. With repeated injury of sufficient severity, fibrogenesis prevails over fibrolysis, resulting in excess ECM deposition, (Figure 3).

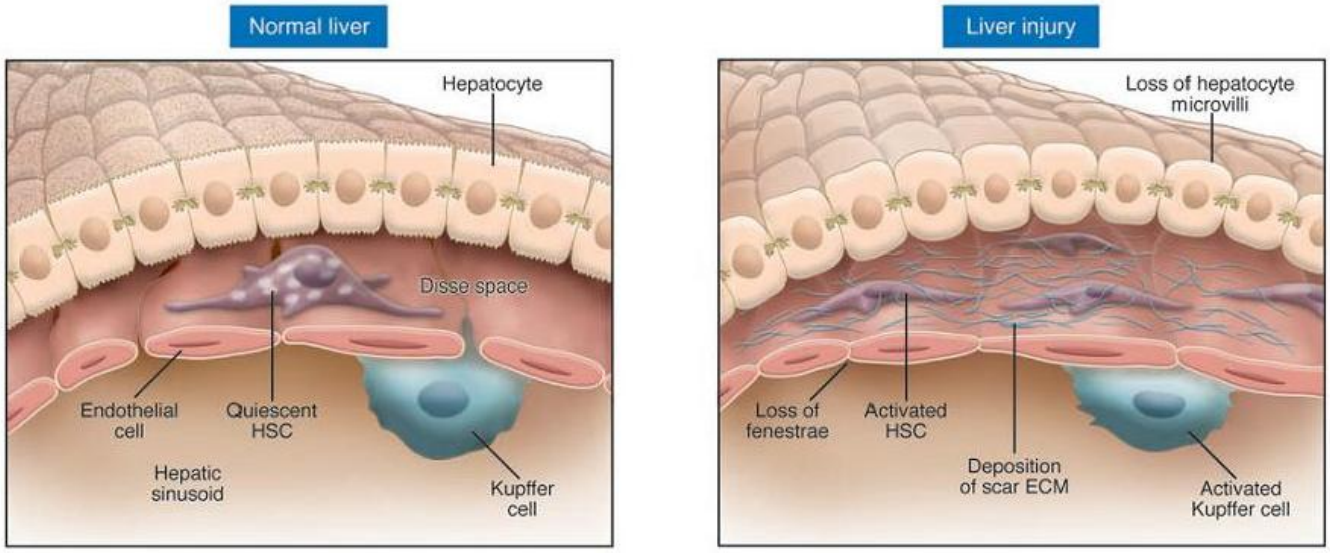

Figure 3: Liver fibrogenesis process

Hepatic stellate cell (HSC) activation leads to accumulation of scar (fibril-forming) matrix, which in turn contributes to the loss of hepatocyte microvilli and sinusoidal endothelial fenestration. Kupffer cells activation accompanies liver injury and contributes to paracrine activation of HSC. (Figure from Iredale JP. Journal of Clinical Investigation 2007) (24)

ii. ECM producing cells

1. Hepatic stellate cell

The identification of stellate cell activation as a key event in fibrogenesis has provided an important framework for conceptualizing the liver's response to injury. HSC activation is a highly regulated process and consists of two major phases: *initiation* (also called a "preinflammatory stage") and *perpetuation*, schematically presented in Figure 4 and 5.

a. Initiation of HSC activation

After liver injury, the HSC undergoes a complex transformation or activation process where the cell changes from a quiescent, resting, vitamin A-rich cell to an activated, proliferating, fibrogenic, and contractile myofibroblast-like cell. Cellular changes accompanying HSC activation comprise morphological changes such as the appearance of the cytoskeletal protein smooth muscle α-actin (α-SMA), a loss in the cellular vitamin A stores, an increase in the appearance of rough endoplasmic reticulum and an increase in DNA synthesis and cellular proliferation (18). This activation process is also associated with acquisition by HSC of the capacity to respond to cytokines and to produce large amounts of matrix protein (18).

Activation of hepatic stellate cells is driven by factors produced by neighbouring cells, including injured hepatocytes, sinusoidal endothelium and Kupffer cells, and by remodelling of the surrounding matrix. Thus, parenchymal injury promotes activation of Kupffer cells, endothelial cells and platelets, and an influx of leucocytes. Those cellular events result in the generation of lipid peroxides, reactive oxygen species (ROS), and a number of cytokines such as TGF-β, the most potent fibrogenic cytokine for the HSC, and PDGF, the most potent mitogen for HSC. These factors promote induction of specific sets of transcription factors in hepatic stellate cells, resulting in induction or *de novo* expression of a variety of cytokines and chemokines and of their receptors, which are involved in fibrogenesis (20). Endothelial cells and platelets are also implicated in the HSC activation through the conversion of TGF-β from the latent to active profibrogenic form or as an important source of paracrine stimuli, including EGF, PDGF and TGF-β (25). Cytokines such as PDGF and TGF-β secreted by HSC create an autocrine loop, which is an important mechanism for perpetuating HSC activation (26).

HSC activation is also associated with an increase in cell contractility. Endothelin-1 (ET-1) is the major contractile stimulus for HSCs (27). Activated HSCs also produce nitric oxide (NO), a physiological antagonist of ET-1. The contractility of HSC may be a major determinant of early and late increases in portal resistance during liver fibrosis and cirrhosis (18) (Figure 4).

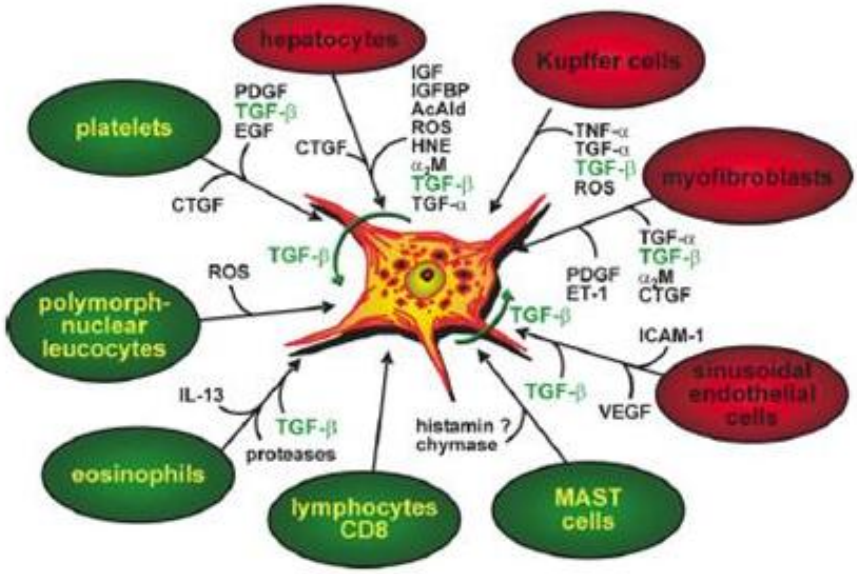

Figure 4: Hepatic stellate cell trans-differentiation / activation

Summary of cellular interactions of immigrated inflammatory cells (green) and resident liver cells (red) with HSCs in the process of trans-differentiation of quiescent cells into proliferative, matrix producing myofibroblastic-like cells (activated HSCs). (Figure from Gressner et al. Comparative Hepatology 2007) (28)

b. Perpetuation of HSC activation

Perpetuation of HSC activation involves a series of phenotypic changes which collectively lead to the accumulation of ECM. These changes include proliferation, contractility, fibrogenesis, chemotaxis and matrix degradation. (a) ***Proliferation*** is driven by paracrine and autocrine mediators, including PDGF, ET-1, thrombin, insulin-like growth factor (IGF), and TGF-β (18). (b) ***Contractility*** of HSCs may be a major determinant of early and late increases in portal resistance during liver fibrosis and cirrhosis. A key contractile stimulus towards HSCs is ET-1 (29). While most studies implicate calcium signalling in response to ET-1-induced contractility (30), a recent study contradicts that view by demonstrating calcium-independent contractile force in stellate cells (31). (c) ***Fibrogenesis*** is the acquired capacity of HSC to produce large amount of fibrillar matrix proteins accumulating in scar tissue. A large number of fibrogenic factors have been identified, including interleukin (IL)-1β, TNF-α, lipid peroxides, but none is as potent as TGF-β (32). (d) ***Chemotaxis*** is the attraction of HSCs at the wounded site. It may results from both proliferation and directed migration into regions of injury. A number of chemoattractants have been identified. PDGF, monocyte chemotactic protein-1 (MCP-1), and CXCR3 appear to be prominent (33-36). Recently, a study demonstrates that PDGF-stimulated chemotaxis is associated with cell spreading at the tip, movement of the cell body towards the stimulant, and retraction of trailing protrusions associated with transient myosin phosphorylation (37).

(e) ***Matrix degradation****:* quantitative and qualitative changes in the activity of MMPs and TIMPs play a key role in ECM remodeling in liver fibrogenesis (38).

A growing number of transcription factors have been identified in HSCs, yet these only represent a small amount of the total number of factors contributing to transcriptional control. HSC activation may be controlled by widely divergent regulatory pathways including transcription factors that contribute to stellate cell activation (e.g., Foxf1 and JunD), inhibition of cell growth (e.g., KLF6), cell survival (e.g., NFκB), and the maintaining of HSCs in the quiescent phenotype (e.g., Lhx2) (18).

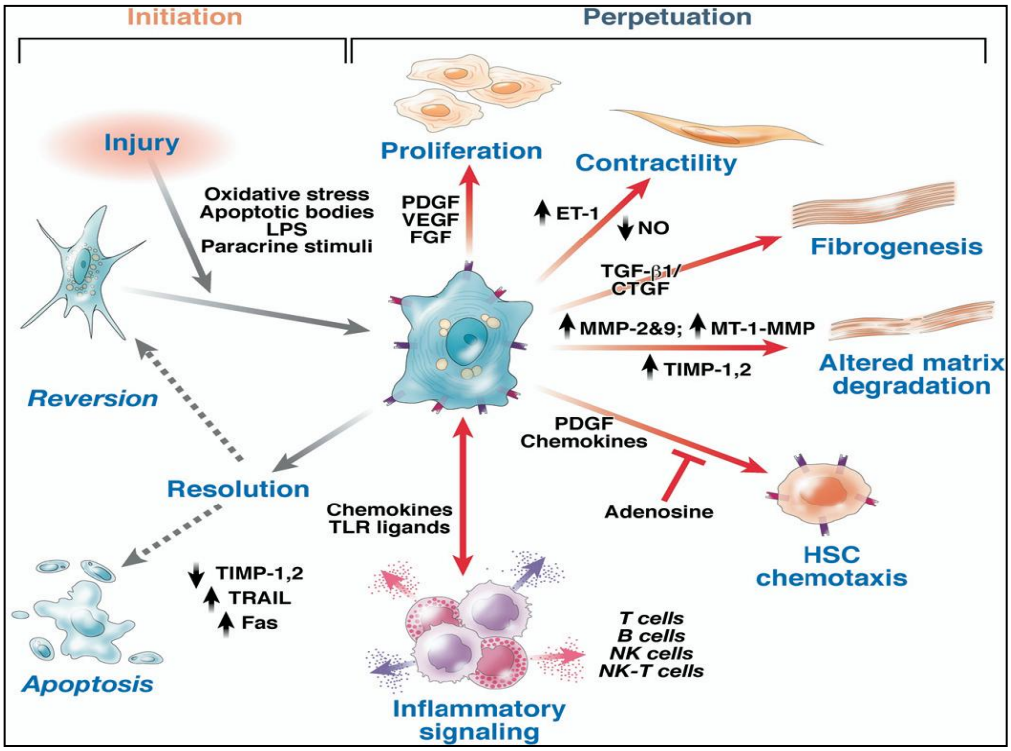

Figure 5: Pathways of hepatic stellate cell activation

Features of HSC activation can be distinguished between those that stimulate initiation and those that contribute to perpetuation. Following liver injury, HSCs undergo activation by soluble stimuli that include oxidant stress signals (reactive oxygen intermediates), apoptotic bodies, lipopolysaccharide (LPS), and paracrine stimuli from neighboring cell types including Kupffer cells, sinusoidal endothelium and hepatocytes. Perpetuation follows, characterized by major phenotypic changes including proliferation, contractility, fibrogenesis, altered matrix degradation, chemotaxis, and inflammatory signaling. During resolution of liver injury, activated HSCs and myofibroblast have been demonstrated to undergo apoptosis. It is also possible that spontaneous reversion to a more quiescent phenotype might occur. (Figure from Friedman SL. Gastroenterology 2008) (39)

2. Other (myo)fibroblastic cells involved in liver fibrosis

Although HSCs are the main producers of ECM components in the liver, other cell types contribute significantly to the synthesis of one or more of these macromolecules. It is increasingly clear that these fibrogenic cells derive not only from resident HSCs, but also from portal fibroblasts. Additionally, circulating fibrocytes, bone marrow, and epithelial–mesenchymal cell transition, may participate to the process, at least under specific conditions (39). Portal fibroblasts appear to be specially important in cholestatic liver diseases and ischemia. In contrast, progressive recruitment of bone marrow–derived cells may occur over time, such that these cells can represent a substantial fraction of the total fibrogenic population in more chronic injury. Bone marrow recruitment of mesenchymal cells remains a somewhat confusing event because of contradictory findings that on the one hand, bone marrow may provide fibrogenic cells, yet on the other hand autologous bone marrow and marrow-derived endothelial progenitor cells can be anti-fibrotic. It remains unclear which cells within marrow contribute to fibrogenesis and which might be anti-fibrotic, and/or what mediators regulate these apparently divergent activities of bone marrow–derived cells (39) (Figure 6).

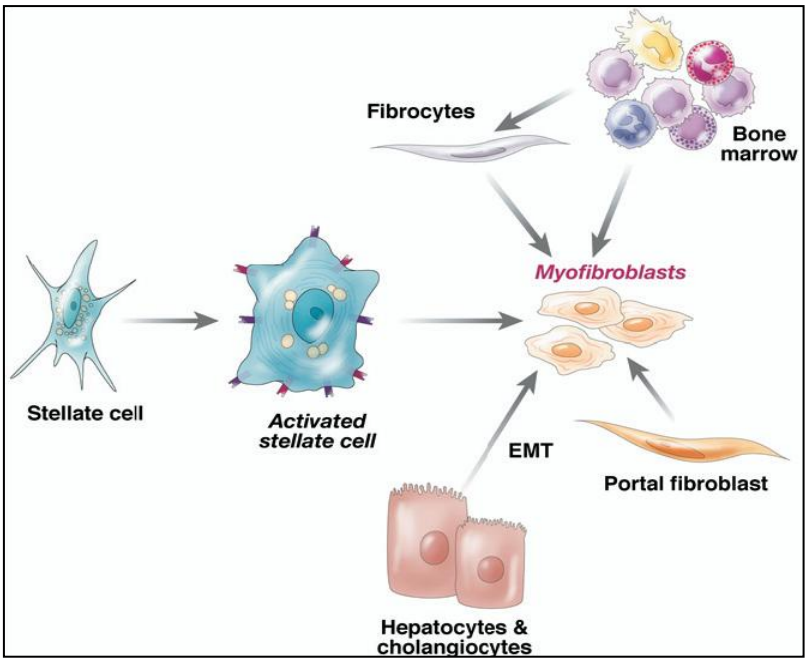

Figure 6: Contributions of activated stellate cells and other fibrogenic cell types to hepatic fibrosis

Multiple sources of fibrogenic myofibroblasts are likely in liver injury depending on the site and nature of the injury. While resident stellate cells appear to be the most likely source, periportal fibroblast may be prominent in biliary injury, whereas bone marrow and possible epithelial-mesenchymal transition may contribute as well. (Figure from Friedman SL. Gastroenterology 2008) (39)

c. How to treat hepatic fibrosis?

Currently, no specific therapy for fibrosis is available. Three approaches aiming at the reduction of excessive scar formation are theoretically possible. The first one would consist in the stimulation of specific proteolytic pathways in order to accelerate the degradation of the excessive ectopic ECM. The second approach would aim at altering the quality of the most abundant ECM proteins such as collagens. This would result in the deposition of a loose scar tissue prone to be rapidly degraded by physiological remodelling processes. The third approach would target HSCs, main effector cells, inhibiting the excessive synthesis of extracellular macromolecules, preventing their activation and proliferation and/or precipitating cell death by apoptosis. As fibrotic response is a physiological wound response involving common pathways irrespectively of the organ/tissue considered, the ideal treatment should be targeted to the liver. Considerable research on those three directions is on the way to identify strategies to successfully prevent fibrosis.

d. How to study hepatic fibrosis?

i. *In vivo* animal models

1. Repeated wound-healing

Following acute liver injury, restoration of normal architecture results from an intricate inflammatory reaction and matrix remodelling process that combines matrix synthesis and fibrolysis, together with liver cell proliferation to make up for cell loss. In contrast, chronic liver injury is associated with prolonged and dysregulated wound healing, characterized by an imbalance between excessive matrix synthesis, altered matrix degradation, and by hepatocyte loss not fully compensated for by proliferation.

Carbon tetrachloride (CCl_4) is a pro-toxin, extensively used for decades to induce liver injury in rodents (40). CCl_4 is transformed by cytochrome P450 (CYP) (mainly by CYP2E1) in a toxic metabolite that induces hepatocyte necrosis in the centrolobular area. In response to necrose, phagocytosis by macrophages and Kupffer cells is activated, inflammatory cells are recruited and a wound healing response occurs leading, when injury is chronic or repeated, to central-central, centro-portal bridging fibrosis or cirrhosis (3) (Figure 7). In this model, anti-fibrotic effects of tested drugs or interventions may therefore result either from a direct effect on fibrogenic cells, ECM remodelling or from anti-inflammatory effects.

There are others hepatotoxic substances able to induce liver fibrosis such as diethylnitrosamine (DEN) and thioacetamide (TAA). These two models induce haemorrhagic

centrilobular necrosis, destruction of sinusoidal endothelial cells leading to coagulation (DEN model) or centrilobular hepatocyte death (TAA model) respectively, resulting to liver fibrosis emerging from the central vein eventually leading to central-central bridging fibrosis (3).

2. Nutritional

Abuse of alcohol and steatohepatitis associated to metabolic syndrome exhibit similar histological changes in hepatocyte lipids overload (steatosis), hepatocyte ballooning (necrosis), polymorphonuclear neutrophil infiltration and the development of perisinusoidal fibrosis (41). Although fibrosis associated with alcohol and metabolic syndrome is common in humans, this is not the case in rodents. Alcohol-induced liver fibrosis in rodents is very difficult to obtain as a result of the absence of deliberate chronic alcoholism limiting alcohol intake. One way to circumvent this problem consists of intragastric infusion of alcohol. However, only early or mild fibrosis is observed, cirrhosis being absent even with more prolonged exposure to ethanol.

Similarly, feeding a high fat diet, while inducing severe metabolic changes, is un-consistently associated with perisinusoidal fibrosis and even for long period of time is seldom associated with significant fibrosis. An alternative model for metabolic steatohepatitis is the methionine and choline deficient (MCD) diet. This model is often used to investigate the pathogenesis of fatty liver disease because it rapidly induces steatosis and necro-inflammation and over longer periods causes hepatic fibrosis (42, 43). Thus this model mimics histological changes, and their evolution, seen in human NASH (Figure 7) (see section “Animal models to study NASH" for details of the model).

3. Bile duct ligation

Bile duct ligation (DBL) represents a rapid and consistent method to induce liver fibrosis and cirrhosis in rats, and less consistently in mice. Hepatic fibrosis induced by BDL is unique in that the primary pathological lesions occur surrounding the bile duct epithelium (Figure 7). The manoeuvre of BDL introduces biomechanical stress to biliary epithelium and initially triggers the compensatory proliferation and expansion of biliary epithelial cells (BECs) (44). Following this epithelial mitogenic phase, chronic obstruction of bile duct causes massive activation of myofibroblasts in the periductal region and ultimately results in biliary fibrosis/cirrhosis. There is little doubt that portal myofibroblast activation is one of the key steps that initiate fibrotic lesions in this model. However, the exact origin of these periductal myofibroblasts remains largely unknown, although it is often presumed that they are from

local activation of residential fibroblasts or HSCs. The rapid progression to cirrhosis and death might limit BDL application in chronic fibrosis studies and makes it difficult to carry out a long-term investigation of liver cirrhosis (45).

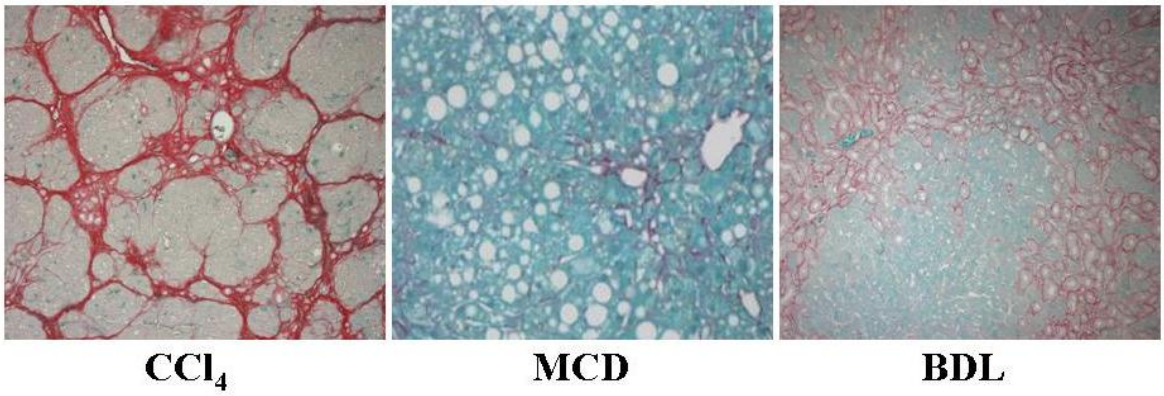

Figure 7: Animal models of hepatic fibrosis

Representative photomicrographs of Sirius red stained liver sections from mice injected with carbon tetrachloride (CCl_4) or fed a methionine and choline deficient (MCD) diet or submitted to a bile duct ligation (BDL). Demonstrating that various stimuli induce different types of fibrosis varying in the potential for progression, the topography and the cell types involved. (magnification x 20)

ii. In Vitro models

1. Primary HSC

Primary quiescent HSCs isolated from mouse and rat livers retain the important capacity to spontaneously plastic-activate in culture into myofibroblastic-like cells, mimicking the activation process observed *in vivo* during hepatic fibrogenesis. The isolation of quiescent HSCs from rat liver typically allows the isolation up to 4–5 x 10^7 viable cells. While methods for stellate cell isolation were initially developed in rats and then adapted to humans, the development of transgenic and knockout mouse models has more recently required the isolation of murine stellate cells (18). Density gradient separation remains the most widely used approach for HSCs isolation (see Annexe). This method favours isolation of low density cells that are relatively vitamin A-rich and are thus of the quiescent phenotype. By contrast, in animals with liver injury, large numbers of HSCs are recovered from higher density gradient layers. Such vitamin A-poor cells are typically more activated in terms of cytoskeletal markers and ECM gene expression (18). Another cell isolation approach, avoiding density gradients, is fluorescent cell sorting based on endogenous vitamin A auto-fluorescence (46).

Lower yields and dependence on costly technology greatly limit its applicability, although it remains valuable for obtaining ultra-purified stellate cells preparations.

In vitro, spontaneous activation of HSC recapitulates the fibrogenic process, thus, one of the most important advantages for primary HSC isolation is the possibility to evaluate the impact of therapeutic drugs, which could be used for the prevention or treatment of the liver fibrosis. By contrast, the poor transfectability of primary HSC and the absence of an efficient procedure reliable to bank these cells remain the most important disadvantages to allow on-demand usage of these primary cells for different research applications.

2. Cell lines

To overcome the limitations of primary HSCs, immortalized rat (HSC-T6) (47) and human HSC (LX-1, LX-2, and hTERT-HSC) (48, 49) cell lines have been developed. Established cell lines will, by definition, differ to some extent in their molecular phenotype from *in situ* or cultured primary cells as they are immortal. The LX-1 and LX-2 lines represent such reagents and the LX-2 line in particular, with its high transfectability and ability to withstand serum free conditions, provide important new tools in the elucidation of HSC biology and the discovery of anti-fibrotic therapies. The most important inconvenient of these cell lines is that all cells are immortalized into the activated phenotype impeding the study of the initiation of HSC activation, the initial and pivotal step in the fibrotic response.

3. Non-alcoholic steatohepatitis

a. Definition

Non-alcoholic steatohepatitis is defined by both histologic (steatohepatitis) and clinical (non-alcoholic) criteria. The histologic abnormalities of non-alcoholic steatohepatitis (NASH) are identical to those in alcohol-induced steatohepatitis and include steatosis (macro > micro), hepatocytes ballooning degeneration (usually zone 3), mixed lobular inflammation with scattered polymorphonuclear neutrophils and mononuclear cells, and, at times, other features, such as lipogranulomas, acidophil bodies, Mallory's hyaline, zone 3 perisinusoidal fibrosis, and megamitochondria. For the diagnosis of NASH, a liver biopsy is still required and therefore remains the gold standard. Only information from biopsy allows grading and staging of the disease (50). This latter information is crucial for patient management because simple

non-alcoholic fatty liver (NAFL) has a benign prognosis, whereas NASH can be progressive and lead to end-stage liver disease.

b. Risk factors and epidemiology

Obesity, hyperglycaemia, type 2 diabetes mellitus (T2DM), and hypertiglyceridaemia are risk factors for NASH and NASH severity (51). Genetic factors undoubtedly predispose to NAFLD/NASH (52, 53).

Palekar et al (54) developed a clinical model that sums 5 risks factors for NASH identified by multivariate logistic regression. These factors include age 50 or older, female sex, aspartate aminotransferase (AST) level of 45 IU or greater, body mass index (BMI) of 30 Kg/m² or greater, AST/ALT ratio of 0.80 or greater, and hyaluronic acid level of 55 µg/l or greater. Combining 3 or more of these factors yielded a sensitivity of 73.7% and a specificity of 65.7% for detecting NASH with receive operating curve (ROC) of 0.763. On the basis of estimates obtained from selected series, the prevalence of NASH in the general population of Western countries is considered to be around 2 and 3%, 19% in obese population and 36,4% in morbidly obese subjects (51, 55, 56).

Because of its association with obesity and with insulin resistance, NASH is today regarded as the hepatic complication of the metabolic syndrome, which is characterized by insulin resistance, hyperinsulinemia, pro-inflammatory and procoagulant changes, and a predisposition to type 2 diabetes, dyslipidemia, premature atherosclerosis and other disorders (57).

c. Pathogenesis

Elements of pathogenesis will be briefly exposed here and have been reviewed in depth by Farrell and Larter (58).

i. Liver steatosis and hepatic insulin resistance

The macrovesicular steatosis observed in NAFLD/NASH is due to excessive accumulation of triglycerides (TG) in the liver. Several cumulative mechanisms participate to the development of liver steatosis: impaired hepatic free fatty acids (FFA) oxidation, enhanced FFA delivery and extraction and increased hepatic *de novo* lipogenesis. Impaired or limited release of Very Low Density Lipoprotein (VLDL) may participate (59) (Figure 8). VLDL-TG production is also augmented due to increased availability of fatty acids from

intrahepatic and visceral origin. Enhanced TG excretion is however not sufficient to prevent hepatic fat accumulation (59). *De novo* lipogenesis is stimulated by glucose and hyperinsulinaemia through activation of carbohydrate response element binding protein (ChREBP) and sterol regulatory element-binding protein 1 (SREBP-1c) (59) (Figure 8).

Insulin is the principal regulator of whole body glucose homeostasis. It promotes glucose disposal in muscles and adipose tissue, and prevents the liver from producing more glucose by inhibition of glycogenolysis and gluconeogenesis. The failure of the latter, due to fatty acids and inflammatory-driven hepatic insulin resistance, is, to a large extent, responsible for the development of fasting hyperglycaemia and persistent stimulation of insulin production by pancreatic β-cells (Figure 8).

ii. The adipose tissue

Overloaded adipose tissue releases FFA and produces numerous chemokines and (adipo-) cytokines that exert effects on insulin sensitivity, metabolism, immunity and inflammation in a paracrine as well as in an endocrine fashion. In addition, in obesity, the adipose tissue contains an increased number of macrophages secreting inflammatory factors that can directly modulate adipocytokine production as well as influence insulin sensitivity and enhance low-grade chronic inflammation both locally, in the adipose tissue, and systematically (60).

iii. Transition from simple steatosis to progressive fibrosing NASH

The mechanisms governing the transition from inert fatty liver to steatohepatitis with progressive fibrosis involve (a) the activation of a pro-oxidative and hepatotoxic cascades linked to altered lipid metabolism, mitochondrial dysfunction and distorted signal transduction along the insulin-signaling and related intracellular pathways, and (b) chronic systemic low grade inflammation and an altered balance of adipo-cytokines production associated with obesity (59), favouring inflammatory and fibrotic processes in the liver.

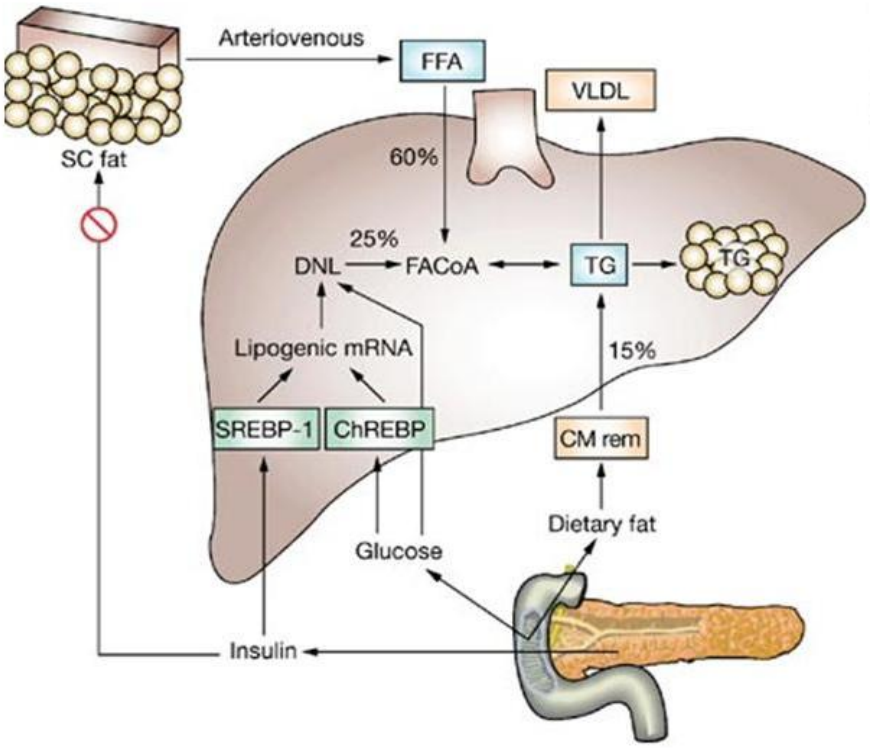

Figure 8: Contribution of different pools to intra-hepatocellular triglycerides in non-alcoholic fatty liver disease

Approximately 60–80% of hepatocellular lipids derive from the circulation, mainly originating from subcutaneous fat. Chronic overnutrition and hyperinsulinemia in obesity and hyperglycaemia in type 2 diabetes mellitus will increase the contribution of de novo lipogenesis and thereby augment the cellular pool of activated fatty acids. According to the hypothesis of defective mitochondrial function in insulin-resistant states, fatty-acid oxidation would be reduced, rendering more long-chain fatty acids bound to coenzyme A available for lipoprotein synthesis and secretion, which was found to be reduced in patients with non-alcoholic steatohepatitis. Subsequently, flux of hepatocellular fatty acids would be directed into storage of any excess of triglycerides, leading to elevated levels of hepatocellular lipids in obesity and type 2 diabetes mellitus. ChREBP, carbohydrate response element binding protein; CM rem, chylomicron remnants; DNL, de novo lipogenesis; FACoA, long-chain fatty acids bound to coenzyme A; FFA, free fatty acids; SC, subcutaneous; SREBP-1, sterol regulatory element-binding protein 1; TG, triglycerides; VLDL, very low density lipoproteins. (Figure from Roden M., Nature Clinical Practice Endocrinology & Metabolism 2006) (61)

d. Animal models to study NASH

i. Genetically obese (ob/ob) mice

Ob/ob mice, leptin-deficient because of a mutation in the ob gene encoding for leptin, represent a naturally occurring model of NAFLD. In the absence of leptin, a satiety hormone synthesized by the white adipose tissue, mice are hyperphagic, obese, insulin resistant,

hyperinsulinaemic, hyperglycaemic, hyperlipidaemic and spontaneously develop fatty liver, but not NASH. Indeed there is no inflammation and ob/ob mice are resistant to fibrosis (42).

However, obese ob/ob mice may develop steatohepatitis when challenged with a dose of lipopolysaccharide (LPS) endotoxin (62) unharmful in wild type (Wt) animals. Recently, low norepinephrine activity in ob/ob mice show to increase hepatic natural killer T (NKT) cells apoptosis and to deplete liver NKT cells, promoting proinflammatory polarization of hepatic cytokine production that sensitizes the liver to LPS toxicity (63).

Moreover, studies have shown that ob/ob mice were more vulnerable to acute liver damage induced by ischemiae-reperfusion or ethanol (64). In ob/ob mice expression of the proinflammatory cytokine TNF-α is increased in white adipose tissue and liver, and insulin resistance, fatty liver disease and susceptibility to dammage are significantly improved by inhibiting TNF-α activity (65).

ii. Methionine and choline deficient (MCD) diet model

Administration of a methionine and choline deficient (MCD) diet to rodents causes progressive fibrosing steatohepatitis pathologically similar to human metabolic steatohepatitis.

Elimination of methionine and choline from the diet causes fat to accumulate rapidly within the liver. In this situation, steatosis is the result of impaired hepatic TG secretion, which in turn is attributable to defective assembly of VLDL. Methionine and choline are important precursors of phosphatidylcholine, the principal phospholipid comprising the outer coat of VLDL particles (66). Choline deficiency results in reduced fatty acid β-oxidation and reduced triacylglycerol clearance by the liver. When these nutrients are in short supply, VLDL production is impaired and triglycerides accumulate in hepatocytes. Methionine deficiency leads to reduction in liver glutathione and increase in ROS (e.g. via CYP2E1) (3). ROS-induced hepatocyte damage and inflammatory recruitment lead to chronic hepatic inflammation and pericellular and perisinusoidal fibrosis that can progress to cirrhosis (45). This severe and progressive liver injury distinguishes the MCD model of fatty liver from others whether induced by high fat diet or genetic defects, in which inflammation and fibrosis are rare and seldom progressive (66).

Although the MCD model mimicks pathological changes seen in human NASH, the patho-physiological mechanisms are likely to be differents as, by contrast to human with

NASH, those mice are not obese (rather cachectic) and exhibit systemic hypersensitivity to insulin together with relative hepatic insulin resistance (67).

iii. High-fat diet model

Development of mild steatohepatitis is only observed when animals are force-fed a high fat diet for long period to obtain chronic over-caloric consumption.

The effects of giving a high-fat diet to rodents can be highly variable. Some studies show clear induction of steatosis and steatohepatitis, whereas others show very few, if any, liver abnormalities (68-71). Some of this variability could be explained by the influence of rodent strain which is known to be important in the susceptibility to several forms of liver disease.

Thus, although some high-fat-feeding models appear well suited for NASH research, the inconsistency in fibrosis development and the challenge to reproduce them reliably between different laboratories may limit their utility and popularity.

4. The transcription factors peroxisome proliferator-activated receptors (PPARs)

Peroxisome proliferator-activated receptors (PPARs) belong to the nuclear receptors superfamily which are ligand-activated transcription factors. Three related PPAR isotypes were identified and named PPARα (NR1C1), PPARβ/δ (NR1C2) and PPARγ (NR1C3) (72). The human and mouse PPARγ genes extend over more than 100kb of genomic DNA and give rise to three mRNAs, PPARγ1, PPARγ2, and PPARγ3, that differ at their 5'-end as a consequence of alternate promoter usage and splicing (73).

a. Tissue distribution

In the adult rat, relatively high levels of PPAR-α mRNA are detected in brown fat, liver, kidney, heart, and mucosa of stomach and duodenum. Retina, adrenal gland, skeletal muscle, and pancreatic islets also express significant amounts of PPARα mRNA (74). In the human, its levels in the liver appear lower than in the rodent liver (75).

PPARγ has a restricted pattern of expression in adult rodents, white and brown adipose tissues being the major sites of expression (74). The intestinal mucosa also expresses high levels of PPARγ in the colon and caecum but less in the small intestine (76). Strikingly,

PPARγ is abundant in lymphoid tissues such as the spleen (red and white pulp) and Peyer's patches in the digestive tract (74), and in cells of the monocyte/macrophage lineage (77). Finally, PPARγ is also expressed at low levels in the liver and skeletal muscle (78).

In adult rats, PPARδ is abundantly and ubiquitously expressed, often at higher levels than PPARα and PPARγ. It also remains the most expressed isotype in the adult nervous system (74). It is only weakly expressed in liver compared to other tissues (74). Although it is abundant in skeletal and cardiac muscle, PPARδ cannot be detected by *in situ* hybridization in smooth muscle cells of the digestive tract. In testis, its expression is very high in Sertoli cells (74). PPARδ, expressed in epidermal keratinocytes (79), is implicated in their differentiation and contributes to the so-called "regenerative skin phenotype" characterizing the late phase of wound healing (80).

b. Structure of PPARs and mechanisms of action

The PPAR genes characterized to date reveal a common organization of the translated region in six coding exons with the following distribution: one exon for the N-terminal A/B domain, two exons for the DNA-binding domain (DBD) (one for each of the two zinc fingers), one exon for the hinge region, and two exons for the ligand-binding domain (LBD). The DBD is the most conserved domain between all nuclear receptors, and indeed is the hallmark of the superfamily. It is formed by two zinc finger-like motifs folded in a globular structure that recognize a DNA target composed of 6 nucleotides (73) (Figure 9).

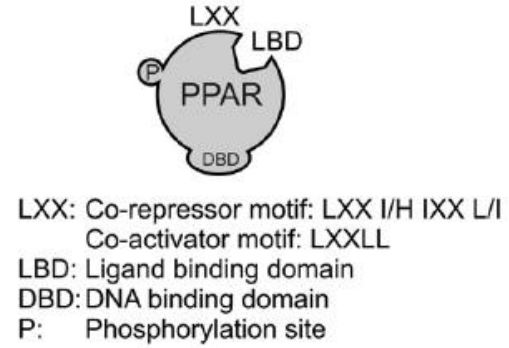

Figure 9: General structure of PPARs

Peroxisome proliferator-activated receptors (PPARs) is composed of a ligand-binding domain (LBD), a DNA-bonding domain, a phosphorylation site (P) and a co-repressor/activator motif (LXX). (Figure from Bragt M.C.E. Physiology and Behavior 2008) (73)

PPARs activate transcription of their target genes as a heterodimer with their DNA binding partner the retinoid X receptor (RXR) (73). RXR, a common DNA binding partner of the thyroid/steroid receptor family, including PPAR, can be activated by the endogenous agonist 9-cis retinoic acid (73). This complex initiates gene transcription after binding to the PPAR response element (PPRE) in enhancer sites of regulated genes. The PPRE is a direct repeat (DR) of two core recognition motifs with a consensus sequence AGGTCA and is spaced by one nucleotide, also called DR1. Additional co-factor proteins are recruited to the PPAR:RXR complex, which play an important role in determining the physiological response to PPAR ligands. Co-factors can either activate (co-activators) or repress (co-repressors) the transcriptional activity of PPARs. The activity of PPARs is fine tuned by their phosphorylation status (73) (Figure 10). Phosphorylation can result in changed affinity for ligands, RXR, co-factors or DNA binding sequence of target genes. Multiple kinase pathways have been implicated in the phosphorylation of PPARs, including cAMP-dependent protein kinase (PKA), c-jun terminal kinase (JNK) and mitogen-activated protein kinases (MAPK) (81). However, the physiological relevance of various modes of phosphorylation is not yet fully understood (73).

Because RXR is a common DNA binding partner to many nuclear receptors of the thyroid/steroid receptor superfamily, competition between PPAR and these receptors can occur. *In vivo*, such competition is likely to occur only when the amounts of RXR are limited. Whether the relative amounts of thyroid hormone receptor (TR), PPARs and RXR meet these conditions in any tissue *in vivo* is so far unknown.

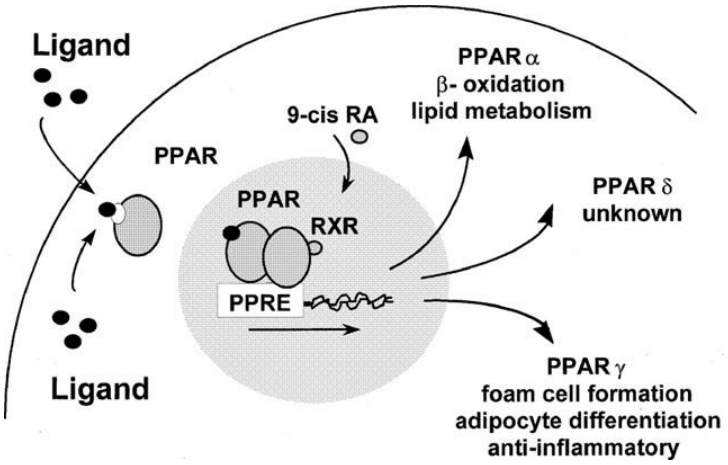

Figure 10: PPAR activation pathway

Activation of the PPAR receptors leads to an accumulation in the nucleus, where they heterodimerize with RXR. The PPAR : RXR heterodimer binds to DNA sequences called PPAR response elements (PPRE), leading to the transcription of the PPAR- responsive gene. (Figure from Bishop-Bailey D. British Journal of Pharmacology 2000) (82)

i. Ligands

Natural and synthetic ligands are determined for each PPAR isoform in both functional (cell-based transactivation efficiency) and *in vitro* interaction assays (Table 1). The identification of unsaturated fatty acids (UFAs) as PPAR ligands provides firm evidence that at least part of the PPAR-dependent transcriptional activity of fatty acids results from a direct interaction of the nuclear receptor with these molecules. PPARα exhibit the highest affinity for the UFAs. By contrast, saturated fatty acids are poor PPAR ligands in general. Among synthetic ligands, compounds of the fibrate family and their derivatives (Wy-14,643) have been widely used to characterize PPARα functions. Amongst the natural ligands for PPARγ, several UFAs such as oleate, linoleate, eicosapentanoic, and arachidonic acids can bind PPARγ as well as a prostanoid called 15-Deoxy-Δ12,14-prostaglandine J2, which is a PGD2 derivative. Thiazolidinediones (TZDs), synthetic PPARγ ligands which include pioglitazone, rosiglitazone and troglitazone, are a class of antidiabetic drugs.

Intriguingly, the screenings for natural and synthetic ligands were not very successful in identifying PPARδ ligands. Bezafibrate is a *Xenopus* PPARδ-specific ligand, but its activity is much weaker on the mammalian PPARδ (83) (Table 1).

Ligands	**PPARs**
Natural ligands	
MUFA	α and δ
PUFA	α, δ and γ
Saturated fatty Acids	α and δ
Eicosanoids	α
15-Deoxy-Δ12, 14-PGJ2	γ
Leukotriene B4	γ

Ligands	**PPARs**
Synthetic ligands	
Wy14,643 (Pirinixic acid)	α
Fatty acyl-coA dehydrogenase inhibitors	α
Leukotriene B4 analogs	α
GW409544	α
GW2433 (fibrate analog)	α and δ
GW2331 (fibrate analog)	α and δ
Benzafibrate	δ
Hypolipidemic and hypoglycelic agents	δ
GW61049x	δ
Pioglitazone	α and γ
Rosiglitazone	γ
Troglitazone	γ
Ragaglitazar	γ
Farglitazar	γ
NSAIDs	γ
Ciprofibrate	γ

Table 1. Natural and Synthetics ligands of PPARs *(72, 73, 83, 84)*

ii. Target genes

Studies have demonstrated that, in the liver, PPARα directly regulates genes involved in fatty acid uptake [fatty acid binding protein (FABP)], β-oxidation [Acyl-CoA oxidase (ACO)] and ω-oxidation (cytochrome P450) (85). Regarding mitochondrial β-oxidation, PPARα activation stimulates the expression of the medium-chain acyl-CoA dehydrogenase (MCAD), the mitochondrial form of hydroxymethylglutaryl-CoA synthase (HMGCS1), involved in ketone body synthesis, as well as carnitine palmitoyl transferase I (CPT-I), also known as a PPARδ target. In the intestine, fatty acids are able to induce the expression of a FABP, and this effect is mimicked by a clofibrate-enriched diet, thus suggesting that PPARα can control the cellular fatty acid flux in the intestinal cell. A stimulatory effect of PPARα on the pyruvate dehydrogenase kinase 4 (PDK4) gene expression and activity is described in rodent and human skeletal muscles (86). PPARα is also shown to prevent inflammation through the induction of the inhibitor of NF-κB alpha (IκBα), resulting in the inhibition of the nuclear factor-kappa B (NF-κB), a key regulator of inflammation (87, 88).

Gene expression profiling by microarray suggests that the detectable changes in gene expression induced by PPARγ ligands occurs mostly in the adipocyte. These include genes involved in glucose uptake [c-Cbl-associated protein (CAP) and glucose transporter 4 (GLUT4)], in lipid uptake and storage [CD36, aP2, LPL, FABP, and acyl-CoA synthase (ACS)], and in energy expenditure [glycerol kinase (GyK), uncoupling protein (UCP) 2 and UCP3] (89). Apart from genes that are directly involved in lipid and glucose homeostasis, PPARγ agonists such as TZDs also modulate the expression of secreted signalling molecules or adipokines in fat including down-regulation of leptin (90) and TNFα (91) and up-regulation of adiponectin (92). PPARγ activation also appears to increase glucose oxidation in the muscle and decrease gluconeogenesis in the liver, in part, by down-regulating PDK4 and phosphoenolpyruvate carboxykinase (PEPCK), respectively (89).

A selective PPARδ ligand is capable of regulating genes important for fatty acid catabolism such as CPT1, UCP2 and UCP3, increasing the fatty acid oxidation rate in muscle cells (85) (Table 2).

Target genes	PPARs
ACO	α
CYP4A1	α
CYP4A6	α
MCAD	α
HMGCS1	α
L-FABP	α and γ
PDK4	α and γ
CPT-I	α and δ
H-FABP	δ
UCP2 and 3	δ and γ
CD36	δ and γ
LPL	δ and γ
ACS	δ and γ
Adiponectin	γ
aP2	γ
GLUT4	γ
CAP	γ
PEPCK	γ
TNFa	γ
Leptin	γ
Gyk	γ

Table 2. Target genes of PPARs *(73, 85, 86, 89-92)*

c. PPARγ in whole body physiology

PPARγ plays a role in various physiological and pathophysiological events, including adipocyte differentiation (93) and the response to insulin. PPARγ activation enhances the lipid storage capacity of the adipose mass, and also increases the number of small, insulin-sensitive adipocytes so as to improve insulin sensitivity (94). PPARγ is implicated in the regulation of lipid metabolism (95) as well as the maturation of monocyte / macrophages and the control of inflammatory reactions (77).

PPARγ deficient ($PPAR\gamma^{-/-}$) mice embryos die at embryonic day 9.5–10 due to placental dysfunction (96). Moderate reduction of PPARγ activity by heterozygous PPARγ deficiency decreases TG content of white adipose tissue (WAT), skeletal muscle, and liver due to increased leptin expression, enhanced fatty acid combustion and decreased lipogenesis, thereby protecting against high-fat (HF) diet-induced obesity and insulin resistance (94).

d. Therapeutic potential of PPARγ ligands

i. Insulin sensitizing effect

Clinical studies with pre-diabetic and diabetic subjects failed to demonstrate an effect of PPARα agonists on plasma glucose and insulin levels. Only for PPARγ there are convincing results demonstrating that PPARγ activation improves insulin sensitivity (94). PPARγ activation increases glucose uptake and glycogen synthesis by skeletal muscle. Treatment reduces hepatic glucose production and subsequent release by a decreased gluconeogenesis (73). In general, human intervention studies with PPARγ agonists report reduced fasting insulin concentrations, glucose concentrations, and improved whole body insulin sensitivity (73).

Several innovative studies involving targeted deletion of the receptor in experimental animal models have assisted in understanding the function of PPARγ specifically in adipose tissue and skeletal muscle, and the secondary effects in other organs, including the liver and pancreas (both of which express low levels of PPARγ) (97). Targeted deletion of PPARγ in fat tissue resulted in marked reduction in the number of adipocytes (97). In addition, it results in elevated levels of plasma non-esterified free fatty acids (NEFA) and TG, and decreased levels of plasma leptin and adiponectin. These mice were also significantly more susceptible to high-fat diet-induced steatosis, hyperinsulinaemia, and insulin insensitivity (in fat and liver, but not muscle). TZDs fail to reduce plasma NEFA and to correct insulin resistance in those animals (97). The importance of PPARγ outside the adipose tissue is highlighted in mice with skeletal muscle-specific loss of PPARγ showing a 80% reduction in insulin-stimulated glucose disposal rates that is not improve with TZD treatment (97).

ii. Fibrosis

Several observations suggest that PPARγ is an important transcription factor in fibrogenesis, in particular on the control of HSC activation. Indeed, forced expression of PPARγ by adenoviral transfection is sufficient to reverse the morphology of activated HSCs to the quiescent phenotype (98). PPARγ is expressed in quiescent, vitamin A-rich cells in normal rat liver and decreased expression is associated with activation of HSCs *in vitro* (99). PPARγ activation inhibited proliferation, migration, and production of collagen I by rat HSCs *in vivo* and *in vitro* (100).

Moreover, *in vivo*, TZDs prevent the development of hepatic fibrosis in several rats' models (100).

iii. NASH

The association between NASH and insulin resistance has proned the use of PPARγ agonists to treat this disease.

TZDs dramatically improve insulin resistance in skeletal muscle, adipose tissue and liver, increasing plasma adiponectin levels and fatty acid oxidation and decreasing fatty acid synthesis (101). Pioglitazone (PGZ) and rosiglitazone (RGZ) were evaluated in pilot studies in patients with NASH (102, 103), and they ameliorate steatosis. PGZ appears to have an additional therapeutic benefit on fibrosis compared to RGZ (104, 105). Recent data from our laboratory demonstrate that pioglitazone alleviates steatohepatitis induced by the MCD diet, an effect associated with correction of intrahepatic insulin resistance *in vivo* in mice (67).

The positive effect of PPARγ agonists on NASH development could be linked to the beneficial effect of these drugs on type 2 diabetes mellitus, their insulin sensitizing properties and their anti-inflammatory and/or anti-fibrotic activities, components implicated in the development of NASH. The mechanism of action remains, however, ill-clarified (Figure 11).

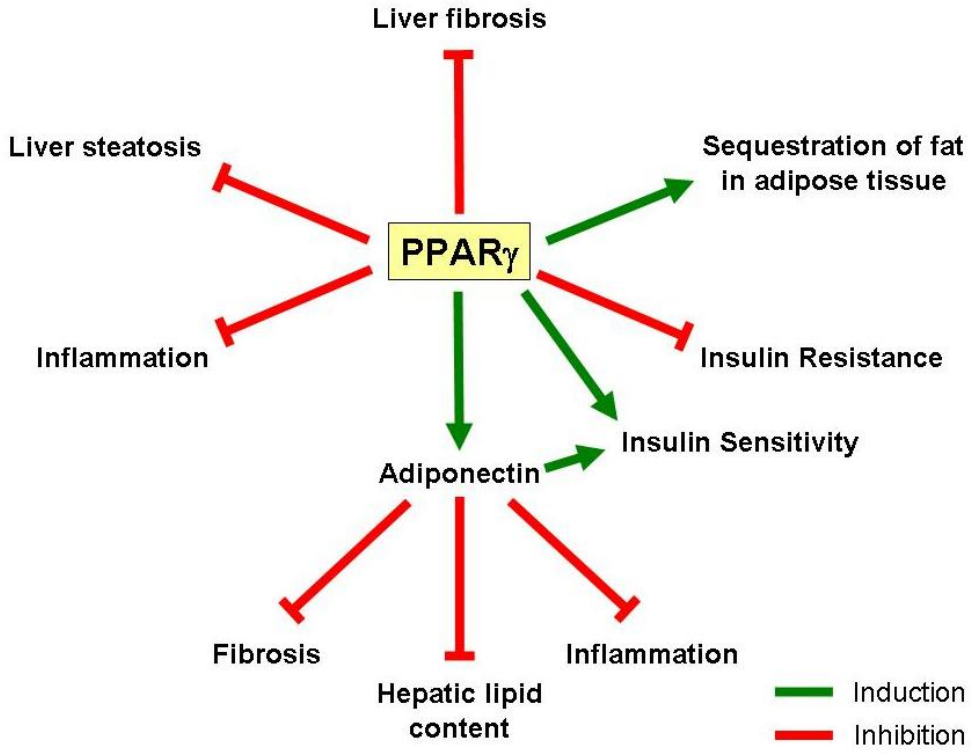

Figure 11: PPARγ and NASH

Metabolic effects of activated PPARγ which could explain its beneficial impact on non-alcoholic steatohepatitis (NASH) development in rodents.

5. Adiponectin, an adipocyte-derived PPARγ regulated gene

Adipose tissue, once considered simply a lipid storage depot, is now known to be a dynamic endocrine organ that secretes various factors with local or more distant action (adipokines). Obese and type 2 diabetic patients exhibit altered profiles of adipokines. Adiponectin is one of the most abundant plasma proteins (~1–17 mg/ml) and circulating levels decrease in obesity (106) as well as in patients with cardiovascular diseases, hypertension, metabolic syndrome, NASH and hepatic fibrosis (107), all states frequently associated with insulin resistance. However, whether this apparent parallelism between low plasma adiponectin levels and insulin resistance represents a cause and effect relationship is not known (107).

a. Structure

Adiponectin structurally belongs to the complement 1q family and is known to form a characteristic homomultimer. The most basic form is the trimer (LMW). Adiponectin also forms two higher ordered structures through the non-covalent binding of two trimers (hexamers) (MMW) and six trimers (18 mers) (HMW). These higher ordered complexes are described as medium molecular weight (hexamers) and high molecular weight (12–18 mers) forms of adiponectin (108). Studies have suggested that high molecular weight adiponectin may be biologically active and critical for enhancing insulin sensitivity (108) (Figure 12).

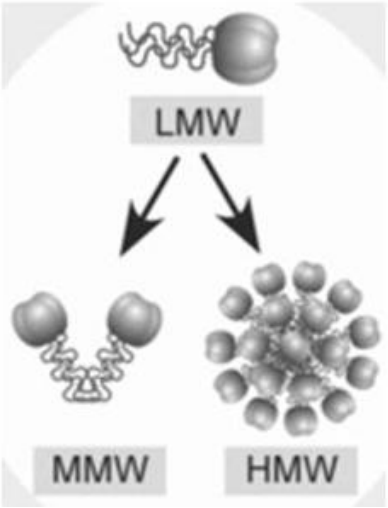

Figure 12: Forms of adiponectin
Oligomerization of full-length Adiponectin into trimers (LMW), hexamers (MMW) and oligomers (HMW) (Figure from Fang and Sweeney. Biochem. Soc. Trans. 2006) (106)

b. Regulation

Adipose tissue is considered as the major site of endogenous adiponectin production, even though other potential sources such as muscle cells, cardiac myocytes, or endothelial cells are also reported (109). TNFα suppresses the transcription of adiponectin in 3T3-L1 adipocytes, which may be an underlying mechanism for the lower adiponectin levels in obesity (110). Insulin sensitizer PPARγ agonists increase adiponectin levels in mice and humans, as well as in 3T3-L1 adipocytes *in vitro* (107). These effects seem to be associated with small-sized adipocytes (94), adipocytes differentiation (93), direct transcriptional activation of genes via PPRE (92) and increased insulin action (94).

c. Mechanisms of action

Adiponectin receptors (AdipoR1/2) serve as receptors for globular and full-length adiponectin and mediate increased AMPK and PPARα activation, fatty-acid oxidation and glucose uptake (111).

i. Activation of downstream signal

AdipoR1 and AdipoR2 are integral membrane proteins with an intracellular N-terminus, a predicted seven-transmembrane (7TM) motif domain and an extracellular C-terminus (111). The locations of the N-terminus and the C-terminus of human AdipoRs are opposite to the topology of all known G-coupled protein receptors (GPCRs). In addition, the downstream signalling molecules of adiponectin, such as AMPK and PPARα, do not seem to be linked to the G protein-signalling pathway. Thus the 7TM containing AdipoRs may belong to a new receptor family, which are structurally and functionally distinct from GPCRs (111).

Recent work by Mao and colleagues identify the first AdipoR1/R2 interacting protein, APPL1. APPL1, a 70 amino acid adaptor protein, contains several protein interaction domains including a pleckstrin homology domain, a phosphotyrosine (PTB) binding motif and a BAR (Bin-Amphysin-Rvs)-domain. The authors demonstrate direct binding of the APPL1-PTB domain with the AdipoR1 intracellular region (112). This is the first evidence susceptible to explain the mechanism by which AdipoR1 induces activation of AMPK. However, exact mechanisms of interaction between AdipoR2 and PPARα remain unknown (Figure 13).

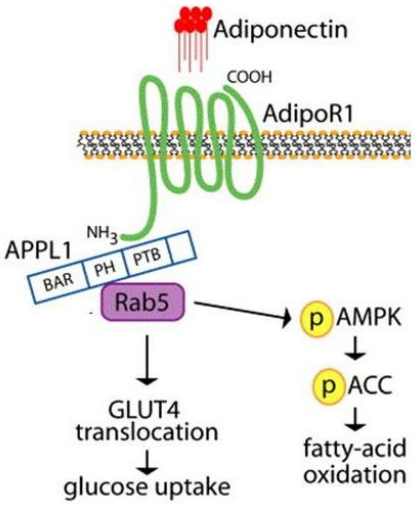

Figure 13: Proposed mechanism for AdipoR1 stimulated activation of the AMPK pathway
APPL1 binds AdipoR1 and is involved in adiponectin-dependent phosphorylation of AMPK, GLUT4 translocation, glucose uptake, and fatty acid oxidation. Its interaction partner Rab5 is important for GLUT4 translocation. (Figure from Hosch S.E. Cell Metabolism 2006) (113)

ii. The adiponectin receptor type 1 (AdipoR1)

1. Tissue/cellular distribution and regulation of gene expression

AdipoR1 is a receptor for globular adiponectin, ubiquitously express but most abundantly in adipose tissue and skeletal muscle (111).

AdipoR1 mRNA expression in skeletal muscle increases after fasting, and refeeding rapidly restores gene expression to levels equal to the original fed state. Moreover, expression of AdipoR1 decreases significantly in muscle and adipose tissue of insulin-resistant ob/ob mice. These observations suggest that insulin may negatively regulate AdipoR1 mRNA levels (114).

2. Down stream control of lipogenesis and fatty acid β-oxidation through AMPK

In vivo, adiponectin stimulate phosphorylation and activation of AMPK in skeletal muscle and liver. The activation of AMPK stimulates glucose uptake (115) and reduces expression levels of molecules involved in gluconeogenesis such as PEPCK and glucose-6-phosphatase (G6Pase) in hepatocytes (116). Furthermore it also stimulates phosphorylation and inhibition of acetyl CoA carboxylase (ACC) leading to a decrease in the concentration of malonyl CoA (117). Malonyl CoA is an allosteric inhibitor of CPT-I, the enzyme that controls the transfer of long chain fatty acyl CoA molecules into mitochondria. Thus, a decrease in its concentration increases fatty acid oxidation (115, 118). This pathway is thought to be central

to the effects of AMPK to reduce lipid stores in muscle and liver (119). Transcriptional control exerted by AMPK may be important for liver steatosis because AMPK activation suppresses expression of SREBP-1c, a transcription factor that controls the transcription of nearly all the enzymes involved in *de novo* lipogenesis (120, 121).

Targeted disruption of AdipoR1 results in the abrogation of adiponectin-induced AMPK activation (111). Moreover, blocking AMPK activation by use of a dominant negative mutant inhibited each of these effects, indicating that stimulation of glucose utilization and fatty acid combustion by adiponectin occurs through activation of AMPK (122) (Figure 14).

iii. The adiponectin receptor type 2 (AdipoR2)

1. Tissue/cellular distribution and regulation of gene expression

AdipoR2 is a receptor for full-length adiponectin, abundantly expressed in mouse liver, to lesser extend in adipose tissue and muscle (111).

As AdipoR1, AdipoR2 mRNA expression in skeletal muscle increase after fasting, and refeeding rapidly restore it to levels equal to the original fed state. Moreover, expression of AdipoR2 significantly decreases in muscle and adipose tissue of insulin-resistant ob/ob mice. These observations suggest that insulin may also negatively regulate AdipoR2 mRNA levels (114).

2. Down stream control of fatty acid β-oxidation and inflammation through activation of PPARα

Beside activation of AMPK upon binding to AdipoR1, adiponectin can also interact with the AdipoR2 resulting in the activation of PPARα, a transcription factor that controls β-oxidation of lipids (111, 123). Treatment of lipoatrophic or obese diabetic mice with adiponectin or overexpression of adiponectin in ob/ob mice results in increased expression levels of PPARα target genes such as CD36, acyl-coenzyme A oxidase, UCP 2 and increases the level of expression of PPARα *in vivo* (111). This suggests that adiponectin enhances fatty acid combustion and energy consumption, at least partly via PPARα activation, leading to decreased TG content in the liver and skeletal muscle and thus co-ordinately increases *in vivo* the insulin sensitivity (Figure 14).

Adiponectin as well as ligand activation of PPARα are able to induce the expression of the inhibitor of NFκB-α (IκBα) (124). This is a protein that binds to NFκB and prevents its nuclear translocation and, subsequent, the transcription of pro-inflammatory genes (125).

Therefore, induction of IκBα via PPARα is positively correlated with a decrease in inflammation, which is beneficial to prevent or counter the low level chronic inflammation, characteristic of the metabolic syndrome (Figure 14).

d. Adiponectin properties

i. Metabolic effects

Adiponectin has anti-diabetic properties due to insulin-mimetic and insulin-sensitizing actions, while anti-inflammatory and anti-atherosclerotic effects are also consistently reported.

The insulin-mimetic and insulin-sensitizing effects of adiponectin on liver and/or skeletal muscle are clearly shown by injection of adiponectin. This acutely decreases blood glucose in normal mice, ameliorates and/or preventes insulin-resistance associated with diet-induced obesity and improves glucose tolerance upon administration to various obese or lipoatrophic insulin-resistant animal models. The direct insulin-sensitizing effect of globular adiponectin (gAd) is further demonstrated by the fact that gAd transgenic ob/ob mice exhibited attenuated insulin resistance and diabetes compared with ob/ob mice (106). Similarly, transgenic overexpression of adiponectin prevented diet-induced metabolic complications in rats (106). In addition, many interesting phenotypic consequences, although not always consistent, are noted using adiponectin-KO mice generated by various groups (110) (Figure 14). The potent and widespread physiological effects of adiponectin therefore make this adipokine extremely attractive as a drug discovery target (106).

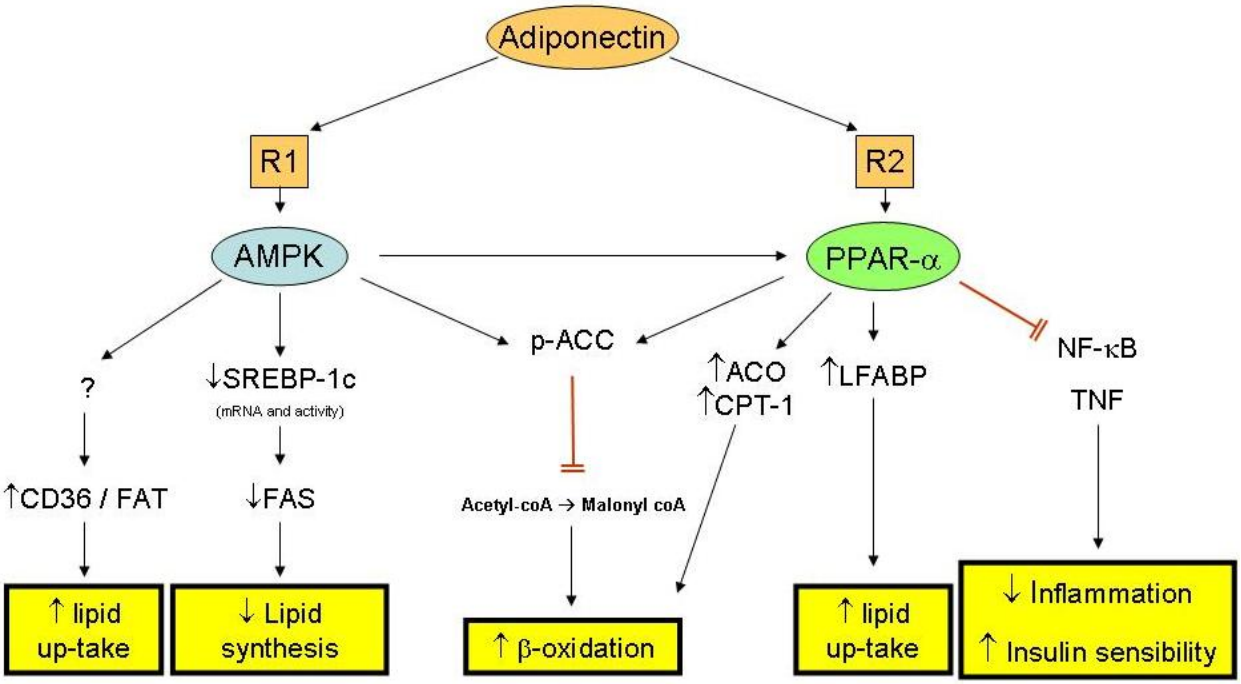

Figure 14: Adiponectin, downstream targets and metabolic effects
Interaction of adiponectin with its receptors AdipoR1 and R2 induces the activation of AMPK and PPARα pathway, respectively, and resulting in various metabolic effects.

ii. Adiponectin and inflammation

Obesity is characterized by low-grade systemic inflammation. Several clinical studies demonstrate the inverse relationship between plasma adiponectin levels and several inflammatory markers including C-reactive protein (CRP) (126). Both IL-6 and TNF-α are important pro-inflammatory (adipo)cytokines, which contribute to regulation of CRP production in liver (127). Experimental studies demonstrated that adiponectin expression is negatively regulated by pro-inflammatory cytokines including IL-6 and TNF-α, whereas adiponectin modulates the action and production of TNF-α in various tissues.

Adiponectin attenuates inflammatory responses to multiple stimuli by modulating signaling pathways in a variety of cell types. Its anti-inflammatory properties may be a major component of its beneficial effects on cardiovascular and metabolic disorders including atherosclerosis and insulin resistance (126).

iii. Adiponectin and Fibrosis

Adiponectin has anti-fibrotic properties. Mice lacking adiponectin are exquisitely sensitive to hepatic fibrosis while supra-physiological levels of adiponectin induced by

adenovirus infection prevents CCl_4-induced fibrosis (128). Several studies show that HSCs express adiponectin receptors (128, 129) and recently high molecular weight (HMW) adiponectin has been shown to inhibit proliferation of the human HSC line hTERT and primary rat activated HSCs via activation of AMPK through suppression of ROS production and subsequent inhibition of the Akt pathway (130). These experimental findings imply that adiponectin has a suppressive effect on liver fibrogenesis by inhibition of proliferation of activated HSCs. However, the role of AMPK on the HSC complete trans-differentiation phenomenon remains to be elucidated. The reverse proposition that hypoadiponectinaemia may therefore explain, at least partly, increased susceptibility to fibrosis in obesity has not been tested.

iv. Adiponectin and NASH

Subjects with NAFLD exhibit decreased adiponectin levels (131, 132), which are negatively correlated with hepatic TG content. The direct role of adiponectin in NAFLD is still unclear, but this hormone is supposed to improve primarily glucose and lipid metabolism. Adiponectin inhibits the expression of tumor necrosis factor (TNF)-α, implicated in NASH pathogenesis (45, 126). Among other factors released within the adipose tissue, TNFα promotes lipolysis and increases FFAs (45). Thus adiponectin would be beneficial in NASH by reducing FFA and by exerting anti-inflammatory effects by opposing the synthesis and release of TNFα from macrophages within adipose tissue in obesity (133). Indeed, in a mouse model of NASH, administration of adiponectin is associated with decreases in hepatic lipid contents and serum ALT levels (111). It has also been suggested that adiponectin could exert some of its hepatic lipid modulatory and anti-inflammatory effects via PPARα (111), the pharmacological activation of which completely reverses experimental steatohepatitis (133). Targher et al. recently showed that adiponectin levels were closely associated with severity of liver histology including hepatic steatosis, necroinflammation and fibrosis. Although all three components of hepatic histology were associated with low adiponectin levels, only steatosis and necroinflammation were found to be independent predictors in multivariate analysis (134).

6. The AMP-activated protein kinase (AMPK)

a. Structure and regulation

AMPK is a metabolic sensor with high sensitivity for the cellular energy status. It is a heterotrimeric protein consisting of a catalytic (α) and regulatory (β and γ) subunits (135). Each α and β subunit is encoded by 2 genes (α1 and α2 or β1 and β2), whereas the γ subunit is encoded by 3 genes (γ1, γ2 and γ3). The protein kinase complex is activated in response to an increase in the ratio of AMP to ATP within the cell. Binding of AMP activates AMPK allosterically and induces phosphorylation of a threonine residue (Thr-172) within the activation domain of the α subunit by an upstream kinase, the tumor suppressor LKB1 (135). Furthermore, binding of AMP inhibits the dephosphorylation of Thr-172 by protein phosphatases, whereas a high concentration of ATP inhibits AMPK activation (136).

AMPK is activated by a wide array of metabolic stresses, including hypoxia, ischemia, oxidative and hyperosmotic stresses, and rise in intracellular calcium ions (137-139). Furthermore, exercise and glucose deprivation also activate AMPK, which suggests a role in exercise adaptations and β cell function. In general, activation of AMPK triggers catabolic pathways that produce ATP, and turns off anabolic pathways that consume ATP, to maintain cellular energy stores (138, 140). Metformin and TZDs, two widely prescribed drugs for the treatment of type 2 diabetes mellitus (T2DM), are also reported to increase AMPK activity (141), underscoring the potential role of the AMPK pathway in the treatment of T2DM.

Pharmacological activation of AMPK can be achieved by treatment of cells with an artificial activator, 5-aminoimidazole-4-carboxamide riboside (AICAR). AICAR is taken up by the cells and phosphorylated to form –aminoimidazole-4-carboxamide-1-D-ridofuranosyl-5'-monophosphate (ZMP), an AMP mimetic, and confers the activating effects of AMP on the AMPK pathway (142). However, ZMP is reported to affect other AMP-regulated enzymes (143, 144), and therefore caution is required in interpretation of data that involves the use of AICAR. Intravenous injection of leptin was found to induce fatty acid oxidation via inhibition of ACC and activate AMPKα2 in skeletal muscle in a biphasic manner (119). As described above, adiponectin also activates AMPK.

An important question is to what extent the α1 and α2 catalytic subunits could have specific targets. AMPK α2 isoform is proposed to play a major role in controlling metabolism in skeletal muscle (145). To get more insight into this issue, mice invalidated for each gene

have been created. Mice lacking the α1 isoform present no defect in glucose homoeostasis, as assessed by the glucose tolerance test (145). By contrast, mice lacking the α2 isoform clearly exhibit glucose intolerance and reduced insulin sensitivity (146). While the double AMPKα1-α2 knockout mice models are embryonic lethal (146).

b. Down stream targets

i. Rapid phosphorylation

In the liver, AMPK is known to phosphorylate various key enzymes involved in lipid and glucose homeostasis but also in protein synthesis and cell proliferation (147).

In lipid homeostasis, AMPK phosphorylates multiple targets in order to acutely, first, switch off anabolic pathways, resulting in the decrease of lipogenesis, cholesterol, triglyceride and malonyl CoA syntheses, and second, switch on alternative catabolic pathways, resulting in the increase of FA β-oxidation (Table 3).

Activated AMPK is also implicated in the regulation of the hepatic glucose homeostasis by phosphorylation of the transducer of regulated CREB activity 2 (TORC2) resulting in its decreased activity, and consequently in a decrease of the hepatic gluconeogenic program (Table 3).

Moreover, several studies have demonstrated that AMPK activation directly limits translational initiation, protein synthesis and cell proliferation (Table 3). This effect is mediated through phosphorylation and consequent inhibition of translation elongation factor 2 (EF2) and/or suppression of mammalian target of rapamycin (mTOR) activity, via direct phosphorylation of mTOR or indirectly through phosphorylation and activation of TSC2 (Table 3).

The transcription co-activator, p300, is phosphorylated by AMPK which inhibits interaction of p300 with PPARγ as well as with RXRand the thyroid hormone receptor, resulting in decreased transcriptional activity of the nuclear receptors (Table 3).

Hepatic Target Proteins	Enzymatic properties	Biological effects
ACC1	↓ Activity	↓ Lipogenesis
ACC2	↓ Activity	↑ Oxidation
HMGCoA reductase	↓ Activity	↓ Cholesterol synthesis
GPAT	↓ Activity	↓ Triglyceride synthesis
Malonyl-CoA decarboxylase	↑ Activity	↓ Malonyl CoA
TORC2	↓ Activity	↓ gluconeogenic program
eEF2 kinase	↑ Activity	↓ Protein synthesis
PFK-2/FBPase-2	Weak kinetic effects	↓ Glucokinase translocation
mTOR	↓ Activity	↓ Protein synthesis
TSC2	↑ Activity	↓ Protein synthesis
Co-activator p300	↓ Activity	↓ Transcriptional activity

Table 3: AMPK hepatic target proteins
(Modified from Viollet B. J Physiol 2006) (147, 148)

ii. Gene regulation

Although the action of AMPK in systemic energy balance is achieved by rapid and direct phosphorylation of metabolic enzymes, longer-term effects on gene expression are also clearly demonstrated. This derives from the very interestingly finding that AMPKα2-containing complexes are found in both the nucleus and the cytoplasm, raising the possibility that AMPK may regulate gene expression, directly or by the phosphorylation of nuclear factors (147). Indeed, various studies establish that AMPK plays an important role in the regulation of glycolytic, gluconeogenic and lipogenic genes through the phosphorylation of the key transcription factors involved in these different programs (Table 4).

Hepatic AMPK-targeted transcription factors	Phosphorylation effect	Target gene(s)
ChREBP	↓ DNA binding	Glycolytic and lipogenic genes
FoxO1	↓ Protein stability	G6Pase
HNF4	↓ Protein stability	L-PK, ApoCIII,…
SREBP-1c	↓ Gene expression	Glycolytic and lipogenic genes
TORC2	↑ Cytoplasmic sequestration	Gluconeogenic genes

Table 4: AMPK hepatic target genes
(Viollet B. J Physiol 2006) (147)

c. Pathways controlled by AMPK

i. Glucose utilization

AMPK contributes to the regulation of glucose uptake by skeletal muscle, cardiac muscle and adipocytes. Physical exercise or experimentally induce contraction of skeletal muscle activates AMPK, in association with an acute, insulin-independent increase in glucose transport into muscle (149). Furthermore, studies of AICAR-treated muscle provide evidence that AMPK increases glucose uptake by promoting GLUT4 translocation to the cell surface and GLUT4 gene transcription (149, 150).

The role of AMPK in glucose transport has been investigated using a transgenic mouse model overexpressing a dominant-negative kinase-dead subunit (AMPKα2DN) in skeletal muscle and heart (149). There was no change in steady-state levels of muscle GLUT4 or glucose uptake (149), suggesting that AMPK does not play a role in basal glucose uptake. On the other hand, hypoxia-stimulated glucose uptake and GLUT4 translocation are completely blocked in AMPKα2DN mice. It is shown that AMPK is able to phosphorylate insulin receptor substrate-1 (IRS-1) on Ser-789 *in vitro* (150, 151). However, AMPK activity is not the operative serine kinase in the studied insulin-resistant animals (152). AMPK may also regulate glucose transport through GLUT1, involving either AMPK α1 or α2 depending on the stimulus (150).

ii. Fatty acid metabolism

Activation of AMPK by AICAR inhibits fatty acid synthesis in rat adipocytes and both fatty acid and cholesterol synthesis in rat hepatocytes by inactivation of ACC and HMG-CoA reductase, respectively (149). AMPK activation also down-regulates anabolic pathways such as fatty acid synthesis at the level of gene expression. These effects may be due to its ability to down-regulate key transcription factors such as SREBP-1c, ChREBP, or HNF-4α (147). In addition to inhibiting anabolic pathways and thus conserving ATP, AMPK also stimulates catabolic pathways that generate ATP, including fatty acid oxidation. Most fatty acids are oxidized in mitochondria, and their entry into the organelle is blocked by malonyl-CoA, because it inhibits CPT-I (147). Malonyl-CoA is produced by one of the target enzymes for AMPK, ACC, which exists as two isoforms, ACC1 and ACC2. ACC1 is cytosolic and appears to be involved mainly with fatty acid synthesis, whereas ACC2 is associated with mitochondria and may have a special role in producing the malonyl-CoA (147). As well as stimulating fatty acid oxidation by this mechanism, in cardiac muscle AMPK activation has

been shown to stimulate fatty acid uptake by translocation of the CD36 (fatty acid translocase) protein to the plasma membrane (153) (Figure 15).

iii. Cell cycle and protein synthesis

Recent findings suggest that AMPK inhibits cell growth and proliferation, and also regulates apoptosis. This is not surprising given that cell growth, DNA replication, and mitosis are all major consumers of ATP, and also that the upstream regulator of AMPK, LKB1, is known to be a tumor suppressor. Several groups have reported that AMPK activation causes G1/S phase cell cycle arrest in different cell lines, and that this is associated with accumulation of the tumor suppressor p53 and of the cyclin-dependent kinase inhibitors p21 and p27, which act downstream of p53 (130, 154, 155). Another potential mechanism to explain these effects is that AMPK has been found to reduce the cytoplasmic/nuclear ratio of the RNA-binding protein HuR, reducing its ability to stabilize mRNAs encoding critical cell regulators such as cyclins A and B1 (156).

AMPK activation may also inhibit cell proliferation owing to its general effects on biosynthesis, including its ability to inhibit fatty acid synthesis [which is elevated in many cancer cells (157)] and the mTOR pathway (158). The mTOR pathway is a critical activator of cell growth and proliferation. It is activated by growth factors such as insulin and IGF1 via the phosphatidylinositol (PI) 3-kinase and PKB/Akt signaling pathway. The mTOR pathway is thought to stimulate translation and hence cell growth, by two mechanisms: (a) activation of ribosomal protein S6 kinase (S6K1); and (b) increased phosphorylation of elongation factor-4E binding protein 1 (4E-BP1), which stimulates the initiation step of translation (159) (Figure 15).

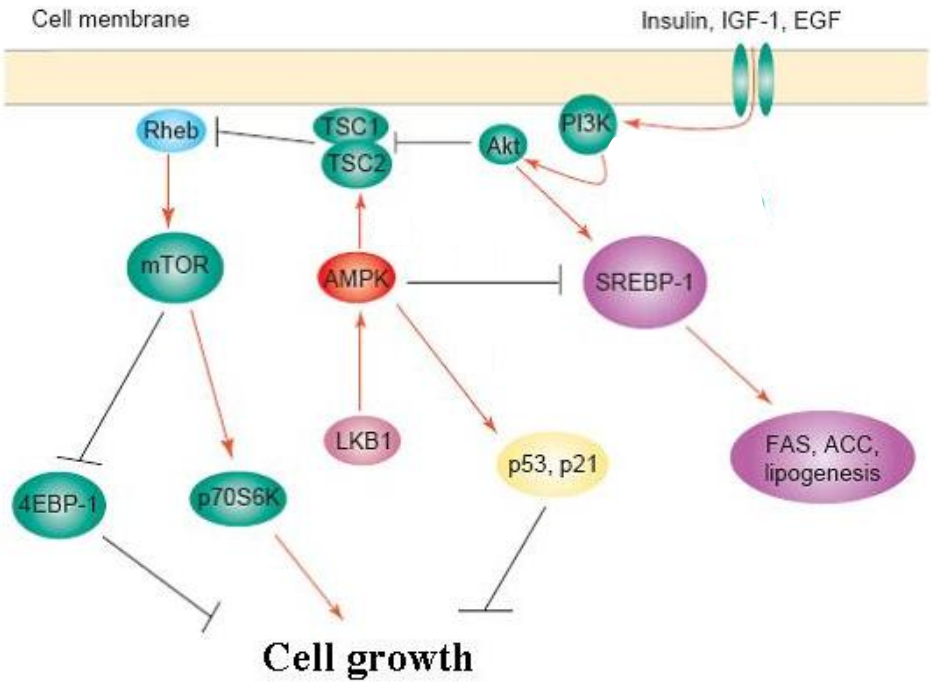

Figure 15: AMPK action in cell growth, protein synthesis and lipid metabolism
AMPK might regulate cell growth, protein synthesis and lipid metabolism by various pathways. These include: positive regulation of p53 and p21; activating TSC2, which inhibits protein synthesis; and reducing the expression of the transcriptional activator SREBP-1, which inhibits de novo fatty acid synthesis. The tumor suppressor TSC2 is a GTPase-activating protein (GAP) that forms a complex with TSC1 and stimulates the intrinsic GTPase activity of Rheb, which leads to the formation of its inactive form, Rheb–GDP. Stimulation by mitogens such as insulin, insulin-like growth factor 1 (IGF-1) and epidermal growth factor (EGF) leads to the phosphorylation and inactivation of TSC2 by Akt. This, in turn, enables the activation of its downstream kinase, mTOR, by Rheb-GTP. Phosphorylation of the translational regulators p70S6K and 4EBP-1 by mTOR stimulates protein synthesis and cell proliferation. (Figure from Luo Z. et al. TRENDS in Pharmacological Sciences 2005) (57)

iv. Inflammation

There is recent evidence that AMPK participates in modulating acute inflammatory reactions. For example, activation of AMPK by AICAR or metformin is associated with diminished nuclear translocation of NFκB in TNFα-stimulated endothelial cells (160, 161), with reduced murine neurophil proinflamatory activity *in vitro* (162). It inhibits the production of IL-6 and IL-8, two pro-inlammatory cytokines, in human adipose tissue as well as in human and rat skeletal muscle cells (163) and suppresses pro-inflammatory response in macrophages promoting their polarization to an anti-inflammatory functional phenotype (164).

Moreover, recent studies demonstrate that the anti-inflammatory property of adiponectin could be mediated trough the activation of AMPK in endothelial cells (165, 166).

v. Response to oxidative stress

Oxidative stress, caused by an imbalance between the production of reactive oxygen species (ROS) and a biological system's ability to readily detoxify the reactive intermediates or easily repair the resulting damage, causes ATP depletion (167) resulting in AMPK activation. Several studies have also demonstrated that ROS can activate AMPK by direct phosphorylation of Thr172 *in vitro*, without changing the cellular AMP/ATP ratio (168, 169). ROS induce *in vitro* the mRNA expression of an AMPK target gene, the PPARγ-coactivator-1 protein (PGC-1) α, by a mechanism AMPK-independent and counteracted by changes in ROS levels within the skeletal muscle cells (170). In addition, the AMPK-independent effect of hydrogen peroxide (H_2O_2), for stimulation of glucose uptake in mouse skeletal muscle, has been confirmed recently (171).

However, how AMPK is regulated under conditions of oxidative stress is poorly understood.

II. Hypothesis – Aims

Fibrosis: Activation of hepatic stellate cells (HSCs) is a central event in fibrosis. Several reports have demonstrated that acting on HSC trans-differentiation and on activated HSC may represent an effective target for anti-fibrotic therapeutic strategy. *In vivo* studies have demonstrated that thiazolidinediones (TZD) drugs, PPARγ agonists currently used for the treatment of type 2 diabetes, have anti-fibrotic properties in rats. However the anti-fibrotic mechanism of PPARγ remained to be elucidated.

The direct ligand activation of PPARγ in HSC, an adiponectin dependent effect and/or a consequence of PPARγ-mediated modulation of inflammation, are 3 non-mutually exclusive mechanisms by which PPARγ agonist may exert their anti-fibrotic effects (Figure 16). **Our first aim is to determine the mechanisms implicated in the anti-fibrotic effect of PPARγ activation using *in vivo* model and *in vitro* primary HSC isolated.** (Study 1)

AMPK is an energy sensor monitoring systemic and cellular energy status. Studies have demonstrated that AMPK activation by adiponectin, an adipocytokine with anti-fibrotic properties, or by synthetic molecules, AICAR, resulted in a decreased PDGF-induced proliferation of rat liver myofibroblasts. **Our second aim is to investigate the role of AMPK on the initiation of HSCs activation, the initial cellular event in fibrogenesis, *in vitro* and its impact on liver fibrosis development *in vivo*.** (Study 2)

NASH: Non-alcoholic steatohepatitis (NASH), the hepatic complication of the metabolic syndrome, is characterized by fatty infiltration of the liver, inflammation, hepatocellular damage and fibrosis. PPARγ agonists augment insulin-mediated adipose tissue uptake and storage of FFAs and also inhibit hepatic fatty acid synthesis through the activation of adenosine monophosphate (AMP)-activated protein kinase (AMPK) by adiponectin. Thus, local effects of PPARγ agonists in adipose tissue can result in reduced insulin resistance (IR) in distant sites, leading to a reduction of circulating FFAs, glucose production, visceral fat accumulation and liver steatosis. PPARγ has also anti-inflammatory actions (Figure 16).

Clinical trials have shown that PPARγ activation by pioglitazone or rosiglitazone improved NASH development. In mice pioglitazone prevents MCD-induced steatohepatitis development. However, nothing is known about the mechanism implicated in this preventive effect of pioglitazone. Some evidences seemed to implicate adiponectin in this effect.

Indeed, adiponectin, a PPARγ-regulated gene, is decreased in patients with NASH, and TZD treatment increases circulating adiponectin. Interaction of adiponectin with its specific receptors resulted in the activation of two downstream targets: AMPK and PPARα. AMPK is implicated in the regulation of lipid and glucose metabolism and PPARα plays a key role in inflammatory reaction.

Therefore we hypothesize that **the preventive effect of pioglitazone on the MCD-induced steatohepatitis development in mice is associated with adiponectin and consequent activation of AMPK and/or PPARα pathways. The testing of this hypothesis is our third aim.** (Study 3)

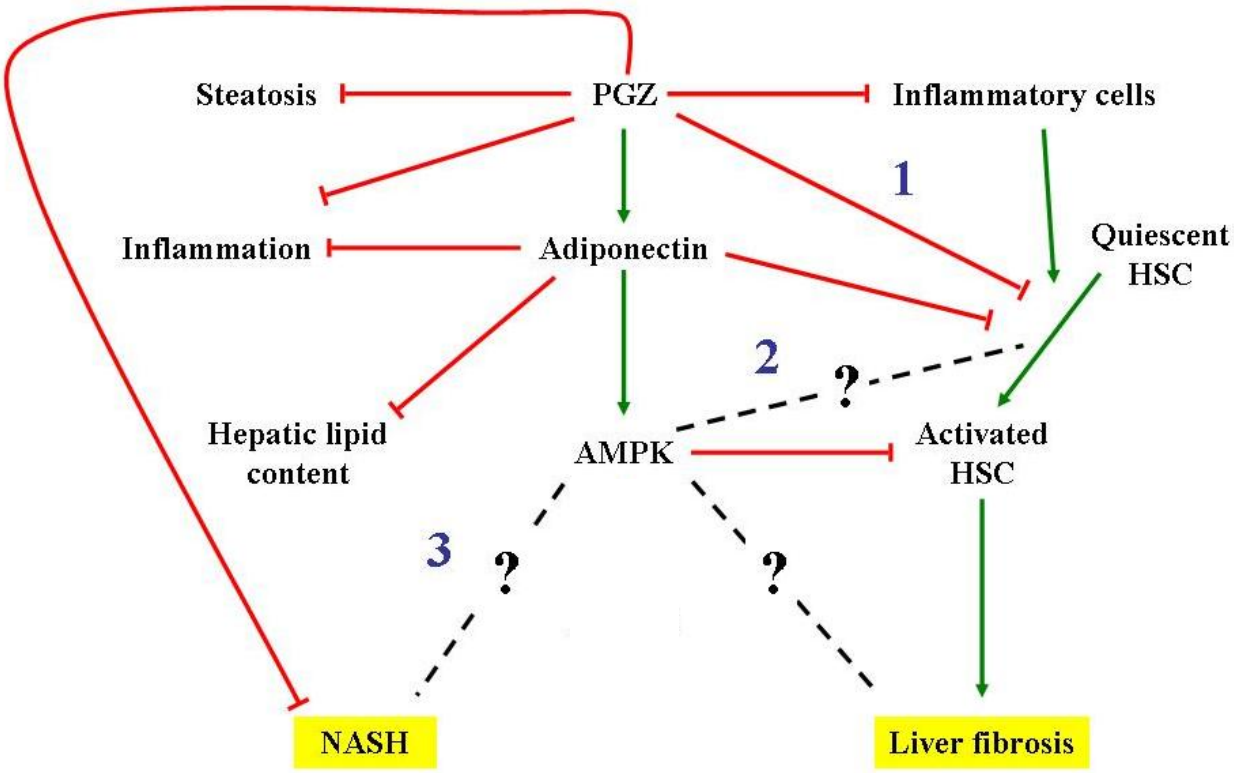

Figure 16: Hypothesis to inhibit liver fibrosis and NASH development

III. Results

Study 1: PPARγ ligand Pioglitazone does not prevent hepatic fibrosis in mice

PPARγ has been proposed as a potential target for fibrosis therapy. The aim of this first study was to understand the mechanism(s) implicated in this effect.

In rats, quiescent HSCs express PPARγ and its expression and activity decreased during HSC trans-differentiation/activation *in vitro* and *in vivo* in rats (99, 100, 172). Previous studies have demonstrated that PPARγ activation and forced expression in rat HSCs prevented their trans-differentiation/activation and reverted their phenotype to that of quiescent cells, respectively (98, 173, 174). In addition, adiponectin is able to inhibit activated HSC proliferation through activation of AMPK (130). *In vivo*, treatment of rats with TZD prevented hepatic fibrosis resulting from chronic toxic injury or bile duct ligation (100, 172).

In order to test the relative contribution of such additional mechanisms for the anti-fibrotic effect of PPARγ agonists, we planned to make use of genetically modified animals.

The first steps in this study were to evaluate the impact of PPARγ agonist pioglitazone on hepatic fibrosis development in mice *in vivo* and to verify whether direct PPARγ stimulation in primary mouse HSCs prevent their trans-differentiation *in vitro*.

In vitro, we demonstrate that PPARγ expression is lost during HSC trans-differentiation/activation in mouse cells as it was in rat cells. PPARγ activation by pioglitazone or 15-deoxy-Δ12,14 prostaglandin J_2 (15d-PGJ_2) induced the expression of CD36, a PPARγ-regulated gene, maintained the PPARγ protein expression but did not alter the trans-differentiation/activation of HSC, as confirmed by collagen-α1 mRNA and α-SMA expression, in cultured murine HSCs as it did in rat HSCs. *In vivo*, although inducing a significant increase of serum adiponectin level, pioglitazone treatment did not prevent the CCl_4-induced liver fibrosis in mice.

In conclusion, our *in vitro* as well as *in vivo* studies demonstrate that, although having anti-fibrotic properties in rats, PPARγ stimulation by PGZ does not prevent activation of HSC *in vitro*, nor hepatic fibrogenesis *in vivo* in mice. Direct anti-fibrotic effect of such substances remains to be demonstrated in humans and if effective, it will be important to determine the mechanisms involved.

This study is presented next and has been published in *International Journal of Molecular Medecine.*

Study 1

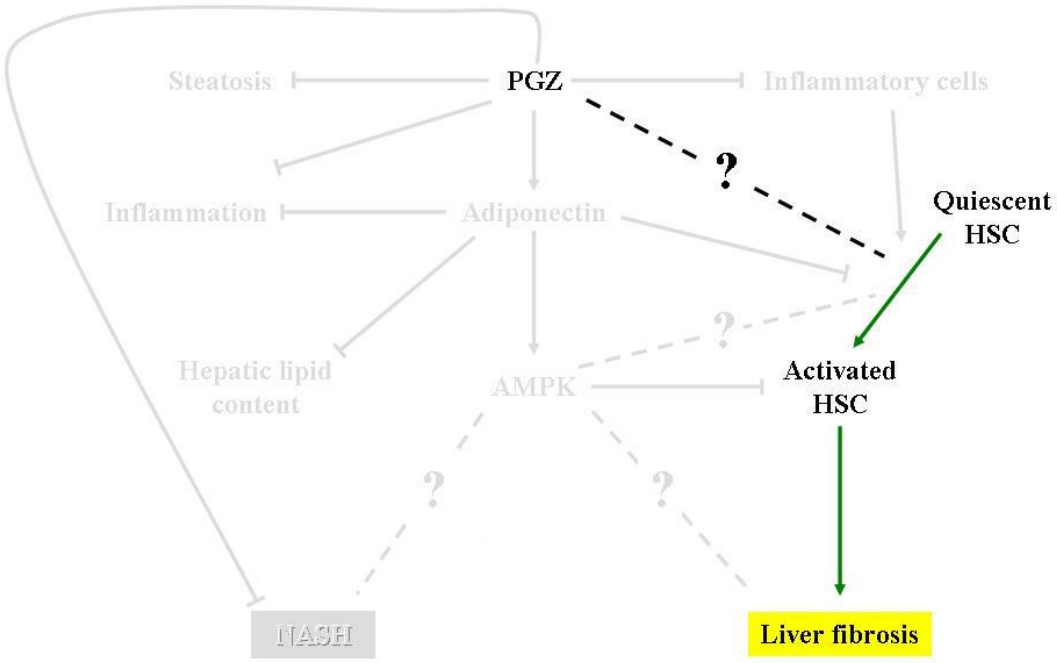

Figure 17: Evaluation of the impact of PGZ on hepatic fibrogenesis in mice

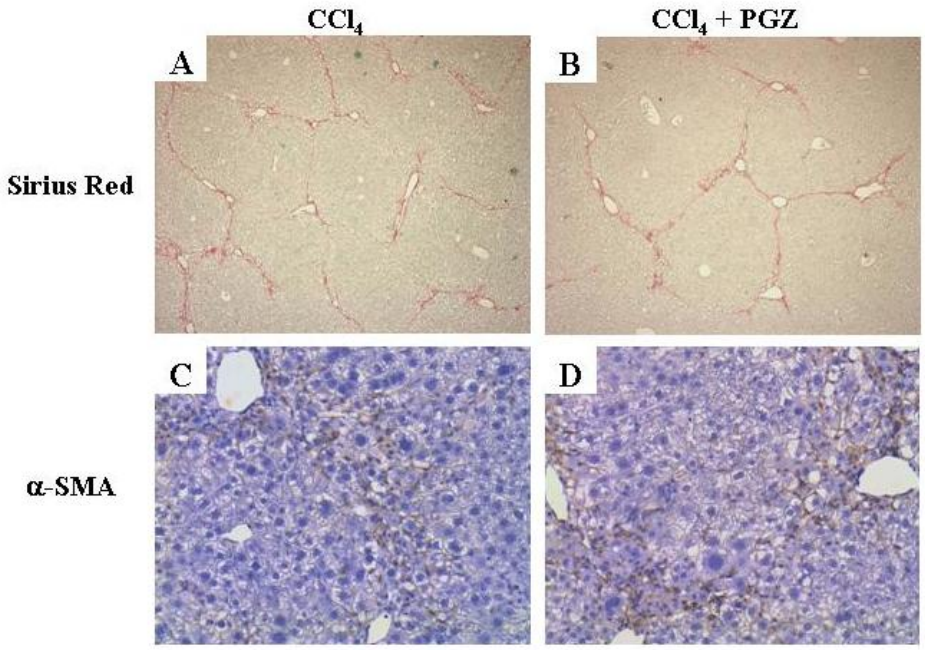

Effect of PGZ on hepatic fibrosis induced by CCl_4 in Balb/C mice

INTERNATIONAL JOURNAL OF MOLECULAR MEDICINE 19: 105-112, 2007

Peroxisome proliferator-activated receptor γ ligand, Pioglitazone, does not prevent hepatic fibrosis in mice

ALAIN DA SILVA MORAIS, JORGE ABARCA-QUINONES, YVES HORSMANS, PETER STÄRKEL and ISABELLE A. LECLERCQ

Laboratoire de Gastroentérologie, Université Catholique de Louvain (UCL), Brussels, Belgium

Received June 20, 2006; Accepted August 29, 2006

Abstract. During hepatic fibrogenesis, quiescent hepatic stellate cells (HSCs) undergo phenotypic transformation into activated matrix-producing cells. This process is recapitulated in primary HSCs cultured on plastic. Based on studies in rats, peroxisome proliferator-activated receptor γ (PPARγ) has been suggested to play a key role in the control of HSC activation. Indeed, in rats, PPARγ expression is depleted in activated HSCs. PPARγ ligands inhibit HSC activation and prevent hepatic fibrosis *in vivo*. Here we evaluated the impact of PPARγ agonists on hepatic fibrogenesis in mice both *in vitro* and *in vivo*. Primary HSCs from Balb/C mice were cultured with PPARγ ligands Pioglitazone (PGZ) or 15-deoxy-Δ12,14 prostaglandin J_2 (15d-PGJ_2). PPARγ mRNA expression was stable during culture-activation of HSCs. However, PPARγ protein was only found in quiescent HSCs but not in fully activated cells. Exposure of HSCs to PPARγ agonists maintained the expression of PPARγ, and trans-activated this transcription factor as demonstrated by gelshift assay and by induction of CD36, a PPARγ-regulated gene. However, PPARγ ligands did not alter the induction of Collagen-I mRNA or α-smooth muscle actin (α-SMA) in cultured HSCs. To test the effect of PPARγ agonist PGZ *in vivo*, hepatic fibrosis was evaluated in Balb/C or C57BL6/J mice treated with CCl_4 (three times a week for 4 weeks; or corn oil for controls), and fed a normal or a PGZ-supplemented diet (0.01% *wt/wt*). PGZ treatment was associated with increased serum adiponectin concentrations but did not decrease the severity of hepatic fibrosis induced by CCl_4. Our data demonstrate that, although having anti-fibrotic properties in rats, PPARγ agonists do not prevent activation of HSCs *in vitro*, nor hepatic fibrogenesis *in vivo* in mice.

Correspondence to: Dr Isabelle Leclercq, Laboratoire de Gastroentérologie, Université Catholique de Louvain, GAEN 53/79, Avenue Mounier 53, B-1200 Brussels, Belgium
E-mail: isabelle.leclercq@gaen.ucl.ac.be

Abbreviations: 15d-PGJ2 , 15-deoxy-Δ12,14 prostaglandin J_2; α-SMA, α-smooth muscle actin; Col-·I, Collagen-·I; DMEM, Dulbecco's modified Eagle's medium; DMSO, dimethyl sulfoxide; ECM, extracellular matrix; FBS, foetal bovine serum; HSC, hepatic stellate cell; PGZ, Pioglitazone; PPARγ, peroxisome proliferator- activated receptor γ

Key words: PPARγ, hepatic stellate cell, Pioglitazone, hepatic fibrogenesis, mouse

Introduction

Liver fibrosis is the consequence of most types of chronic liver disease and results from excess deposition of extracellular matrix (ECM) components generated mainly by hepatic stellate cells (HSCs) (1,2). In the normal liver, HSCs play a key role in the storage and transport of vitamin A (3). In response to liver injury, or spontaneously when cultured on plastic, these cells activate or trans-differentiate into myofibroblastic-like cells, acquiring contractile, proliferative, pro-inflammatory and fibrogenic properties (4,5). Most of the anti-fibrotic treatments currently under evaluation aim at inhibiting the activation of HSCs (6,7). The identification of key cytokines, transcription factors and molecular mechanisms controlling HSC activation is believed to lead to pathophysiological-based strategies to treat liver fibrosis.

Peroxisome proliferator-activated receptor γ (PPARγ), a member of the steroid/retinoid nuclear hormone receptor superfamily of ligand-activated transcription factors (8), has been proposed as a potential molecular target for inhibition of HSC trans-differentiation. PPARγ has been shown to be expressed in quiescent HSCs and its expression and activity decreased during HSC activation *in vitro* and *in vivo* in rats (6,7,9). The treatment of rat HSCs with ligands for PPARγ prevented their activation *in vitro*. In addition, forced expression of PPARγ in culture-activated HSCs by means of adenoviral transfection has been shown to revert their phenotype to that of quiescent cells (10-12).

In vivo, treatment of rats with thiazolidinediones drugs [Pioglitazone (PGZ) or rosiglitazone], which are synthetic ligands for PPARγ, prevent hepatic fibrosis resulting from chronic toxic injury or bile duct ligation (6,7,13). Despite this potent preventive effect, PGZ has limited efficacy in the treatment of pre-established hepatic fibrosis. Indeed, we recently published that PGZ halts the progression of hepatic fibrosis only when the treatment is administered early in the course of toxic or metabolic disease (14).

PPARγ activation plays a role in various physiological and pathophysiological events, including the stimulation of adipocyte differentiation, the response to insulin and the regulation of lipid metabolism as well as the maturation of

monocyte/macrophages and the control of inflammatory reaction (15). Therefore, besides direct action on HSCs, PPARγ stimulation may also interfere with the fibrotic process via modulation of adipocytokine production or as a consequence of its anti-inflammatory properties. The use of genetically modified mice is therefore a good tool to explore the implication of such additional mechanisms for the anti-fibrotic effect of PPARγ agonists. As a prerequisite to such studies, the anti-fibrotic properties of PPARγ agonists need to be evaluated in mice.

Thus we analysed the regulation of PPARγ expression during the culture activation of mouse primary HSCs as well as the impact of PPARγ agonist on matrix production and HSC activation. We also examined the effect of treatment with the PPARγ agonist PGZ on CCl_4 -induced hepatic fibrosis in mice *in vivo*. Surprisingly, and contrasting with observations in rats, PGZ did not prevent hepatic fibrosis in mice. Moreover, although we found PPARγ to be expressed in quiescent HSCs and downregulated during their activation, PPARγ agonists did not prevent collagen I expression nor myofibroblastic trans-differentiation in cultured murine HSCs.

Materials and methods

Animal studies. Female Balb/C and C57BL6/J mice, were obtained from Elevage Janvier (Le Genest Saint Isle, France). All animals were kept in a temperature- and humidity-controlled environment in a 12-h light-dark cycle. They were allowed free access to water and food. The animals were handled according to the guidelines for humane care for laboratory animals established by the Université Catholique de Louvain (UCL), and the study protocol was approved by the local ethics committee. To examine the effect of Pioglitazone (PGZ) on hepatic fibrosis, 8-week-old Balb/C mice were randomly divided into 4 experimental groups (n=5 per group). Mice were injected with CCl_4 (400 µl/kg body weight in corn oil) intra-peritoneally three times a week for 4 weeks and fed a standard powdered diet (Pavan Service Carfil Quality, Oud-Thurnout, Belgium) (CCl_4 group) or a PGZ-supplemented diet (CCl_4 +PGZ group). The PGZ-supplemented diet was prepared by mixing PGZ (Takeda Chemical Industries, Osaka, Japan) with the powdered standard diet to obtain a 0.01% Pioglitazone diet (*wt/wt*). As controls, mice received intra-peritoneal injections of corn oil (3 times/week for 4 weeks) and were fed a normal diet (control group) or the PGZ-supplemented diet (PGZ group). A similar experiment was repeated on the female C57BL6/J mice.

At the time of sacrifice (48 h after the last injection of CCl_4), blood was collected by cardiac puncture and the liver and abdominal subcutaneous fat rapidly excised. Part of the liver was fixed in 4% formalin, embedded in paraffin and used for histological analyses. The remaining liver and the subcutaneous adipose tissue were snap frozen in liquid nitrogen and kept at -80˚C until use.

Isolation and characterization of hepatic stellate cells. Primary HSCs were isolated from female Balb/C mice by *in situ* pronase-collagenase digestion of the liver followed by others (16). Five mouse livers were perfused for each isolation. After isolation, the cells were re-suspended in Dulbecco's modified Eagle's medium (DMEM; Invitrogen, Merelbeke, Belgium) supplemented with 20% foetal bovine serum (FBS, Invitrogen), 100 units/ml penicillin and 100 µg/ml streptomycin (Invitrogen). Primary HSCs were cultured in cell culture dishes at 37˚C in a humidified atmosphere with 5% CO_2 and 95% air. At day 1, the medium was removed and replaced by DMEM supplemented with 5% FBS.

The purity of the cultures was evaluated by examining the characteristic stellate shape of the cells with phase-contrast microscopy and by the presence of lipid droplets by auto-fluorescence using an excitation light of 320 nm. After the first replacement of medium (day 1), purity was >90%. At day 9 the cells were passaged by treatment with 5 ml of Trypsin-EDTA 0.5X (Invitrogen) per dish for 7 min at 37˚C. After addition of 5 ml of DMEM with 20% FBS, the cells were collected and washed twice in PBS, and seeded in DMEM supplemented with 5% FBS.

HSC treatment. To analyse the effect of PPARγ agonists on HSC biology, HSCs were incubated with DMEM supplemented with 5% FBS containing PGZ 10 µM (Takeda Chemical Industries), or vehicle (DMSO). In separate experiments, cells were incubated with the most potent PPARγ activator 15-deoxy-Δ12,14 prostaglandin J_2 (15d-PGJ_2) 10 µM (Sigma Aldrich, ref. no. D8440, Bornem, Belgium) or vehicle (ethanol 0.5%). Treatment was initiated at day 1 or day 3 after plating as indicated in the Results section. Medium was renewed every 2 days and the cells were passaged at day 9.

Total RNA extraction. Total RNA was extracted from cultured HSCs or from liver or adipose tissue using the TriPure isolation reagent kit (Roche Diagnostics Belgium, Vilvoorde). cDNA was prepared by reverse transcription of 1 µg total hepatic RNA using random primers and M-MLV (Moloney murine leukemia virus) reverse transcriptase (Gibco BRL, Merelbeke, Belgium). To assess the expression of PPARγ mRNA in HSCs during culture conditions, gene amplification was conducted using TaqDNA polymerase (Amersham Biosciences, Diegem, Belgium) and primers (sense, 5'-aagagatcacagagtatgcc-3' and anti-sense, 5'-cttcacagcaaactcaaac-3'). This expression was compared to that of Ribosomal protein L19 (RPL19) RNA (primers: sense, 5'-agtatgctcaggcttcagaa-3'; and anti-sense, 5'-gcaggtctaagaccaaggaa-3') serving as control (17). The cycle conditions were 94˚C for 5 min, 94˚C for 1 min, 56˚C for 1 min and 72˚C for 1 min (30 cycles) and then 72˚C for 10 min.

To quantify gene expression, real-time PCR analysis was carried out with the GeneAmp 5700 sequence detection system and software (Applied Biosystems, Den Ijssel, Netherlands) using SYBR-Green for detection. RPL19 RNA was chosen as an invariant standard. Adiponectin, CD36, Collagen-I (Col-I), PPARγ total and RPL19 primers were designed using the Primer Express design software (Applied Biosystems). The following primers were used: adiponectin: sense, 5'-gcagagatggcactcctgga-3' and anti-sense, 5'-cccttcag ctcctgtcattcc-3'; CD36: sense, 5'-tccagccaatgcctttgc-3' and anti-sense, 5'-ttctgcactgaaaaagtaatctcca-3'; Col-I: sense, 5'-ttcacctacagcacgcttgt-3' and anti-sense, 5'-tcatcgaatacaaaaccacc

aaga-3'; PPARγ total: sense, 5'-ctgctcaagtatggtgtccatga-3' and anti-sense, 5'-tgaataaagatggagtcctcatctca-3'; and RPL19: sense, 5'-gaaggtcaaagggaatgtgttca-3' and anti-sense, 5'-acaagctgaaggcagacaagg-3'. cDNA derived from adipose tissue or the liver was used to prepare standard dilution curves. PCR reactions were performed according to the standardized thermal profile of the system previously set by the manufacturer. All tissue and standard curve samples were run in duplicate at the same time in a single 96-well reaction plate (MicroAmp Optical, Applied Biosystems) using the appropriate primers. Results are expressed as relative gene expression (RGE) using the ΔCt method (User bulletin 2, Applied Biosystems).

Histology, immunohistochemistry and immunocyto-chemistry. Mouse livers were fixed in 4% neutral buffered formalin overnight, processed to paraffin blocks, sectioned, and stained with hematoxylin and eosin or sirius red (to visualize collagen deposition) by using standard techniques. Immunodetection for α-smooth muscle actin (α-SMA) was performed as previously described (18), using mouse monoclonal anti-α-SMA (Clone 1A4; 1:100) and the EnVision Dako mouse as secondary antibody. All reagents were from DakoCytomation (Via Real, USA), unless indicated otherwise.

For immunocytochemistry experiments, the cells were seeded on plastic Thermanox™ coverslips (25 mm in diameter, Nunc, Rochester, NY, USA). At determined times (ranging from 1 to 12 days) the coverslips were washed once in PBS and the cells were fixed by immersion in formaldehyde 4% at 4˚C for 5 min. Endogenous peroxidases were inhibited by incubating the coverslips in methanol with 0.1% H_2O_2. After immersion in PBS containing 10% normal goat serum for 20 min, the coverslips were incubated with either mouse monoclonal anti-α-SMA antibody (1:300) (Clone 1A4), mouse monoclonal anti-Desmin antibody (1:500) (Clone D33), rabbit polyclonal anti-GFAP antibody (1:1000) (Clone 6F2) or anti-PPARγ antibody (1:50) (H-100; Santa-Cruz, Heidelberg, Germany) overnight at 4˚C. After washing in PBS, the coverslips were incubated with the appropriate peroxidase-conjugated secondary antibody at room temperature for 1 h. Peroxidase activity was revealed with 3-amino-9-ethyl-carbazole (DakoCytomation). Slides were then counter-stained in haematoxylin and eosin and examined under the microscope. The percentage of positive cells was determined by counting the stained cells versus the total number of cells.

Preparation of cell lysates and nuclear extracts. Lysates for Western blot analyses were obtained by incubating the cells in 500 µl of buffer containing 150 mM NaCl; 1.5 mM $MgCl_2$; 10% Glycerol; 0.1% Triton X-100; 1 mM EGTA; 50 mM HEPES and 2 µg/ml of aprotinin and of leupeptin; for 5 min at 37˚C. The resulting lysates were collected and clarified by centrifugation (10 min at 12,000 x g). Nuclear extracts were prepared using the nuclear extract kit (Active Motif, Rixensart, Belgium), and stored at -80˚C. The protein contents were determined using a BCA protein assay with serum albumin as a standard (Pierce Chemical, Rockford, IL, USA).

Western blotting. Proteins from HSC lysates were separated by SDS-PAGE and transferred onto PVDF transfer membranes (PolyScreen). Fifty-five micrograms of proteins were loaded for the detection of PPARγ and α-SMA. Homogenates from adipose tissue were used as positive controls for PPARγ Western blots. The membranes were then stripped (Pierce's restore Western blot stripping, Milwaukee, WI, USA) and reprobed with ß-actin antibody to assess equal protein load. The following antibodies and conditions were used: a rabbit polyclonal anti-PPARγ antibody (H-100; Santa-Cruz, Heidelberg, Germany; 1:1000; overnight), a mouse monoclonal anti-α-SMA antibody (Clone 1A4, DakoCytomation, 1:5000; 1 h); a mouse monoclonal anti-ß-actin antibody (Clone AC-15, Sigma, Heidelberg, Germany; 1:80.000; 1 h); secondary peroxidase-conjugated AffiniPure goat anti-mouse or goat anti-rabbit antibodies (Jackson ImmunoResearch, Cambridgeshire, UK) for ß-actin and α-SMA or PPARγ, respectively. The antigen-antibody reaction was visualized using the Western lightning chemiluminescence reagent plus (PerkinElmer) detection system followed by exposure of the membranes to a Kodak X-Omat Blue XB film. The quantification of immune-reactive proteins was obtained by densitometry using the Gel Doc 2000 device and software (Bio-Rad, Nazareth, Belgium).

Electrophoretic mobility shift assays (EMSA). Ten micrograms of nuclear proteins were incubated for 20 min on ice in binding buffer (Tris-HCl 10 mM pH 7.5, NaCl 50 mM, EDTA 1 mM, DTT 1 mM, glycerol 5%) containing 1 µg poly(dI-dC) (2 µg/µl) and 0.5 ng of γ-32P end-labelled double-stranded oligonucleotides (20.000 cpm). Nuclear extracts (5 µg) from COS-7 transfected with PPARγ (Active Motif, Rixensart, Belgium) were used as positive control. DNA protein complexes were separated by electrophoresis (200 V, 2 h) on a 5% polyacrylamide gel (29:1 cross-linking) in a 1X TBE buffer (88 mmol/l TRIS, 88 mmol/l boric acid, 2 mmol/l EDTA). Gels were dried and exposed to a Kodak BioMax MS Film (Amersham International plc, Little Chalfont, UK) for 24 h. Pre-annealed chromatography-purified double-stranded oligonucleotides containing the peroxisome-proliferator-responsive element (PPRE) (5'-TGCACATTTCACCCAGAGAGAAGGGATTGA-3') were used as a probe (7). To confirm the identity of the protein/DNA binding, a supershift analysis was performed as follows: NE were pre-incubated with 2 µl of specific antibody (2 µg/µl) (PPARγ H-100; Santa-Cruz) for 20 min on ice. Then the binding buffer, dI-dC and probe were added and the mixture was incubated for a further 20 min on ice.

Biochemical assays. The level of adiponectin in serum was determined using a mouse adiponectin RIA kit (Linco Research, MO, USA). The hydroxyproline content was determined on liver samples hydrolyzed in 5 ml 6 M HCl at 110˚C for 18-24 h as previously reported (19) using hydroxy-proline 40 µg/ml (Sigma Aldrich) as a standard.

Statistical analysis. Results are expressed as mean ± standard deviation (SD). Statistical differences between groups were tested using one way analysis of variance (ANOVA). Statistical significance was assumed for p values <0.05.

INTERNATIONAL JOURNAL OF MOLECULAR MEDICINE 19: 105-112, 2007

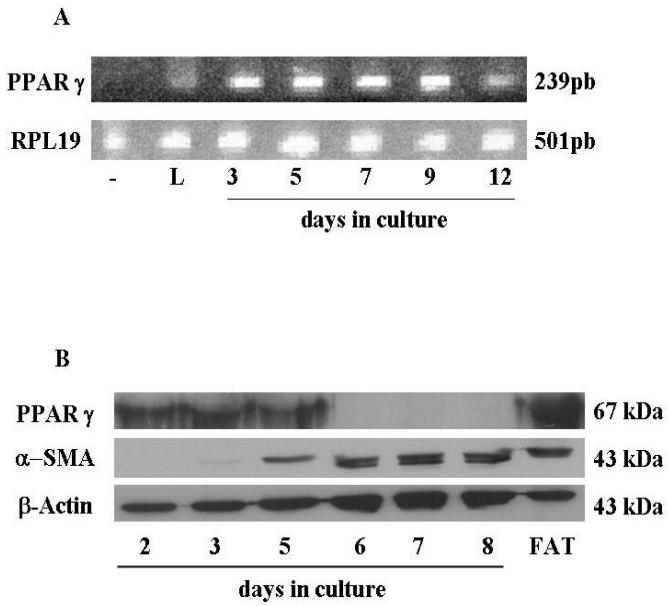

Figure 1. PPARγ mRNA and protein expression in cultured mouse primary HSC. (A) Expression of PPARγ and RPL19 (housekeeping gene) mRNA evaluated by PCR as described in the Materials and methods section. cDNA derived from RNA extracted from whole liver (L). Reaction mixture in which cDNA was omitted served as negative control (-). (B) Representative Western blot showing the evolution of PPARγ protein expression in HSC during culture. The initial blot has been stripped and reprobed with α-smooth muscle actin (α-SMA) and ß-actin antibodies to assess for HSC activation and equivalence of protein loading, respectively. Protein extracted from adipose tissue (FAT) served as positive control for PPARγ protein expression. Primary mouse (Balb/c) HSC were cultured in DMEM supplemented with 5% FBS, and cell lysates were prepared at the indicated time points.

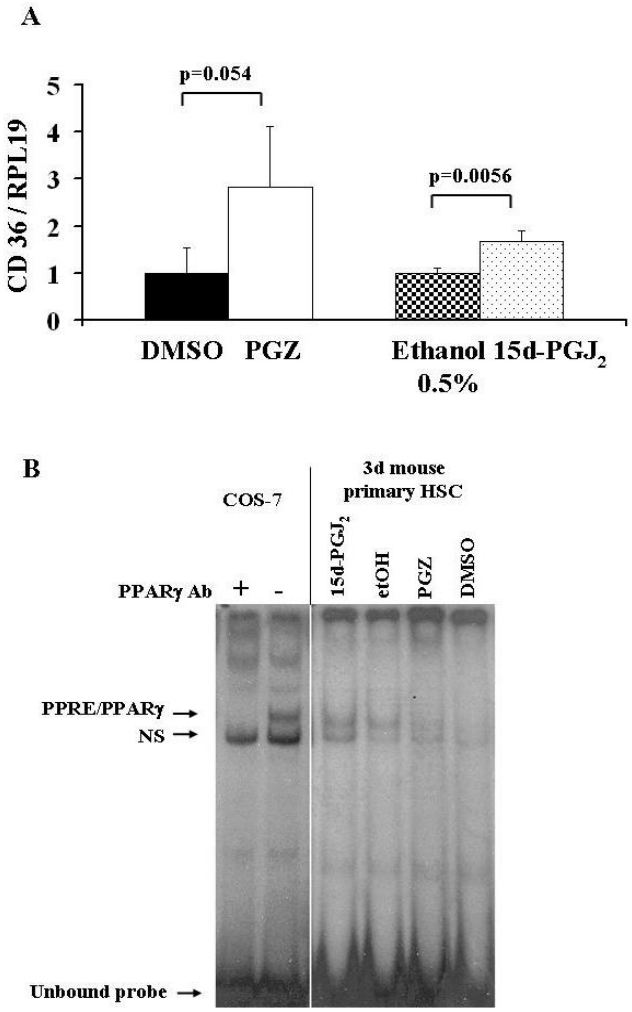

Figure 2. Pioglitazone induces the expression of the PPARγ-regulated CD36 gene and PPRE binding in cultured HSC. (A) Bar graphs represent the level of CD36 mRNA expression as determined by real-time PCR in primary HSC from Balb/C mouse livers cultured from day 1 to day 7 in DMEM supplemented with Pioglitazone (PGZ) 10 μM or DMSO (vehicle), or in the presence of 15d-PGJ_2 10 μM or ethanol 0.5% (vehicle). Results have been normalised to the expression of RPL19 mRNA as an invariant control. Data are expressed as mean ± SD on n=10 culture dishes from 2 different cell preparations. p values are given for PPARγ agonist-treated cells versus their respective controls. (B) Electromobility shift assay and supershift on nuclear fractions of 3-day-old HSC exposed for 2 h to PGZ (10 μM) or DMSO as vehicle, or to 15d-PGJ_2 or ethanol as vehicle. Nuclear extracts from PPARγ-transfected COS-7 cells were used as positive control. (NS, non specific bands).

Results

PPARγ expression in cultured HSCs. We evaluated the expression of PPARγ in quiescent HSCs (day 3) and its regulation during activation of HSCs under culture conditions. Quiescent HSCs and HSCs cultured for up to 9 days expressed PPARγ mRNA at similar levels (Fig. 1A). After 12 days in culture (i.e. after one passage at day 9), we observed a decreased expression of PPARγ mRNA (Fig. 1A). The decreased expression of PPARγ mRNA after long-term culture and passage has been confirmed by quantification of PPARγ transcripts by real-time PCR (not shown). We then evaluated the expression of PPARγ protein by Western blotting. The presence of PPARγ protein was readily demonstrated in HSCs cultured for up to 5 days, but the protein was no longer detected in HSCs cultured for longer periods (6, 7 or 8 days) (Fig. 1B). As demonstrated by α-SMA expression, the loss of PPARγ protein detection occurred when HSCs underwent activation into myofibroblasts. Thus, after 5 days in culture, there was a marked decrease in PPARγ protein expression, while transcript expression was maintained for up to 9 days, suggesting that the inhibition of protein occurs first at the post-transcriptional then at the transcriptional level during the culture activation of HSCs.

Functionality of PPARγ in cultured HSCs. To assess whether the PPARγ transcription factor is functionally active in HSCs, we analysed the mRNA expression of a PPARγ-regulated gene, CD36, in cultured HSCs by real-time PCR. Primary HSCs have been cultured from day 1 to 7 in DMEM supplemented with PGZ 10 μM, or DMSO (vehicle) or in the presence of the potent PPARγ ligand 15d-PGJ_2 10 μM, or ethanol 0.5% used as vehicle. The CD36 mRNA expression was increased in cells treated with PPARγ agonists (Fig. 2A), suggesting the functionality of PPARγ in cultured HSCs. To confirm these results we performed EMSA using a typical peroxisome proliferator responsive element (PPRE) as target oligonucleotide. After 3 days in culture, HSCs were exposed for 2 h to PGZ (10 μM), 15d-PGJ_2 (10 μM) or vehicle (DMSO or ethanol, respectively). Nuclear proteins were then extracted and subjected to a gel shift assay. Nuclear extracts from PPARγ-transfected COS-7 cells served as positive controls. As shown in Fig. 2B, a retarded band was observed in PGZ-

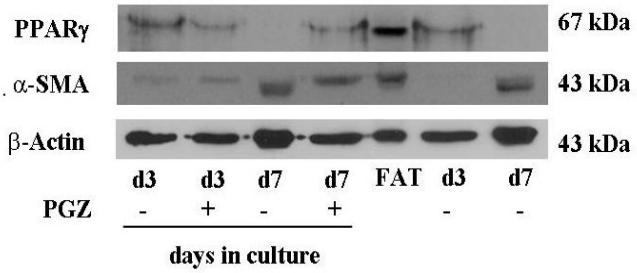

Figure 3. Effect of PGZ treatment on PPARγ and α-SMA protein expression in murine HSC. Representative Western blot for PPARγ in HSC cultured from day 1 to day 7 in DMEM containing 5% FBS supplemented with PGZ 10 μM (+) or DMSO as vehicle (-). Cell lysates were prepared at day 3 or at day 7. The initial blot has been stripped and reprobed with α-smooth muscle actin (α-SMA) and ß-actin antibodies. Proteins extracted from adipose tissue (FAT) served as positive control.

compared to DMSO-treated HSCs. Similarly, the retarded band was of stronger intensity in 15d-PGJ_2-treated cells than in the ethanol controls. To note, a PPRE binding complex was seen in. ethanol- but not in DMSO-treated cells. Supershift assay confirmed the presence of PPARγ in the protein/DNA retarded complex.

Effect of PPARγ ligands on PPARγ protein expression in cultured HSCs. To evaluate the impact of PPARγ ligand on PPARγ protein expression in our culture system, murine primary HSCs were cultured with PGZ (10 μM), or vehicle 24 h after seeding. Lysates were prepared at day 3 and day 7, and used for Western blot analysis. At day 3, PPARγ protein was expressed at similar intensity in HSCs whether cultured in the presence or in the absence of PGZ (Fig. 3). At day 7, PPARγ protein was not detected in control cells. However, culture of HSCs in the presence of PGZ was associated with the persistence of PPARγ protein expression (Fig. 3). This treatment did not affect the trans-differentiation of the cells as confirmed by the α-SMA protein expression in the different groups of treated HSCs (Fig. 3).

Effects of PPARγ agonists on HSC activation. To assess the effects of PPARγ activation on fibrogenesis *in vitro*, we evaluated Collagen-I mRNA expression by real-time PCR in HSCs cultured for 4 days in the presence of PGZ (10 μM) or 15d-PGJ_2 (10 μM). As shown in Fig. 4A and B, treatment with PGZ or 15d-PGJ_2 from day 3-7 did not affect the expression of Collagen-I mRNA, relative to vehicle-treated cells. Similarly, no change in Collagen-I mRNA was seen in HSCs exposed to PPARγ ligands as early as 24 h after seeding (from day 1-5). As expected, the proportion of HSCs expressing α-SMA increased progressively with time in culture so that 22 and 76% of HSCs were α-SMA positive at day 3 and 7, respectively. To evaluate the impact of PGZ treatment on HSC activation, we incubated the cells with PGZ (10 μM) or DMSO 24 h after plating and evaluated the number of α-SMA expressing cells at day 3 and day 7. As shown in Fig. 4C, the percentage of HSCs expressing the α-SMA protein was similar in the PGZ and the DMSO-treated HSCs, demonstrating that PGZ does not prevent the spontaneous activation of murine HSCs in culture.

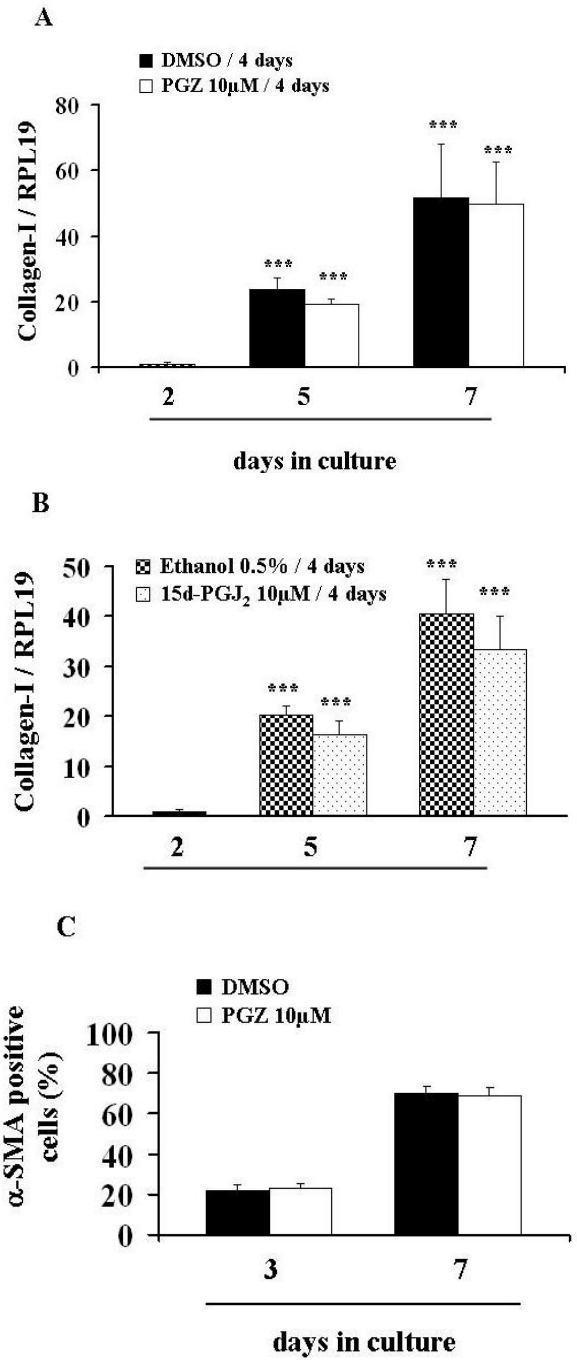

Figure 4. PPARγ ligands PGZ and 15d-PGJ_2 do not alter Collagen-I mRNA expression or α-SMA expression during culture activation of murine HSC. Graph bars represent collagen mRNA expression quantitated by real-time PCR in primary HSC cultured in the presence of (A) PGZ 10 μM (open bars) or DMSO (vehicle, black bars); or (B) 15d-PGJ_2 (hatched bars) or ethanol 0.5% (vehicle, grey bars). Cells were exposed to PPARγ ligand or vehicles for 4 days (i.e. from day 1-5, or from day 3-7). Individual values represent the ratio of Collagen-I mRNA to RPL19 mRNA. The value obtained for cDNA derived from 2-day-old untreated HSC has been arbitrarily set at one. Data are mean ± SD (arbitrary units) for n=10 dishes per group, from 3 different cell preparations. (C) α-SMA immunopositive cells (% of total cell number) in HSC cultured in the presence of PGZ 10 μM (open bars) or DMSO (vehicle, black bars) for 3 or 7 days. $^{***}p<0.001$ compared to 2-day-old, untreated HSC. There is no significant difference between PGZ- and DMSO-treated cells, nor between 15d-PGJ_2- and ethanol-treated HSC.

Effect of PPARγ agonist PGZ on hepatic fibrogenesis in vivo. To determine whether PGZ has anti-fibrotic properties *in vivo* in mice, we induced hepatic fibrosis in female Balb/C or

INTERNATIONAL JOURNAL OF MOLECULAR MEDICINE 19: 105-112, 2007

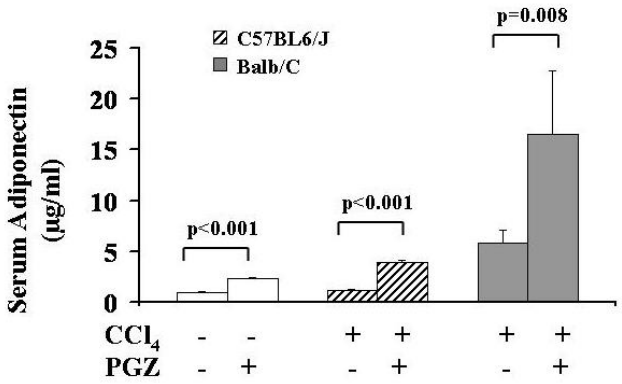

Figure 5. PGZ administered as a food-supplemented diet induces adiponectin in C57BL6/J and Balb/C mice. Serum adiponectin levels in mice treated with CCl_4 (400 µl/kg body weight, 3 times a week) for 4 weeks (C57BL6/J mice, hatched bars; Balb/C mice, grey bars) or vehicle (C57BL6/J mice, open bars) and fed the PGZ-supplemented diet (+) or the control diet (-). Data are expressed as mean ± SD in µg/ml for n=5 per group.

C57BL6/J mice by repeated intra-peritoneal injections of CCl_4 for 4 weeks. During this period, mice were fed a PGZ-supplemented diet (0.01% *wt/wt*) (n=5) or a standard mouse chow (n=5). Mice fed a PGZ-supplemented diet or a standard chow and injected with corn oil served as non-fibrotic controls.

In CCl_4-Balb/C mice, treatment with PGZ induced a 3-fold induction of adiponectin mRNA expression in adipose tissue (4.39±2.21 versus 1.19±0.7 arbitrary units in controls; p=0.03). This was paralleled by a 3-fold increase in serum adiponectin in PGZ-treated versus untreated CCl_4-Balb/C mice (Fig. 5). Administration of CCl_4 to Balb/C mice induced liver fibrosis with formation of collagen bridges between central veins (Fig. 6A). PGZ treatment did not significantly alter the severity of fibrosis induced by CCl_4 as demonstrated by Sirius red staining (Fig. 6B). Moreover, the amount and distribution of activated HSCs expressing α-SMA were not different whether CCl_4-Balb/C mice were treated or not with PGZ (Fig. 6C and D). In keeping with the histological findings, hepatic hydroxyproline content (Fig. 6E) and induction of hepatic Collagen-I mRNA (Fig. 6F) were at least as high in PGZ-treated than in untreated CCl_4-Balb/C mice.

To ensure that this absence of anti-fibrotic effect was not strain-dependent, we repeated the experiment on C57BL6/J mice. As in the Balb/C mice, PGZ treatment of the C57BL6/J mice induced the expression of adiponectin transcripts in adipose tissue (not shown) and circulating levels of adiponectin (Fig. 5). As reported by others (20), a similar CCl_4 regimen resulted in liver fibrosis of a lesser severity in C57LB6/J than in Balb/C mice demonstrated by peri-centrolobular fibrosis with incomplete bridges (not shown), lower hepatic hydroxyproline content (Fig. 6E) and lower levels of hepatic Collagen-I mRNA (Fig. 6F). Thus, as observed in Balb/C mice, PGZ treatment did not reduce the severity of CCl_4-induced fibrosis in C57BL6/J mice.

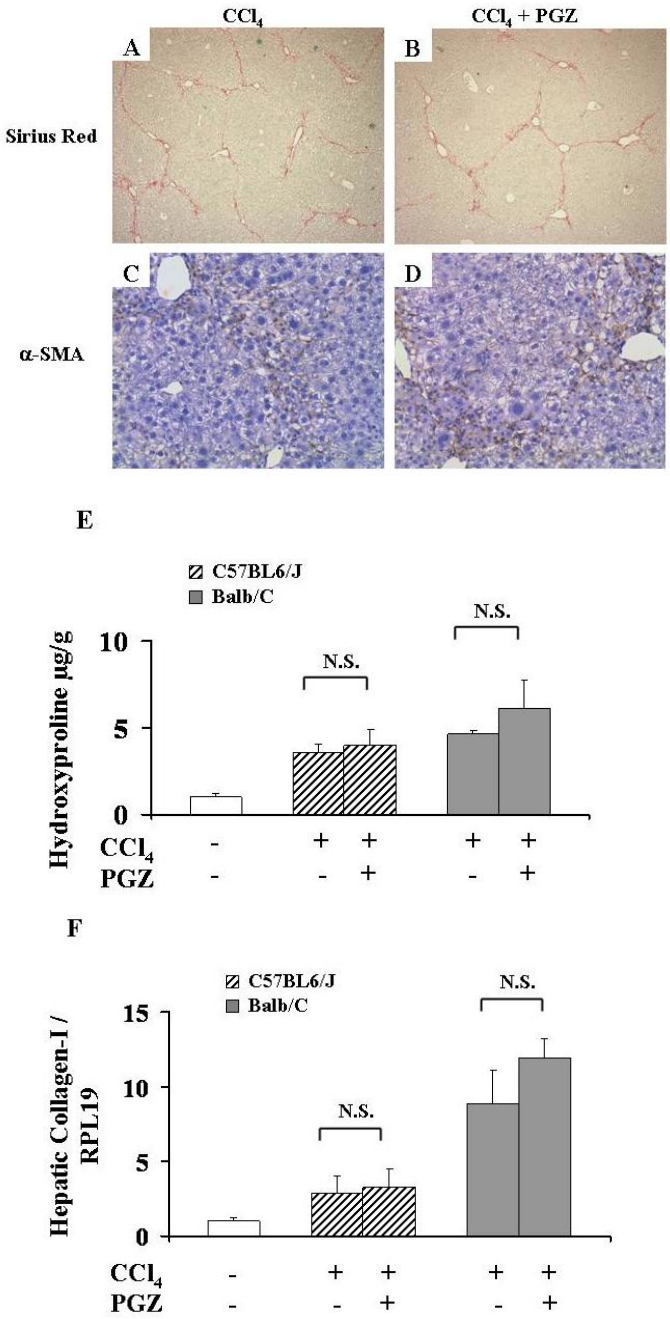

Figure 6. Effect of PGZ on hepatic fibrosis induced by CCl_4 in C57BL6/J and Balb/C mice. Representative photomicrographs of Sirius red-stained liver sections (A and B, collagen in red) or α-SMA immunostained sections (C and D, α-SMA positive cells in brown) from C57BL6/J mice who received IP injections of CCl_4 (400 µl/kg body weight, 3 times/week for 4 weeks) and fed the control diet (A and C) or a PGZ-supplemented diet (0.01% *wt/wt*; B and D). Hepatic Collagen-I mRNA expression determined by real-time PCR (E) and quantification of hepatic hydroxyproline content (F) in C57BL6/J (hatched bars) and Balb/C (grey bars) mice treated with CCl_4 (400 µl/kg body weight, 3 times/week for 4 weeks) and fed a PGZ-supplemented diet (+) or the control diet (-). Open bars represent values obtained for the livers of untreated mice. Collagen I mRNA values were normalized to those of RPL19 regarded as an invariant control. Data are expressed as mean ± SD (n=5 per group). N.S., the absence of statistical significance.

Discussion

The thiazolidinediones (TZDs), a new class of insulin sensitising anti-hyperglycemic agents, have been identified as high-affinity ligands for PPARγ, a nuclear hormone receptor that plays a central role as a regulator of terminal adipocyte differentiation (21). It has been shown that, in rats, TZDs significantly reduce the severity of hepatic fibrosis (7).

This raises the possibility that TZDs may be used for the prevention and treatment of hepatic fibrosis, and as drugs of particular interest for fibrosis associated with the metabolic syndrome or non-alcoholic steatohepatitis.

Based on their studies of rat HSCs, Tsukamoto and group have proposed the concept that PPARγ is a key regulator of HSC biology, maintaining HSCs in their quiescent phenotype (10). In accordance with observations in rat cells (9), we found PPARγ protein to be expressed in quiescent primary HSCs of mouse origin. Exposure of these cells to PPARγ agonist PGZ activated the transcription factor as demonstrated by the induction of the PPARγ/PPRE binding complex by EMSA as well as by induced expression of CD36, a PPARγ-regulated gene. As in rat cells, cultured-activation of mouse HSCs was associated with a decreased expression of PPARγ, and their treatment with PPARγ ligand prevented the reduction in PPARγ protein expression during culture-induced activation. Despite the presence of functional and ligand-responsive PPARγ, the activation of this transcription factor failed to prevent, or even attenuate, the activation of mouse HSCs *in vitro*, as it did in rat cells (7,9). Indeed, induction of Collagen-I mRNA and of α-SMA during culture was not modified by exposure of the cells to PPARγ ligands PGZ or 15d-PGJ_2.

In rats, two specific mechanisms have been proposed to explain the anti-fibrotic effect of PPARγ agonists. The first one is based on the observations that PPARγ expression is lost in activated HSCs and that forced expression of PPARγ by mean of viral transfection is sufficient to revert HSCs to their quiescent phenotype. By analogy to the adipogenic role of PPARγ on adipocytes, this transcription factor might thus be necessary for HSCs to retain their 'adipogenic' phenotype, which is characterized by their ability to concentrate vitamin A in lipid droplets and by their quiescence in terms of the proliferation and production of extracellular matrix. The second mechanism involves the direct participation of PPARγ in the transcriptional regulation of genes specific to fibrogenesis. In a recent study, Yavrom *et al* showed that, although no PPRE sequence was found in the promoter of the rat Collagen-I gene, PPARγ suppresses the proximal Collagen-I promoter via inhibition of p300-facilitated NF-I binding to DNA in rat HSCs (22). Our observations firmly demonstrated that ligand stimulation of PPARγ in mice HSCs, although having transcriptional activity, did not act as a molecular switch to prevent spontaneous activation of the cells during culture on plastic. Moreover, this transcription factor did not appear to participate in the transcriptional control of the Collagen-I gene involved in fibrogenesis. Promoter analysis will be needed to confirm this.

We show here, in two different strains of mice, that PPARγ agonist PGZ did not exert anti-fibrotic properties in mice *in vivo*. Indeed, PGZ had no impact on hepatic fibrosis, induction of hepatic Collagen-I gene expression or activation of hepatic stellate cells induced by chronic administration of CCl_4. This is in sharp contrast with several reports on the anti-fibrotic properties of PPARγ agonist drugs in various models of fibrosis in rats (6,7,13). In the literature, this anti-fibrotic effect has been related to inhibition of HSC activation (7, 9, 13). Therefore, if direct regulation of HSC biology is the principal mechanism implicated in the anti-fibrotic effect of PPARγ agonists in rats, the absence of preventive effect of PGZ on hepatic fibrosis *in vivo* in mice is not surprising in light of our *in vitro* results.

A common observation in all studies published to date is that TZD treatment induces the expression of an adipocyte-specific secretory protein, adiponectin (23). Adiponectin has anti-fibrotic properties. Mice lacking adiponectin are exquisitely sensitive to hepatic fibrosis while supra-physiological levels of adiponectin induced by adenovirus infection prevent CCl_4-induced fibrosis in wild-type mice (24). In our study, as in similar studies in mice (23, 25), PGZ administered as a food mixture increased the expression of adiponectin mRNA in adipose tissue as well as serum levels of adiponectin by a factor 2 to 3. Despite this, PGZ did not protect against fibrosis. This suggests that the rise in adiponectin levels, as obtained by PGZ treatment, is insufficient to provide protection against hepatic fibrosis. Unfortunately, the increase of PGZ doses above the therapeutic range used in this study does not further increase adiponectin levels (25). Alternatively, as PPARγ regulates many functions in adipocytes (24), as well as in inflammatory cells (26, 27), the fibro-protective properties of adiponectin may be counterbalanced by the fibro-permissive effect of other factors regulated by PPARγ.

In summary, ligand activation of PPARγ by PGZ does not prevent hepatic fibrogenesis in mice. This is related to the fact that the transcription factor does not control the activation of murine HSCs nor the transcription of fibrogenic genes such as Collagen-I. In addition, the modulation of the production of adiponectin by therapeutic doses of PGZ has a negligible impact on hepatic fibrogenesis.

Acknowledgments

We thank Professor Albert Geerts, Laboratory for Molecular Liver Cell Biology, Faculty of Medicine and Pharmacy, Free University of Brussels (VUB), for the expert technical advice regarding the isolation of primary HSC; and Martine Petit et Valérie Lebrun for the technical assistance. This work was supported by a grant from the Belgian 'Fonds National de la Recherche scientifique' (FNRS convention no. 3.4507.04), by grant 05/10-328 (action de recherche concertée de la direction de la recherche scientifique de la communauté française de Belgique), and by a grant from the university (Fonds Spécial de Recherche, Université Catholique de Louvain). IL is a research associate with the FNRS.

References

1. Friedman SL: Liver fibrosis - from bench to bedside. J Hepatol 38 (suppl 1): 38-53, 2003.
2. Gressner AM: Transdifferentiation of hepatic stellate cells (Ito cells) to myofibroblasts: a key event in hepatic fibrogenesis. Kidney Int (suppl 54): 39-45, 1996.
3. Moriwaki H, Blaner WS, Piantedosi R and Goodman DS: Effects of dietary retinoid and triglyceride on the lipid composition of rat liver stellate cells and stellate cell lipid droplets. J Lipid Res 29: 1523-1534, 1988.
4. Hautekeete ML and Geerts A: The hepatic stellate (Ito) cell: its role in human liver disease. Virchows Arch 430: 195-207, 1997.
5. Friedman SL: Molecular regulation of hepatic fibrosis, an integrated cellular response to tissue injury. J Biol Chem 275: 2247-2250, 2000.

6. Marra F, Efsen E, Romanelli RG, Caligiuri A, Pastacaldi S, Batignani G, *et al*: Ligands of peroxisome proliferator-activated receptor gamma modulate profibrogenic and proinflammatory actions in hepatic stellate cells. Gastroenterology 119: 466-478, 2000.
7. Galli A, Crabb DW, Ceni E, Salzano R, Mello T, Svegliati-Baroni G, *et al*: Antidiabetic thiazolidinediones inhibit collagen synthesis and hepatic stellate cell activation *in vivo* and *in vitro*. Gastroenterology 122: 1924-1940, 2002.
8. Spiegelman BM and Flier JS: Adipogenesis and obesity: rounding out the big picture. Cell 87: 377-389, 1996.
9. Miyahara T, Schrum L, Rippe R, Xiong S, Yee HF Jr, Motomura K, *et al*: Peroxisome proliferator-activated receptors and hepatic stellate cell activation. J Biol Chem 275: 35715-35722, 2000.
10. Hazra S, Miyahara T, Rippe RA and Tsukamoto H: PPAR gamma and hepatic stellate cells. Comp Hepatol 3 (suppl 1): 7, 2004.
11. Hazra S, Xiong S, Wang J, Rippe RA, Krishna V, Chatterjee K, *et al*: Peroxisome proliferator-activated receptor gamma induces a phenotypic switch from activated to quiescent hepatic stellate cells. J Biol Chem 279: 11392-11401, 2004.
12. She H, Xiong S, Hazra S and Tsukamoto H: Adipogenic transcriptional regulation of hepatic stellate cells. J Biol Chem 280: 4959-4967, 2005.
13. Kon K, Ikejima K, Hirose M, Yoshikawa M, Enomoto N, Kitamura T, *et al*: Pioglitazone prevents early-phase hepatic fibrogenesis caused by carbon tetrachloride. Biochem Biophys Res Commun 291: 55-61, 2002.
14. Leclercq IA, Sempoux C, Starkel P and Horsmans Y: Limited therapeutic efficacy of pioglitazone on progression of hepatic fibrosis in rats. Gut 55: 1020-1029, 2006.
15. Moore KJ, Rosen ED, Fitzgerald ML, Randow F, Andersson LP, Altshuler D, *et al*: The role of PPAR-gamma in macrophage differentiation and cholesterol uptake. Nat Med 7: 41-47, 2001.
16. Geerts A, Eliasson C, Niki T, Wielant A, Vaeyens F and Pekny M: Formation of normal desmin intermediate filaments in mouse hepatic stellate cells requires vimentin. Hepatology 33: 177-188, 2001.
17. Colin IM, Nava E, Toussaint D, Maiter DM, Vandenhove MF, Luscher TF, *et al*: Expression of nitric oxide synthase isoforms in the thyroid gland: evidence for a role of nitric oxide in vascular control during goiter formation. Endocrinology 136: 5283-5290, 1995.
18. Starkel P, Sempoux C, Leclercq IA, Herin M, Deby C, Desager JP, *et al*: Oxidative stress, KLF6 and transforming growth factor-beta up-regulation differentiate non-alcoholic steatohepatitis progressing to fibrosis from uncomplicated steatosis in rats. J Hepatol 39: 538-546, 2003.
19. Leclercq IA, Farrell GC, Schriemer R and Robertson GR: Leptin is essential for the hepatic fibrogenic response to chronic liver injury. J Hepatol 37: 206-213, 2002.
20. Shi Z, Wakil AE and Rockey DC: Strain-specific differences in mouse hepatic wound healing are mediated by divergent T helper cytokine responses. Proc Natl Acad Sci USA 94: 10663-10668, 1997.
21. Lehmann JM, Moore LB, Smith-Oliver TA, Wilkison WO, Willson TM and Kliewer SA: An antidiabetic thiazolidinedione is a high affinity ligand for peroxisome proliferator-activated receptor gamma (PPAR gamma). J Biol Chem 270: 12953-12956, 1995.
22. Yavrom S, Chen L, Xiong S, Wang J, Rippe RA and Tsukamoto H: Peroxisome proliferator-activated receptor gamma suppresses proximal alpha1(I) collagen promoter via inhibition of p300-facilitated NF-I binding to DNA in hepatic stellate cells. J Biol Chem 280: 40650-40659, 2005.
23. Combs TP, Wagner JA, Berger J, Doebber T, Wang WJ, Zhang BB, *et al*: Induction of adipocyte complement-related protein of 30 kilodaltons by PPAR gamma agonists: a potential mechanism of insulin sensitization. Endocrinology 143: 998-1007, 2002.
24. Kamada Y, Tamura S, Kiso S, Matsumoto H, Saji Y, Yoshida Y, *et al*: Enhanced carbon tetrachloride-induced liver fibrosis in mice lacking adiponectin. Gastroenterology 125: 1796-1807, 2003.
25. Kubota N, Terauchi Y, Kubota T, Kumagai H, Itoh S, Satoh H, *et al*: Pioglitazone ameliorates insulin resistance and diabetes by both adiponectin-dependent and -independent pathways. J Biol Chem 281: 8748-8755, 2006.
26. Jiang C, Ting AT and Seed B: PPAR-gamma agonists inhibit production of monocyte inflammatory cytokines. Nature 391: 82-86, 1998.
27. Ricote M, Li AC, Willson TM, Kelly CJ and Glass CK: The peroxisome proliferator-activated receptor-gamma is a negative regulator of macrophage activation. Nature 391: 79-82, 1998.

Study 2: The AMP-activated protein kinase is not a determinant check point in liver fibrogenesis

AMPK is an energy sensor that contributes to maintain the energy balance in the cell (138). It allows a shift toward catabolic functions when energy stores are low and allows to perform energy storing or energy demanding functions (such as lipid storage and protein synthesis) when energy is available.

Trans-differentiation of quiescent HSCs, into extracellular matrix producing, proliferative and contractile myofibroblast-like cells (activated HSCs) is a complex energetically demanding process. It is likely to require sufficient metabolic resources to complete. Previous studies have demonstrated that adiponectin inhibits activation and may induce apoptosis of fully activated myofibroblasts originating from rat HSC (130). Moreover, AMPK activation by high molecular weight adiponectin, AICAR, metformin or transduction of constitutively active AMPK result in the inhibition of the PDGF-stimulated proliferation of human activated HSC line hTERT and human or rat myofibroblast derived from HSCs (130, 175). These results suggest that AMPK may represent a novel modulator of the activated phenotype of human and rat HSCs.

Here we evaluated the impact of AMPK activation and partial inhibition on the critical step of fibrosis: the initiation of activation of quiescent HSC (trans-differentiation/activation) *in vitro*. We also evaluated its impact on fibrogenic response *in vivo*.

We showed that activation of HSCs into myofibroblasts i*n vitro* is associated with increased AMPK activity probably due to the stabilization of the enzyme complex. Deletion of the AMPKα1 catalytic subunit, resulting in decreased AMPK activity in HSC, did not alter the initiation of HSC activation. AMPK activation by treatment with AICAR, mimicking a state of supra-physiological energy depletion, decreased significantly collagen mRNA expression and cell proliferation. *In vivo*, the stimulation of AMPK, in mice fed MCD diet with metformin, or the lack of AMPKα1, in CCl_4-injected knockout mice, did not alter the hepatic fibrogenesis.

Our data demonstrate, for the first time, that AMPK stimulates HSC initial activation/trans-differentiation *in vitro*. By contrast, dramatic reduction in AMPK activity, as in AMPK$\alpha1^{-/-}$ mice, did not alter fibrotic response to CCl_4 suggesting that AMPK does not operate a decisive control on fibrogenesis.

Study 2

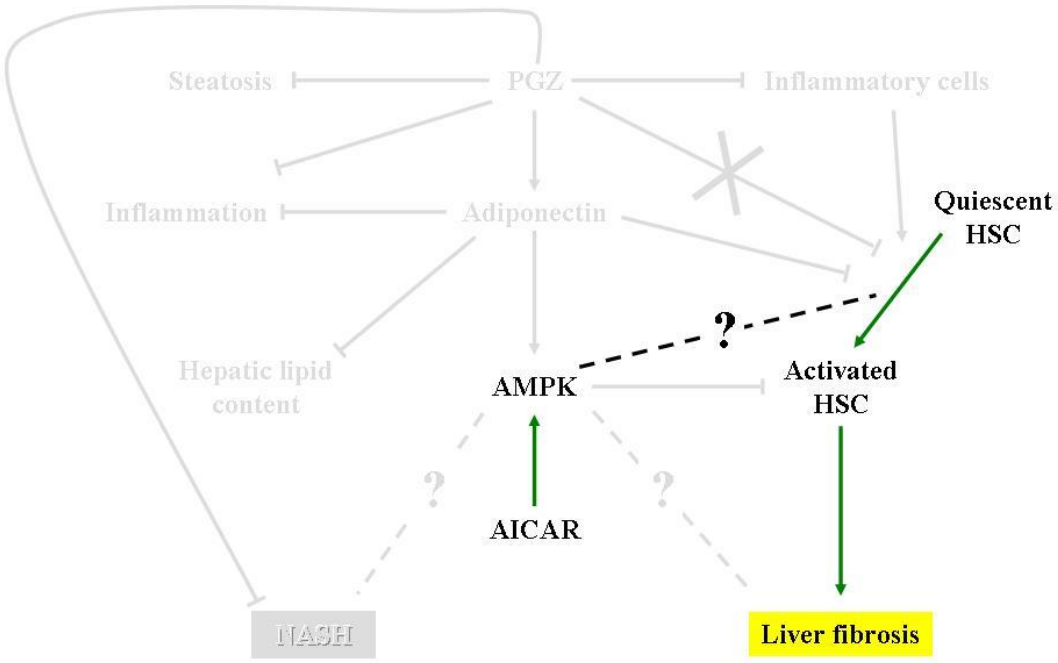

Figure 18: Evaluation of the impact of AMPK on HSC activation and hepatic fibrogenesis in mice

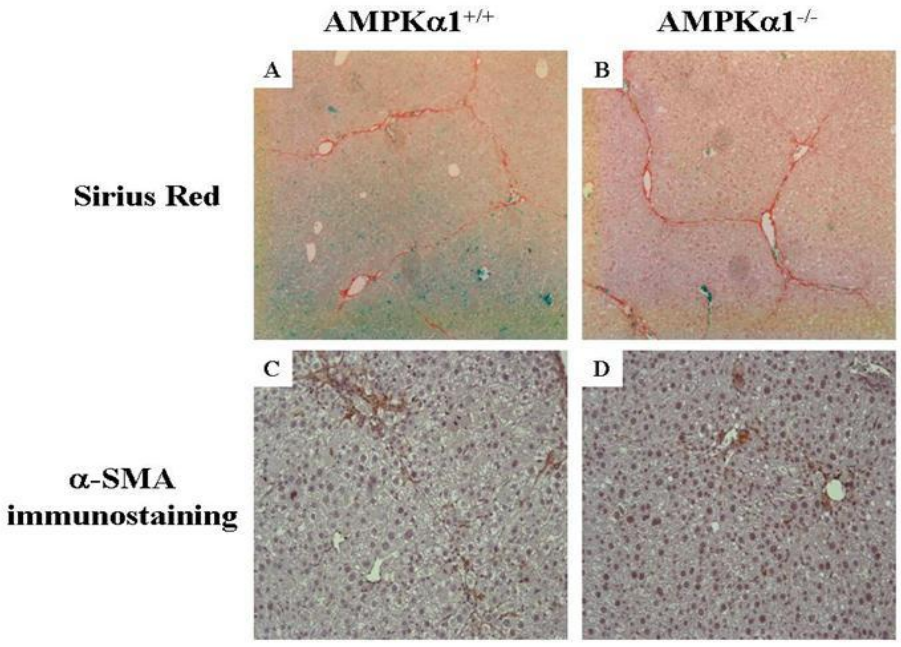

Impact of AMPKα1 deletion on CCl_4-induced liver fibrosis

The AMP-activated protein kinase is not a determinant check point in liver fibrogenesis

List of abbreviations:

α-SMA: alpha smooth muscle actin; AICAR: 5-aminoimidazole-4-carboxamide ribonucleoside; AMPK: AMP-activated protein kinase; BrdU: Bromodeoxyuridine; CCl_4: carbon tetrachloride; DMEM: Dulbecco's Modified Eagle's Medium; FBS: Foetal Bovine Serum; HSC: Hepatic Stellate Cell; HSP-90: heat shock protein 90; ICAM-1: Inter-Cellular Adhesion Molecule 1; MCP-1: Monocyte chemotactic protein-1 ; mTOR: mammalian target of rapamycin, p70S6K: p70 *Ribosomal* S6 Kinase; PDGF: Platelet-derived growth factor; PPARα: Peroxisome proliferator-activated receptor alpha; PTEN: Phosphatase and TENsin homolog; RPL19: ribosomal protein L19, TGF-β1: Transforming growth factor beta-1

Financial support:

This work was supported by grant from the Belgian 'Fonds National de la Recherche scientifique" (FNRS conventions n°3.4507.04 and 3.4578.07), by grant ARC-05/10-328 (Action de Recherche Concertée de la Direction de la Recherche Scientifique de la Communauté Française de Belgique), and by grant from the university (Fonds Spécial de Recherche, Université catholique de Louvain) to Isabelle A. Leclercq. BG was recipient of the ICP "Michel de Visscher" Fellowship. IL is research associate with the FNRS.

Abstract

Background: Trans-differentiation of quiescent hepatic stellate cells (HSCs) into extracellular matrix producing, proliferative and contractile myofibroblast-like cells (activated HSCs) is an energy-demanding pathway involves in fibrogenesis. The AMP-activated protein kinase (AMPK) plays a key role in the regulation of cellular energy homeostasis. **Methods:** To evaluate the impact of AMPK on the HSC trans-differentiation *in vitro* and *in vivo*, primary HSCs were isolated from mice lacking the AMPK α1 catalytic subunit (AMPKα$1^{-/-}$) and their littermates (AMPKα$1^{+/+}$) and liver fibrosis was induced in AMPKα$1^{-/-}$ and $^{+/+}$ mice by repeated injections of CCl_4. **Results:** AMPK activity and expression are significantly increased in primary HSCs during trans-differentiation, associated with specific upregulation of mRNA expression of the AMPKγ3 regulatory subunit. Although it inhibited early proliferation of HSC, AMPKα1 deletion neither alters collagen gene induction during HSC activation *in vitro* nor CCl_4-induced hepatic fibrogenesis development *in vivo*. However, activation of AMPK by AICAR inhibited HSC proliferation and collagen-α1 expression. **Conclusion:** Our data demonstrate that HSC trans-differentiation is associated with increased AMPK activity that could be related to the stabilisation of AMPK heterotrimeric complex by upregulation of its γ3 subunits. Targeted activation of AMPK in HSC may represent a tool for the treatment of fibrosis. By contrast deletion of AMPKα1 in mice did not prevent CCl_4-induced fibrogenesis and is therefore an unlikely mechanism to explain increased fibrosis associated with obesity and metabolic syndrome.

Introduction

Trans-differentiation of quiescent HSC into myofibroblast-like cells is a key cellular event in fibrogenesis. During this process, HSC acquire the capacity to proliferate, contract, migrate and produce large amounts of extracellular matrix (ECM) components forming scar tissue. Inhibition or blockade of HSC trans-differentiation to maintain them in their quiescent state is therefore an attractive strategy for the treatment of liver fibrosis.

Obesity and metabolic syndrome are associated with increased risk for developing liver fibrosis and increased fibrosis severity in patients with non-alcoholic steatohepatitis (NASH) or other chronic liver injuries such as viral hepatitis C (1). In humans, plasma adiponectin concentrations markedly decrease in obese and type 2 diabetes patients (2). Decreased adiponectin levels are closely associated with the degree of hepatic steatosis, necroinflammation and fibrosis in NASH (3). Studies in rodents demonstrated that adiponectin has a suppressive effect on liver fibrogenesis: Mice lacking adiponectin develop a more severe carbon tetrachloride (CCl_4)-induced hepatic fibrosis than the wild-type mice and injection of adenovirus producing adiponectin before CCl_4 treatment prevents liver fibrosis in wild-type mice. *In vitro* studies confirmed that adiponectin directly impacts on HSC inhibiting proliferation, migration, and expression of fibrogenic genes, and, perhaps induce apoptosis of activated cells (4, 5).

Adiponectin mediates its metabolic effects through receptor-dependent activation of adenosine monophosphate (AMP)-activated protein kinase (AMPK) and PPARα (2). AMPK, a serine/threonine heterotrimeric protein kinase composed by a catalytic alpha (α) and regulatory beta (β) and gamma (γ) subunits, is a fuel-sensing enzyme which plays a central role in the regulation of cellular energy homeostasis (6). Upon activation, AMPK stimulates ATP-generating catabolic pathways, such as glycolysis and lipid oxidation, and turns off energy-consuming processes, such as glycogen, lipid and protein synthesis, to restore energy balance (7), (8). In addition, AMPK also regulates both cell growth and proliferation and cell cycling (9, 10). Indeed, several studies have shown that AMPK activation by the widely used AMP-mimetic 5-aminoimidazole-4-carboxamide ribonucleoside (AICAR) caused cell cycle arrest in hepatoma HepG2 cells (11), mouse embryonic fibroblasts (10), human aortic muscle cells and rabbit aortic strips (9).

Recent studies from Brenner's and Marra's groups have explored the possibility that adiponectin inhibits fibrogenesis by activation of AMPK in HSC (12, 13). They both demonstrated that activation of AMPK by high molecular weight adiponectin, AICAR,

metformin or adenovirus-mediated expression of a constitutively active form of AMPK inhibited the PDGF-stimulated proliferation of human activated HSC line hTERT and myofibroblasts derived from primary human or rat HSCs (12, 13). By contrast, AMPK activation had little impact on the production of extracellular matrix components such as collagen I-α1 (12).

Those studies provide some insight into the mechanisms by which adiponectin may limit fibrosis progression. However, the role of AMPK on the complex processes of activation and trans-differentiation of HSCs into myofibroblast-like cells, the critical initiating step in fibrogenesis, remains to be investigated and its importance for fibrosis *in vivo* to be demonstrated.

To explore these questions, we first determine AMPK activity during *in vitro* trans-differentiation of primary murine HSC and analyse the consequences of AMPK activation, or conversely the loss of AMPK function, on this process. In a second time, we evaluate the importance of AMPK on CCl_4-induced hepatic fibrogenesis development *in vivo* in mice.

Materials and methods

Animals studies

Female AMPKα1 null-mice (AMPKα1$^{-/-}$) and their littermates (AMPKα1$^{+/+}$) were kindly provided by B. Viollet, Institut Cochin, Paris (14). All animals were kept in a temperature and humidity-controlled environment with a 12 h light–dark cycle and *ad libitum* access to water and diet. The animals were handled according to the guidelines for humane care for laboratory animals in accordance with EU Regulation and the study protocol was approved by the local ethics committee.

To determine the impact of AMPK on hepatic fibrogenesis, 10 weeks-old AMPKα1$^{-/-}$ and AMPKα1$^{+/+}$ (Wt) mice were injected intra-peritoneally with CCl_4 (400µL/kg body weight in corn oil) or vehicle three times a week for 4 weeks. At the time of sacrifice (48 h after the last injection of CCl_4), blood was collected by cardiac puncture and the liver and abdominal subcutaneous fat rapidly excised. Part of the liver was fixed in 4% formalin, embedded in paraffin and used for histological analyses; the remaining liver and the subcutaneous adipose tissue were snap frozen in liquid nitrogen and kept at -80°C until use.

Isolation and treatment of hepatic stellate cells

Primary HSCs were isolated from female Balb/C, AMPKα1$^{-/-}$ and AMPKα1$^{+/+}$ mice as described previously (15). Primary HSCs were cultured in DMEM + 20% FBS at 37°C in a humidified atmosphere with 5% CO_2 and 95% air. After 24 hours, the medium was removed and replace by DMEM supplemented with 5% FBS.

The purity of cultures was evaluated by examining the characteristic stellate shape of the cells with phase-contrast microscopy and the presence of lipid droplets by auto-fluorescence using an excitation wavelength of 320 nm. After the first replacement of medium (day 1), purity was above 90%.

To analyse the impact of AMPK activation on HSC biology, primary cells were incubated with DMEM supplemented with 5% FBS containing AICA riboside (AICAR) 250µM (BIOMOL International, USA) for 48 hours. Treatment was initiated at day 3 after plating (quiescent HSCs). Medium was renewed every 2 days and cells passaged at day 9.

Histology and immunohistochemistry.

Sections were stained with hematoxylin/eosin, sirius red (to visualize collagen deposition) or α-SMA (Clone 1A4, Dako, Belgium) using standard techniques (15).
Hepatic stellate cells were seeded on plastic Thermanox™ Coverslips (Nunc, USA). At determined times (ranging from 1 to 9 days) the coverslips were washed once in PBS and cells fixed by immersion in formaldehyde 4% at 4°C for 5 min. Endogenous peroxidases were inhibited by incubating the coverslips in methanol with 0.1% H_2O_2. After immersion in PBS containing 10% Normal Goat Serum for 20 min, coverslips were incubated with mouse monoclonal anti-α-SMA antibody (1:300) (Clone 1A4, Dako, Belgium) overnight at 4°C. After washing in PBS, coverslips were incubated with the appropriate peroxidase-conjugated secondary antibody at room temperature during 1h. Peroxidase activity was revealed with 3-amino-9-ethylcarbazole (DakoCytomation). Slides were then counter stained in haematoxylin-eosin and examined under the microscope.

Biochemical assays.

Hydroxyproline content was determined on liver samples hydrolyzed in 5mL 6M HCl at 110 degrees for 18-24 hours as previously reported (16) using hydroxyproline 40µg/ml (Sigma Aldrich, Belgium) as a standard.

HSC proliferation

Quantitative evaluation of HSC proliferation was evaluated by BrdU incorporation using the Cell Proliferation ELISA (colorimetric) (Roche Diagnostics, Belgium). Murin primary HSC were cultured in a 96-well plate at a concentration of 2000 cells per well. At day 3, HSCs were incubated in DMEM with 5% FBS supplemented or not with AICAR 250µM for 48 hours and proliferation test performed at the indicated time points.

Total RNA extraction, Reverse Transcription and Quantitative PCR

Total RNA was extracted from cultured HSCs using the TRIpure Isolation Reagent (Roche Diagnostics, Belgium). cDNA was obtained by reverse transcription of 1µg total RNA using random primers and M-MLV reverse transcriptase (Gibco BRL, Belgium). mRNA expression levels were quantitated by realtime PCR (RT-qPCR) as previously described (15). Primer

pairs for transcripts of interest were designed using the Primer Express design software (Applied Biosystems) and listed in Table 1. RPL19 RNA was chosen as an invariant standard. Results were expressed as fold expression relative to expression in the control group (value set at 1) using the delta Ct method (17).

Preparation of cell lysates and Western Blot analysis

Lysates for western blot analyses and AMPK activity were obtained as previously described (15). Protein concentrations were determined using a BCA protein assay with serum albumin as a standard (Pierce Chemical, USA). Proteins from HSC lysates were separated by SDS-PAGE and transferred onto PVDF Transfer membrane (PolyScreen, NEN Life Science Products, USA). The membranes were then exposed to the following antibodies: AMPKα1 or AMPKα2, phospho-(Thr172)-AMPKα, p70S6K, phospho-(Thr389)-p70S6K (Cell Signaling, USA) and Heat Shock Protein 90 (HSP-90) (BD Transduction Laboratories, USA). The quantification of immune-reactive proteins was obtained by densitometry using the Gel Doc^{TM} XR System 170-8170 device and software (Bio-Rad, USA). Intensity of HSP-90 band was used as a loading control.

AMPK assay

Total AMPK activity was assayed on cell lysates after precipitation with 10% (*w*/*v*) poly(ethylene glycol) 6000 (Merck, Belgium) as previously described (18).

To measure the AMPKα1 and α2 activities, 100µg protein from cell lysates were immunoprecipitated with protein-G-sepharose and isoform specific antibodies to the α1 or α2 catalytic subunits of AMPK (Cell Signaling) for 1h at 4°C. One unit of AMPK activity corresponds to 1 nmol of product formed per min under the assay conditions (19).

Statistical analysis

Results are expressed as mean ± standard deviation (SD). Statistical differences between groups were tested using one way analysis of variance (ANOVA). Statistical significance was assumed for p values <0.05

Results

AMPK expression and activity in cultured HSCs

Quiescent HSC significantly express the AMPKα1 but little of the AMPKα2 catalytic subunit (Figure 1B) mainly in their non-phosphorylated (inactive) form. Culture-activation of primary HSC from a quiescent (day 3) into a myofibroblastic-activated phenotype (day 7) is associated with a significant increase in both AMPKα1 and α2 protein expression (Figure 1A), with AMPKα1 being much higher than α2 activity (Figure 1B). During this process, AMPK phosphorylation (on Thr172) and the activity of both catalytic subunits increase.

AMPKgamma 3 (AMPKγ3) regulatory subunit mRNA increased during HSC trans-differentiation

Because AMPK is a heterotrimeric complex (6), gene expression for the catalytic (α) and regulatory (β and γ) subunit isoforms has been evaluated during time in culture. As depicted in Figure 2, regulatory AMPKγ3 subunit gene expression increases significantly during the trans-differentiation of the quiescent HSCs (day 2) into the activated phenotype (day 7). By contrast, the mRNA expression of AMPKγ1/2 or of AMPKα1/2, β1/2 remains constant (Figure 2).

Impact of AMPK activation on HSC trans-differentiation

To evaluate the impact of AMPK activation on HSC trans-differentiation, primary HSCs isolated from Wt mice, are incubated with AICAR (250µM) for 48 hours between day 3 (quiescent phenotype) and day 5 (early-activated phenotype). This treatment results in a significant increase of total AMPK activity measured in cell lysates at day 5 compared to cells incubated with vehicle (CTL) (Figure 3A). This is paralleled by a marked phosphorylation (Thr172) of AMPK, above the level observed in untreated HSCs (Figure 3B).

AMPK may participate to the control of protein synthesis and cell proliferation (20, 21), inhibiting those processes when energy resources are low. Indeed, AMPK is able to phosphorylate and inactivate mTOR, thereby reducing phosphorylation of p70S6K and consequently protein synthesis (20). In untreated cells, increased AMPK activity during cell activation is associated with increased phosphorylation of p70S6K and cell proliferation (Figures 3B and E). Upon AICAR treatment, supra-physiological activation of AMPK is associated with a complete inhibition of p70S6K phosphorylation and inhibition of cell proliferation (Figures 3B and E). We also observe a significant inhibition of AMPK and

p70S6K protein expression after treatment with AICAR (Figure 3B). This could be related with the inhibition of cell proliferation, and consequently cell number, observed after supra-physiological activation of AMPK. The physiological up-regulations of collagen-αI mRNA and α-SMA expression that occur in cultured HSCs are repressed upon exposure to AICAR (Figures 3C and D).

Taken together, pharmacological activation of AMPK inhibits proliferation, collagen-αI and α-SMA expression during HSC activation *in vitro*.

Effect of AMPKα1 deletion on HSC activation

HSCs isolated from mice lacking AMPKα1, the prominent catalytic subunit in HSCs, were used to determine the dependence on increased activity of AMPK for HSCs activation. Collagen-αI and α-SMA mRNA expressions and cell proliferation were evaluated and compared to Wt cells. Compared to cells from AMPKα$1^{+/+}$ mice, phospho-AMPK was negligible in activated AMPKα$1^{-/-}$ cells (data not show). As observed in Figure 4C, collagen-α1 mRNA expression in HSCs isolated from Wt and AMPKα$1^{-/-}$ mice increased during early trans-differentiation, and the lack of the AMPKα1 catalytic subunit did not significantly altered it (Figure 4C). α-SMA mRNA expression increased significantly in Wt HSCs and deletion of AMPKα1 catalytic subunit did not alter the significant increased expression in the early steps of HSC activation (Figure 4D). This supports that the absence of the AMPKα1 catalytic subunit does not alter the phenotypic changes and the induction of pro-fibrogenic genes during early activation phenomenon. HSCs proliferation has been evaluated at day 3 (quiescent cells) and day 5 (early activated cells) following 24 hours exposure to BrdU. In Wt cells, BrdU incorporation was significantly higher at day 5 than at day 3. By contrast, between day 3 and day 5 there was no change in DNA synthesis in AMPKα$1^{-/-}$ HSC (Figure 4A). This is confirmed by α-SMA immunostaining (Figure 4B).

AMPKα1 deletion, leading to reduced AMPK activity, is associated with inhibition of cell proliferation but it does not alter the increase expression of collagen-αI nor the increased expression of α-SMA observed during the trans-differentiation phenomenon.

Lack of AMPKα1 catalytic subunit did not alter hepatic fibrogenesis in mice

To determine whether AMPK is implicated in the development of hepatic fibrogenesis *in vivo*, we repeatedly injected AMPKα1$^{-/-}$ mice with CCl_4 and compared the fibrotic response with that of their Wt littermates. In AMPKα1$^{-/-}$ mice, hepatic AMPK activity is 75% lower than in Wt due to the abolition of AMPKα1 activity which is not compensated for by an up-regulation of AMPKα2 (Figure 5A-B). The Thr172 phosphorylation of AMPK was similar in CTL and CCl_4 treated livers (Figure 5A). In addition, neither total hepatic AMPK nor AMPKα2 activities are significantly altered by CCl_4 (Figure 5 B and C). In AMPKα1$^{+/+}$ mice, CCl_4 treatment induced hepatic fibrosis as shown by the formation of collagen bridges between central veins, visualized by Sirius Red staining, and the increased α-SMA positive cells, corresponding to activated HSCs (Figures 6A and C). The deletion of the AMPKα1 catalytic subunit does not significantly alter the development of the CCl_4-induced liver fibrosis in these mice (Figures 6B and D). In keeping with the histological findings, hepatic hydroxyproline content is as high in AMPKα1$^{-/-}$ as in AMPKα1$^{+/+}$ mice (Figure 6E).

Fibrogenesis in the CCl_4 model is classically accompanied by significant increased in collagen-α1, alpha smooth muscle actin (α-SMA), transforming growth factor beta (TGFβ)-1 (22), associated with HSCs activation, as well as monocyte chemoattractant protein-1 (MCP-1) (23) and intracellular adhesion molecule-1 (ICAM-1) (24) expressions, reflecting inflammatory cell recruitment during the wound healing process. As expected, this is the case in CCl_4-treated AMPKα1$^{+/+}$ mice (Figure 7). The expression of these genes is not altered by the lack of the AMPKα1 catalytic subunit (Figure 7), confirming that life long low AMPK activity does not perturb the wound healing response, and that both the inflammatory and the fibrogenic components of this process are maintained.

Discussion

Activation and trans-differentiation of hepatic stellate cells (HSCs) is a key cellular event for hepatic fibrogenesis. This process, characterized by important morphological and phenotypical alterations, is energetically demanding and requires sufficient metabolic resources (10). At a cellular level, AMPK gauges cellular energy status, and accordingly operates a coordinated switch between adenosine triphosphate (ATP)-consuming pathways and energy producing pathways (10). It also operates a control on cell cycle progression in close adequacy with the availability of energy resources (10). Our results showed that trans-differentiation of quiescent primary mice HSC into a myofibroblastic-like cell phenotype in culture, mimicking the activation process observed *in vivo* during hepatic fibrogenesis, is characterized by an increased AMPK activity, mainly sustained by the AMPKα1 catalytic subunit. mRNA levels for the catalytic subunits remaining stable, increased AMPK protein and kinase activities are not dependent on enhanced gene expression. Rather, increased γ3 subunit, the muscle-specific AMPK gamma isoform (25), may induce stabilisation of the AMPK complex and explain the enhanced protein levels and participate to augmented activity observed during HSCs activation. As AMPKγ3 is an isoform preponderantly seen in muscle cells, this increased expression may be part of the changes in gene expression associated with myofibroblastic transformation. These results are thus compatible with the operation of switch towards energy mobilization and production necessary to meet the needs for the trans-differentiation processes.

AMPK exercises an inhibitory control on protein synthesis and cell growth (26, 27), protects cells from apoptosis induced by glucose starvation (20, 28), probably through the inhibition of the mTOR pathway. mTOR is a ubiquitously expressed and highly conserved serine/threonine kinase that affects a number of key cell functions including protein synthesis and cell proliferation. AMPK can inactivate mTOR by 2 means: direct inhibitory phosphorylation of mTOR/Raptor and phosphorylation and activation of TSC2. Inhibition of mTOR results in a decrease phosphorylation of the p70 *Ribosomal* S6 Kinase (p70S6K) (20, 29). Thus, AMPK may directly and indirectly (via TSC2) suppress mTOR activity to limit protein synthesis, in conditions of energy storage. Intriguingly, Alessi *et al.* has recently reported that AMPK activators provide protection against the development of tumors in a mouse model where mTOR is activated via reduced expression of PTEN and LKB1 (30). This suggested that AMPK regains the control over the mTOR pathway when it is activated at "supra-physiological" levels. During culture activation of HSCs, increased AMPK activity is

associated with increased phosphorylation of p70S6K, suggesting that inhibition of such pathways does not occur when necessary energy resource can be mobilized or alternatively, that the inhibitory influence of AMPK over this pathway could be overcame by other stimuli facilitating protein synthesis and cell cycle progression.

Studies report that AMPK activation suppresses proliferation in vascular smooth muscle cells (9, 31) and cancer cells (32). Similarly, it has recently been shown that AMPK activation inhibits and negatively modulates the activated phenotype and proliferation of both human and rat activated-HSCs (12, 13). However, these studies evaluate the impact of AMPK on the activated phenotype of HSCs and not on the trans-differentiation mechanism *in vitro*, mimicking the activation process observed *in vivo* which is one of the main characteristic phenomenons implicated in the development of hepatic fibrosis. Here we also show that supra-physiological activation of AMPK induced by treatment with AICAR inhibitss of cell proliferation, α-SMA expression and collagen-α1 production that are normally seen during plastic activation of quiescent HSC. This is associated with the inhibition of p70S6K phosphorylation suggesting a decrease in the protein synthesis pathway. These results support the concept that the use of drugs activating AMPK, which have a proven beneficial action on liver glucose and lipid metabolism, may also have anti-fibrotic properties.

Some authors propose that if AMPK activation, by adiponectin or drugs, results in decreased activated-HSC proliferation and eventually in reducing fibrosis development, the opposite may be true. In other words, the absence of adiponectin, as observed in obese humans, may be associated with low AMPK activation and increased HSC trans-differentiation, participating in increased fibrosis and increased risk for fibrosis development in these patients. Preliminary observations (B. Guigas and I. Leclercq, unpublished observations) show that aging mice lacking AMPKα1 subunit develop discreet spontaneous perisinusoidal fibrosis (data not shown). However, this phenomenon remains to be explained. It could be associated with the loss of collagenase yield and the mitochondrial dysfunctions observed in these mice (data not shown).

To verify the hypothesis that decreased AMPK activity can be associated with increased risk for fibrosis development, we analyse trans-differentiation of HSC isolated from AMPKα1$^{-/-}$ mice, and compare them to AMPKα1$^{+/+}$ HSC. In the former cells, AMPKα1 is absent, and residual AMPK activity is only supported by the AMPKα2 subunit, resulting in a significant reduction of overall AMPK activity. Conversely to our expectation, cell proliferation normally initiated by plating on plastic is quasi absent in AMPKα1$^{-/-}$ HSC. By contrast, these

cells retain the capacity to induce collagen-α1 and α-SMA expression. This suggests that in the absence of AMPKα1 or in association with decreased overall AMPK activity, HSCs are able to trans-differentiate, but not to proliferate during this process, as if the deficient AMPK system is not sufficient to stimulate the generation of energy for the two processes simultaneously. If this occurs also *in vivo*, AMPKα1 deletion will confer relative protection against fibrosis.

In vivo, the fibrotic response to repeated injections of CCl_4 is not altered in AMPKα1$^{-/-}$ mice. Deposition of scar tissue occurs to a similar extent in AMPKα1$^{+/+}$ and AMPKα1$^{-/-}$ mice. In addition, hepatic fibrosis development is similarly associated with increased expressions of α-SMA, TGFβ-1, MCP-1 and ICAM-1 in both strains. Moreover, the number of activated HSC, as identified by α-SMA immunostaining or by α-SMA gene expression, appears similar in the AMPKα1$^{-/-}$ and Wt strains. There is thus a discrepancy between reduced cell proliferation observed *in vitro* during early trans-differentiation process in AMPKα1 deficient cells and an unaltered fibrotic response *in vivo* in AMPKα1$^{-/-}$ mice. Reduced AMPK may limit mobilisation of sufficient amounts of energy for several cellular processes to occur simultaneously and explain the dissociation between preserved fibrogenesis but inhibition of proliferation in early steps of HSC activation *in vitro*. However at a late stage, when the cells are in a steady state of activation, it is conceivable that energy demand drops, energy mobilized by low AMPK activity may be directed towards cell proliferation.

AMPK is recognised as a pivotal kinase, acting as a switch for orienting metabolic functions towards catabolism or rather towards ATP synthetic processes according to cell energy status and nutrient availability. Thereby AMPK act as a regulator of cellular energy homeostasis. The observations made here suggest that AMPK does not operate a decisive control on its numerous downstream functions, but rather that it allows or favours cell viability according to cellular resources or prevented some of them to maintain it.

In conclusion, our results support the proposition that stimulation of the AMPK regulator of energy status in the cells may represent a target for the treatment of hepatic fibrosis. However, as AMPK is probably also required to orchestrate metabolism and cell functions during tissue rebuilding, associated with the wound healing process, specific targeting of AMPK in HSCs will probably be needed. Increased hepatic fibrosis in adiponectin deficient mice (4) could be related to the absence of AMPK activation. If so, mice with low AMPK activity should have a similar phenotype than in adipo$^{-/-}$ mice. This is not the case. Our results using AMPK deficient cells and animals do thus not provide support to the hypothesis that low AMPK

stimulation, such as expected from low adiponectin stimulus, explains increased susceptibility to fibrosis.

Table

Table 1. Sequences of Primers

Gene	Primer Sequences	GeneBank accession #
α-SMA	**Forward: 5'**- TCCTGACGCTGAAGTATCCGATA-**3'** **Reverse: 5'**- GGTGCCAGATCTTTTCCATGTC-**3'**	**NM_007392**
AMPKα1	**Forward: 5'**- TCGGCACCTTCGGGAAA-**3'** **Reverse: 5'**- GTTGAGTATCTTCACAGCCACTTTATGT-**3'**	**NM_001013367**
AMPKα2	**Forward: 5'**- CGCCTCTCATCGCAGACA-**3'** **Reverse: 5'**- CTTGGGCTTCGTTGTGTTGA-**3'**	**NM_178143**
AMPKβ1	**Forward: 5'**- AGGACACGGGCATCTCTTGT-**3'** **Reverse: 5'**- GTGGTTCAGCATGACGTGGTT-**3'**	**NM_031869**
AMPKβ2	**Forward: 5'**- TGTTATGCTGAACCATCTCTATGCA-**3'** **Reverse: 5'**- GCGTGGTGACATACTTCTTCTTGT-**3'**	**NM_182997**
AMPKγ1	**Forward: 5'**- TGCCATGGTCCGTACTACCA-**3'** **Reverse: 5'**- CGGAGACTCGGTGCTGTACA-**3'**	**NM_016781**
AMPKγ2	**Forward: 5'**- AACGTACAATAACTTGGACATCACAGT-**3'** **Reverse: 5'**- GCACTTCACCACACCCTCAA-**3'**	**NM_145401**
AMPKγ3	**Forward: 5'**- CACGGGAACAGGTGCATAGG-**3'** **Reverse: 5'**- GGAGACCACGCCCAGAAGA-**3'**	**NM_153744**
Col-αI	**Forward: 5'**- TTCACCTACAGCACGCTTGT-**3'** **Reverse: 5'**- TCATCGAATACAAAACCACCAAGA-**3'**	**NM_007742**
ICAM-1	**Forward: 5'**- CCGCAGGTCCAATTCACACT-**3'** **Reverse: 5'**- CAGAGCGGCAGAGCAAAAG-**3'**	**NM_010493**
MCP-1	**Forward: 5'**- CCACTCACCTGCTGCTACTCAT-**3'** **Reverse: 5'**- CTGCTGGTGATCCTCTTGT-**3'**	**NM_011333**
RPL19	**Forward: 5'**- GAAGGTCAAAGGGAATGTGTTCA-**3'** **Reverse: 5'**- ACAAGCTGAAGGCAGACAAGG-**3'**	**NM_009078**
TGF-β1	**Forward: 5'**- CCTGCAAGACCATCGACATG-**3'** **Reverse: 5'**- GAGCCTTAGTTTGGACAGGATCTG-**3'**	**NM_011577**

α-SMA: alpha smooth muscle actin; AMPK: AMPK-activated protein kinase; Col-αI: Collagen alpha 1; ICAM-1: Inter-Cellular Adhesion Molecule 1; MCP-1: Monocyte chemotactic protein-1; RPL19: ribosomal protein L19; TGF-β1: Transforming Growth Factor beta-1

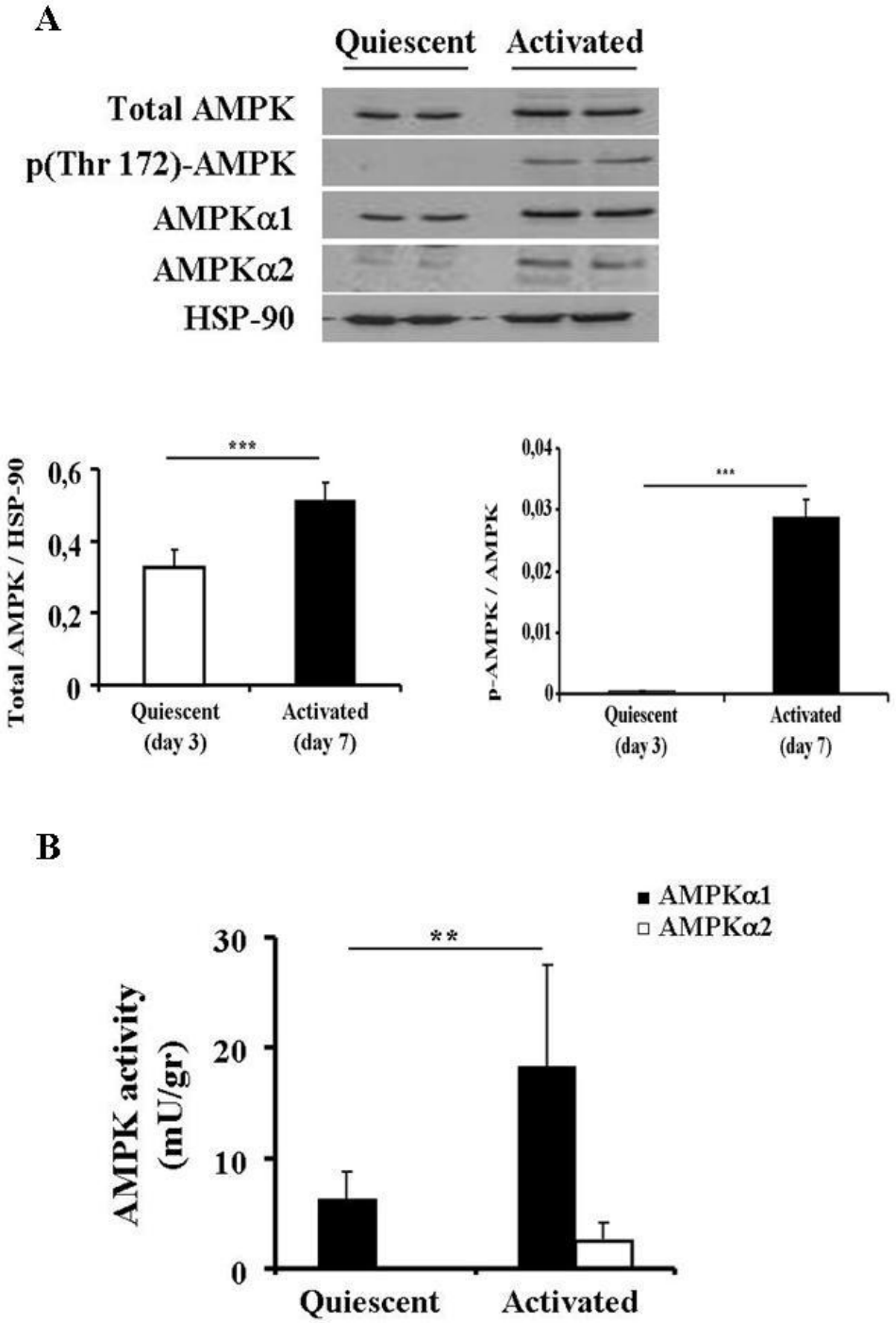

Figure 1: Increased AMPK activity and protein expression during HSC trans-differentiation

(A) Representative western blot for total AMPK, phospho(Thr172)-AMPK (p-AMPK), AMPKα1 and α2 catalytic subunits and HSP-90. The bar graph represents total AMPK/HSP-90 and p-AMPK/total AMPK ratio, determined by densitometric analysis and expressed as arbitrary units, quiescent (day 3) and activated (day 7) HSC. Data normalized to HSP-90 for western blot are expressed in arbitrary units as mean ± SD (n=5 per group). (B) Bar graph represents hepatic AMPKα1 and AMPKα2 activities, measured as described in Materials and Methods section. ** $p<0.05$ and *** $p<0.001$ compared to quiescent HSC.

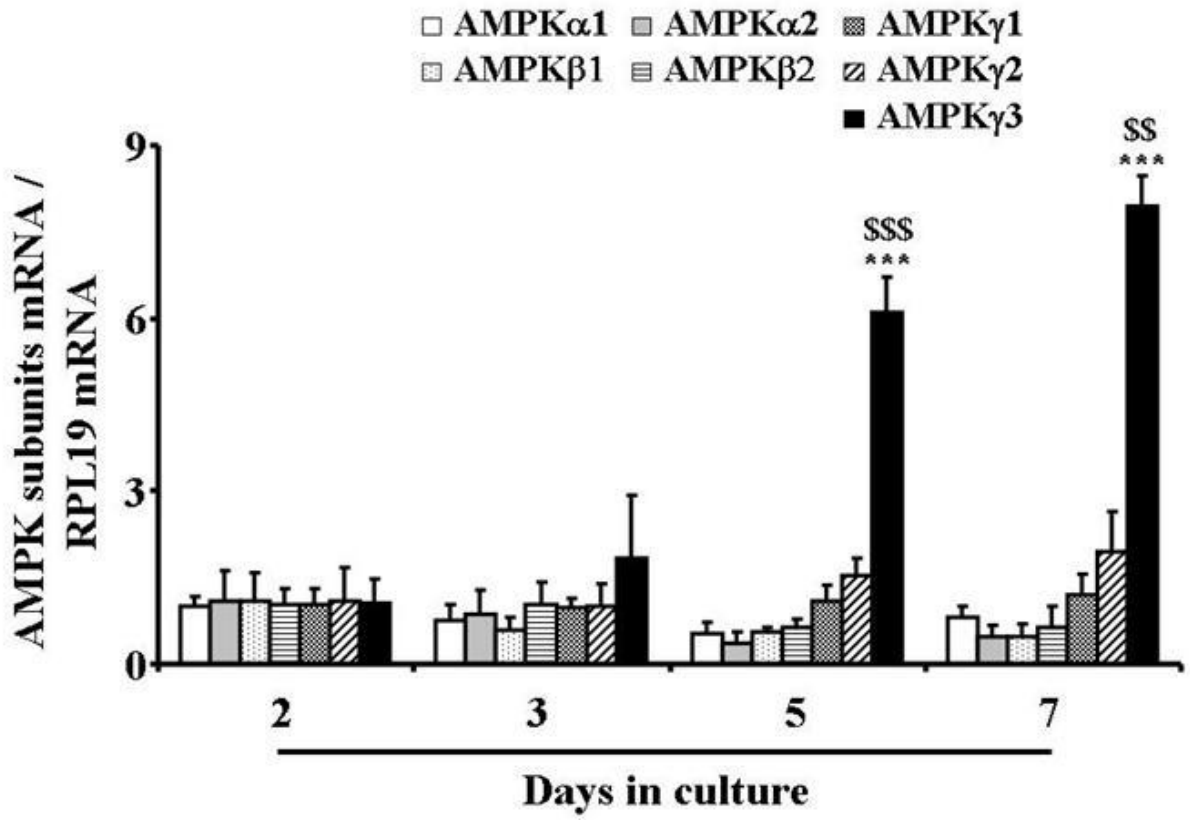

<u>Figure 2:</u> AMPK subunits gene expression increased during HSC trans-differentiation
Bar graph represents AMPK subunits mRNA expression quantitated by RT-qPCR in primary HSC in culture. RT-qPCR data are normalised to the expression of RPL19 mRNA regarded as an invariant control. Data are expressed in arbitrary units as mean ± SD on n=12 culture dishes from 3 different cell preparations. *** $p<0.001$ compared to AMPK subunit at the same time point, $^{\$\$}$ $p<0.05$ and $^{\$\$\$}$ $p<0.001$ compared to AMPKγ3 subunit.

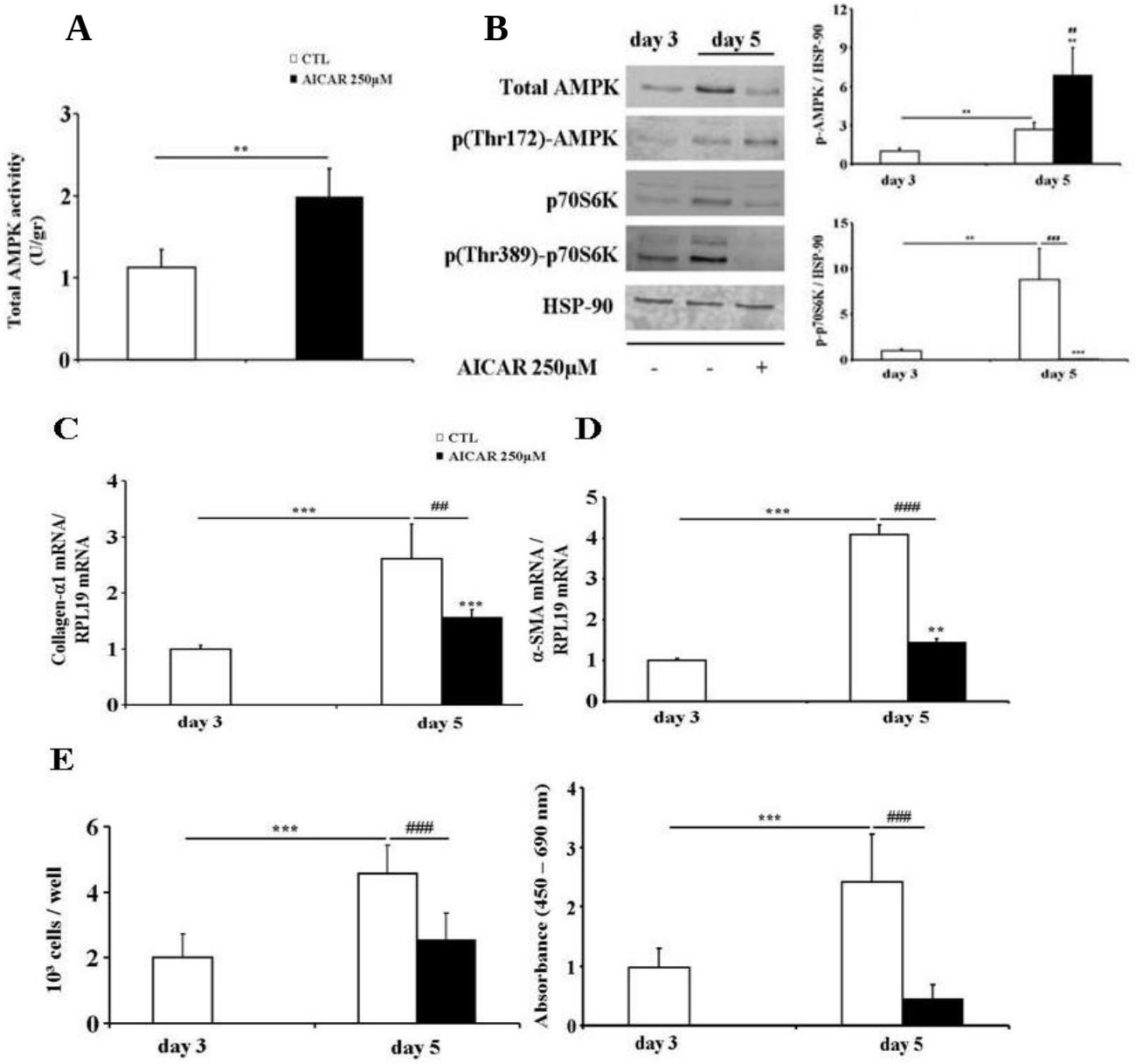

Figure 3: Impact of AMPK activation on murine HSC trans-differentiation

Bar graphs represent (A) total AMPK activity, (C) collagen-α1 and (D) α-SMA mRNA expressions, quantitated by RT-qPCR, and (E) cell count and cell proliferation, measured as described in Materials and Methods section, in HSC isolated from Wt mice and treated with AICAR 250µM between day 3 (quiescent phenotype) and day 5 (early activated phenotype). Results (mean ± SD on n=10 culture dishes from 3 different cell preparations) are normalised to the expression of RPL19 mRNA regarded as an invariant control. ** $p<0.05$ and *** $p<0.001$ compared to CTL, ## $p<0.05$ and ### $p<0.001$ compared to AICAR. (B) Representative western blot for total AMPK, phosphor(Thr172)-AMPK (p-AMPK), p70S6K, phosphor(Thr389)-p70S6K (p-p70S6K) in HSC isolated from Wt mice and treated with AICAR 250µM between day 3 (quiescent phenotype) and day 5 (early activated phenotype). The bar graph represents total p-AMPK/HSP-90 and p-p70S6K/HSP-90 ratio, determined by densitometric analysis and expressed as arbitrary units. Data normalized to HSP-90 for western blot are expressed in arbitrary units as mean ± SD (n=5 per group). ** $p<0.05$ and *** $p<0.001$ compared to HSC day 3 and ### $p<0.001$ compared to HSC day 5 in CTL conditions.

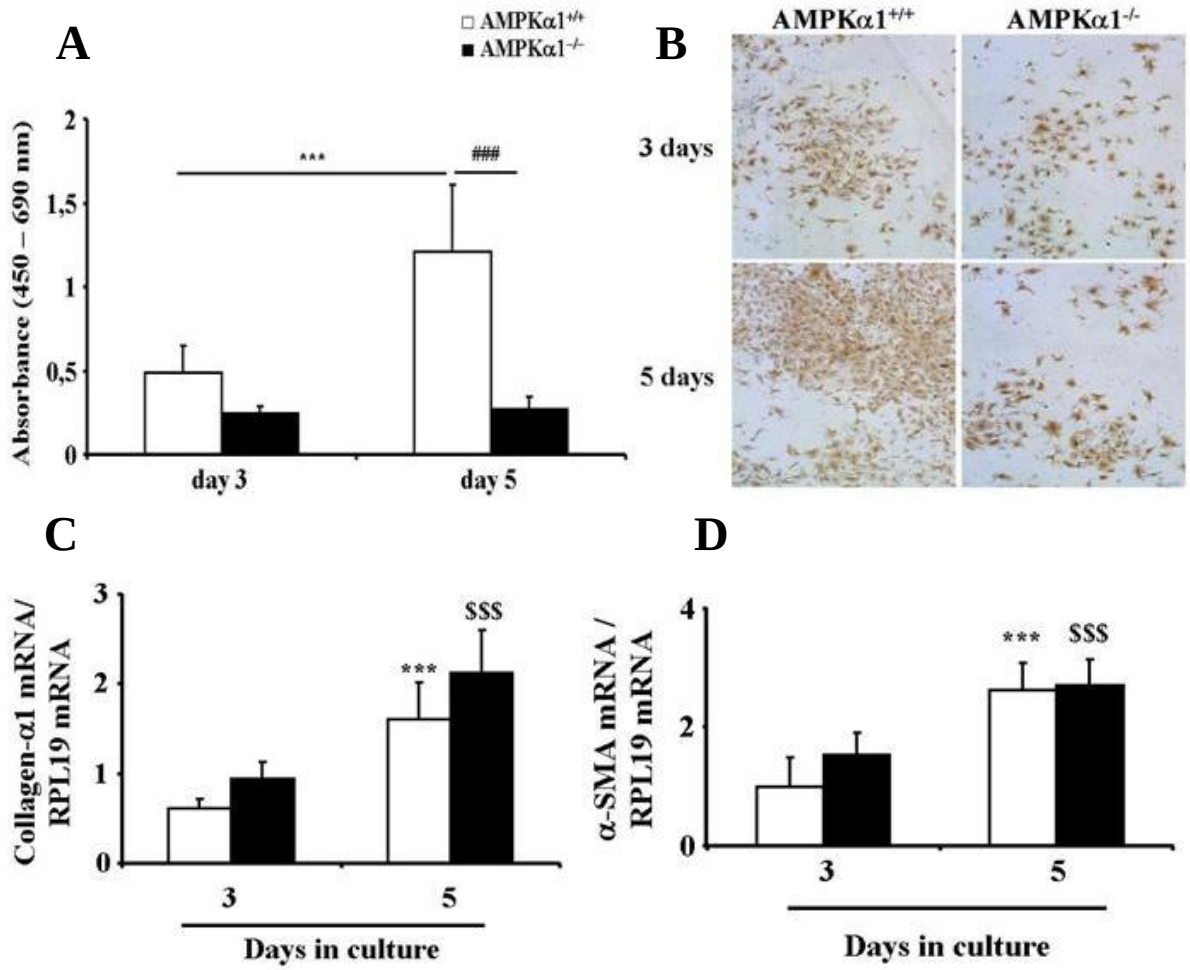

Figure 4: Impact of AMPKα1 deletion on HSC trans-differentiation

(A) Bar graph representing the cell proliferation. HSC isolated from Wt and AMPKα1$^{-/-}$ mice were incubated 24h with BrdU. A colorimetric assay (based on BrdU incorporation detected by a BrdU-antibody peroxidase conjugate) was carried out as described in Materials and Methods section. The colour intensity at 450 nm correlates directly to the amount of BrdU incorporated into the DNA, which in turn represents proliferation. (B) Representative photomicrographs of α-SMA immunostained HSCs isolated from AMPKα1$^{+/+}$ and $^{-/-}$ mice and fixed at day 3 and day 5 after isolation. Bar graph represent collagen-α1 (C) and α-SMA (D) mRNA expressions quantitated by RT-qPCR in primary HSC isolated from Wt and AMPKα1$^{-/-}$ mice during time in culture. RT-qPCR data are normalised to the expression of RPL19 mRNA regarded as an invariant control. Data are expressed in arbitrary units as mean ± SD on n=10 culture dishes from 3 different cell preparations. Experiments were performed in triplicates; data are expressed in arbitrary units as mean ± SD. *** $p<0.001$ compared to Wt, $^{\$\$}$ $p<0.05$ and $^{\$\$\$}$ $p<0.001$ compared to AMPKα1$^{-/-}$ and $^{\#\#\#}$ $p<0.001$ Wt versus AMPKα1$^{-/-}$ HSC.

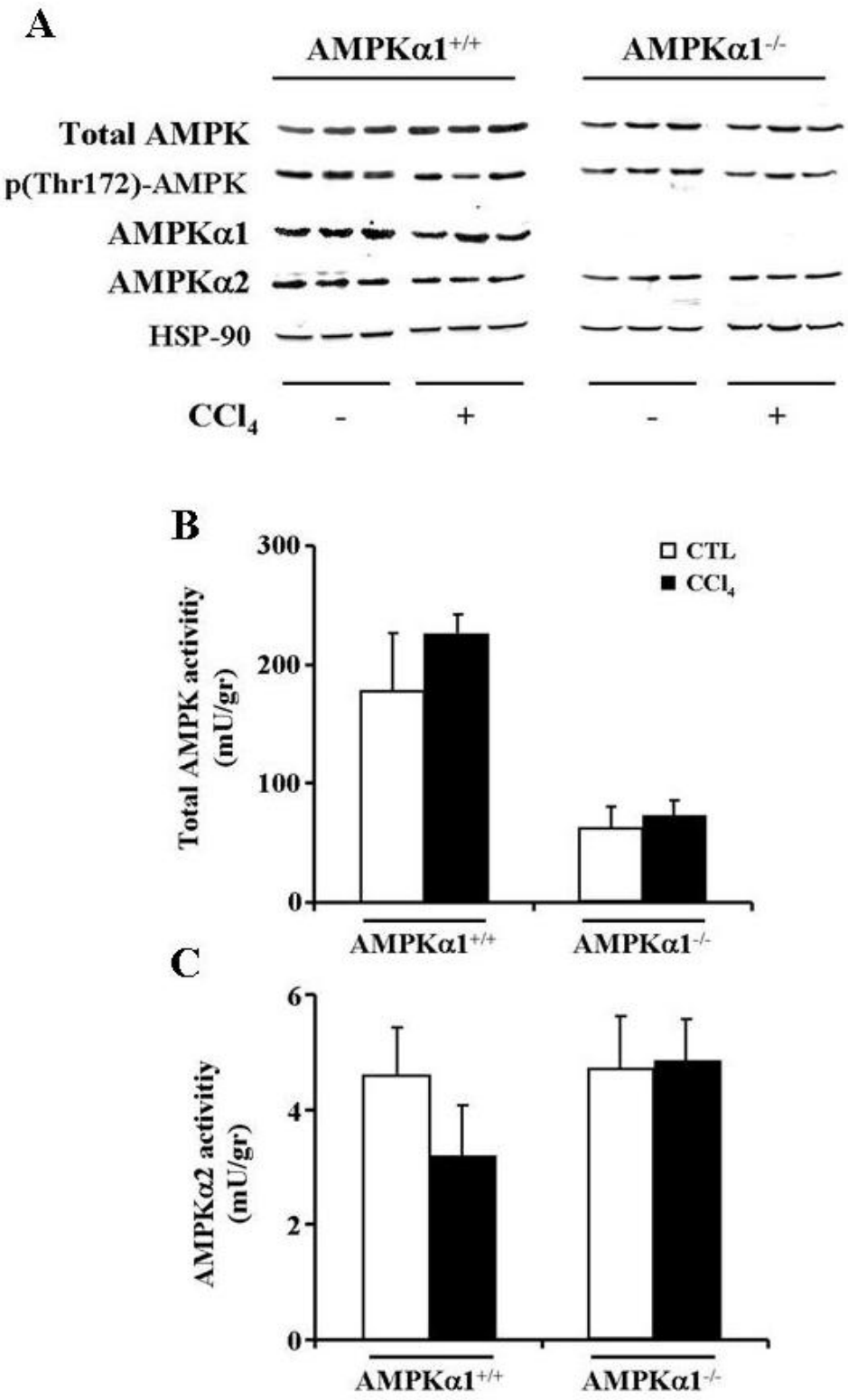

Figure 5: Impact of CCl_4 on total AMPK and AMPKα2 activities

(A) Representative western blot for total AMPK, phospho(Thr172)-AMPK (p-AMPK), AMPKα1 and α2 catalytic subunits and HSP-90 and bar graphs representing (B) total AMPK and (C) AMPKα2 activities, measured as described in Materials and Methods section, in livers of AMPKα1$^{+/+}$ and $^{-/-}$ mice treated with corn oil (CTL) or CCl_4 (400µl/Kg body weight, 3 X/wk for 4 weeks). Results are expressed as mean ± SD on n=5 per group.

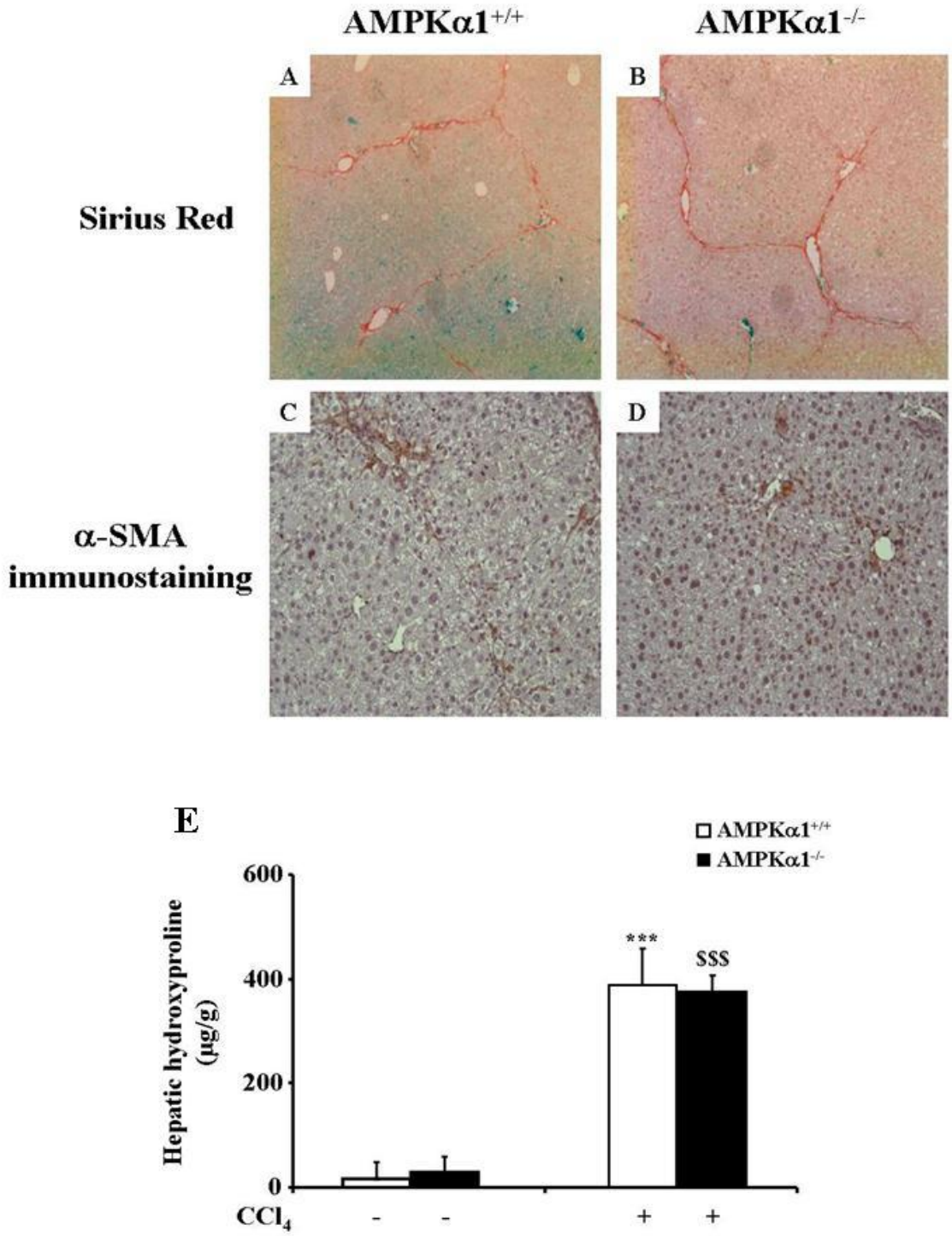

Figure 6: Impact of AMPKα1 on CCl_4-induced liver fibrosis

Representative photomicrographs of (A and B) Sirius red and (C and D) α-SMA immunostaining liver sections from AMPKα1$^{+/+}$ and $^{-/-}$ mice receiving repeated injections of CCl_4 for 4 weeks (n=5 per group). (E) Bar graph represents quantification of hepatic hydroxyproline content and (measured as described in Materials and Methods section, in livers of AMPKα1$^{+/+}$ and $^{-/-}$ mice treated with corn oil (CTL) or CCl_4 (400µl/Kg body weight, 3 X/wk for 4 weeks). Results, expressed as mean ± SD on n=5 per group, are normalised to the expression of RPL19 mRNA regarded as an invariant control. Data are expressed in arbitrary units. *** $p<0.001$ compared to AMPKα1$^{+/+}$ CTL and $^{\$\$\$}$ $p<0.001$ compared to AMPKα1$^{-/-}$ in control conditions.

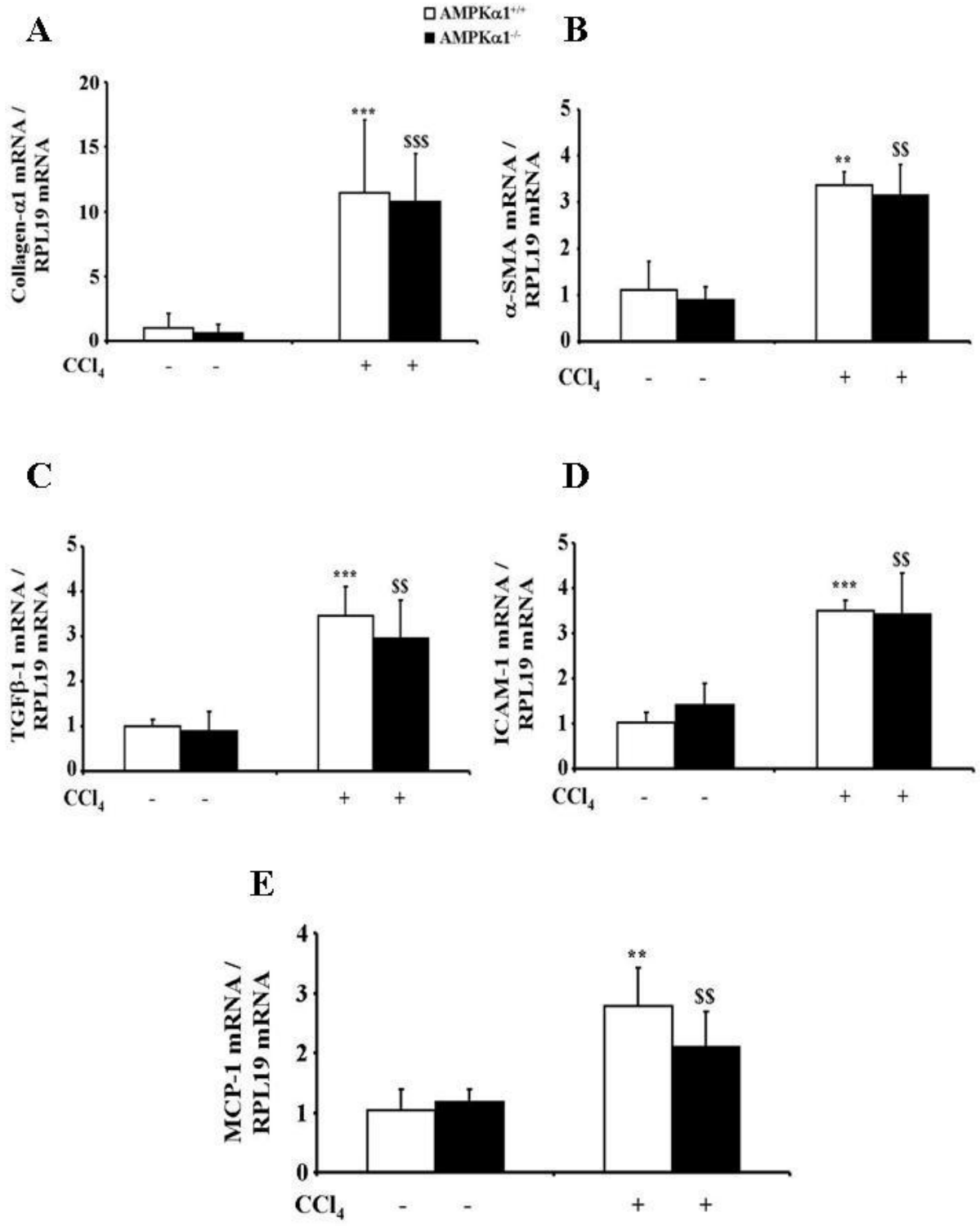

<u>Figure 7:</u> Impact of AMPKα1 deletion on HSC activation *in vivo*

Bar graphs represent (A) collagen-α1, (B) α-SMA, (C) TFGβ-1, (D) ICAM-1 and (E) MCP-1 mRNA expression quantitated by RT-qPCR in livers of AMPKα1$^{+/+}$ and $^{-/-}$ mice treated with corn oil (CTL) or CCl_4 (400µl/Kg body weight, 3 X/wk for 4 weeks). Results, expressed as mean ± SD on n=5 per group, are normalised to the expression of RPL19 mRNA regarded as an invariant control. Data are expressed in arbitrary units. ** $p<0.05$, *** $p<0.001$ compared to AMPKα1$^{+/+}$ CTL and $^{\$\$}$ $p<0.05$, $^{\$\$\$}$ $p<0.001$ compared to AMPKα1$^{-/-}$ in control conditions.

References

1. Clark JM, Brancati FL, Diehl AM. Nonalcoholic fatty liver disease. Gastroenterology 2002;122:1649-1657.
2. Yamauchi T, Nio Y, Maki T, Kobayashi M, Takazawa T, Iwabu M, Okada-Iwabu M, et al. Targeted disruption of AdipoR1 and AdipoR2 causes abrogation of adiponectin binding and metabolic actions. Nat Med 2007;13:332-339.
3. Targher G, Bertolini L, Rodella S, Zoppini G, Scala L, Zenari L, Falezza G. Associations between plasma adiponectin concentrations and liver histology in patients with nonalcoholic fatty liver disease. Clin Endocrinol (Oxf) 2006;64:679-683.
4. Kamada Y, Tamura S, Kiso S, Matsumoto H, Saji Y, Yoshida Y, Fukui K, et al. Enhanced carbon tetrachloride-induced liver fibrosis in mice lacking adiponectin. Gastroenterology 2003;125:1796-1807.
5. Ding X, Saxena NK, Lin S, Xu A, Srinivasan S, Anania FA. The roles of leptin and adiponectin: a novel paradigm in adipocytokine regulation of liver fibrosis and stellate cell biology. Am J Pathol 2005;166:1655-1669.
6. Hardie DG. Minireview: the AMP-activated protein kinase cascade: the key sensor of cellular energy status. Endocrinology 2003;144:5179-5183.
7. Hardie DG, Salt IP, Hawley SA, Davies SP. AMP-activated protein kinase: an ultrasensitive system for monitoring cellular energy charge. Biochem J 1999;338 (Pt 3):717-722.
8. Kahn BB, Alquier T, Carling D, Hardie DG. AMP-activated protein kinase: ancient energy gauge provides clues to modern understanding of metabolism. Cell Metab 2005;1:15-25.
9. Igata M, Motoshima H, Tsuruzoe K, Kojima K, Matsumura T, Kondo T, Taguchi T, et al. Adenosine monophosphate-activated protein kinase suppresses vascular smooth muscle cell proliferation through the inhibition of cell cycle progression. Circ Res 2005;97:837-844.
10. Jones RG, Plas DR, Kubek S, Buzzai M, Mu J, Xu Y, Birnbaum MJ, et al. AMP-activated protein kinase induces a p53-dependent metabolic checkpoint. Mol Cell 2005;18:283-293.
11. Imamura K, Ogura T, Kishimoto A, Kaminishi M, Esumi H. Cell cycle regulation via p53 phosphorylation by a 5'-AMP activated protein kinase activator, 5-

aminoimidazole- 4-carboxamide-1-beta-D-ribofuranoside, in a human hepatocellular carcinoma cell line. Biochem Biophys Res Commun 2001;287:562-567.

12. Caligiuri A, Bertolani C, Guerra CT, Aleffi S, Galastri S, Trappoliere M, Vizzutti F, et al. Adenosine monophosphate-activated protein kinase modulates the activated phenotype of hepatic stellate cells. Hepatology 2008;47:668-676.
13. Adachi M, Brenner DA. High molecular weight adiponectin inhibits proliferation of hepatic stellate cells via activation of adenosine monophosphate-activated protein kinase. Hepatology 2008;47:677-685.
14. Jorgensen SB, Viollet B, Andreelli F, Frosig C, Birk JB, Schjerling P, Vaulont S, et al. Knockout of the alpha2 but not alpha1 5'-AMP-activated protein kinase isoform abolishes 5-aminoimidazole-4-carboxamide-1-beta-4-ribofuranosidebut not contraction-induced glucose uptake in skeletal muscle. J Biol Chem 2004;279:1070-1079.
15. Da Silva Morais A, Abarca-Quinones J, Horsmans Y, Starkel P, Leclercq IA. Peroxisome proliferated-activated receptor gamma ligand, Pioglitazone, does not prevent hepatic fibrosis in mice. Int J Mol Med 2007;19:105-112.
16. Leclercq IA, Farrell GC, Schriemer R, Robertson GR. Leptin is essential for the hepatic fibrogenic response to chronic liver injury. J Hepatol 2002;37:206-213.
17. Livak KJ, Schmittgen TD. Analysis of relative gene expression data using real-time quantitative PCR and the 2(-Delta Delta C(T)) Method. Methods 2001;25:402-408.
18. Mitchelhill KI, Stapleton D, Gao G, House C, Michell B, Katsis F, Witters LA, et al. Mammalian AMP-activated protein kinase shares structural and functional homology with the catalytic domain of yeast Snf1 protein kinase. J Biol Chem 1994;269:2361-2364.
19. Guigas B, Bertrand L, Taleux N, Foretz M, Wiernsperger N, Vertommen D, Andreelli F, et al. 5-Aminoimidazole-4-carboxamide-1-beta-D-ribofuranoside and metformin inhibit hepatic glucose phosphorylation by an AMP-activated protein kinase-independent effect on glucokinase translocation. Diabetes 2006;55:865-874.
20. Inoki K, Zhu T, Guan KL. TSC2 mediates cellular energy response to control cell growth and survival. Cell 2003;115:577-590.
21. Luo Z, Saha AK, Xiang X, Ruderman NB. AMPK, the metabolic syndrome and cancer. Trends Pharmacol Sci 2005;26:69-76.
22. Wallace K, Burt AD, Wright MC. Liver fibrosis. Biochem J 2008;411:1-18.

23. Imamura M, Ogawa T, Sasaguri Y, Chayama K, Ueno H. Suppression of macrophage infiltration inhibits activation of hepatic stellate cells and liver fibrogenesis in rats. Gastroenterology 2005;128:138-146.
24. Knittel T, Dinter C, Kobold D, Neubauer K, Mehde M, Eichhorst S, Ramadori G. Expression and regulation of cell adhesion molecules by hepatic stellate cells (HSC) of rat liver: involvement of HSC in recruitment of inflammatory cells during hepatic tissue repair. Am J Pathol 1999;154:153-167.
25. Mahlapuu M, Johansson C, Lindgren K, Hjalm G, Barnes BR, Krook A, Zierath JR, et al. Expression profiling of the gamma-subunit isoforms of AMP-activated protein kinase suggests a major role for gamma3 in white skeletal muscle. Am J Physiol Endocrinol Metab 2004;286:E194-200.
26. Martin KA, Blenis J. Coordinate regulation of translation by the PI 3-kinase and mTOR pathways. Adv Cancer Res 2002;86:1-39.
27. Sakamoto K, Hirshman MF, Aschenbach WG, Goodyear LJ. Contraction regulation of Akt in rat skeletal muscle. J Biol Chem 2002;277:11910-11917.
28. Shaw RJ, Bardeesy N, Manning BD, Lopez L, Kosmatka M, DePinho RA, Cantley LC. The LKB1 tumor suppressor negatively regulates mTOR signaling. Cancer Cell 2004;6:91-99.
29. Gwinn DM, Shackelford DB, Egan DF, Mihaylova MM, Mery A, Vasquez DS, Turk BE, et al. AMPK phosphorylation of raptor mediates a metabolic checkpoint. Mol Cell 2008;30:214-226.
30. Huang X, Wullschleger S, Shpiro N, McGuire VA, Sakamoto K, Woods YL, McBurnie W, et al. Important role of the LKB1-AMPK pathway in suppressing tumorigenesis in PTEN-deficient mice. Biochem J 2008;412:211-221.
31. Nagata D, Takeda R, Sata M, Satonaka H, Suzuki E, Nagano T, Hirata Y. AMP-activated protein kinase inhibits angiotensin II-stimulated vascular smooth muscle cell proliferation. Circulation 2004;110:444-451.
32. Rattan R, Giri S, Singh AK, Singh I. 5-Aminoimidazole-4-carboxamide-1-beta-D-ribofuranoside inhibits cancer cell proliferation in vitro and in vivo via AMP-activated protein kinase. J Biol Chem 2005;280:39582-39593.

This manuscript is still under preparation

The authors will be: Alain da Silva Morais[1]

Jorge Abarca-Quinones[1]

Bruno Guigas[2,3]

Benoit Viollet[4,5]

Peter Stärkel[1]

Isabelle A. Leclercq[1].

[1]Gastroenterology Laboratory, Université catholique de Louvain (UCL), Brussels, Belgium; [2]Hormone and Metabolic Research Unit, Université catholique de Louvain (UCL) and de Duve Institute, Brussels, Belgium; [3]Department of Molecular Cell Biology, Leiden University Medical Center, Leiden, The Netherlands; [4]Department of Endocrinology, Metabolism and Cancer and [5]INSERM U567, CNRS UMR 8104, Institut Cochin, Université Paris 5, Paris, France.

I will thank them for their precious contribution.

Financial support:

This work was supported by grant from the Belgian 'Fonds National de la Recherche scientifique" (FNRS conventions n°3.4507.04 and 3.4578.07), by grant ARC-05/10-328 (Action de Recherche Concertée de la Direction de la Recherche Scientifique de la Communauté Française de Belgique), and by grant from the university (Fonds Spécial de Recherche, Université catholique de Louvain) to Isabelle A. Leclercq. BG was recipient of the ICP "Michel de Visscher" Fellowship. IL is research associate with the FNRS.

Acknowledgments

We thank Professor Louis Hue, Hormone and Metabolic Research Unit, Université catholique de Louvain (UCL) and de Duve Institute, for critical reading of the manuscript. Anti-AMPKα1 and anti-AMPKα2 antibodies provided by G. Hardie from Dundee University, Dundee, Scotland.

Study 3: Prevention of steatohepatitis by pioglitazone: implication of adiponectin-dependent inhibition of SREBP-1c and inflammation

NASH associates steatosis, inflammation, fibrosis and insulin resistance (176). PPARγ agonist drugs are used in the treatment of diabetes (94). They favour fat storage in adipose tissue, reduce the release of FFA and metabolic anti-inflammatory mediators by adipose tissue and restore insulin sensitivity. PPARγ activation by pioglitazone or rosiglitazone improves NASH development in human (102, 103, 105). In mice pioglitazone prevents MCD-induced steatohepatitis development. However, the mechanism implicated in this preventive effect of pioglitazone remains ill-clarified. Circulating levels of adiponectin, an adipocytokine with anti-inflammatory and insulin-sensitising properties, is decreased in NASH patients (132). Adiponectin, trough its specific receptors, activates AMPK and PPARα, involved in the regulation of lipid and glucose metabolism as well as in the control of inflammatory reaction (88, 177, 178).

In order to test whether the beneficial effects of PPARγ agonists on steatohepatitis are dependent on adiponectin, we compared the effects of pioglitazone on MCD-induced steatohepatitis in control mice and mice lacking adiponectin. We observe that PGZ treatment does not prevent the steatohepatitis development in mice lacking adiponectin by contrast with wild type mice. Thus, our data demonstrate that the beneficial effect of PGZ on MCD-induced steatohepatitis in mice is strictly dependent on adiponectin.

To evaluate whether it involves adiponectin receptor-dependent activation of AMPK and/or PPARα, we analyse those cellular pathways in MCD-fed wild type mice and mice lacking the AMPKα1 catalytic subunit with and without pioglitazone. We show that PGZ treatment is apparently not associated with increased AMPK activity, nor with signs of PPARα activation, in MCD-induced steatohepatitis. By contrast, we observe the inhibition of SREBP-1c by pioglitazone treatment suggesting that the repression of *de novo* lipogenesis by pioglitazone is likely to participate to beneficial effect of this drug on steatohepatitis.

The mechanisms by which PGZ and adiponectin control SREBP-1c and inflammation remain to be elucidated.

This study is presented next will be published in *Journal of Hepatology* (available online).

Study 3

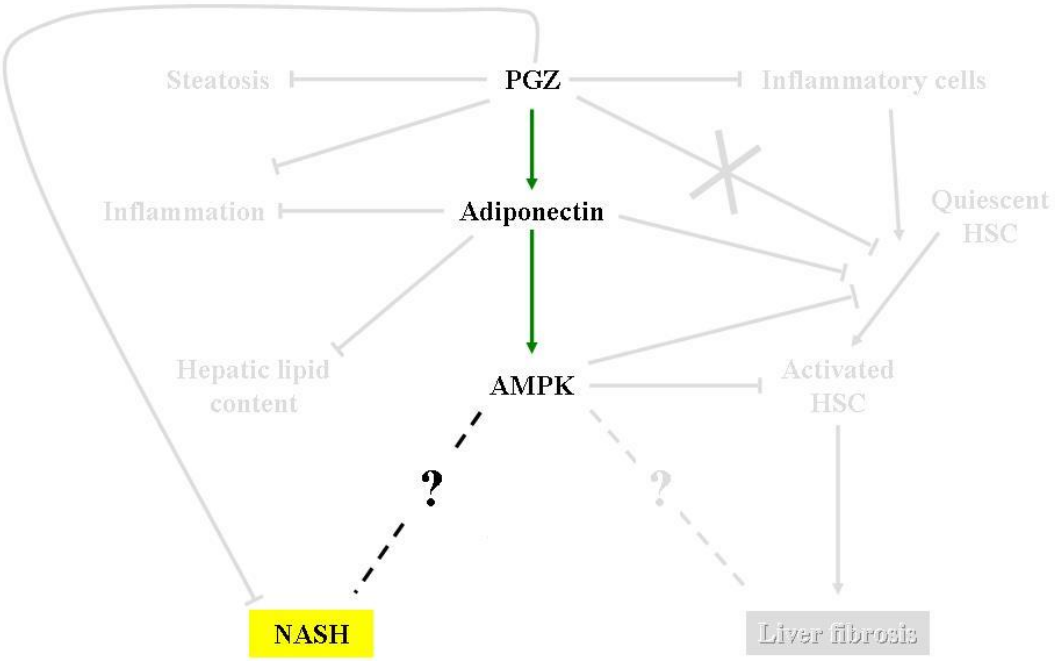

Figure 19: Evaluation of the impact of the axis PGZ-adiponectin-AMPK on NASH development in mice

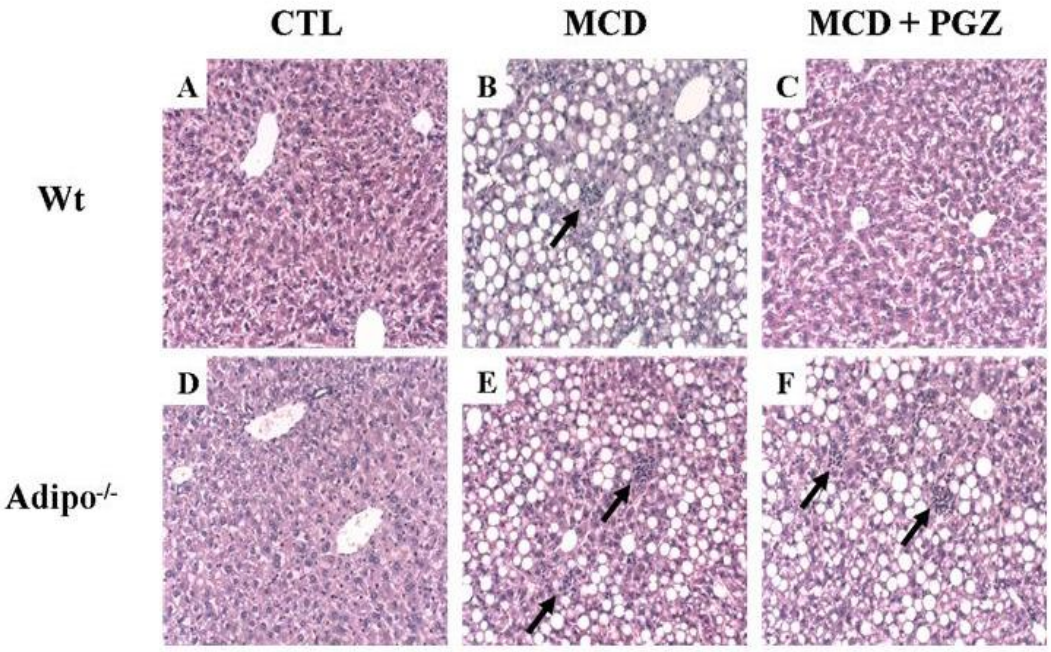

The preventive effect of PGZ on MCD-induced steatohepatitis is dependent on adiponectin

A. Da Silva Morais et al. / Journal of Hepatology xxx (2009) xxx-xxx

Journal of Hepatology

Prevention of steatohepatitis by pioglitazone: Implication of adiponectin-dependent inhibition of SREBP-1c and inflammation ☆

Alain Da Silva Morais [1], Valérie Lebrun [1], Jorge Abarca-Quinones [1], Sonia Brichard [2], Louis Hue [3], Bruno Guigas [3,4], Benoit Viollet [5,6], Isabelle A. Leclercq [1,*]

[1]*Laboratoire de Gastro-entérologie, Université catholique de Louvain, GAEN 53/79, Avenue Mounier, 53, B-1200 Brussels, Belgium*
[2]*Endocrinology and Metabolism Unit, Université catholique de Louvain (UCL), Brussels, Belgium*
[3]*Hormone and Metabolic Research Unit, Université catholique de Louvain (UCL) and Institute of Cellular Pathology, Brussels, Belgium*
[4]*Department of Molecular Cell Biology, Leiden University Medical Center, Leiden, The Netherlands*
[5]*Department of Endocrinology, Metabolism and Cancer*
[6]*INSERM U567, CNRS UMR 8104, Institut Cochin, Universite´ Paris 5, Paris, France*

Background/Aims: Peroxisome proliferator-activated receptor gamma (PPARγ) agonist drugs, like pioglitazone (PGZ), are proposed as treatments for steatohepatitis. Their mechanisms of action remain ill-clarified.

Methods: To test the hypothesis that PGZ improves steatohepatitis through adiponectin-dependent stimulation of AMPK and/or PPARα, mice licking adiponectin (Adipo$^{-/-}$) or the AMPKα1 catalytic subunit (AMPKα1$^{-/-}$) or wild-type (Wt) mice were fed the methionine and choline deficient (MCD) diet, supplemented or not with PGZ.

Results: In Wt mice, PGZ increased circulating levels of adiponectin and reduced the severity of MCD-induced steatohepatitis but there was no evidence of activation of AMPK or PPARα and their downstream targets. By contrast, PGZ completely repressed nuclear translocation of SREBP-1c, a key transcription factor for de novo lipogenesis. This effect was lacking in Adipo$^{-/-}$ mice in which PGZ failed to prevent steatohepatitis. Surprisingly, AMPKα1$^{-/-}$ mice were resistant to MCD-induced steatohepatitis, a status also associated with repression of SREBP-1c.

Conclusion: The preventive effect of PGZ on MCD-induced steatohepatitis depends on adiponectin upregulation but apparently does not involve AMPK or PPARα activation. The inhibition of SREBP-1c and dependent repression of lipogenesis are likely to participate in this effect. The mechanisms by which PGZ and adiponectin control SREBP-1c and inflammation remain to be elucidated.

Keywords: MCD diet; AMPK; PPARalpha; SREBP-1c; Mouse

Received 26 August 2008; received in revised form 4 October 2008; accepted 11 October 2008
Associate Editor: C.P. Day

☆ The authors declare that they do not have anything to disclose regarding funding from industries or conflict of interest with respect to this manuscript.

*Corresponding author. Tel.: +32 2 764 52 73; fax: +32 2 764 53 46.
E-mail address: isabelle.leclercq@uclouvain.be (I.A. Leclercq).

Abbreviations: Adipo, adiponectin; AdipoR, adiponectin receptor; AMPK, AMP-activated protein kinase; ACC, acetyl-CoA carboxylase; ACO, acyl CoA oxidase; cDNA, complementary deoxyribonucleic acid; FA, fatty acid; FAS, fatty acid synthase; HSP-90, heat shock protein 90; IκBα, inhibitor of NF-κB alpha; MCD, methionine and choline deficient; mTOR, mammalian target of rapamycin; NASH, non-alcoholic steatohepatitis; NF-jB, nuclear factor-kappa B; p70S6K, p70 *Ribosomal* S6 Kinase, PGC-1α, peroxisome proliferator-activated receptor-gamma coactivator 1 alpha; PGZ, pioglitazone; PPAR, peroxisome proliferator-activated receptor; RPL19, ribosomal protein L19; SCD-1, stearoyl-CoA desaturase 1; SREBP-1c, sterol regulatory element binding protein 1c; TNF, tumor necrosis factor; Wt, wild-type.

0168-8278/$34.00
doi:10.1016/j.jhep.2008.10.027

DOCTOPIC: Cirrhosis and its Complications

Please cite this article in press as: Da Silva Morais A et al., Prevention of steatohepatitis by pioglitazone: Implication of ..., J Hepatol (2008), doi:10.1016/j.jhep.2008.10.027

1. Introduction

Non-alcoholic steatohepatitis (NASH), histologically characterised by steatosis, hepatocellular damage, inflammation and variable fibrosis, is often seen in patients with obesity and/or insulin resistance [1]. NASH is therefore now recognised as the hepatic complication of the metabolic syndrome [2]. To date, there is no con-sensus on efective therapy [3]. Clinical studies provide evidence that insulin-sensitizing thiazolidinedione (TZD) drugs may be beneficial [4-6]. The mechanism of action of TZD in NASH is however incompletely understood. Three strategies of action, possibly acting in synergy, could be proposed: (i) TZD stimulate adipocyte proliferation and fat mass expansion favouring the storage of fat in adipose tissue, sparing peripheral tissues, such as liver, from fat accumulation and lipotoxicity [7], (ii) TZD modulate adipocytokine release, in particular they induce the production of adiponectin, favouring increased fatty acid (FA) oxidation, decreased lipogenesis [8] and decreased inflammation and/or (iii) TZD may modulate lipid metabolism, hepatic inflammation and fibrosis by activation of peroxisome proliferator-activated receptor gamma (PPARγ), PPARα, adiponectin or other cytokines [9-11].

TZD induces the expression of adiponectin by the adipose tissue, and adiponectin is believed to mediate some of the TZD's metabolic effects in target tissues, in particular, insulin sensitization [12]. Adiponectin increases FA β-oxidation in muscle [13] and decreases hepatic lipid content in ob/ob mice [14]. Also, adiponectin has direct anti-fibrotic [15] and anti-inflammatory properties [16].

In the liver, adiponectin signals through two receptors, AdipoR1 and AdipoR2, which activate two distinct pathways. AdipoR1 is ubiquitously expressed, while AdipoR2 is most abundantly expressed in the liver [17]. Downstream of AdipoR1, adiponectin activates the AMP-activated protein kinase (AMPK), a pivotal kinase for the regulation of cellular energy homeostasis. In particular, activation of AMPK stimulates FA β-oxidation and inhibits hepatic *de novo* lipogenesis [18,19]. Activated, AMPK also negatively regulates transcription and activation of sterol regulatory element binding protein-1c (SREBP-1c), which controls the expression of nearly all genes required for de novo synthesis of FAs and triglyceride synthesis [18]. AdipoR2 preferentially recruits PPARα, to stimulate oxidation of lipids and prevent inflammation through inhibition of NF-κB [16].

We previously demonstrated that pioglitazone (PGZ), a synthetic PPARγ activator, prevents steatohepatitis in mice [20]. In this work, we used adiponectin deficient mice (Adipo-/-) to determine whether adiponectin is required for the preventive effect of PGZ. In order to assess the pathway recruited by adiponectin, we analysed the PPARα and AMPK pathways and used mice with impaired AMPK activity.

2. Materials and methods

2.1. Animals studies

AMPKα1 null-mice (AMPKα1$^{-/-}$) and AMPKα1$^{+/+}$ littermates were kindly provided by B. Viollet, Institut Cochin, Paris [21]. Adiponectin-knockout mice (Adipo$^{-/-}$) [22] were bred in our animal facility. C57BL6/J (Wt) mice were used as controls. All animals were kept in a temperature and humidity-controlled environment in a 12 h light-dark cycle. At all times, they were allowed free access to water and diet. The animals were handled according to the guidelines for humane care for laboratory animals in accordance with EU Regulation and the study protocol was approved by the local ethics committee.

Female (10 weeks old) Adipo$^{-/-}$, AMPKα1$^{-/-}$ and control mice were randomly assigned to one of the 3 dietary groups and received (a) a standard powdered diet (Pavan Service Carfil Quality, Belgium) (control group), (b) a methionine-choline deficient diet (cat. no 960439, ICN, USA) (MCD group) or (c) a MCD diet supplemented with PGZ 0.01% (*wt/wt*) (MCD + PGZ group) for 5 weeks (n = 5 mice/group). At the time of sacrifice (between 8:00 and 10:00 AM), blood was collected, the liver rapidly excised and weighed. A part of the liver was fixed in 4% formalin, the other immediately snap-frozen and kept at _80 °C until use.

In a separate experiment, C57BL6/J mice received a single dose of PGZ (100 mg/kg body weight) by gavage and were sacrificed after 0, 30 min, 12 h, 24 h, and 48 h (n = 5-6 mice/time point).

2.2. Total RNA extraction, Reverse Transcription and Quantitative PCR

Total RNA was extracted using TRIpure Isolation Reagent (Roche Diagnostics, Belgium). cDNA were synthesized and served as template to quantitate hepatic mRNA expression using real time PCR as previously described [23]. Primer pairs for transcripts of interest were designed using the Primer Express design software (Applied Biosystems) and listed in Table 1. RPL19 RNA was chosen as an invariant standard. Results were expressed as fold expression relative to expression in the control group (value set at 1) using the delta Ct method [23].

2.3. Western blot analyses

Liver homogenates, nuclear extracts and cytosolic fractions were prepared and protein concentrations determined as described else-where [24]. Proteins were separated by SDS-PAGE and transferred onto PVDF membrane (PolyScreen, NEN Life Science Products, USA). The membranes were then exposed to antibodies raised against:
AMPKα1, AMPKα2, phospho-AMPKα (Thr 172) (Cell Signaling, USA), SREBP-1c (Santa-Cruz, USA), phospho-mTOR (Thr 2446) (Cell Signaling, USA), mTOR (Cell Signaling, USA), phospho-p70S6K (Thr 389) (Cell Signaling, USA), p70S6K (Cell Signaling, USA), Ikbα (Santa-Cruz, USA). The quantification of immune-reactive proteins was obtained by densitometry using the Gel Doc™ XR System 170-8170 device and software (Bio-Rad, USA). Expression of Heat Shock Protein (HSP)-90 (BD Transduction Laboratories, USA) or b-actin (Sigma, Germany) was used as a loading control.

2.4. AMPK assay

Total AMPK activity was assayed on liver homogenates after precipitation with 10% (*wt/v*) poly(ethylene glycol) 6000 (Merck, Belgium) [25]. 100 µg protein from liver homogenates were immunoprecipitated with protein-G-sepharose and isoform specific antibodies to the α1 or α2 catalytic subunits of AMPK (Cell Signaling) measure the AMPKα1 and α2 activities [26]. One unit of AMPK activity corresponds to 1 nmol of product formed per min under the assay conditions.

Table 1
Sequences of primers.

Gene	Primer sequences	GeneBank accession #
ACO	Forward: 5' -CACAGCAGTGGGATTCCAAAT-3' Reverse: 5' -CGTCTGCAGCATCATAACAGTGT-3'	NM_015729
FAS	Forward: 5 -GATCCTGGAACGAGAACACGAT-3' Reverse: 5 -AGAGACGTGTCACTCCTGGACTT-3	NM_007988
IκBα	Forward: 5' -CGCTTGGTGGACGATCG-3' Reverse: 5' -TTGCTCGTACTCCTCGTCCTTC-3	NM_010907
PPARa	Forward: 5' -CAACGGCGTCGAAGACAAA-3 Reverse: 5' -TGACGGTCT CCACGGACAT-3'	NM_011144
PGC-1a	Forward: 5 -CAAGCCAAACCAACAACTTTATCTCT-3 Reverse: 5 -CACACTTAAGGTGCGTTCAATAGTC-3	NM_008904
RPL19	Forward: 5' -GAAGGTCAAAGGGAATGTGTTCA-3' Reverse: 5' -ACAAGCTGAAGGCAGACAAGG-3'	NM_009078
SCD-1	Forward: 5' -CCAGAATGACGTGTACGAATGG-3 Reverse: 5 -GCGTGTGTTTCTGAGAACTTGTG-3	NM_009127
SREBP-1c	Forward: 5' -CTGGCACTAAGTGCCCTCAAC-3' Reverse: 5' -GCCACATAGATCTCTGCCAGTGT-3'	NM_011480

ACO, acyl coenzyme-A oxidase; FAS, fatty acid synthase; IκBα, inhibitor of NFκB alpha; PGC-1α, peroxisome proliferator-activated receptor gamma coactivator 1 alpha; PPARα, peroxisome proliferator-activated receptor alpha; RPL19, ribosomal protein L19; SCD-1, stearoyl-CoA desaturase 1; SREBP-1c, sterol regulatory element binding protein 1c.

2.5. Histology examination

Hepatic steatosis was assessed on haematoxylin/eosin-stained liver sections as the percentage of hepatocytes containing lipid vacuoles. Hepatic inflammation was quantified as the ratio of the area of inflam-matory foci (defined as groups of five or more inflammatory cells) to the total area of the section [27].

2.6. Biochemical assays

The level of adiponectin in serum was determined using a mouse adiponectin RIA kit (Linco Research, USA). Total liver lipid were extracted using methanol and chloroform and quantitated using the vanillin-phosphoric acid reaction [20].

2.7. Statistical analysis

Results are expressed as mean ± SD. Statistical differences between groups were tested using one way analysis of variance (ANOVA). Statistical significance was assumed for $p < 0.05$.

3. Results

3.1. Pioglitazone prevents MCD diet-induced steatohepatitis

Wild-type C57BL6/J mice fed the MCD diet develop macrovesicular steatosis and foci of mixed inflammation (Fig. 1B). Consistent with a previous report [20], PGZ reduced the severity of steatohepatitis induced by MCD diet as seen on histopathology (Fig. 1C) and confirmed by a significant decrease in hepatic lipid content and in hepatic inflammatory area (Table 2). While not significantly affected by MCD diet alone, PGZ induced a 6-fold increase in serum adiponectin level (Table 2).

3.2. The anti-steatohepatitis effect of pioglitazone is dependent on adiponectin

Adipo$^{-/-}$ mice fed MCD diet developed a significant steatohepatitis, although of lesser severity than Wt mice (Fig. 1E and Table 2). By contrast to Wt mice, PGZ treatment did not prevent the MCD-induced steatohepatitis in Adipo$^{-/-}$ mice (Fig. 1F). PGZ had no impact on hepatic inflammation and, if anything worsened the hepatic lipid accumulation induced by the MCD diet (Table 2). These observations imply that the protective effect of PGZ on steatohepatitis depends on adiponectin.

3.3. Is an adiponectin-dependent activation of PPARa involved in the anti-steatohepatitis effect of PGZ?

Adiponectin through receptors AdipoR1 and R2 activates AMPK and PPARα, respectively [17].

Acyl-coA oxidase (ACO) is a PPARα-dependent, rate limiting enzyme in FA β-oxidation [28]. No changes in the mRNA levels of ACO were observed whatever the condition or strain considered (Fig. 2A). IκBα is a PPARα-regulated anti-inflammatory gene encoding for a protein that stabilise NF-κB under the inactive form [29]. Hepatic IκBα mRNA and protein levels were comparable in CTL and MCD-fed Wt mice. Administration of PGZ did not significantly induce IκBα (Fig. 2B and C). Similar results were obtained in Adipo$^{-/-}$ mice.

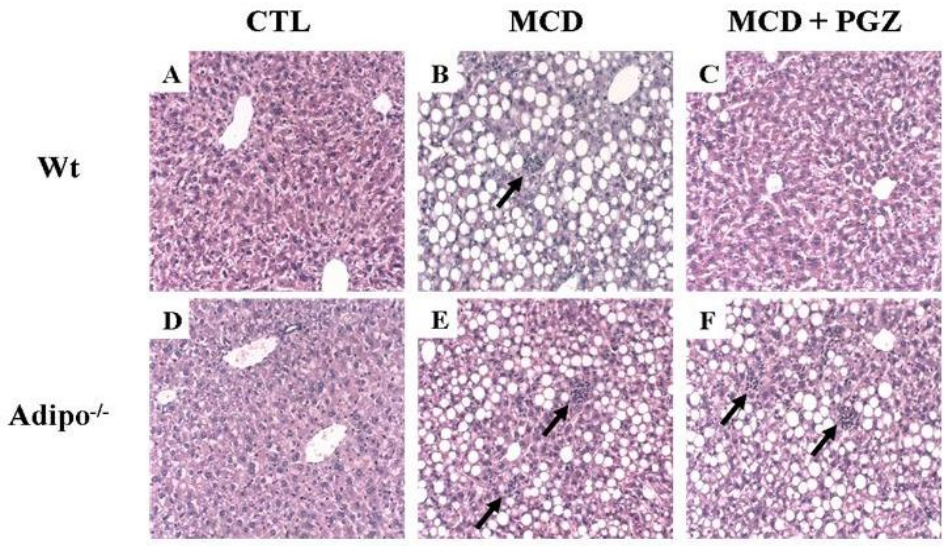

Fig. 1. The preventive effect of PGZ on MCD-induced steatohepatitis is dependent on adiponectin. Representative photomicrographs of haematoxylin/eosin-stained liver sections from C57BL6/J (Wt) and Adiponectin deficient (Adipo$^{-/-}$) mice fed the control diet (A and D), MCD diet (B and E) or PGZ-supplemented MCD diet (0.01% wt/wt) (C and F) for 5 weeks (n = 5 per group). Arrows point towards foci of inflammatory cells. Note that PGZ prevents steatosis and inflammation induced by the MCD diet in Wt but not in Adipo$^{-/-}$ mice.

3.4. Is an adiponectin-dependent activation of AMPK involved in the anti-steatohepatitis effect of PGZ?

In Wt mice, MCD diet did not alter Thr172 phosphorylation of AMPK (Fig. 3B) and AMPKα1/α2 activities (Fig. 3A). In PGZ-treated MCD-fed mice, we failed to evidence any changes in AMPK phosphorylation and activity (Fig. 3A and B). We therefore examined whether PGZ treatment induced activation of downstream targets of AMPK either by rapid phosphorylation or by longer-lasting gene regulation. Acetyl-CoA carboxylase (ACC) is directly phosphorylated and inactivated by AMPK [30]. PGZ treatment to MCD-fed mice did not significantly alter the phosphorylation state of ACC (Fig. 3B). AMPK is known to inactivate the mammalian Target of Rapamycin Complex 1 (mTORC1) by direct phosphorylation (Thr 2446) or by phosphorylation and activation of its upstream regulator, the tumor suppressor complex 2 (TSC2) [31]. Inhibition of mTOR leads to a decrease phosphorylation of the p70 *Ribosomal* S6 Kinase (p70S6K) [32]. MCD diet reduced mTOR expression but without significant change in the p-mTOR/mTOR or p-p70S6K/p70S6K ratio.

PGZ treatment did not alter mTOR expression, nor the phosphorylation state of mTOR and p70S6K (Fig. 3C). AMPK also regulates gene transcription, repressing ACC while increasing PGC1α gene expression [33]. As shown in Fig. 3D, in the liver of Wt mice, ACC mRNA levels were unaltered by MCD diet and PGZ treatment. MCD diet increased significantly PGC-1α mRNA but this expression was not enhanced by treatment with PGZ.

Activated AMPK negatively regulates SREBP-1c by repression of gene transcription and inhibition of nuclear translocation [18], leading to repression of lipogenic genes FAS and SCD-1. Administration of the MCD diet to Wt mice significantly decreased SREBP-1c mRNA, and PGZ further reduced those levels (Fig. 4A). Importantly, while the cytosolic pool of SREBP-1c protein remained unaffected by experimental conditions (Fig. 4B), nuclear SREBP-1c (nSREBP-1c), was virtually undetectable under PGZ treatment (Fig. 4C). Despite this, there was only a modest reduction in hepatic FAS mRNA (-20%) in PGZ treated MCD mice versus MCD-fed mice (Fig. 4D). As previously described [34], MCD diet repressed SCD-1 mRNA and PGZ induced no further change (not shown).

Table 2
Efect of PGZ on hepatic lipid content, inflammation and serum adiponectin.

Mouse strain	Hepatic lipid content (mg/100 mg liver ± SD)		Hepatic inflammation (% of total hepatic area ± SD[a])		Serum adiponectin (μg/ml ± SD)	
	Wt	Adipo$^{-/-}$	Wt	Adipo$^{-/-}$	Wt	Adipo$^{-/-}$
CTL	15.7 ± 1.1	15.6 ± 2.1	0.003 ± 0.002	0.004 ± 0.003	7.7 ± 2.3	<DL [b]
MCD	38. 9 ± 5.6 ***	25.6 ± 1.2$^{**,\$\$}$	0.4 ± 0.1***	0.2 ± 0.1$^{***,\$}$	11.1 ± 2.2	<DL [b]
MCD + PGZ	22.8 ± 3.2 $^{**,\#\#}$	31.3 ± 3.9$^{**,\#\#\#}$	0.1 ± 0.1$^{\#\#}$	0.2 ± 0.1	46.8 ± 2.1$^{***,\#\#\#}$	<DL [b]

$^{**}p < 0.01$ and $p < 0.001$ compared to CTL. $^{\#\#}p < 0.01$ and $^{\#\#\#}p < 0.001$ in PGZ treated compared to MCD. $^{\$}p < 0.05$ and $^{\$\$}p < 0.01$ in Adipo$^{-/-}$ versus Wt (C57BL6/J) fed the MCD diet for 5 weeks (n = 5 per group).

[a] See Section 2 for details on quantification.

[b] <DL: Below the detection limit for the assay used.

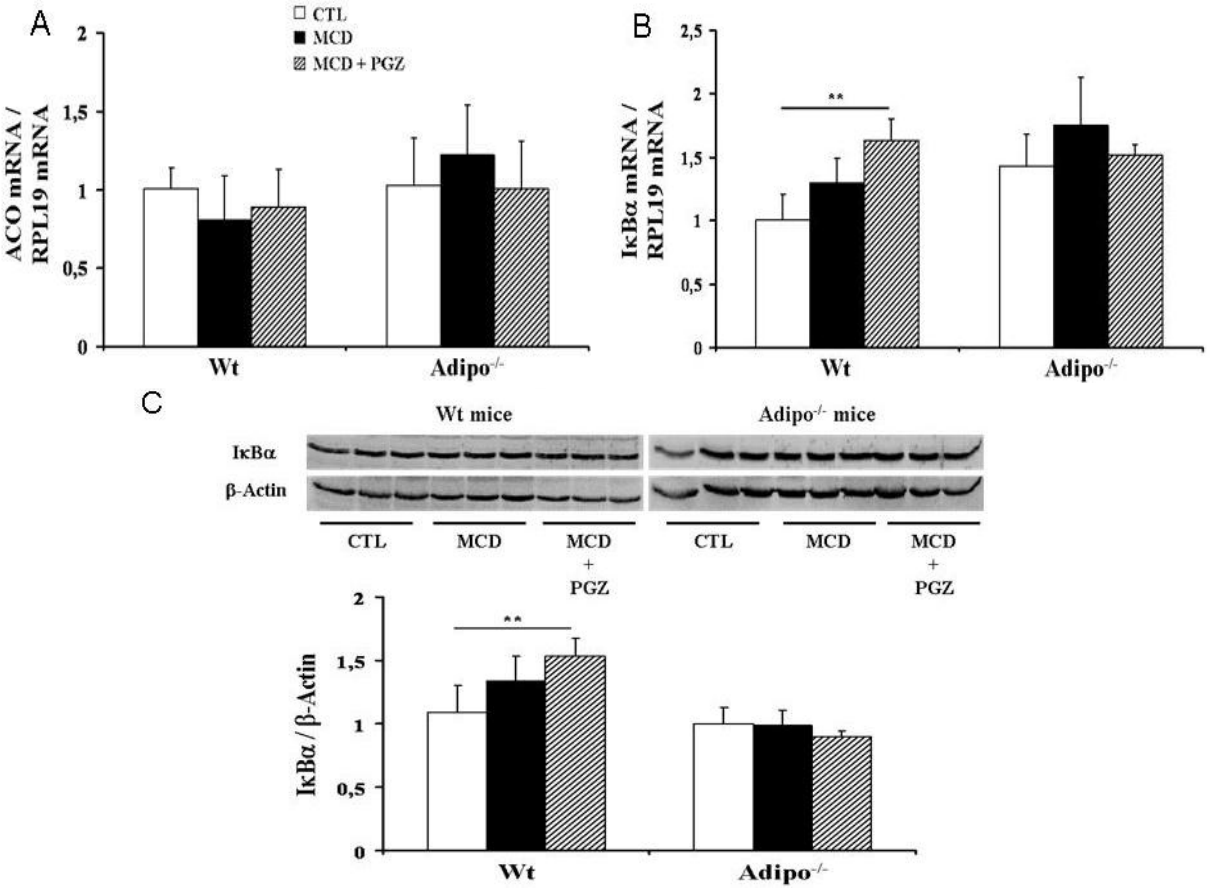

Fig. 2. The preventive effect of PGZ is not mediated trough PPARα pathway. Bar graphs of ACO (A) and IκBα (B) mRNA expression quantitated by RT-qPCR, and representative western blot for IκBα and b-actin (C) in livers of C57BL6/J (Wt) and Adipo$^{-/-}$ mice fed the control (open bar), the MCD (black bar) or the PGZ-supplemented MCD diets (hatched bar) for 5 weeks. mRNA results (mean ± SD) are normalised to the expression of RPL19 mRNA and protein results to that of b-actin (n = 5 per group).

3.5. AMPK targets in adiponectin-deficient mice

Compared to Wt mice, the deletion of the adiponectin gene did not significantly modify the phosphorylation (Fig. 3B) or the activity of AMPK (not shown) whether fed the control or the MCD diet with or without PGZ. Although lower than in Wt mice, ACC expression and phosphorylation were unchanged whether Adipo$^{-/-}$ mice were fed the CTL, the MCD or the MCD+PGZ diet (Fig. 3B). As in Wt mice there was a stepwise decrease in SREBP-1c mRNA levels in Adipo$^{-/-}$ mice when fed the control, the MCD or the MCD+PGZ diet (Fig. 4A). In sharp contrast to Wt mice, in Adipo$^{-/-}$ mice, no decrease in nSREBP-1c was seen upon MCD diet and no abolition of this signal upon PGZ treatment (Fig. 4C). Also, no change in FAS mRNA was seen in response to PGZ (Fig. 4D).

Together, those observations suggest that decreased SREBP-1c and alleged consequences on lipogenesis may represent an adiponectin-dependent mechanism by which PGZ ameliorates steatohepatitis. However, in the absence of demonstrated change in AMPK activity, it is difficult to assume that adiponectin-dependent activation of AMPK mediates this effect.

3.6. AMPKα1$^{-/-}$ are resistant to MCD diet-induced steatohepatitis

As AMPK stimulates β-oxidation and inhibits lipogenesis, we hypothesized that mice with deficient AMPK activity would develop worse steatohepatitis under MCD diet and would be insensitive to the protective effect of PGZ if this effect is AMPK-dependent.

The absence of AMPKα1 catalytic subunit in the liver of AMPKα1$^{-/-}$ was not compensated for by an increase in α2 expression or activity (Fig. 5A-C). This resulted in a lower phosphorylation of AMPK (Fig. 5A) and an 80% decrease in total AMPK activity (not shown), which was not modulated by MCD diet or PGZ (Fig. 5A-C).

Liver histology appeared normal in CTL-fed AMPKα1$^{-/-}$ mice (Fig. 6A and D). MCD diet induced a macrovesicular hepatic steatosis in AMPKα1$^{+/+}$ mice (Fig. 6B) but the severity of hepatic inflammation was however lower than observed in Wt C57BL6/J mice (Tables 2 and 3). This may be explained by differences in genetic backgrounds [35,36]. Surprisingly, MCD-induced steatohepatitis was far less severe AMPKα1$^{-/-}$ than in $^{+/+}$ littermates (Fig. 6E), as confirmed by

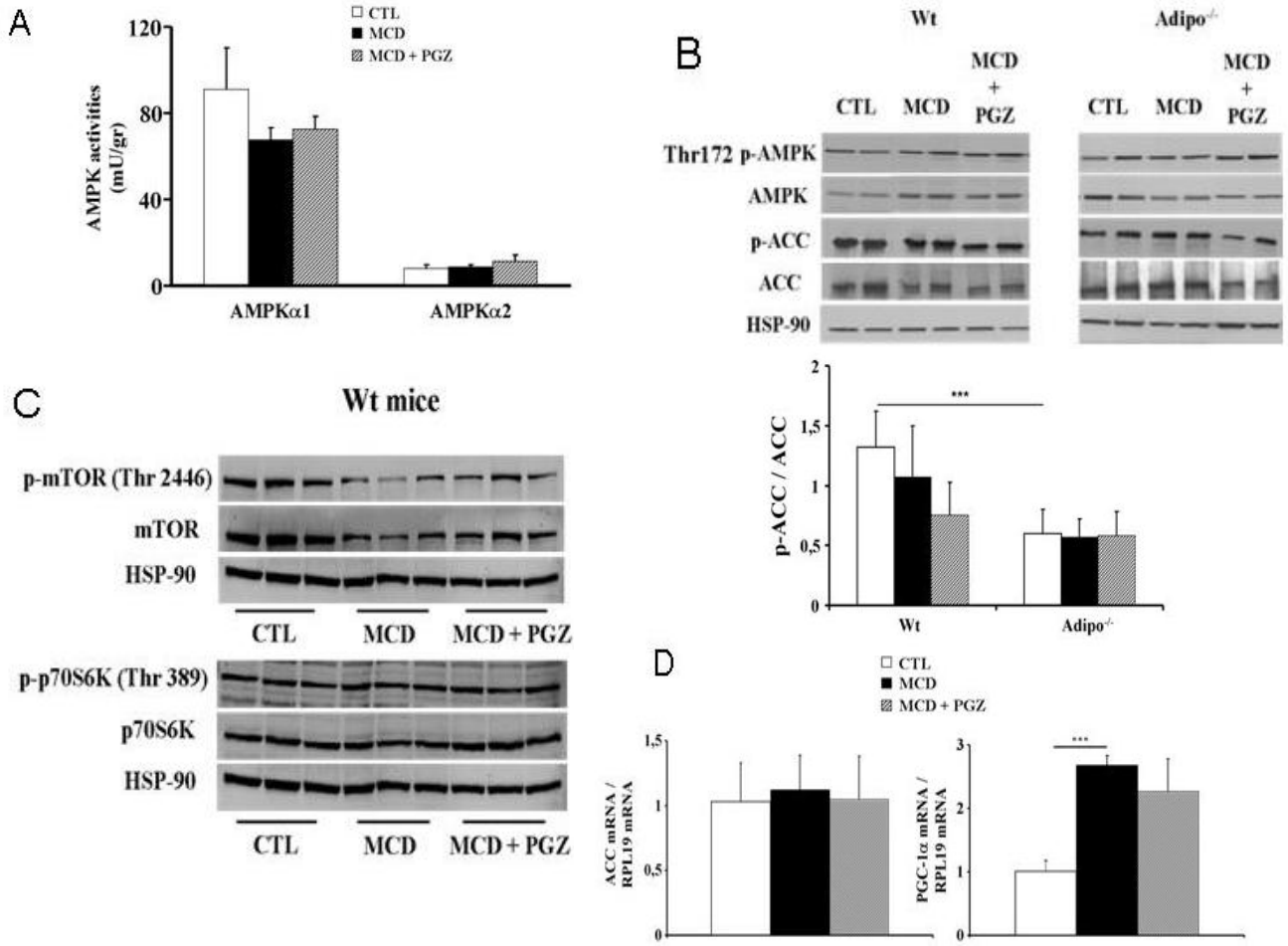

Fig. 3. Administration of PGZ does not alter AMPK activity. (A) Bar graph represents hepatic AMPKa1 and AMPKa2 activities, measured as described in Section 2. (B) Representative western blot for phosphoThr172-AMPK (p-AMPK) and total AMPK, phosphoSer79-ACC (p-ACC) and ACC and HSP-90. The bar graph represents p-ACC/ACC ratio determined by densitometric analysis and expressed as arbitrary units. (C) Representative western blot for phospho-mTOR (Thr 2446) (p-mTOR), mTOR, phospho-p70S6K (Thr 389) (p-p70S6K) and p70S6K and HSP90, and (D) ACC and PGC-1α mRNA expression quantitated by RT-qPCR in Wt mice fed the control (open bar), the MCD (black bar) or the PGZ-supplemented MCD diets (hatched bar) for 5 weeks (n = 5 per group). Data normalized to HSP90 for western blot or to the expression of RPL19 mRNA regarded as an invariant control for RT-qPCR are expressed in arbitrary units as mean ± SD (n = 5 per group). *** $p < 0.001$ compared to Wt CTL.

the quantification of inflammatory infiltration and hepatic lipid content (Table 3). Furthermore, irrespective of the size of fat droplets, the proportion of hepatocytes containing a vacuole of fat was also lower in AMPKα1$^{-/-}$ than in $^{+/+}$ mice (45 ± 20% versus 91 ± 5%, respectively; p = 0.004). PGZ ameliorated MCD-induced steatohepatitis in AMPKα1$^{+/+}$ but not in AMPKα1$^{-/-}$ mice, although it substantially increased adiponectin (Fig. 6F and Table 3).

SREBP-1c mRNA levels were similar in AMPKα1$^{+/+}$ and $^{-/-}$ livers under the control diet (Fig. 7A). As in Wt C57BL6/J, MCD diet decreased and PGZ abolished nSREBP-1c in AMPKα1$^{+/+}$. By contrast, nSREBP-1c was dramatically low in AMPKα1$^{-/-}$ fed control diet and completely abrogated under the MCD diet (Fig. 7B). In control conditions, despite the striking difference in nSREBP1c, FAS mRNA expression was similar in both genetic groups. However, abrogation of nSREBP-1c in mice fed MCD-diet is associated with a significant downregulation of FAS mRNA that remained unchanged under PGZ treatment (Fig. 7C).

These data support the proposition that AMPK activity is necessary for SREBP-1c activation and that chronic loss of nSREBP-1c may partly explain the resistance of AMPKα1$^{-/-}$ mice to MCD diet-induced steatohepatitis.

4. Discussion

In the present work, we report that pioglitazone (PGZ) is ineffective to prevent MCD-induced steatohepatitis in adiponectin-deficient mice. Several studies have proposed PPARγ agonists thiazolidinediones (TZD) as a therapeutic option for non-alcoholic steatohepatitis (NASH) [4,5,20]. Adiponectin, an adipocytokine partly by PPARγ, has been recognised as a pivotal mediator for TZD effects on glucose homeostasis, insulin sensitivity and lipid metabolism [7,8,12]. Circulating adiponectin levels were decreased in NASH patients [37] and TZD administration increased serum concentrations of adiponectin [38]. Previous studies [20,39] as well as the present data, consistently report the association

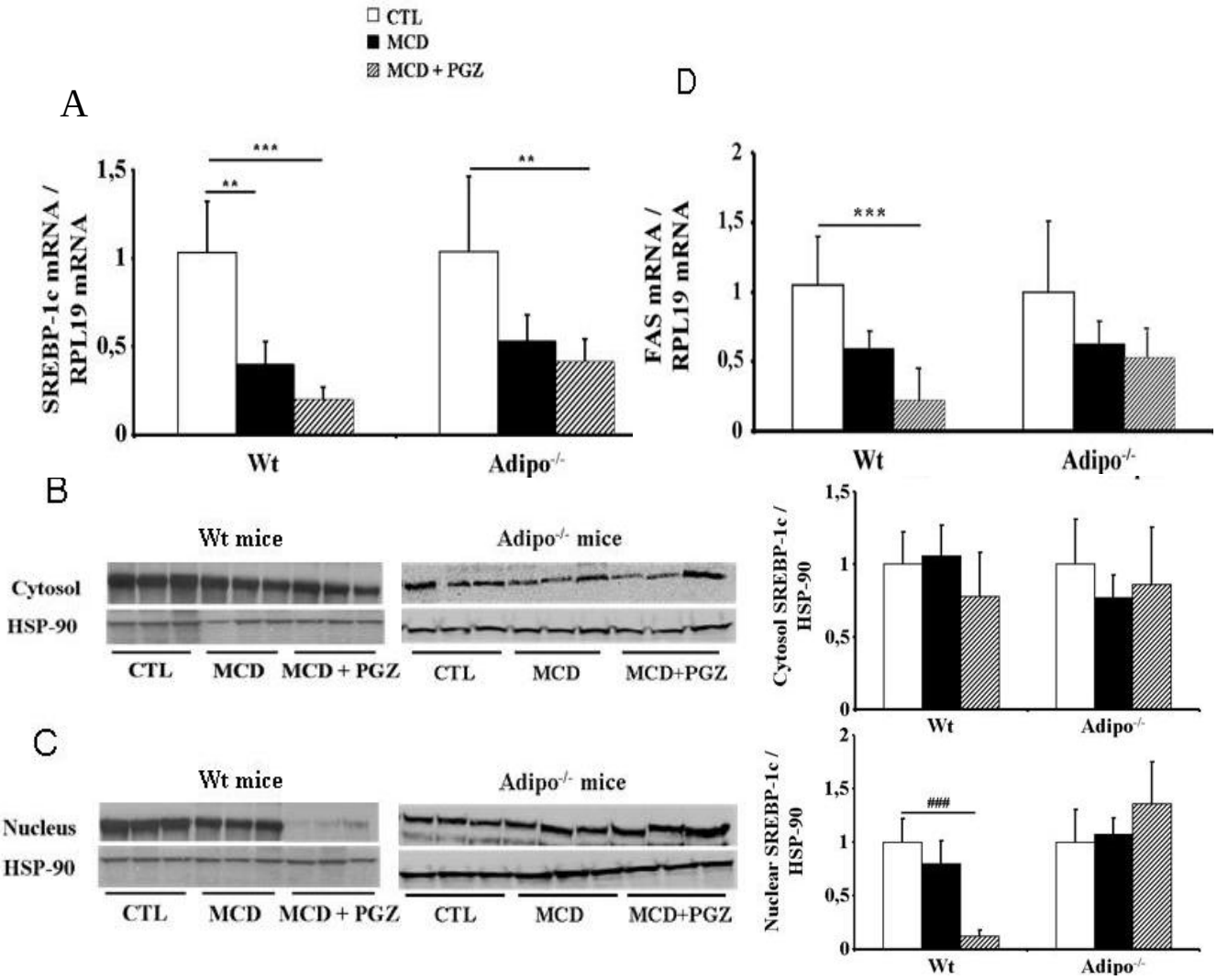

Fig. 4. Effect of MCD diet and PGZ on SREBP-1c, FAS and SCD-1 mRNA. Bar graph represents hepatic SREBP-1c mRNA expression quantitated by RT-qPCR (A), representative western blot for cytosol (B) and nuclear protein expressions of SREBP-1c (C) with bar graph of densitometric analysis, and (D) FAS mRNA expression quantitated by RT-qPCR in livers of Wt and Adipo$^{-/-}$ mice fed the control (open bar), the MCD (black bar) or the PGZ-supplemented MCD diets (hatched bar) for 5 weeks. Western blot data are normalized to HSP90 used as loading control, RT-qPCR data are normalised to the expression of RPL19 mRNA regarded as an invariant control. Data are expressed as mean ± SD Arbitrary Units (n = 5 per group). *** *p < 0.001* compared to CTL, $^{###}$ *p < 0.001* compared to MCD-fed mice.

between the beneficial effect of TZD on MCD diet-induced steatohepatitis and increased serum levels of adiponectin. The absence of PGZ effect in mice lacking adiponectin unambiguously establishes that PGZ reduces steatohepatitis in an adiponectin-dependent fashion in this model. Moreover, as obesity, hyperinsulinemia and insulin resistance are not pathogenically involved in MCD-steatohepatitis [40], mechanisms other that adiponectin-dependent insulin sensitization are likely to be implicated.

Adiponectin signals through two receptors. Their activation concurs with the decreases of hepatic de novo lipogenesis and the increase of FA oxidation [13,14]. In rodent livers, upon activation of AdipoR1, adiponectin increases AMPK activity, stimulates FA oxidation and suppresses endogenous glucose production [30,41]. In our study, despite elevated circulating levels of adiponectin by chronic PGZ treatment, we failed to evidence AMPK activation in the liver at the time point considered.

However, a single dose of PGZ increased serum adiponectin and liver AMPK activity (not shown), as it has been reported by others using short-term PGZ administration protocols [42,43]. The administration of the drug in a food mixture as well as the duration of the treatment may explain the absence of increased AMPK activity in our long-term in vivo study. This view is in accordance with the study of Bergheim et al. in which chronic administration of metformin, a potent activator of AMPK, was not associated with detectable changes in p-AMPK in mouse livers [44].

We evaluated activation of downstream targets of AMPK-dependent on rapid phosphorylation or on longer-lasting gene regulation. In cell culture systems, AMPK activation, obtained by exposure to the AMPK activator AICA riboside (AICAR) or by viral transfection of constitutively active form of AMPK, inhibits ACC and FAS gene transcription [45,46]. AMPK-dependent inhibition of SREBP-1c and of de novo lipogenesis has been observed after treatment with PGZ or administration

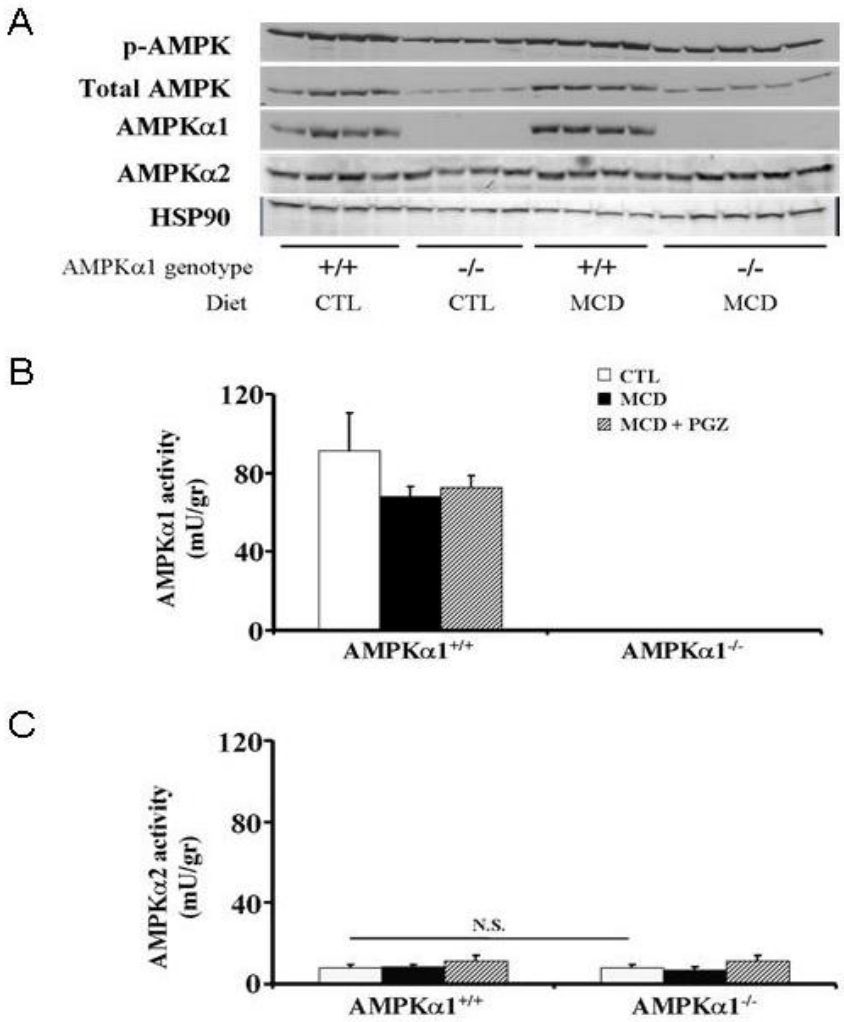

Fig. 5. AMPK activity and expression in AMPKα1$^{+/+}$ and AMPKα1$^{-/-}$ mice. (A) Representative western blot of phosphor(Thr172)-AMPK (p-AMPK), total AMPK, AMPKα1 and AMPKα2 in liver homogenates of AMPKα1$^{+/+}$ and AMPKα1$^{-/-}$ mice fed the control diet (CTL) or the MCD diet for 5 weeks (n = 5 per group). Western blot are normalized to HSP90 used as loading control. Bar graphs represent (B) AMPKα1 and (C) AMPKα2 activities in liver homogenates of AMPKα1$^{+/+}$ and AMPKα1$^{-/-}$ mice fed the control (open bar), the MCD (black bar) or the PGZ-supplemented MCD diets (hatched bar) for 5 weeks. (N.S. for not significant).

of AICAR in rats [47]. On the other hand, the expression of PGC-1α increases in rat skeletal muscle upon treatment with AICAR [48] while PGC-1α mRNA expression has been shown to be drastically reduced in hepatocytes lacking both AMPKα1 and α2 subunits [49]. In our model, hepatic mRNA levels of ACC, FAS, SREBP-1c and PGC-1α remained unchanged in mice fed the PGZ-supplemented MCD diet compared to mice fed the MCD diet alone. ACC and mTOR are well known downstream targets of AMPK [33]. ACC is a particularly sensitive marker of AMPK activation since, *in vitro*, maximal phosphorylation occurs when only a small proportion of AMPK has been phosphorylated [50]. We failed to evidence significant modification of phosphorylation of those substrates under PGZ treatment. In addition, AMPKα1 deficiency does not increase the susceptibility to MCD diet-induced steatohepatitis.

It is therefore tempting to conclude that AMPK is not implicated in mediating the adiponectin-dependent effect of PGZ on steatohepatitis.

ACC is a rate controlling enzyme for the synthesis of malonyl-CoA, a pivotal switch for lipid fate since it is a critical precursor for FA synthesis and a potent inhibitor of mitochondrial FA oxidation [19]. Total ACC protein, the ratio p-ACC/ACC, and presumably malonyl-CoA content, remained unchanged upon PGZ treatment. Moreover, PGZ treatment did not change the mRNA expression of ACO, a PPARα-regulated gene and key enzyme for FA b-oxidation. Based on those observations, increased lipid burning is unlikely to be involved in the anti-steatohepatitis effect of PGZ in this model.

In our study, as in others [36,51], MCD diet in Wt mice decreases nuclear translocation, and consequently activity of

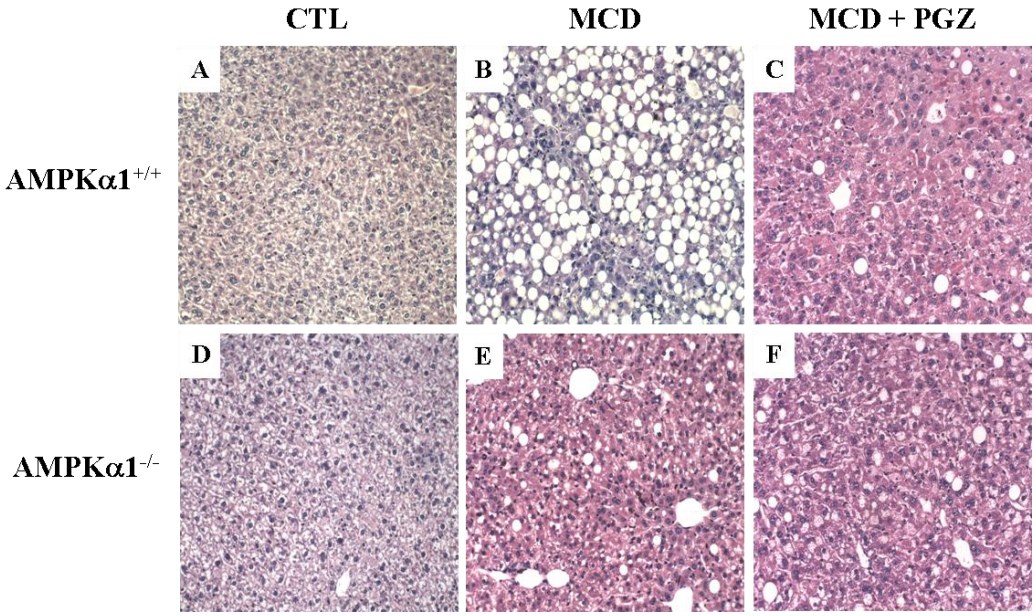

Fig. 6. MCD-induced steatohepatitis and effect of PGZ treatment in mice lacking AMPKα1. Representative photomicrographs of haematoxylin/eosin-stained liver sections from AMPKα1+/+ and AMPKα1$^{-/-}$ mice fed the control diet (A and D), the MCD diet (B and E) or the PGZ-supplemented MCD diet (0.01% wt/wt) (C and F) for 5 weeks (n = 5 per group).

Table 3
Efect of PGZ on hepatic lipid content, inflammation and serum adiponectin in AMPKα1$^{-/-}$ mice

Mouse strain	Hepatic lipid content (mg/100 mg liver ± SD)		Hepatic inflammation (% of total hepatic area ± SD) [a]		Serum adiponectin (μg/ml ± SD)	
	AMPKα1$^{+/+}$	AMPKα1$^{-/-}$	AMPKα1$^{+/+}$	AMPKα1$^{-/-}$	AMPKα1$^{+/+}$	AMPKα1$^{-/-}$
CTL	16.3 ± 0.9	14.2 ± 1.3	0.006 ± 0.005	0.009 ± 0.006	8.2 ± 2.5	9.8 ± 2.9
MCD	40.3 ± 6.6 ***	23.2 ± 7.4	0.08 ± 0.02 ***	0.04 ± 0.03$^{\$,*}$	10.8 ± 2.5	11.9 ± 2.6
MCD + PGZ	23.1 ± 2.8 $^{**,\#\#}$	18.7 ± 1.2 **	0.04 ± 0.02 $^{\#\#}$	0.03 ± 0.03	46.2 ± 1.9 $^{***,\#\#\#}$	86.8 ± 27.2 $^{***,\#\#\#}$

** p < 0.01 and *** p < 0.001 compared to CTL. $^{\#\#}$ p < 0.01 and $^{\#\#\#}$ p < 0.001 in PGZ treated compared to MCD. $^{\$}$p < 0.05 in AMPKα1$^{-/-}$ versus Wt (AMPKα1$^{+/+}$) fed the MCD diet (n = 5 per group).
[a] See Section 2 for details on quantification.

SREBP-1c, the transcription factor controlling nearly all the genes required for *de novo* synthesis of FAs and triglycerides in the liver [18]. FAS mRNA and SCD-1 mRNA and proteins decrease also although not proportionally. Thus, an apparent adaptative transcriptional repression of lipogenesis occurs in MCD-fed mice, possibly linked to reduced food intake and hypoinsulinemia [52]. Based on downregulation of SREBP-1c and FAS, but not of SCD-1, mRNA levels, Ota and co-workers proposed decreased lipogenesis and insulin sensitization as mechanisms for prevention of MCD diet-induced steatohepatitis in obese and diabetics OLETF rats by PGZ [39]. As supporting evidence, SREBP-1c overexpression in transgenic mice leads to fatty liver while inactivation of SREBP-1c gene in the livers of *ob/ob* mice lowers by 50% hepatic triglyceride content [53,54]. We show here that PGZ abrogates SREBP-1c nuclear translocation and represses FAS gene expression. This suggests that, in the absence of significant change on mechanisms regulating b-oxidation, including ACO mRNA and p-ACC/ACC ratio, inhibition of SREBP-1c, may lower lipogenesis underneath a certain treshold resulting in reduced liver steatosis. Decreased nSREBP-1c associated with protection from steatohepatitis is observed in AMPKα1$^{-/-}$ mice fed the MCD diet as well as in Wt MCD-fed mice treated with PGZ. In contrast, PGZ treatment failed to repress SREBP-1c and to lessen the severity of steatosis in Adipo$^{-/-}$ mice. Thus inhibition of SREBP-1c is associated with the anti-steatohepatitis effect of PGZ, is dependent on adiponectin but, it is probably not related to AMPK activation. The mechanisms for the adiponectin-dependent inhibition of SREBP-1c remain to be elucidated.

Beside steatosis, PGZ also reduces hepatic inflammation in MCD livers. This may relate to the anti-inflammatory properties of adiponectin [16]. Our observation that loss of adiponectin function does not shift the baance towards increased inflammation weakened this possibility, but does not exclude it considered the relative adiponectin resistance in MCD mice [55]. Adiponectin [17] and PGZ [11] can activate PPARα. This transcription factor controls the expression of IκBα, key regulator of inflammation. IκBα mRNA and

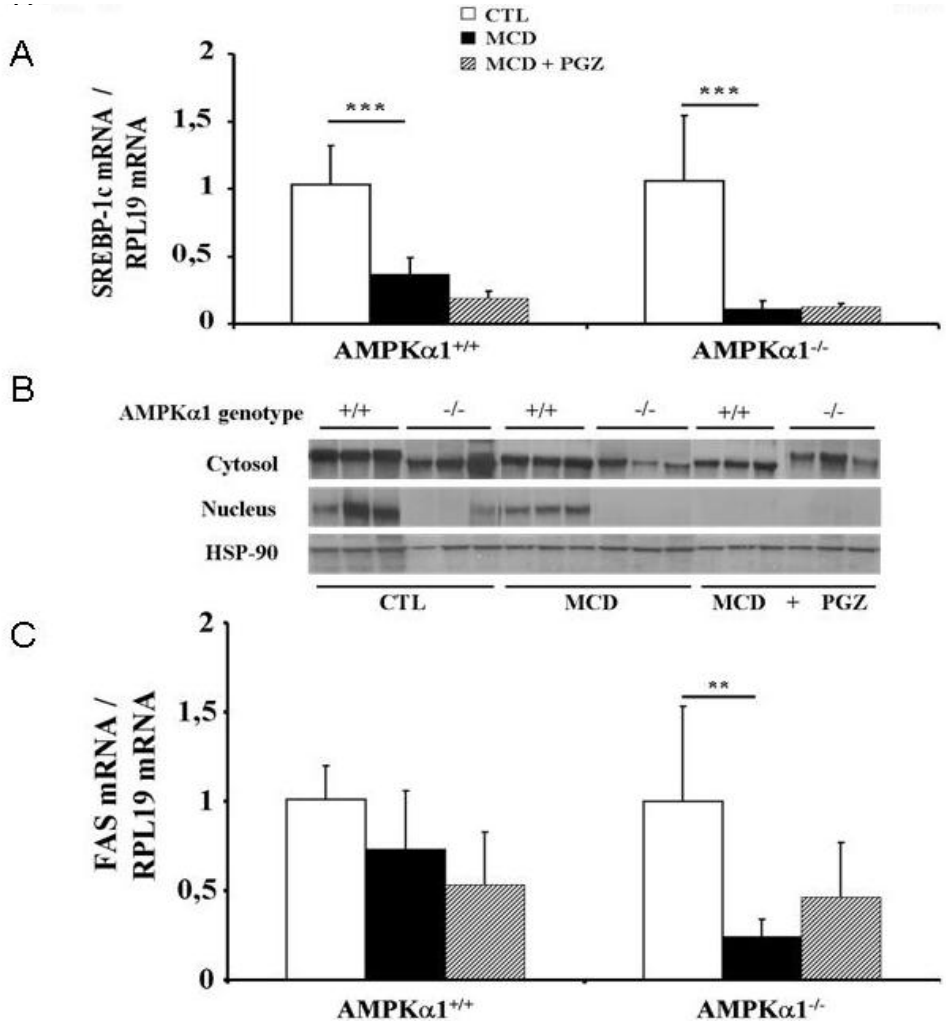

Fig. 7. AMPK is necessary for proper SREBP-1c activation. Bar graphs represent (A) SREBP-1c and (C) FAS mRNA expressions quantitated by RT-qPCR in livers of AMPKα1+/+ and AMPKα1-/- mice fed the control (open bar), the MCD (black bar) or the PGZ-supplemented MCD diets (hatched bar) for 5 weeks. Results (mean ± SD; n = 5 per group) are normalised to the expression of RPL19 mRNA regarded as an invariant control. ** *p < 0.01* and *** *p < 0.001* compared to CTL. (B) Representative western blot for cytosol and nuclear protein expressions of SREBP-1c in AMPKa1$^{+/+}$ and AMPKa1$^{-/-}$ mice fed the control, the MCD or the PGZ-supplemented MCD diets for 5 weeks.

proteins were negligibly elevated upon PGZ treatment providing little support for a PPARα-dependent control of inflammation in this setting. Also, direct modulation of inflammation has not been retained as a primary mechanism for modulation of steatohepatitis severity by PPARα in studies using PPARα$^{-/-}$ mice [56] or specific PPARα agonists [57]. Finally, PGZ may regulate inflammatory response through activation of PPARγ in inflammatory cells, in an adiponectin independent manner. If this was a prominent mechanism of action, then we would expect a reduction of hepatic inflammation in PGZ-treated Adipo$^{-/-}$ mice. But this is not the case. Thus, either steatosis and inflammation are ameliorated simultaneously by related or independent mechanisms both mediated by adiponectin, or reduced inflammation is the consequence of reduced steatosis or vice versa. It remains to be investigated whether and how SREBP-1c or other transcription factors, such as the recently described XBP1 [58], might link steatosis and inflammation.

This study also points towards a conflicting implication of AMPK in steatosis. It was anticipated that reduced AMPK activity would inhibit fatty acid oxidation and repress lipogenesis [30,33,41] and thereby confer increased susceptibility to diet-induced steatosis in AMPKα1$^{-/-}$ mice. But, AMPKα1$^{-/-}$ mice are surprisingly protected from MCD diet-induced steatohepatitis. Similar contra-intuitive effects have been observed in situations in which AMPK was activated by AICAR or liver specific delivery of adenovirus encoding constitutively active AMPK and resulted in increased, rather than decreased, liver fat [45]. These results call for further studies to resolve the paradigm that AMPK activation can both increase and reduce hepatic lipid content and clarify the experimental conditions and the metabolic context in which AMPK would participate to one or the other effect.

The present study demonstrates that the preventive effect of PGZ on MCD-induced steatohepatitis requires adiponectin. Both PGZ treatment and reduced AMPK activity as in AMPKa1$^{-/-}$ mice protect from steatohepatitis and profoundly inhibit nuclear translocation of SREBP-1c, while in Adipo$^{-/-}$ mice, PGZ does not prevent steatohepatitis nor repress SREBP-1c. The inhibition of SREBP-1c and dependent lipogenesis represents a likely mechanism of protection from MCD diet- induced steatohepatitis. As this cannot be forecast from the study of this animal model, further studies in humans are needed to decide whether SREBP-1c and hepatic lipogenesis may represent therapeutic targets for steatohepatitis.

Acknowledgments

Anti-AMPKα1 and anti-AMPKα2 antibodies provided by G. Hardie from Dundee University, Dundee, Scotland. Adiponectin deficient founders were generated by N. Maeda, Osaka University, Japan [22]. This work was supported by a grant from the Belgian 'Fonds National de la Recherche scientifique" (FNRS conventions Nos. 3.4507.04 and 3.4578.07), by grant ARC-05/10-328 (Action de Recherche Concertée de la Direction de la Recherche Scientifique de la Communauté Française de Belgique), and by a grant from the university (Fonds Spécial de Recherche, Université´ catholique de Louvain). BG was recipient of the ICP "Michel de Visscher" Fellowship. IL is research associate with FNRS.

References

[1] Dixon JB, Bhathal PS, O'Brien PE. Nonalcoholic fatty liver disease: predictors of nonalcoholic steatohepatitis and liver fibrosis in the severely obese. Gastroenterology 2001;121:91-100.
[2] Marchesini G, Brizi M, Bianchi G, Tomassetti S, Bugianesi E, Lenzi M, et al. Nonalcoholic fatty liver disease: a feature of the metabolic syndrome. Diabetes 2001;50:1844-1850.
[3] Torres DM, Harrison SA. Diagnosis and therapy of nonalcoholic steatohepatitis. Gastroenterology 2008;134:1682-1698.
[4] Neuschwander-Tetri BA, Brunt EM, Wehmeier KR, Oliver D, Bacon BR. Improved nonalcoholic steatohepatitis after 48 weeks of treatment with the PPAR-gamma ligand rosiglitazone. Hepatology 2003;38:1008-1017.
[5] Promrat K, Lutchman G, Uwaifo GI, Freedman RJ, Soza A, Heller T, et al. A pilot study of pioglitazone treatment for nonalcoholic steatohepatitis. Hepatology 2004;39:188-196.
[6] Ratziu V, Giral P, Jacqueminet S, Charlotte F, Hartemann- Heurtier A, Serfaty L, et al. Rosiglitazone for nonalcoholic steatohepatitis: one-year results of the randomized placebo-controlled Fatty Liver Improvement with Rosiglitazone Therapy (FLIRT) Trial. Gastroenterology 2008;135:100-110.
[7] Teranishi T, Ohara T, Maeda K, Zenibayashi M, Kouyama K, Hirota Y, et al. Effects of pioglitazone and metformin on intracellular lipid content in liver and skeletal muscle of individuals with type 2 diabetes mellitus. Metabolism 2007;56: 1418-1424.
[8] Miyazaki Y, Mahankali A, Wajcberg E, Bajaj M, Mandarino LJ, DeFronzo RA. Effect of pioglitazone on circulating adipocytokine levels and insulin sensitivity in type 2 diabetic patients. J Clin Endocrinol Metab 2004;89:4312-4319.
[9] Jiang C, Ting AT, Seed B. PPAR-gamma agonists inhibit production of monocyte inflammatory cytokines. Nature 1998;391:82-86.
[10] von Knethen A, Brune B. PPARgamma - an important regulator of monocyte/macrophage function. Arch Immunol Ther Exp (Warsz) 2003;51:219-226.
[11] Orasanu G, Ziouzenkova O, Devchand PR, Nehra V, Hamdy O, Horton ES, et al. The peroxisome proliferator-activated receptor-gamma agonist pioglitazone represses inflammation in a peroxisome proliferator-activated receptor-alpha-dependent manner in vitro and in vivo in mice. J Am Coll Cardiol 2008;52:869-881.
[12] Nawrocki AR, Rajala MW, Tomas E, Pajvani UB, Saha AK, Trumbauer ME, et al. Mice lacking adiponectin show decreased hepatic insulin sensitivity and reduced responsiveness to peroxisome proliferator-activated receptor gamma agonists. J Biol Chem 2006;281:2654-2660.
[13] Fruebis J, Tsao TS, Javorschi S, Ebbets-Reed D, Erickson MR, Yen FT, et al. Proteolytic cleavage product of 30-kDa adipocyte complement-related protein increases fatty acid oxidation in muscle and causes weight loss in mice. Proc Natl Acad Sci USA 2001;98:2005-2010.
[14] Xu A, Wang Y, Keshaw H, Xu LY, Lam KS, Cooper GJ. The fat-derived hormone adiponectin alleviates alcoholic and nonalcoholic fatty liver diseases in mice. J Clin Invest 2003;112:91-100.
[15] Kamada Y, Tamura S, Kiso S, Matsumoto H, Saji Y, Yoshida Y, et al. Enhanced carbon tetrachloride-induced liver fibrosis in mice lacking adiponectin. Gastroenterology 2003;125:1796-1807.
[16] Yokota T, Oritani K, Takahashi I, Ishikawa J, Matsuyama A, Ouchi N, et al. Adiponectin, a new member of the family of soluble defense collagens, negatively regulates the growth of myelomonocytic progenitors and the functions of macrophages. Blood 2000;96:1723-1732.
[17] Yamauchi T, Kamon J, Ito Y, Tsuchida A, Yokomizo T, Kita S, et al. Cloning of adiponectin receptors that mediate antidiabetic metabolic effects. Nature 2003;423:762-769.
[18] Horton JD. Sterol regulatory element-binding proteins: transcrip-tional activators of lipid synthesis. Biochem Soc Trans 2002;30: 1091-1095.
[19] Dobrzyn P, Dobrzyn A, Miyazaki M, Cohen P, Asilmaz E, Hardie DG, et al. Stearoyl-CoA desaturase 1 deficiency increases fatty acid oxidation by activating AMP-activated protein kinase in liver. Proc Natl Acad Sci USA 2004;101:6409-6414.
[20] Leclercq IA, Lebrun VA, Starkel P, Horsmans YJ. Intrahepatic insulin resistance in a murine model of steatohepatitis: effect of PPARgamma agonist pioglitazone. Lab Invest 2007;87:56-65.
[21] Jorgensen SB, Viollet B, Andreelli F, Frosig C, Birk JB, Schjerling P, et al. Knockout of the alpha2 but not alpha1 5 -AMP-activated protein kinase isoform abolishes 5-aminoimidazole-4-carboxamide-1-beta-4-ribofuranosidebut not contraction-induced glucose uptake in skeletal muscle. J Biol Chem 2004;279:1070-1079.
[22] Maeda N, Shimomura I, Kishida K, Nishizawa H, Matsuda M,Nagaretani H, et al. Diet-induced insulin resistance in mice lacking adiponectin/ACRP30. Nat Med 2002;8:731-737.
[23] Da Silva Morais A, Saliez A, Leclercq I, Horsmans Y, Starkel P. Inhibition of the Ras oncoprotein reduces proliferation of hepatocytes in vitro and in vivo in rats. Clin Sci (Lond) 2008;114: 73-83.
[24] Da Silva Morais A, Abarca-Quinones J, Horsmans Y, Starkel P, Leclercq IA. Peroxisome proliferated-activated receptor gamma ligand, Pioglitazone, does not prevent hepatic fibrosis in mice. Int J Mol Med 2007;19:105-112.
[25] Mitchelhill KI, Stapleton D, Gao G, House C, Michell B, Katsis F, et al. Mammalian AMP-activated protein kinase shares structural and functional homology with the catalytic domain of yeast Snf1 protein kinase. J Biol Chem 1994;269:2361-2364.
[26] Guigas B, Bertrand L, Taleux N, Foretz M, Wiernsperger N, Vertommen D, et al. 5-Aminoimidazole-4-carboxamide-1-beta- D-ribofuranoside and metformin inhibit hepatic glucose phosphorylation by an AMP-activated protein kinase-independent effect on glucokinase translocation. Diabetes 2006;55:865-874.
[27] Leclercq IA, Farrell GC, Sempoux C, dela Pena A, Horsmans Y. Curcumin inhibits NF-kappaB activation and reduces the severity of experimental steatohepatitis in mice. J Hepatol 2004;41: 926-934.
[28] Rao MS, Reddy JK. PPARalpha in the pathogenesis of fatty liver disease. Hepatology 2004;40:783-786.
[29] Delerive P, Gervois P, Fruchart JC, Staels B. Induction of IkappaBalpha expression as a mechanism contributing to the anti-inflammatory activities of peroxisome proliferator-activated receptor-alpha activators. J Biol Chem 2000;275:36703-36707.
[30] Tomas E, Tsao TS, Saha AK, Murrey HE, Zhang C, Itani SI, et al. Enhanced muscle fat oxidation and glucose transport by ACRP30 globular domain: acetyl-CoA carboxylase inhibition and AMP-activated protein kinase activation. Proc Natl Acad Sci USA 2002;99:16309-16313.
[31] Gwinn DM, Shackelford DB, Egan DF, Mihaylova MM, Mery A, Vasquez DS, et al. AMPK phosphorylation of raptor mediates a metabolic checkpoint. Mol Cell 2008;30:214-226.
[32] Inoki K, Zhu T, Guan KL. TSC2 mediates cellular energy response to control cell growth and survival. Cell 2003;115: 577-590.

33] Viollet B, Foretz M, Guigas B, Horman S, Dentin R, Bertrand L, et al. Activation of AMP-activated protein kinase in the liver: a new strategy for the management of metabolic hepatic disorders. J Physiol 2006;574:41-53.
[34] Rizki G, Arnaboldi L, Gabrielli B, Yan J, Lee GS, Ng RK, et al. Mice fed a lipogenic methionine-choline-deficient diet develop hyper metabolism coincident with hepatic suppression of SCD-1. J Lipid Res 2006;47:2280-2290.
[35] Okumura K, Ikejima K, Kon K, Abe W, Yamashina S, Enomoto N, et al. Exacerbation of dietary steatohepatitis and fibrosis in obese, diabetic KK-A(y) mice. Hepatol Res 2006;36:217-228.
[36] Rinella ME, Elias MS, Smolak RR, Fu T, Borensztajn J, Green RM. Mechanisms of hepatic steatosis in mice fed a lipogenic methionine choline-deficient diet. J Lipid Res 2008;49:1068-1076.
[37] Kaser S, Moschen A, Cayon A, Kaser A, Crespo J, Pons-Romero F, et al. Adiponectin and its receptors in non-alcoholic steatohepatitis. Gut 2005;54:117-121.
[38] Maeda N, Takahashi M, Funahashi T, Kihara S, Nishizawa H, Kishida K, et al. PPARgamma ligands increase expression and plasma concentrations of adiponectin, an adipose-derived protein. Diabetes 2001;50:2094-2099.
[39] Ota T, Takamura T, Kurita S, Matsuzawa N, Kita Y, Uno M, et al. Insulin resistance accelerates a dietary rat model of nonalcoholic steatohepatitis. Gastroenterology 2007;132:282-293.
[40] Rinella ME, Green RM. The methionine-choline deficient dietary model of steatohepatitis does not exhibit insulin resistance. J Hepatol 2004;40:47-51.
[41] Yamauchi T, Kamon J, Minokoshi Y, Ito Y, Waki H, Uchida S, et al. Adiponectin stimulates glucose utilization and fatty-acid oxidation by activating AMP-activated protein kinase. Nat Med 2002;8:1288-1295.
[42] Saha AK, Avilucea PR, Ye JM, Assifi MM, Kraegen EW, Ruderman NB. Pioglitazone treatment activates AMP-activated protein kinase in rat liver and adipose tissue in vivo. Biochem Biophys Res Commun 2004;314:580-585.
[43] LeBrasseur NK, Kelly M, Tsao TS, Farmer SR, Saha AK, Ruderman NB, et al. Thiazolidinediones can rapidly activate AMP-activated protein kinase in mammalian tissues. Am J Physiol Endocrinol Metab 2006;291:E175-E181.
[44] Bergheim I, Guo L, Davis MA, Lambert JC, Beier JI, Duveau I, et al. Metformin prevents alcohol-induced liver injury in the mouse: critical role of plasminogen activator inhibitor-1. Gastroenterology 2006;130:2099-2112.
[45] Foretz M, Ancellin N, Andreelli F, Saintillan Y, Grondin P, Kahn A, et al. Short-term overexpression of a constitutively active form of AMP-activated protein kinase in the liver leads to mild hypoglycemia and fatty liver. Diabetes 2005;54: 1331-1339.
[46] Gaidhu MP, Fediuc S, Ceddia RB. 5-Aminoimidazole-4-carbox-amide-1-beta- D-ribofuranoside-induced AMP-activated protein kinase phosphorylation inhibits basal and insulin-stimulated glucose uptake, lipid synthesis, and fatty acid oxidation in isolated rat adipocytes. J Biol Chem 2006;281:25956-25964.
[47] Tomita K, Azuma T, Kitamura N, Nishida J, Tamiya G, Oka A, et al. Pioglitazone prevents alcohol-induced fatty liver in rats through upregulation of c-Met. Gastroenterology 2004;126: 873-885.
[48] Suwa M, Nakano H, Kumagai S. Effects of chronic AICAR treatment on fiber composition, enzyme activity, UCP3, and PGC-1 in rat muscles. J Appl Physiol 2003;95:960-968.
[49] Guigas B, Taleux N, Foretz M, Detaille D, Andreelli F, Viollet B, et al. AMP-activated protein kinase-independent inhibition of hepatic mitochondrial oxidative phosphorylation by AICA riboside. Biochem J 2007;404:499-507.
[50] Goransson O, McBride A, Hawley SA, Ross FA, Shpiro N, Foretz M, et al. Mechanism of action of A-769662, a valuable tool for activation of AMP-activated protein kinase. J Biol Chem 2007;282:32549-32560.
[51] Larter CZ, Yeh MM, Haigh WG, Williams J, Brown S, Bell-Anderson KS, et al. Hepatic free fatty acids accumulate in experimental steatohepatitis: role of adaptive pathways. J Hepatol 2008;48:638-647.
[52] Horton JD, Bashmakov Y, Shimomura I, Shimano H. Regulation of sterol regulatory element binding proteins in livers of fasted and refed mice. Proc Natl Acad Sci USA 1998;95:5987-5992.
[53] Yahagi N, Shimano H, Hasty AH, Matsuzaka T, Ide T, Yoshikawa T, et al. Absence of sterol regulatory element-binding protein-1 (SREBP-1) ameliorates fatty livers but not obesity or insulin resistance in Lep(ob)/Lep(ob) mice. J Biol Chem 2002;277: 19353-19357.
[54] Shimomura I, Bashmakov Y, Horton JD. Increased levels of nuclear SREBP-1c associated with fatty livers in two mouse models of diabetes mellitus. J Biol Chem 1999;274:30028-30032.
[55] Larter CZ, Yeh MM, Williams J, Bell-Anderson KS, Farrell GC. MCD-induced steatohepatitis is associated with hepatic adiponectin resistance and adipogenic transformation of hepatocytes. J Hepatol 2008;49:407-416.
[56] Ip E, Farrell GC, Robertson G, Hall P, Kirsch R, Leclercq I. Central role of PPARalpha-dependent hepatic lipid turnover in dietary steatohepatitis in mice. Hepatology 2003;38:123-132.
57] Ip E, Farrell G, Hall P, Robertson G, Leclercq I. Administration of the potent PPARalpha agonist, Wy-14,643, reverses nutritional fibrosis and steatohepatitis in mice. Hepatology 2004;39: 1286-1296.
[58] Kaser A, Lee AH, Franke A, Glickman JN, Zeissig S, Tilg H, et al. XBP1 links ER stress to intestinal inflammation and confers genetic risk for human inflammatory bowel disease. Cell 2008;134:743-756.

IV. Discussion and perspectives

PPARγ – adiponectin – AMPK axis in the control of hepatic fibrogenesis

PPARγ and hepatic fibrosis

HSCs, being the main matrix producing cells in hepatic wound-healing, play a pivotal role in liver fibrogenesis (13). Hence, interfering with the activation, the proliferation and ECM production by HSC represents one attractive potential therapeutic option for liver fibrosis.

In rats, TZD treatment prevents fibrosis development and, to a lesser extend, fibrosis progression (100). This effect may be attributable to at least 3, most likely cooperative, mechanisms. First, direct PPARγ activation in HSC may interfere with fibrogenesis. Indeed, PPARγ has been shown to be expressed in quiescent HSC, while this expression is lost during HSC trans-differentiation (99). Exposure of quiescent rat HSC in culture to TZD prevents their activation (100, 172). On the contrary, forced expression of PPARγ in culture activated rat HSC, by mean of adenoviral transfection, reverts their phenotype to that of quiescent cells (98, 174). Second, those effects may be indirectly mediated through PPARγ dependent induction of adiponectin. PPARγ agonist drugs stimulate adiponectin expression by the adipose tissue and its release in the circulation (92). Adiponectin has been shown to be anti-fibrogenic as mice lacking adiponectin are exquisitely sensitive to fibrosis while increased adiponectin has been shown to be anti-fibrotic (128). Third, PPARγ and adiponectin, as well as other adipocytokines which regulation is altered upon PPARγ stimulation, modulate maturation and activation of immune and inflammatory cells (77). PPARγ-mediated reduction of inflammation could indirectly reduce the severity of liver fibrosis.

In order to test the relative contribution of each process, we wanted to make use of genetically modified mouse (such as adiponectin deficient mice or mice lacking PPARγ or adiponectin receptor expression in immune cells).

The first step in this experimental protocol was to assess the effect of TZD treatment on fibrogenesis *in vivo* in mice. Surprisingly, and contrasting with results previously obtained in rats by we and others (100, 172, 179), TZD treatment failed to prevent liver fibrosis in mice as classically induced by repeated administration of CCl_4. More surprising were the results we obtained *in vitro* on culture activated primary HSC of mouse origin. We found PPARγ to be

expressed and having DNA binding and transcriptional activity upon ligand activation in quiescent mouse HSC but not in activated HSC. Exposure of quiescent HSC to PPARγ ligands prevented the loss of its expression. However, contrasting with observations in rats HSC (98, 174), we shown that treatment of quiescent HSC with PPARγ agonists failed to interfere with HSC activation, transformation into myofibroblast-like phenotype as well as to prevent the induction of matrix gene expression. Our observations firmly demonstrated that ligand stimulation of PPARγ in mouse HSC, although leading to transcriptional activation, did not act as a molecular switch to prevent activation of murine HSC in culture. Moreover, PPARγ agonist treatment, although leading to increased serum adiponectin levels, failed to exert anti-fibrotic properties *in vivo* in two different strains of mice.

This suggests that the set of gene controlled by PPARγ in HSCs varies between species: PPARγ exerting a control over fibrogenic genes (such as collagen-α1 and α-SMA) in rat's but not in mouse's HSCs. Moreover, our results also shown that increased levels of adiponectin reached upon therapeutic doses of PPARγ agonist are not sufficient to induce evident anti-fibrotic effects in the mouse CCl_4 model of fibrosis.

While *in vitro* studies using fully activated myofibroblasts deriving form human HSC suggested that PPARγ stimulation might modulate the activation of these cells, the effect of PPARγ agonists on activation of quiescent human HSC has not been demonstrated. Those tests are currently hampered owe to the short supply of "normal" liver tissue for research purposes. In NASH clinical trials using TZD (96-98), no or minor effects on the fibrosis component have been reported, providing little support for an anti-fibrotic effect of such drugs. The anti-fibrotic properties of PPARγ agonist drugs remains thus to be demonstrated in humans, but on the basis of the first clinical trials and on our results in mice, PPARγ does not appears as a likely effective target for anti-fibrotic therapy.

Implication of AMPK on liver fibrogenesis

The fibrotic transformation of HSC is a highly energy demanding process as it requires cell proliferation, cell transformation and production of large amounts of matrix and matrix remodelling proteins. It is therefore reasonable to postulate that this process will fail or will be impaired if the cell is not capable of mobilising sufficient energy. AMPK is a fuel-sensitive gauge, able to channel the metabolic machinery towards ATP producing or anabolic energy storage activities depending on the cellular needs and energy resources (138). In that way, it

allows or precludes cellular activities that are otherwise determined by specific stimuli. For example, potent AMPK activation, by manoeuvres mimicking a low energy cellular content status, has been shown to orientate the metabolism towards energy production, and if sufficient energy can not be produced, inhibit protein synthesis and cause cell cycle arrest (155, 180, 181).

During trans-differentiation of HSCs, we have observed an increased protein expression of AMPK and increased AMPK activity. As transcript levels for the catalytic subunits remained unchanged, it is likely that the increased expression of AMPKγ3 mRNA, encoding for a regulatory protein, may participate to the stabilisation of the AMPK complex. This mechanism for AMPK increased activity remains to be demonstrated.

AMPK is able to inactivate mTOR resulting in decreased phosphorylation of p70S6K (182). This leads to a limitation of protein synthesis. Despite the fact that AMPK is activated during HSC trans-differentiation, we observe that p70S6K remains highly phosphorylated. This suggests that, providing that energy production is sufficient, the protein synthesis function may be performed if it receivs an appropriate stimulus. By contrast, when cells are treated with AICAR, mimicking a severely low cellular energy status, AMPK is activated over the "physiological" level seen during normal activation of HSC. In this situation, we observe that p70S6K phosphorylation is inhibited, cell proliferation and cell trans-differentiation are blocked and the collagen production is prevented. Thus, it is like if, when the cells "sense" that energy is not available and when such energy can not be produced, energy demanding pathways such as protein production and cell proliferation are impeded. Similarly, other authors have shown that the proliferative response of fully activated myofibroblasts originating from rat or human HSCs to PDGF (the most potent mitogen for HSC) is reduced upon AMPK activation by AICAR, metformin or adiponectin (130, 175). All together, our results support that, targeting AMPK to increase its activity, might confer anti-fibrotic protection. However, as the AMPK system has multiple functions in diverse cell types, the net result of AMPK activation on fibrogenesis remains to be verified *in vivo*. This could be evaluated in experimental mice models submitted to pharmacological activation of AMPK by treatment with metformin or by injection of a constitutively activated AMPK and chronically administred with CCl_4 to induce hepatic fibrosis.

As AMPK activation by adiponectin has been shown to reduce proliferation of fully activated myofibroblastic cells *in vivo*, some authors (130, 175) have proposed that the reverse might be true. In this view, AMPK$\alpha 1^{-/-}$ mice or mice with reduced AMPK activity should be exquisitely sensitive to fibrosis as are adiponectin deficient mice. If confirms, low

adiponectin levels, as seen in obese patients and patients with metabolic syndrome (132), leading to reduced AMPK stimulation may explain, at least partly, the higher propensity of those patients to develop fibrosis in response to various liver diseases, and in particular in NASH. We decided to test this assumption using mice with low AMPK activity owe to the lack of the alpha1 catalytic subunit of the AMPK complex. In those mice, we verified that AMPK activity is reduced by 80% in total liver and in HSCs, confirming that the lack of AMPKα1 is not compensated for by increased AMPKα2 expression and dependent activity. Although, those mice appears to develop spontaneous perisinusoidal fibrosis with aging (data not shown), the wound healing fibrosis in response to CCl_4 was not different from that of wild type mice. We then studied AMPK$\alpha1^{-/-}$ primary HSCs *in vitro*. Interestingly, low AMPK activity is associated with inhibition of cell proliferation that spontaneously occurs upon plating cells on plastic. By contrast, collagen gene induction and cell transformation were preserved, although the latter event was a bit delayed compared to control cells. This suggests that, in the absence of AMPKα1 or when AMPK activity is abnormally low, HSCs are able to trans-differentiate and produce matrix proteins, but are not able to proliferate, as if the deficient AMPK system was not sufficient to foster or mobilize sufficient energy to complete several energy consuming processes simultaneously. We would like to confirm this hypothesis, by analysing HSCs after long term in culture, i.e. when cells are fully differentiated. If our hypothesis is correct, cell proliferation should increase to the level of wild type HSCs at this time. This will also be in concordance with our *in vivo* finding that fibrotic response of AMPK$\alpha1^{-/-}$ mice is not altered.

Those results supported the hypothesis that AMPK did not operate a decisive control on its numerous downstream functions, but rather that it allows, favours or prevents some of them according to cellular resources. If to be used *in vivo* as anti-fibrotic drug, induction of AMPK activity should be specifically targeted to HSCs. It will be also important to test the consequences of such activation on hepatic cell proliferation, a pivotal process for organ repair. By contrast with the hypothesis proposed by some authors (130, 175), reduced hepatic AMPK activity could probably not be an argument explaining the increased susceptibility to fibrosis development in obesity and in other diseased associated with low circulating adiponectin levels.

In regard of our *in vitro* results, specific activation of AMPK on stellate cells, pharmacologically or by adenoviral transfection, could be considered as a potential therapeutic mechanism to prevent liver fibrosis development in humans. However, this

possibility remains to be demonstrated *in vitro* after isolation of human HSCs from normal liver. Because AMPK$\alpha 1^{-/-}$ mice developed a similar fibrosis that Wt mice and while Adipo$^{-/-}$ mice exhibited a more severe liver fibrosis after treatment with CCl_4, it would be interesting to evaluate the impact of the transfection of the Adipo$^{-/-}$ mice with the constititively activated form of AMPK, resulting in a supra-physiological increase of AMPK activity, during the CCl_4-induced hepatic fibrogenesis.

However, before using for treatment of hepatic fibrosis, the impact of AMPK activation would be evaluated not only on liver cells but also on the entire body because of the pleiotropic effects of AMPK amoung others in cell cycle and protein synthesis.

PPARγ – adiponectin – AMPK axis in the control of NASH

Non-alcoholic steatohepatitis (NASH) is an under-diagnosed liver disease characterised by steatosis, necroinflammation and fibrosis. Human studies with thiazolidinediones, i.e. pioglitazone (PGZ), in subjects with NASH have demonstrated improvement in liver function tests, steatosis and liver inflammation. Such treatment had however little impact, if any, on fibrosis (102, 103). The mechanisms of action of TZD in NASH are incompletely understood. Hence, stimulation of adipocyte differentiation and fat storage in adipocytes preventing lipotoxicity, modulation of adipocytokines release and insulin-sensitization or anti-inflammatory and anti-fibrotic effects represent three potential modus of action of TZD for prevention of NASH development

As previously described by we and others (67, 183), pioglitazone (PGZ) treatment prevents the development of a methionine and choline deficient (MCD) diet-induced steatohepatitis in mice. As PGZ treatment increases significantly the circulating levels adiponectin (92), we evaluated the implication of this adipocytokine on the preventive effect of PGZ on NASH development. By contrast to wild-type (Wt) mice, PGZ failed to prevent steatohepatitis induced by the MCD diet in mice lacking adiponectin (Adipo$^{-/-}$). This firmly establishes that the beneficial effect conferred by PGZ is dependent on adiponectin.

Adiponectin upon binding to its specific receptors, elicits the activation of AMPK and PPARα pathways (111). AMPK exerts a control over *de novo* lipogenesis and lipid burning, while PPARα co-ordinately favours fatty acid oxidation and, by acting on NFκB, has anti-inflammatory properties. Thus activation of hepatic pathways evoked by adiponectin may counteract steatohepatitis by reducing both steatosis and hepatic inflammation through increased lipid burning and inhibition of NFκB pathway, respectively. We therefore analysed

and compared the effect of TZD on those 2 pathways in Wt and Adipo$^{-/-}$ mice fed the MCD diet. Compared to untreated MCD-fed Wt mice (with steatohepatitis), we observed no change in AMPK activity upon PGZ treatment, although such treatment increased significantly serum adiponectin levels. However, a single dose of PGZ increased serum adiponectin and liver AMPK activity (data not shown), as it has been reported by others using short-term PGZ administration protocols (184, 185). The administration of the drug in a food mixture as well as the duration of the treatment may explain the absence of increased AMPK activity in our long-term *in vivo* study.

In our model, hepatic mRNA levels of ACC, FAS, SREBP-1c and PGC-1α, well-defined AMPK target genes, remained unchanged in mice fed the PGZ-supplemented MCD diet compared to mice fed the MCD diet alone. Similarly, we saw no change in the phosphorylation state of down stream AMPK targets. In addition, AMPKα1 deficiency does not increase the susceptibility to MCD-diet induced steatohepatitis. It is therefore tempting to conclude that AMPK is not implicated in mediating the adiponectin-dependent effect of PGZ on steatohepatitis.

The implication of PPARα, which stimulates lipid oxidation and prevents inflammation through inhibition of NFκB (124, 186), in MCD diet-induced steatohepatitis has been established with increased disease severity in PPARα$^{-/-}$ mice while PPARα activation reversed MCD-induced steatohepatitis (187, 188). Here, we observed that the beneficial effect of PGZ on MCD-induced steatohepatitis in mice is not associated with activation of the PPARα-dependent fatty acid β-oxidation. Thus this suggests that increased lipid burning, in response to adiponectin-dependent activation of PPARα, is not likely to be involved in the anti-steatohepatitis effect of PGZ in this model. PPARα also controls the expression of IκBα, a key regulator of inflammation. IκBα mRNA and proteins were negligibly elevated upon PGZ treatment providing little support for a PPARα-dependent control of inflammation in this setting.

This study also points towards conflicting implication of AMPK in steatosis: As AMPK stimulates β-oxidation and inhibits lipogenesis, we hypothesized that mice with deficient AMPK activity (AMPKα1$^{-/-}$ mice) would develop worse steatosis and may be steatohepatitis under MCD diet than wild type littermates and that they would be insensitive to the protective effect of PGZ if this effect is AMPK dependent. Conversely to our expectation, we observed that AMPKα1$^{-/-}$ mice are protected from MCD-induced steatohepatitis development. Similar

contra-intuitive effects have been observed in situations in which AMPK was activated by AICAR or liver specific delivery of adenovirus encoding constitutively active AMPK and resulted in increased, rather than decreased, liver fat (114). These results call for further studies to resolve the paradigm that AMPK activation can both increase and reduce hepatic lipid content and clarify the experimental conditions and the metabolic context in which AMPK would participate to one or the other effect. Thus, we could anticipate that transfection of MCD fed AMPK$\alpha 1^{-/-}$ mice with a constitutively activated form of AMPK would be associated with the development of MCD-induced steatohepatitis. It could also be interesting to evaluate the effect of MCD diet after conditional knockout of AMPKα1 or α2 in the liver of Wt mice, resulting in an eventual compensatory AMPK activity compared to the non-conditional kockout models, adapted to this deficiency.

An important finding was that PGZ abrogates SREBP-1c nuclear translocation and represses FAS gene expression in the MCD model. This suggests that, in the absence of significant change on mechanisms regulating β-oxidation, including ACO mRNA and p-ACC/ACC ratio, inhibition of SREBP-1c, may lower lipogenesis underneath a certain threshold resulting in reduced liver steatosis. Decreased nSREBP-1c associated with protection from steatohepatitis is observed in AMPK$\alpha 1^{-/-}$ mice fed the MCD diet as well as in Wt MCD-fed mice treated with PGZ. In contrast, PGZ treatment failed to repress SREBP-1c and to lessen the severity of steatosis in Adipo$^{-/-}$ mice. Thus inhibition of SREBP-1c is associated with the anti-steatohepatitis effect of PGZ, is dependent on adiponectin but, it is probably not related to AMPK activation.

Our study suggests that the inhibition of SREBP-1c and dependent lipogenesis may represent a likely mechanism of protection from MCD diet-induced steatohepatitis. Leptin signaling has been suggested to be improved in MCD fed mice (189). Leptin increased AMPK activity (119) and suppressed SCD-1 expression (190). SCD-1 reduced expression resulted in decreased hepatic expression of SREBP-1c as demonstrated in mice lacking SCD-1 (191). In the other hand, the reduced expression of SREBP-1c in AMPK$\alpha 1^{-/-}$ mice under normal diet compared to Wt mice could be related to the lack of AMPK, known to induce the phosphoinositide 3-kinases (PI3K)/PKB pathway *in vitro* (192). As PI3K induces the expression of SREBP-1c in the liver (193), the decreased expression of SREBP-1c observed in AMPK$\alpha 1^{-/-}$ mice could be associated with a decreased in the PI3K pathway. Therefore it would be interesting to evaluate the leptin and PI3K signaling pathways *in vivo* in mice fed MCD diet.

Several lines of evidence suggest that SREBP-1c may also represent a therapeutic target for NAFLD/NASH in humans. In obesity, increased adipocyte mass and insulin resistance, especially in visceral adipose tissue, contributes to elevated plasma levels of FFAs through lipolysis. As the rate of hepatic FFA uptake is directly proportional to plasma FFA concentrations, increased lipolysis appears as the major contributor to intrahepatic lipid accumulation. The transcription factor SREBP-1c mediates most of insulin's effects on lipogenesis (194, 195). *De novo* lipogenesis is activated by glucose and hyperinsulinaemia through activation of ChREBP, SREBP-1c, and by low grade inflammation and increased TNF. Increased *de novo* lipogenesis in hepatocytes is indeed observed in NAFLD patients with hepatic insulin resistance. While in normal subjects, the contribution of hepatic *de novo* lipogenesis to the pool of hepatic fatty acids is less than 5%, it increases up to 25 % in NAFLD patients. Conversely, intrahepatic lipids and lipid metabolites directly interfere with insulin signaling, increasing insulin resistance. Therefore, targeting of SREBP-1c may be beneficial for NAFLD/NASH patients, reducing both fat accumulation and improving hepatic insulin resistance.

In our model, PGZ reduces both inflammation and steatosis in an adiponectin dependent fashion. Either steatosis and inflammation are ameliorated simultaneously by related or independent mechanisms both mediated by adiponectin, or reduced inflammation is the consequence of reduced steatosis or *vice versa*. Therefore, according to the experimental evidence discussed above, therapeutic interventions that can enhance the actions of adiponectin, such as increasing plasma adiponectin concentrations by treatment with PGZ or up-regulating/activating adiponectin receptors, could represent attractive strategies to improve metabolic syndrome and to combat NAFLD obesity-related diabetes and vascular diseases, associated with low levels of serum adiponectin, in humans. It remains to investigate whether and how SREBP-1c or other transcription factors, such as the recently described XBP1 (196), a key component of the endoplasmic reticulum stress response, might link steatosis and inflammation. The mechanisms for the adiponectin-dependent inhibition of SREBP-1c remain also to be elucidated.

In this work exploring the role of the cascade PPARγ-adiponectin-AMPK in the pathophysiology of NASH and hepatic fibrosis in mice, we demonstrate that PPARγ has no effect on activation of HSC or fibrogenesis. However, stimulation of AMPK in HSC prevents their activation and proliferation and therefore the anti-fibrotic potential of such as a strategy deserve to be evaluated *in vivo*. PPARγ stimulation, in an adiponectin-dependent manner,

prevents steatosis and inflammation in the MCD-diet model of steatohepatitis. This effect appears to be independent of AMPK activation and to involve inhibition of SREBP-1c. Further studies are mandatory to understand the mechanisms by which PPARγ and adiponectin repress both lipogenesis and inflammation and to determine whether SREBP-1c could represent a therapeutic target for NASH.

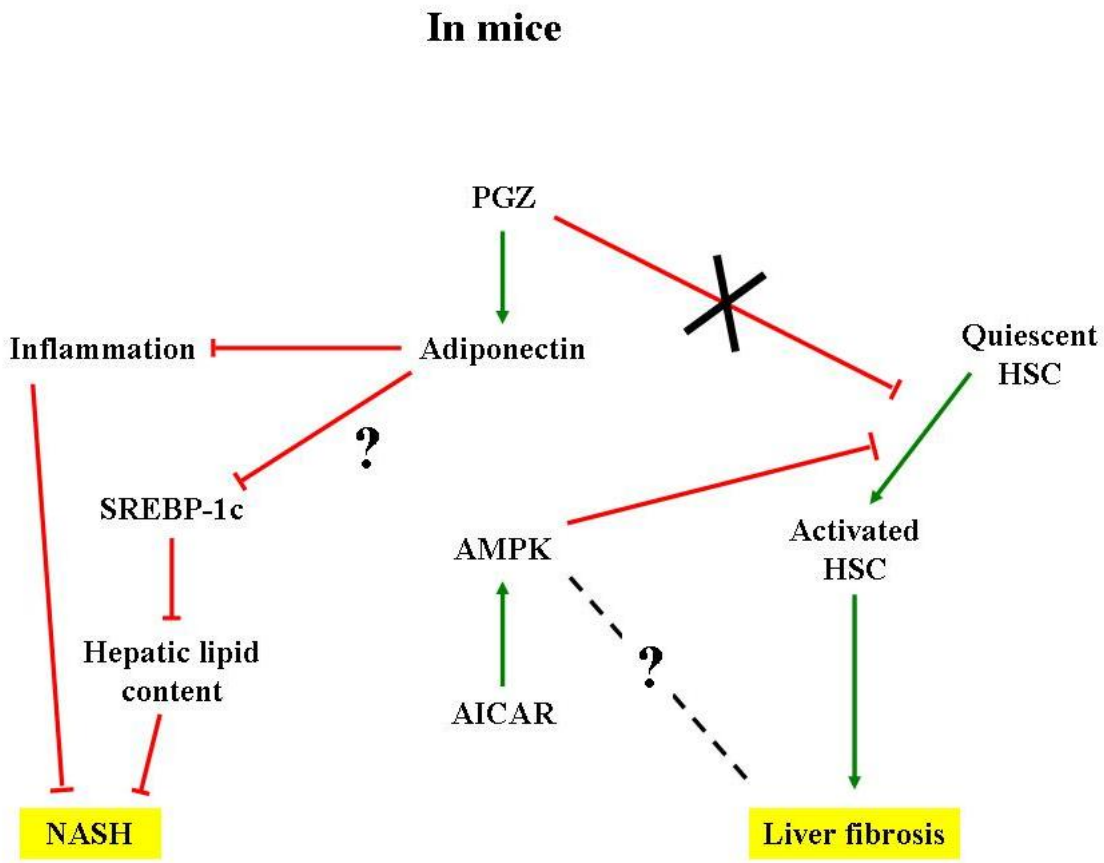

Figure 20: Impact of the axis PGZ-adiponectin-AMPK on liver fibrogenesis and NASH development in mice

V. Other publications

1. **da Silva Morais A**, Saliez A, Leclercq I, Horsmans Y, Stärkel P.
Inhibition of the Ras oncoprotein reduces proliferation of hepatocytes in vitro and in vivo in rats. **Clin Sci (Lond). 2008** Jan;114(1):73-83.

2. Leclercq IA, **Da Silva Morais A**, Schroyen B, Van Hul N, Geerts A.
Insulin resistance in hepatocytes and sinusoidal liver cells: mechanisms and consequences.
J Hepatol. 2007 Jul;47(1):142-56. Review.

VI. Bibliography list

1. Ramadori G, Moriconi F, Malik I, Dudas J. Physiology and pathophysiology of liver inflammation, damage and repair. J Physiol Pharmacol 2008;59 Suppl 1:107-117.
2. Leclercq IA, Da Silva Morais A, Schroyen B, Van Hul N, Geerts A. Insulin resistance in hepatocytes and sinusoidal liver cells: mechanisms and consequences. J Hepatol 2007;47:142-156.
3. Wallace K, Burt AD, Wright MC. Liver fibrosis. Biochem J 2008;411:1-18.
4. Yokota S. Functional differences between sinusoidal endothelial cells and interlobular or central vein endothelium in rat liver. Anat Rec 1985;212:74-80.
5. MacPhee PJ, Schmidt EE, Groom AC. Evidence for Kupffer cell migration along liver sinusoids, from high-resolution in vivo microscopy. Am J Physiol 1992;263:G17-23.
6. Crispe I: The liver: a unique immunologic environment. In: Boyer JL, Ockner R, eds. Progress in liver diseases. Volume 15. Philadelphia: WB Saunders, 1997; 109-124.
7. Friedman SL. Cytokines and fibrogenesis. Semin Liver Dis 1999;19:129-140.
8. Geerts A. History, heterogeneity, developmental biology, and functions of quiescent hepatic stellate cells. Semin Liver Dis 2001;21:311-335.
9. Weiskirchen R, Gressner AM. Isolation and culture of hepatic stellate cells. Methods Mol Med 2005;117:99-113.
10. Geerts A, Niki T, Hellemans K, De Craemer D, Van Den Berg K, Lazou JM, Stange G, et al. Purification of rat hepatic stellate cells by side scatter-activated cell sorting. Hepatology 1998;27:590-598.
11. Rockey DC. Hepatic blood flow regulation by stellate cells in normal and injured liver. Semin Liver Dis 2001;21:337-349.
12. Adams DH, Eksteen B. Aberrant homing of mucosal T cells and extra-intestinal manifestations of inflammatory bowel disease. Nat Rev Immunol 2006;6:244-251.
13. Friedman SL. Molecular regulation of hepatic fibrosis, an integrated cellular response to tissue injury. J Biol Chem 2000;275:2247-2250.
14. Pinzani M, Rombouts K, Colagrande S. Fibrosis in chronic liver diseases: diagnosis and management. J Hepatol 2005;42 Suppl:S22-36.
15. Friedman SL, Rockey DC, McGuire RF, Maher JJ, Boyles JK, Yamasaki G. Isolated hepatic lipocytes and Kupffer cells from normal human liver: morphological and functional characteristics in primary culture. Hepatology 1992;15:234-243.

16. Milani S, Herbst H, Schuppan D, Kim KY, Riecken EO, Stein H. Procollagen expression by nonparenchymal rat liver cells in experimental biliary fibrosis. Gastroenterology 1990;98:175-184.
17. Schuppan D. Structure of the extracellular matrix in normal and fibrotic liver: collagens and glycoproteins. Semin Liver Dis 1990;10:1-10.
18. Friedman SL. Hepatic stellate cells: protean, multifunctional, and enigmatic cells of the liver. Physiol Rev 2008;88:125-172.
19. Sanyal AJ, Bosch J, Blei A, Arroyo V. Portal hypertension and its complications. Gastroenterology 2008;134:1715-1728.
20. Lotersztajn S, Julien B, Teixeira-Clerc F, Grenard P, Mallat A. Hepatic fibrosis: molecular mechanisms and drug targets. Annu Rev Pharmacol Toxicol 2005;45:605-628.
21. Tsukada S, Parsons CJ, Rippe RA. Mechanisms of liver fibrosis. Clin Chim Acta 2006;364:33-60.
22. Gressner AM. Transdifferentiation of hepatic stellate cells (Ito cells) to myofibroblasts: a key event in hepatic fibrogenesis. Kidney Int Suppl 1996;54:S39-45.
23. Benyon RC, Arthur MJ. Extracellular matrix degradation and the role of hepatic stellate cells. Semin Liver Dis 2001;21:373-384.
24. Iredale JP. Models of liver fibrosis: exploring the dynamic nature of inflammation and repair in a solid organ. J Clin Invest 2007;117:539-548.
25. Bachem MG, Melchior R, Gressner AM. The role of thrombocytes in liver fibrogenesis: effects of platelet lysate and thrombocyte-derived growth factors on the mitogenic activity and glycosaminoglycan synthesis of cultured rat liver fat storing cells. J Clin Chem Clin Biochem 1989;27:555-565.
26. Li D, Friedman SL. Liver fibrogenesis and the role of hepatic stellate cells: new insights and prospects for therapy. J Gastroenterol Hepatol 1999;14:618-633.
27. Racine-Samson L, Rockey DC, Bissell DM. The role of alpha1beta1 integrin in wound contraction. A quantitative analysis of liver myofibroblasts in vivo and in primary culture. J Biol Chem 1997;272:30911-30917.
28. Gressner OA, Weiskirchen R, Gressner AM. Evolving concepts of liver fibrogenesis provide new diagnostic and therapeutic options. Comp Hepatol 2007;6:7.
29. Rockey D. The cellular pathogenesis of portal hypertension: stellate cell contractility, endothelin, and nitric oxide. Hepatology 1997;25:2-5.

30. Pinzani M, Failli P, Ruocco C, Casini A, Milani S, Baldi E, Giotti A, et al. Fat-storing cells as liver-specific pericytes. Spatial dynamics of agonist-stimulated intracellular calcium transients. J Clin Invest 1992;90:642-646.
31. Melton AC, Datta A, Yee HF, Jr. [Ca2+]i-independent contractile force generation by rat hepatic stellate cells in response to endothelin-1. Am J Physiol Gastrointest Liver Physiol 2006;290:G7-13.
32. Pietrangelo A. Metals, oxidative stress, and hepatic fibrogenesis. Semin Liver Dis 1996;16:13-30.
33. Kinnman N, Hultcrantz R, Barbu V, Rey C, Wendum D, Poupon R, Housset C. PDGF-mediated chemoattraction of hepatic stellate cells by bile duct segments in cholestatic liver injury. Lab Invest 2000;80:697-707.
34. Ikeda K, Wakahara T, Wang YQ, Kadoya H, Kawada N, Kaneda K. In vitro migratory potential of rat quiescent hepatic stellate cells and its augmentation by cell activation. Hepatology 1999;29:1760-1767.
35. Marra F, Romanelli RG, Giannini C, Failli P, Pastacaldi S, Arrighi MC, Pinzani M, et al. Monocyte chemotactic protein-1 as a chemoattractant for human hepatic stellate cells. Hepatology 1999;29:140-148.
36. Bonacchi A, Romagnani P, Romanelli RG, Efsen E, Annunziato F, Lasagni L, Francalanci M, et al. Signal transduction by the chemokine receptor CXCR3: activation of Ras/ERK, Src, and phosphatidylinositol 3-kinase/Akt controls cell migration and proliferation in human vascular pericytes. J Biol Chem 2001;276:9945-9954.
37. Melton AC, Yee HF. Hepatic stellate cell protrusions couple platelet-derived growth factor-BB to chemotaxis. Hepatology 2007;45:1446-1453.
38. Arii S, Mise M, Harada T, Furutani M, Ishigami S, Niwano M, Mizumoto M, et al. Overexpression of matrix metalloproteinase 9 gene in hepatocellular carcinoma with invasive potential. Hepatology 1996;24:316-322.
39. Friedman SL. Mechanisms of hepatic fibrogenesis. Gastroenterology 2008;134:1655-1669.
40. Plaa GL. Chlorinated methanes and liver injury: highlights of the past 50 years. Annu Rev Pharmacol Toxicol 2000;40:42-65.
41. Bataller R, Brenner DA. Liver fibrosis. J Clin Invest 2005;115:209-218.
42. Leclercq IA, Farrell GC, Schriemer R, Robertson GR. Leptin is essential for the hepatic fibrogenic response to chronic liver injury. J Hepatol 2002;37:206-213.

43. Sahai A, Malladi P, Pan X, Paul R, Melin-Aldana H, Green RM, Whitington PF. Obese and diabetic db/db mice develop marked liver fibrosis in a model of nonalcoholic steatohepatitis: role of short-form leptin receptors and osteopontin. Am J Physiol Gastrointest Liver Physiol 2004;287:G1035-1043.
44. Lunz JG, 3rd, Contrucci S, Ruppert K, Murase N, Fung JJ, Starzl TE, Demetris AJ. Replicative senescence of biliary epithelial cells precedes bile duct loss in chronic liver allograft rejection: increased expression of p21(WAF1/Cip1) as a disease marker and the influence of immunosuppressive drugs. Am J Pathol 2001;158:1379-1390.
45. Marra F, Gastaldelli A, Svegliati Baroni G, Tell G, Tiribelli C. Molecular basis and mechanisms of progression of non-alcoholic steatohepatitis. Trends Mol Med 2008;14:72-81.
46. Matsuura T, Nagamori S, Fujise K, Hasumura S, Homma S, Sujino H, Shimizu K, et al. Retinol transport in cultured fat-storing cells of rat liver. Quantitative analysis by anchored cell analysis and sorting system. Lab Invest 1989;61:107-115.
47. Vogel S, Piantedosi R, Frank J, Lalazar A, Rockey DC, Friedman SL, Blaner WS. An immortalized rat liver stellate cell line (HSC-T6): a new cell model for the study of retinoid metabolism in vitro. J Lipid Res 2000;41:882-893.
48. Schnabl B, Choi YH, Olsen JC, Hagedorn CH, Brenner DA. Immortal activated human hepatic stellate cells generated by ectopic telomerase expression. Lab Invest 2002;82:323-333.
49. Xu L, Hui AY, Albanis E, Arthur MJ, O'Byrne SM, Blaner WS, Mukherjee P, et al. Human hepatic stellate cell lines, LX-1 and LX-2: new tools for analysis of hepatic fibrosis. Gut 2005;54:142-151.
50. Ramesh S, Sanyal AJ. Evaluation and management of non-alcoholic steatohepatitis. J Hepatol 2005;42 Suppl:S2-12.
51. Clark JM, Brancati FL, Diehl AM. Nonalcoholic fatty liver disease. Gastroenterology 2002;122:1649-1657.
52. Angulo P. Nonalcoholic fatty liver disease. N Engl J Med 2002;346:1221-1231.
53. Neuschwander-Tetri BA, Caldwell SH. Nonalcoholic steatohepatitis: summary of an AASLD Single Topic Conference. Hepatology 2003;37:1202-1219.
54. Palekar NA, Naus R, Larson SP, Ward J, Harrison SA. Clinical model for distinguishing nonalcoholic steatohepatitis from simple steatosis in patients with nonalcoholic fatty liver disease. Liver Int 2006;26:151-156.

55. Abrams GA, Kunde SS, Lazenby AJ, Clements RH. Portal fibrosis and hepatic steatosis in morbidly obese subjects: A spectrum of nonalcoholic fatty liver disease. Hepatology 2004;40:475-483.
56. Cortez-Pinto H, de Moura MC, Day CP. Non-alcoholic steatohepatitis: from cell biology to clinical practice. J Hepatol 2006;44:197-208.
57. Luo Z, Saha AK, Xiang X, Ruderman NB. AMPK, the metabolic syndrome and cancer. Trends Pharmacol Sci 2005;26:69-76.
58. Farrell GC, Larter CZ. Nonalcoholic fatty liver disease: from steatosis to cirrhosis. Hepatology 2006;43:S99-S112.
59. Leclercq IA, Horsmans Y. Nonalcoholic fatty liver disease: the potential role of nutritional management. Curr Opin Clin Nutr Metab Care 2008;11:766-773.
60. Shoelson SE, Lee J, Goldfine AB. Inflammation and insulin resistance. J Clin Invest 2006;116:1793-1801.
61. Roden M. Mechanisms of Disease: hepatic steatosis in type 2 diabetes--pathogenesis and clinical relevance. Nat Clin Pract Endocrinol Metab 2006;2:335-348.
62. Yang SQ, Lin HZ, Lane MD, Clemens M, Diehl AM. Obesity increases sensitivity to endotoxin liver injury: implications for the pathogenesis of steatohepatitis. Proc Natl Acad Sci U S A 1997;94:2557-2562.
63. Li Z, Oben JA, Yang S, Lin H, Stafford EA, Soloski MJ, Thomas SA, et al. Norepinephrine regulates hepatic innate immune system in leptin-deficient mice with nonalcoholic steatohepatitis. Hepatology 2004;40:434-441.
64. Chavin KD, Yang S, Lin HZ, Chatham J, Chacko VP, Hoek JB, Walajtys-Rode E, et al. Obesity induces expression of uncoupling protein-2 in hepatocytes and promotes liver ATP depletion. J Biol Chem 1999;274:5692-5700.
65. Li Z, Yang S, Lin H, Huang J, Watkins PA, Moser AB, Desimone C, et al. Probiotics and antibodies to TNF inhibit inflammatory activity and improve nonalcoholic fatty liver disease. Hepatology 2003;37:343-350.
66. Rizki G, Arnaboldi L, Gabrielli B, Yan J, Lee GS, Ng RK, Turner SM, et al. Mice fed a lipogenic methionine-choline-deficient diet develop hypermetabolism coincident with hepatic suppression of SCD-1. J Lipid Res 2006;47:2280-2290.
67. Leclercq IA, Lebrun VA, Starkel P, Horsmans YJ. Intrahepatic insulin resistance in a murine model of steatohepatitis: effect of PPARgamma agonist pioglitazone. Lab Invest 2007;87:56-65.

68. Romestaing C, Piquet MA, Bedu E, Rouleau V, Dautresme M, Hourmand-Ollivier I, Filippi C, et al. Long term highly saturated fat diet does not induce NASH in Wistar rats. Nutr Metab (Lond) 2007;4:4.

69. Ito M, Suzuki J, Tsujioka S, Sasaki M, Gomori A, Shirakura T, Hirose H, et al. Longitudinal analysis of murine steatohepatitis model induced by chronic exposure to high-fat diet. Hepatol Res 2007;37:50-57.

70. Lieber CS, Leo MA, Mak KM, Xu Y, Cao Q, Ren C, Ponomarenko A, et al. Model of nonalcoholic steatohepatitis. Am J Clin Nutr 2004;79:502-509.

71. Svegliati-Baroni G, Candelaresi C, Saccomanno S, Ferretti G, Bachetti T, Marzioni M, De Minicis S, et al. A model of insulin resistance and nonalcoholic steatohepatitis in rats: role of peroxisome proliferator-activated receptor-alpha and n-3 polyunsaturated fatty acid treatment on liver injury. Am J Pathol 2006;169:846-860.

72. Desvergne B, Wahli W. Peroxisome proliferator-activated receptors: nuclear control of metabolism. Endocr Rev 1999;20:649-688.

73. Bragt MC, Popeijus HE. Peroxisome proliferator-activated receptors and the metabolic syndrome. Physiol Behav 2008;94:187-197.

74. Braissant O, Wahli W. Differential expression of peroxisome proliferator-activated receptor-alpha, -beta, and -gamma during rat embryonic development. Endocrinology 1998;139:2748-2754.

75. Palmer CN, Hsu MH, Griffin KJ, Raucy JL, Johnson EF. Peroxisome proliferator activated receptor-alpha expression in human liver. Mol Pharmacol 1998;53:14-22.

76. Saez E, Tontonoz P, Nelson MC, Alvarez JG, Ming UT, Baird SM, Thomazy VA, et al. Activators of the nuclear receptor PPARgamma enhance colon polyp formation. Nat Med 1998;4:1058-1061.

77. Moore KJ, Rosen ED, Fitzgerald ML, Randow F, Andersson LP, Altshuler D, Milstone DS, et al. The role of PPAR-gamma in macrophage differentiation and cholesterol uptake. Nat Med 2001;7:41-47.

78. Gavrilova O, Haluzik M, Matsusue K, Cutson JJ, Johnson L, Dietz KR, Nicol CJ, et al. Liver peroxisome proliferator-activated receptor gamma contributes to hepatic steatosis, triglyceride clearance, and regulation of body fat mass. J Biol Chem 2003;278:34268-34276.

79. Westergaard M, Henningsen J, Svendsen ML, Johansen C, Jensen UB, Schroder HD, Kratchmarova I, et al. Modulation of keratinocyte gene expression and differentiation

by PPAR-selective ligands and tetradecylthioacetic acid. J Invest Dermatol 2001;116:702-712.

80. Romanowska M, al Yacoub N, Seidel H, Donandt S, Gerken H, Phillip S, Haritonova N, et al. PPARdelta enhances keratinocyte proliferation in psoriasis and induces heparin-binding EGF-like growth factor. J Invest Dermatol 2008;128:110-124.
81. Diradourian C, Girard J, Pegorier JP. Phosphorylation of PPARs: from molecular characterization to physiological relevance. Biochimie 2005;87:33-38.
82. Bishop-Bailey D. Peroxisome proliferator-activated receptors in the cardiovascular system. Br J Pharmacol 2000;129:823-834.
83. Zoete V, Grosdidier A, Michielin O. Peroxisome proliferator-activated receptor structures: ligand specificity, molecular switch and interactions with regulators. Biochim Biophys Acta 2007;1771:915-925.
84. Odegaard JI, Ricardo-Gonzalez RR, Red Eagle A, Vats D, Morel CR, Goforth MH, Subramanian V, et al. Alternative M2 activation of Kupffer cells by PPARdelta ameliorates obesity-induced insulin resistance. Cell Metab 2008;7:496-507.
85. Alaynick WA. Nuclear receptors, mitochondria and lipid metabolism. Mitochondrion 2008.
86. Muoio DM, Way JM, Tanner CJ, Winegar DA, Kliewer SA, Houmard JA, Kraus WE, et al. Peroxisome proliferator-activated receptor-alpha regulates fatty acid utilization in primary human skeletal muscle cells. Diabetes 2002;51:901-909.
87. Orasanu G, Ziouzenkova O, Devchand PR, Nehra V, Hamdy O, Horton ES, Plutzky J. The peroxisome proliferator-activated receptor-gamma agonist pioglitazone represses inflammation in a peroxisome proliferator-activated receptor-alpha-dependent manner in vitro and in vivo in mice. J Am Coll Cardiol 2008;52:869-881.
88. Yokota T, Oritani K, Takahashi I, Ishikawa J, Matsuyama A, Ouchi N, Kihara S, et al. Adiponectin, a new member of the family of soluble defense collagens, negatively regulates the growth of myelomonocytic progenitors and the functions of macrophages. Blood 2000;96:1723-1732.
89. Way JM, Harrington WW, Brown KK, Gottschalk WK, Sundseth SS, Mansfield TA, Ramachandran RK, et al. Comprehensive messenger ribonucleic acid profiling reveals that peroxisome proliferator-activated receptor gamma activation has coordinate effects on gene expression in multiple insulin-sensitive tissues. Endocrinology 2001;142:1269-1277.

90. De Vos P, Lefebvre AM, Miller SG, Guerre-Millo M, Wong K, Saladin R, Hamann LG, et al. Thiazolidinediones repress ob gene expression in rodents via activation of peroxisome proliferator-activated receptor gamma. J Clin Invest 1996;98:1004-1009.
91. Peraldi P, Xu M, Spiegelman BM. Thiazolidinediones block tumor necrosis factor-alpha-induced inhibition of insulin signaling. J Clin Invest 1997;100:1863-1869.
92. Maeda N, Takahashi M, Funahashi T, Kihara S, Nishizawa H, Kishida K, Nagaretani H, et al. PPARgamma ligands increase expression and plasma concentrations of adiponectin, an adipose-derived protein. Diabetes 2001;50:2094-2099.
93. Tontonoz P, Hu E, Spiegelman BM. Stimulation of adipogenesis in fibroblasts by PPAR gamma 2, a lipid-activated transcription factor. Cell 1994;79:1147-1156.
94. Yamauchi T, Kamon J, Waki H, Murakami K, Motojima K, Komeda K, Ide T, et al. The mechanisms by which both heterozygous peroxisome proliferator-activated receptor gamma (PPARgamma) deficiency and PPARgamma agonist improve insulin resistance. J Biol Chem 2001;276:41245-41254.
95. Rosen ED, Spiegelman BM. PPARgamma : a nuclear regulator of metabolism, differentiation, and cell growth. J Biol Chem 2001;276:37731-37734.
96. Barak Y, Nelson MC, Ong ES, Jones YZ, Ruiz-Lozano P, Chien KR, Koder A, et al. PPAR gamma is required for placental, cardiac, and adipose tissue development. Mol Cell 1999;4:585-595.
97. Sharma AM, Staels B. Review: Peroxisome proliferator-activated receptor gamma and adipose tissue--understanding obesity-related changes in regulation of lipid and glucose metabolism. J Clin Endocrinol Metab 2007;92:386-395.
98. Hazra S, Xiong S, Wang J, Rippe RA, Krishna V, Chatterjee K, Tsukamoto H. Peroxisome proliferator-activated receptor gamma induces a phenotypic switch from activated to quiescent hepatic stellate cells. J Biol Chem 2004;279:11392-11401.
99. Miyahara T, Schrum L, Rippe R, Xiong S, Yee HF, Jr., Motomura K, Anania FA, et al. Peroxisome proliferator-activated receptors and hepatic stellate cell activation. J Biol Chem 2000;275:35715-35722.
100. Galli A, Crabb DW, Ceni E, Salzano R, Mello T, Svegliati-Baroni G, Ridolfi F, et al. Antidiabetic thiazolidinediones inhibit collagen synthesis and hepatic stellate cell activation in vivo and in vitro. Gastroenterology 2002;122:1924-1940.
101. Lutchman G, Promrat K, Kleiner DE, Heller T, Ghany MG, Yanovski JA, Liang TJ, et al. Changes in serum adipokine levels during pioglitazone treatment for nonalcoholic

steatohepatitis: relationship to histological improvement. Clin Gastroenterol Hepatol 2006;4:1048-1052.

102. Promrat K, Lutchman G, Uwaifo GI, Freedman RJ, Soza A, Heller T, Doo E, et al. A pilot study of pioglitazone treatment for nonalcoholic steatohepatitis. Hepatology 2004;39:188-196.

103. Neuschwander-Tetri BA, Brunt EM, Wehmeier KR, Oliver D, Bacon BR. Improved nonalcoholic steatohepatitis after 48 weeks of treatment with the PPAR-gamma ligand rosiglitazone. Hepatology 2003;38:1008-1017.

104. Belfort R, Harrison SA, Brown K, Darland C, Finch J, Hardies J, Balas B, et al. A placebo-controlled trial of pioglitazone in subjects with nonalcoholic steatohepatitis. N Engl J Med 2006;355:2297-2307.

105. Ratziu V, Giral P, Jacqueminet S, Charlotte F, Hartemann-Heurtier A, Serfaty L, Podevin P, et al. Rosiglitazone for nonalcoholic steatohepatitis: one-year results of the randomized placebo-controlled Fatty Liver Improvement with Rosiglitazone Therapy (FLIRT) Trial. Gastroenterology 2008;135:100-110.

106. Fang X, Sweeney G. Mechanisms regulating energy metabolism by adiponectin in obesity and diabetes. Biochem Soc Trans 2006;34:798-801.

107. Kadowaki T, Yamauchi T. Adiponectin and adiponectin receptors. Endocr Rev 2005;26:439-451.

108. Zou C, Shao J. Role of adipocytokines in obesity-associated insulin resistance. J Nutr Biochem 2008;19:277-286.

109. Wolf AM, Wolf D, Avila MA, Moschen AR, Berasain C, Enrich B, Rumpold H, et al. Up-regulation of the anti-inflammatory adipokine adiponectin in acute liver failure in mice. J Hepatol 2006;44:537-543.

110. Maeda N, Shimomura I, Kishida K, Nishizawa H, Matsuda M, Nagaretani H, Furuyama N, et al. Diet-induced insulin resistance in mice lacking adiponectin/ACRP30. Nat Med 2002;8:731-737.

111. Yamauchi T, Kamon J, Ito Y, Tsuchida A, Yokomizo T, Kita S, Sugiyama T, et al. Cloning of adiponectin receptors that mediate antidiabetic metabolic effects. Nature 2003;423:762-769.

112. Mao X, Kikani CK, Riojas RA, Langlais P, Wang L, Ramos FJ, Fang Q, et al. APPL1 binds to adiponectin receptors and mediates adiponectin signalling and function. Nat Cell Biol 2006;8:516-523.

113. Hosch SE, Olefsky JM, Kim JJ. APPLied mechanics: uncovering how adiponectin modulates insulin action. Cell Metab 2006;4:5-6.

114. Tsuchida A, Yamauchi T, Ito Y, Hada Y, Maki T, Takekawa S, Kamon J, et al. Insulin/Foxo1 pathway regulates expression levels of adiponectin receptors and adiponectin sensitivity. J Biol Chem 2004;279:30817-30822.

115. Winder WW, Hardie DG. AMP-activated protein kinase, a metabolic master switch: possible roles in type 2 diabetes. Am J Physiol 1999;277:E1-10.

116. Lochhead PA, Salt IP, Walker KS, Hardie DG, Sutherland C. 5-aminoimidazole-4-carboxamide riboside mimics the effects of insulin on the expression of the 2 key gluconeogenic genes PEPCK and glucose-6-phosphatase. Diabetes 2000;49:896-903.

117. Park H, Kaushik VK, Constant S, Prentki M, Przybytkowski E, Ruderman NB, Saha AK. Coordinate regulation of malonyl-CoA decarboxylase, sn-glycerol-3-phosphate acyltransferase, and acetyl-CoA carboxylase by AMP-activated protein kinase in rat tissues in response to exercise. J Biol Chem 2002;277:32571-32577.

118. McGarry JD, Brown NF. The mitochondrial carnitine palmitoyltransferase system. From concept to molecular analysis. Eur J Biochem 1997;244:1-14.

119. Minokoshi Y, Kim YB, Peroni OD, Fryer LG, Muller C, Carling D, Kahn BB. Leptin stimulates fatty-acid oxidation by activating AMP-activated protein kinase. Nature 2002;415:339-343.

120. Zhou G, Myers R, Li Y, Chen Y, Shen X, Fenyk-Melody J, Wu M, et al. Role of AMP-activated protein kinase in mechanism of metformin action. J Clin Invest 2001;108:1167-1174.

121. Foretz M, Ancellin N, Andreelli F, Saintillan Y, Grondin P, Kahn A, Thorens B, et al. Short-term overexpression of a constitutively active form of AMP-activated protein kinase in the liver leads to mild hypoglycemia and fatty liver. Diabetes 2005;54:1331-1339.

122. Yamauchi T, Kamon J, Minokoshi Y, Ito Y, Waki H, Uchida S, Yamashita S, et al. Adiponectin stimulates glucose utilization and fatty-acid oxidation by activating AMP-activated protein kinase. Nat Med 2002;8:1288-1295.

123. Rao MS, Reddy JK. PPARalpha in the pathogenesis of fatty liver disease. Hepatology 2004;40:783-786.

124. Delerive P, Gervois P, Fruchart JC, Staels B. Induction of IkappaBalpha expression as a mechanism contributing to the anti-inflammatory activities of peroxisome proliferator-activated receptor-alpha activators. J Biol Chem 2000;275:36703-36707.

125. Baeuerle PA, Baltimore D. I kappa B: a specific inhibitor of the NF-kappa B transcription factor. Science 1988;242:540-546.
126. Ouchi N, Walsh K. Adiponectin as an anti-inflammatory factor. Clin Chim Acta 2007;380:24-30.
127. Blake GJ, Ridker PM. Novel clinical markers of vascular wall inflammation. Circ Res 2001;89:763-771.
128. Kamada Y, Tamura S, Kiso S, Matsumoto H, Saji Y, Yoshida Y, Fukui K, et al. Enhanced carbon tetrachloride-induced liver fibrosis in mice lacking adiponectin. Gastroenterology 2003;125:1796-1807.
129. Ding X, Saxena NK, Lin S, Xu A, Srinivasan S, Anania FA. The roles of leptin and adiponectin: a novel paradigm in adipocytokine regulation of liver fibrosis and stellate cell biology. Am J Pathol 2005;166:1655-1669.
130. Adachi M, Brenner DA. High molecular weight adiponectin inhibits proliferation of hepatic stellate cells via activation of adenosine monophosphate-activated protein kinase. Hepatology 2008;47:677-685.
131. Bugianesi E, Pagotto U, Manini R, Vanni E, Gastaldelli A, de Iasio R, Gentilcore E, et al. Plasma adiponectin in nonalcoholic fatty liver is related to hepatic insulin resistance and hepatic fat content, not to liver disease severity. J Clin Endocrinol Metab 2005;90:3498-3504.
132. Kaser S, Moschen A, Cayon A, Kaser A, Crespo J, Pons-Romero F, Ebenbichler CF, et al. Adiponectin and its receptors in non-alcoholic steatohepatitis. Gut 2005;54:117-121.
133. Larter CZ, Farrell GC. Insulin resistance, adiponectin, cytokines in NASH: Which is the best target to treat? J Hepatol 2006;44:253-261.
134. Targher G, Bertolini L, Rodella S, Zoppini G, Scala L, Zenari L, Falezza G. Associations between plasma adiponectin concentrations and liver histology in patients with nonalcoholic fatty liver disease. Clin Endocrinol (Oxf) 2006;64:679-683.
135. Hardie DG. The AMP-activated protein kinase pathway--new players upstream and downstream. J Cell Sci 2004;117:5479-5487.
136. Davies SP, Helps NR, Cohen PT, Hardie DG. 5'-AMP inhibits dephosphorylation, as well as promoting phosphorylation, of the AMP-activated protein kinase. Studies using bacterially expressed human protein phosphatase-2C alpha and native bovine protein phosphatase-2AC. FEBS Lett 1995;377:421-425.

137. Hawley SA, Pan DA, Mustard KJ, Ross L, Bain J, Edelman AM, Frenguelli BG, et al. Calmodulin-dependent protein kinase kinase-beta is an alternative upstream kinase for AMP-activated protein kinase. Cell Metab 2005;2:9-19.

138. Hardie DG. Minireview: the AMP-activated protein kinase cascade: the key sensor of cellular energy status. Endocrinology 2003;144:5179-5183.

139. Kahn BB, Alquier T, Carling D, Hardie DG. AMP-activated protein kinase: ancient energy gauge provides clues to modern understanding of metabolism. Cell Metab 2005;1:15-25.

140. Carling D. The AMP-activated protein kinase cascade--a unifying system for energy control. Trends Biochem Sci 2004;29:18-24.

141. Fryer LG, Parbu-Patel A, Carling D. The Anti-diabetic drugs rosiglitazone and metformin stimulate AMP-activated protein kinase through distinct signaling pathways. J Biol Chem 2002;277:25226-25232.

142. Corton JM, Gillespie JG, Hawley SA, Hardie DG. 5-aminoimidazole-4-carboxamide ribonucleoside. A specific method for activating AMP-activated protein kinase in intact cells? Eur J Biochem 1995;229:558-565.

143. Longnus SL, Wambolt RB, Parsons HL, Brownsey RW, Allard MF. 5-Aminoimidazole-4-carboxamide 1-beta -D-ribofuranoside (AICAR) stimulates myocardial glycogenolysis by allosteric mechanisms. Am J Physiol Regul Integr Comp Physiol 2003;284:R936-944.

144. Vincent MF, Marangos PJ, Gruber HE, Van den Berghe G. Inhibition by AICA riboside of gluconeogenesis in isolated rat hepatocytes. Diabetes 1991;40:1259-1266.

145. Viollet B, Andreelli F, Jorgensen SB, Perrin C, Flamez D, Mu J, Wojtaszewski JF, et al. Physiological role of AMP-activated protein kinase (AMPK): insights from knockout mouse models. Biochem Soc Trans 2003;31:216-219.

146. Viollet B, Andreelli F, Jorgensen SB, Perrin C, Geloen A, Flamez D, Mu J, et al. The AMP-activated protein kinase alpha2 catalytic subunit controls whole-body insulin sensitivity. J Clin Invest 2003;111:91-98.

147. Viollet B, Foretz M, Guigas B, Horman S, Dentin R, Bertrand L, Hue L, et al. Activation of AMP-activated protein kinase in the liver: a new strategy for the management of metabolic hepatic disorders. J Physiol 2006;574:41-53.

148. Mukhtar MH, Payne VA, Arden C, Harbottle A, Khan S, Lange AJ, Agius L. Inhibition of glucokinase translocation by AMP-activated protein kinase is associated

with phosphorylation of both GKRP and 6-phosphofructo-2-kinase/fructose-2,6-bisphosphatase. Am J Physiol Regul Integr Comp Physiol 2008;294:R766-774.

149. Long YC, Zierath JR. AMP-activated protein kinase signaling in metabolic regulation. J Clin Invest 2006;116:1776-1783.
150. Kemp BE, Stapleton D, Campbell DJ, Chen ZP, Murthy S, Walter M, Gupta A, et al. AMP-activated protein kinase, super metabolic regulator. Biochem Soc Trans 2003;31:162-168.
151. Jakobsen SN, Hardie DG, Morrice N, Tornqvist HE. 5'-AMP-activated protein kinase phosphorylates IRS-1 on Ser-789 in mouse C2C12 myotubes in response to 5-aminoimidazole-4-carboxamide riboside. J Biol Chem 2001;276:46912-46916.
152. Qiao LY, Zhande R, Jetton TL, Zhou G, Sun XJ. In vivo phosphorylation of insulin receptor substrate 1 at serine 789 by a novel serine kinase in insulin-resistant rodents. J Biol Chem 2002;277:26530-26539.
153. Luiken JJ, Coort SL, Willems J, Coumans WA, Bonen A, van der Vusse GJ, Glatz JF. Contraction-induced fatty acid translocase/CD36 translocation in rat cardiac myocytes is mediated through AMP-activated protein kinase signaling. Diabetes 2003;52:1627-1634.
154. Rattan R, Giri S, Singh AK, Singh I. 5-Aminoimidazole-4-carboxamide-1-beta-D-ribofuranoside inhibits cancer cell proliferation in vitro and in vivo via AMP-activated protein kinase. J Biol Chem 2005;280:39582-39593.
155. Jones RG, Plas DR, Kubek S, Buzzai M, Mu J, Xu Y, Birnbaum MJ, et al. AMP-activated protein kinase induces a p53-dependent metabolic checkpoint. Mol Cell 2005;18:283-293.
156. Wang W, Fan J, Yang X, Furer-Galban S, Lopez de Silanes I, von Kobbe C, Guo J, et al. AMP-activated kinase regulates cytoplasmic HuR. Mol Cell Biol 2002;22:3425-3436.
157. Xiang X, Saha AK, Wen R, Ruderman NB, Luo Z. AMP-activated protein kinase activators can inhibit the growth of prostate cancer cells by multiple mechanisms. Biochem Biophys Res Commun 2004;321:161-167.
158. Kimura N, Tokunaga C, Dalal S, Richardson C, Yoshino K, Hara K, Kemp BE, et al. A possible linkage between AMP-activated protein kinase (AMPK) and mammalian target of rapamycin (mTOR) signalling pathway. Genes Cells 2003;8:65-79.
159. Carrera AC. TOR signaling in mammals. J Cell Sci 2004;117:4615-4616.

160. Su RY, Chao Y, Chen TY, Huang DY, Lin WW. 5-Aminoimidazole-4-carboxamide riboside sensitizes TRAIL- and TNF{alpha}-induced cytotoxicity in colon cancer cells through AMP-activated protein kinase signaling. Mol Cancer Ther 2007;6:1562-1571.
161. Huang NL, Chiang SH, Hsueh CH, Liang YJ, Chen YJ, Lai LP. Metformin inhibits TNF-alpha-induced IkappaB kinase phosphorylation, IkappaB-alpha degradation and IL-6 production in endothelial cells through PI3K-dependent AMPK phosphorylation. Int J Cardiol 2008.
162. Zhao X, Zmijewski JW, Lorne E, Liu G, Park YJ, Tsuruta Y, Abraham E. Activation of AMPK attenuates neutrophil proinflammatory activity and decreases the severity of acute lung injury. Am J Physiol Lung Cell Mol Physiol 2008;295:L497-504.
163. Lihn AS, Pedersen SB, Lund S, Richelsen B. The anti-diabetic AMPK activator AICAR reduces IL-6 and IL-8 in human adipose tissue and skeletal muscle cells. Mol Cell Endocrinol 2008;292:36-41.
164. Sag D, Carling D, Stout RD, Suttles J. Adenosine 5'-monophosphate-activated protein kinase promotes macrophage polarization to an anti-inflammatory functional phenotype. J Immunol 2008;181:8633-8641.
165. Chandrasekar B, Boylston WH, Venkatachalam K, Webster NJ, Prabhu SD, Valente AJ. Adiponectin blocks interleukin-18-mediated endothelial cell death via APPL1-dependent AMP-activated protein kinase (AMPK) activation and IKK/NF-kappaB/PTEN suppression. J Biol Chem 2008;283:24889-24898.
166. Devaraj S, Torok N, Dasu MR, Samols D, Jialal I. Adiponectin decreases C-reactive protein synthesis and secretion from endothelial cells: evidence for an adipose tissue-vascular loop. Arterioscler Thromb Vasc Biol 2008;28:1368-1374.
167. Lelli JL, Jr., Becks LL, Dabrowska MI, Hinshaw DB. ATP converts necrosis to apoptosis in oxidant-injured endothelial cells. Free Radic Biol Med 1998;25:694-702.
168. Choi SL, Kim SJ, Lee KT, Kim J, Mu J, Birnbaum MJ, Soo Kim S, et al. The regulation of AMP-activated protein kinase by H(2)O(2). Biochem Biophys Res Commun 2001;287:92-97.
169. Zou MH, Hou XY, Shi CM, Kirkpatick S, Liu F, Goldman MH, Cohen RA. Activation of 5'-AMP-activated kinase is mediated through c-Src and phosphoinositide 3-kinase activity during hypoxia-reoxygenation of bovine aortic endothelial cells. Role of peroxynitrite. J Biol Chem 2003;278:34003-34010.

170. Irrcher I, Ljubicic V, Hood DA. Interactions between ROS and AMP kinase activity in the regulation of PGC-1{alpha} transcription in skeletal muscle cells. Am J Physiol Cell Physiol 2009;296:C116-123.
171. Jensen TE, Schjerling P, Viollet B, Wojtaszewski JF, Richter EA. AMPK alpha1 activation is required for stimulation of glucose uptake by twitch contraction, but not by H2O2, in mouse skeletal muscle. PLoS ONE 2008;3:e2102.
172. Marra F, Efsen E, Romanelli RG, Caligiuri A, Pastacaldi S, Batignani G, Bonacchi A, et al. Ligands of peroxisome proliferator-activated receptor gamma modulate profibrogenic and proinflammatory actions in hepatic stellate cells. Gastroenterology 2000;119:466-478.
173. Hazra S, Miyahara T, Rippe RA, Tsukamoto H. PPAR Gamma and Hepatic Stellate Cells. Comp Hepatol 2004;3 Suppl 1:S7.
174. She H, Xiong S, Hazra S, Tsukamoto H. Adipogenic transcriptional regulation of hepatic stellate cells. J Biol Chem 2005;280:4959-4967.
175. Caligiuri A, Bertolani C, Guerra CT, Aleffi S, Galastri S, Trappoliere M, Vizzutti F, et al. Adenosine monophosphate-activated protein kinase modulates the activated phenotype of hepatic stellate cells. Hepatology 2008;47:668-676.
176. Dixon JB, Bhathal PS, O'Brien PE. Nonalcoholic fatty liver disease: predictors of nonalcoholic steatohepatitis and liver fibrosis in the severely obese. Gastroenterology 2001;121:91-100.
177. Horton JD. Sterol regulatory element-binding proteins: transcriptional activators of lipid synthesis. Biochem Soc Trans 2002;30:1091-1095.
178. Dobrzyn P, Dobrzyn A, Miyazaki M, Cohen P, Asilmaz E, Hardie DG, Friedman JM, et al. Stearoyl-CoA desaturase 1 deficiency increases fatty acid oxidation by activating AMP-activated protein kinase in liver. Proc Natl Acad Sci U S A 2004;101:6409-6414.
179. Leclercq IA, Sempoux C, Starkel P, Horsmans Y. Limited therapeutic efficacy of pioglitazone on progression of hepatic fibrosis in rats. Gut 2006;55:1020-1029.
180. Imamura K, Ogura T, Kishimoto A, Kaminishi M, Esumi H. Cell cycle regulation via p53 phosphorylation by a 5'-AMP activated protein kinase activator, 5-aminoimidazole- 4-carboxamide-1-beta-D-ribofuranoside, in a human hepatocellular carcinoma cell line. Biochem Biophys Res Commun 2001;287:562-567.
181. Igata M, Motoshima H, Tsuruzoe K, Kojima K, Matsumura T, Kondo T, Taguchi T, et al. Adenosine monophosphate-activated protein kinase suppresses vascular smooth

muscle cell proliferation through the inhibition of cell cycle progression. Circ Res 2005;97:837-844.

182. Gwinn DM, Shackelford DB, Egan DF, Mihaylova MM, Mery A, Vasquez DS, Turk BE, et al. AMPK phosphorylation of raptor mediates a metabolic checkpoint. Mol Cell 2008;30:214-226.
183. Ota T, Takamura T, Kurita S, Matsuzawa N, Kita Y, Uno M, Akahori H, et al. Insulin resistance accelerates a dietary rat model of nonalcoholic steatohepatitis. Gastroenterology 2007;132:282-293.
184. Saha AK, Avilucea PR, Ye JM, Assifi MM, Kraegen EW, Ruderman NB. Pioglitazone treatment activates AMP-activated protein kinase in rat liver and adipose tissue in vivo. Biochem Biophys Res Commun 2004;314:580-585.
185. LeBrasseur NK, Kelly M, Tsao TS, Farmer SR, Saha AK, Ruderman NB, Tomas E. Thiazolidinediones can rapidly activate AMP-activated protein kinase in mammalian tissues. Am J Physiol Endocrinol Metab 2006;291:E175-181.
186. Tomas E, Tsao TS, Saha AK, Murrey HE, Zhang Cc C, Itani SI, Lodish HF, et al. Enhanced muscle fat oxidation and glucose transport by ACRP30 globular domain: acetyl-CoA carboxylase inhibition and AMP-activated protein kinase activation. Proc Natl Acad Sci U S A 2002;99:16309-16313.
187. Ip E, Farrell GC, Robertson G, Hall P, Kirsch R, Leclercq I. Central role of PPARalpha-dependent hepatic lipid turnover in dietary steatohepatitis in mice. Hepatology 2003;38:123-132.
188. Ip E, Farrell G, Hall P, Robertson G, Leclercq I. Administration of the potent PPARalpha agonist, Wy-14,643, reverses nutritional fibrosis and steatohepatitis in mice. Hepatology 2004;39:1286-1296.
189. Rinella ME, Elias MS, Smolak RR, Fu T, Borensztajn J, Green RM. Mechanisms of hepatic steatosis in mice fed a lipogenic methionine choline-deficient diet. J Lipid Res 2008;49:1068-1076.
190. Biddinger SB, Miyazaki M, Boucher J, Ntambi JM, Kahn CR. Leptin suppresses stearoyl-CoA desaturase 1 by mechanisms independent of insulin and sterol regulatory element-binding protein-1c. Diabetes 2006;55:2032-2041.
191. Ntambi JM, Miyazaki M, Stoehr JP, Lan H, Kendziorski CM, Yandell BS, Song Y, et al. Loss of stearoyl-CoA desaturase-1 function protects mice against adiposity. Proc Natl Acad Sci U S A 2002;99:11482-11486.

192. Bertrand L, Ginion A, Beauloye C, Hebert AD, Guigas B, Hue L, Vanoverschelde JL. AMPK activation restores the stimulation of glucose uptake in an in vitro model of insulin-resistant cardiomyocytes via the activation of protein kinase B. Am J Physiol Heart Circ Physiol 2006;291:H239-250.

193. Kim JB, Sarraf P, Wright M, Yao KM, Mueller E, Solanes G, Lowell BB, et al. Nutritional and insulin regulation of fatty acid synthetase and leptin gene expression through ADD1/SREBP1. J Clin Invest 1998;101:1-9.

194. Shimano H, Shimomura I, Hammer RE, Herz J, Goldstein JL, Brown MS, Horton JD. Elevated levels of SREBP-2 and cholesterol synthesis in livers of mice homozygous for a targeted disruption of the SREBP-1 gene. J Clin Invest 1997;100:2115-2124.

195. Horton JD, Goldstein JL, Brown MS. SREBPs: activators of the complete program of cholesterol and fatty acid synthesis in the liver. J Clin Invest 2002;109:1125-1131.

196. Kaser A, Lee AH, Franke A, Glickman JN, Zeissig S, Tilg H, Nieuwenhuis EE, et al. XBP1 links ER stress to intestinal inflammation and confers genetic risk for human inflammatory bowel disease. Cell 2008;134:743-756.

197. Kristensen DB, Kawada N, Imamura K, Miyamoto Y, Tateno C, Seki S, Kuroki T, et al. Proteome analysis of rat hepatic stellate cells. Hepatology 2000;32:268-277.

VII.Annexe

Isolation of hepatic stellate cells from mouse liver (Protocol for 5 mice)

The protocol to isolate primary hepatic stellate cells from mice (schematized in Figure 15) has been established from a rat protocol (197)

Material

Female 10 weeks old mice

Collagenase P (Roche)

Pronase E (MERCK)

Dnase I (Roche)

Histodenz (Sigma)

GBSS (Invitrogen)

Medium for pre-perfusion (pH 7.35) **SC1**: 5mM KCl; 1mM $MgCl_2.6H_2O$; 0,3mM $MgSO_4.7H_2O$; 0,3mM $Na_2HPO_4.12H_2O$; 0,2mM KH_2PO_4; 5mM glucose.H_2O; 3mM $NaHCO_3$; 1,5mM $CaCl_2.2H_2O$; 17µM phenol red.

Medium for perfusion (pH 7.35) **SC2**: 0,14M NaCl; 5mM KCl; 1mM $MgCl_2.6H_2O$; 0,3mM $MgSO_4.7H_2O$; 0,3mM $Na_2HPO_4.12H_2O$; 0,2mM KH_2PO_4; 5mM glucose.H_2O; 3mM $NaHCO_3$; 1,5mM $CaCl_2.2H_2O$; 17µM phenol red.

Medium for perfusion (pH 7.35) **GBSS-A**: 0,14M NaCl; 5mM KCl; 0,85mM Na_2HPO_4.anhydre; 0,6mM $NaH_2PO4.2H_2O$; 4,5mM glucose.H_2O; 4mM $NaHCO_3$; 0,5mM EGTA; 10mM HEPES; 17µM phenol red.

Medium for perfusion (pH 7.35) **GBSS-B**: 0,14M NaCl; 5mM KCl; 0,85mM Na_2HPO_4.anhydre; 0,6mM $NaH_2PO4.2H_2O$; 4mM $CaCl_2.2H_2O$; 4mM $NaHCO_3$; 10mM HEPES; 17µM phenol red.

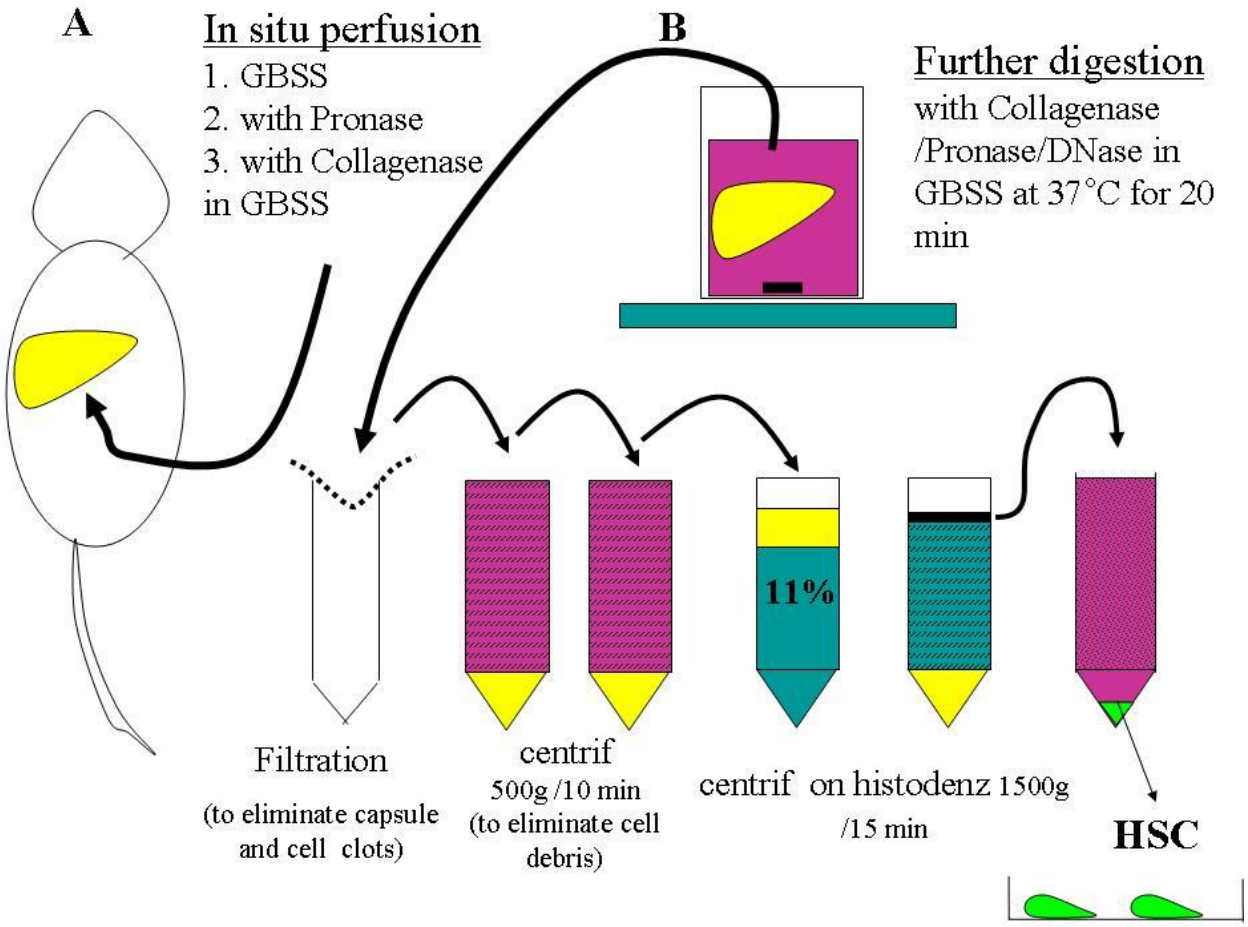

Figure 21: Schematic representation of mice HSC isolation protocol

Preparation

a. Prepare the pronase (100mg pronase E; 0.05%) and collagenase (50mg collagenase P; 0.025%) solutions for perfusion by filtering the enzymes, with a 0.2µm pore size single use sterile syringe filter, into 200ml of SC2.
b. Put the mediums for pre-perfusion (SC1) and perfusion (pronase and collagenase solutions) at 37°C in a water bath.
c. Prepare the Dnase solution (6mg Dnase; 0.2%) by filtration, with a 0.2µm pore size single use sterile syringe filter, into 3ml of GBSS.

Operation

a. Anaesthetize the mouse with Ketamine (0.1%) and Rompun (0.1%) by intra-peritoneal injection.
b. Open the abdominal cavity and expose the portal vein (Picture 1).

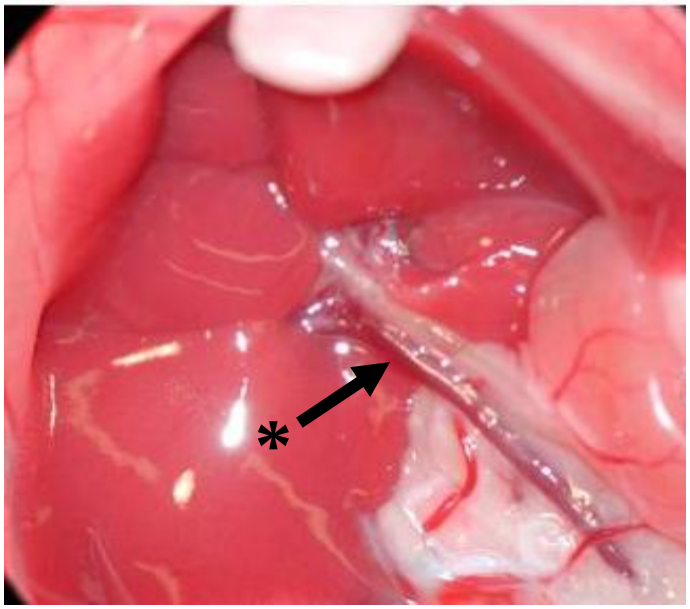

Picture 1: Localization of the portal vein

After opened the abdominal cavity and removed viscera, the portal vein is visualized (*****)

c. Insert a 26G needle into the portal vein and fix it with a clamp.

Perfusion and in situ digestion

a. Start the pre-perfusion with SC1 medium at the rate of approximately 6 - 7 ml/min, cut the Venacava inferior and continue the pre-perfusion for 5 min (Picture 2).

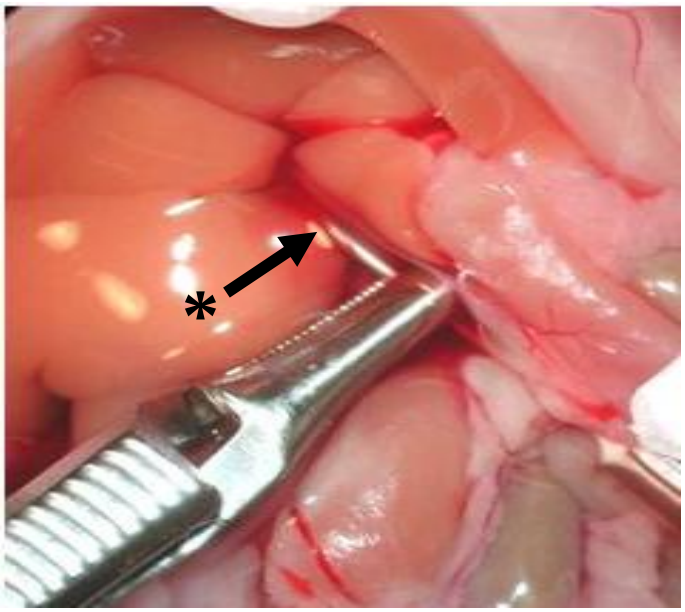

Picture 2: Liver perfusion

A 26G needle is inserted in the portal vein (*****) in order to flush the liver.

b. Perfuse the liver with the pronase solution for 5 min at the same speed (Picture 3).

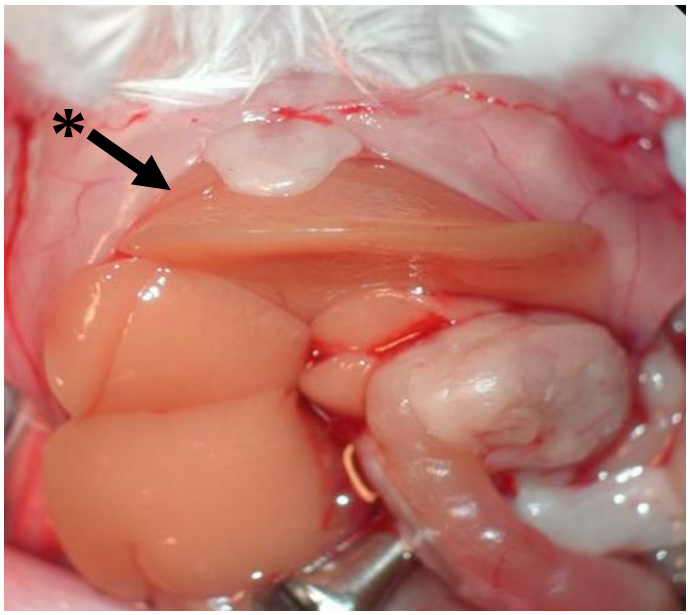

Picture 3: Effect of pronase perfusion

The pronase solution increased significantly the volume of the liver (*****).

c. Perfuse the liver with the collagenase solution for 5 min ate the same speed (Picture 4).

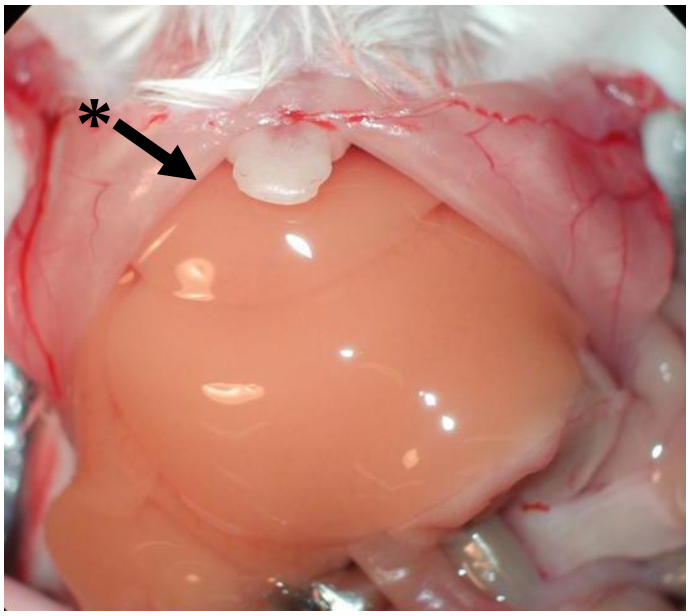

Picture 4: Effect of collagenase perfusion

The collagenase solution damaged the hepatic collagen structure (*****).

d. Carefully take the liver out and put it into 30 ml of cold SC2.
e. Meanwhile put the Dnase solution at 37°C in a water bath.

Digestion

a. When all the digested livers are collected, minced them well into a wide-mouth beaker containing 120ml SC2 medium (digestion medium) composed by 50mg pronase E + 50mg collagenase P, filtered with a 0.2µm pore size single use sterile syringe filter, + 1ml Dnase solution and incubate it for 20 min in a 37°c water bath.
b. Every 2 min, in the first 10min, and every 5 min, in the latest, add 1 drop of NaOH 1M to readjust the pH of the medium.
c. After digestion, filtrate the cell solution medium with a nylon mesh gauze (100µm pore size).
d. Collect the cell solution medium and divide it into 3 falcon tubes (50ml).

Centrifugation, Counting and Plating

a. Centrifuge the falcon tubes 10min 500g at 4°C.
b. Take off the supernatant and resuspend each pellet with 10ml GBSS-B including 0.2ml Dnase solution.
c. Collect the cell solution medium and divide it into 2 falcon tubes (50ml), adjust to 50ml with GBSS-B and centrifuge them 10min 500g at 4°C.
d. Meanwhile prepare the Histodenz solution (gradient solution): 19.25ml GBSS-A including 5.5g Histodenz, gradient 11%.
e. Take off the supernatant, resuspend the pellets with 10ml GBSS-B including 0.2ml Dnase solution.
f. Mix them together in a 50ml falcon tube, add the 19.25ml filtered, through a 0.2µm pore size single use sterile syringe filter, Histodenz solution, and adjust to 50ml with GBSS-B.
g. Divide the total cell solution medium into 4 falcon tubes (15ml) (12.5ml solution per tube) and place 1ml of GBSS-B carefully onto the cell suspension medium.
h. Centrifuge 15min 1500g at 4°C without break.
i. Collect the white layer in two falcon tubes (50ml) containing GBSS-B, adjust them to 50ml with GBSS-B and centrifuge 10min 500g at 4°C.

j. Take off the supernatant and resuspend the pellets with 10ml DMEM supplemented with 20% FBS and antibiotics.
k. Count the cells with a Malassez cell and plate the cells on the cell culture dishes at the appropriate density.

Conditions of culture

Cells are plated with DMEM supplemented with 20% foetal bovine serum (FBS). 24 hours after plating, medium is changed to DMEM containing 5% FBS until used. At day 9, cells are passaged by trypsinisation. The trans-differentiation is assessed by evaluation of two specific markers: α-SMA by immunostaining (Figure 16) and collagen-α1 (Col-α1) gene expression (Figure 17) in primary mouse HSC during time in culture.

As observed in picture 5, the α-SMA staining increased significantly during time in culture.

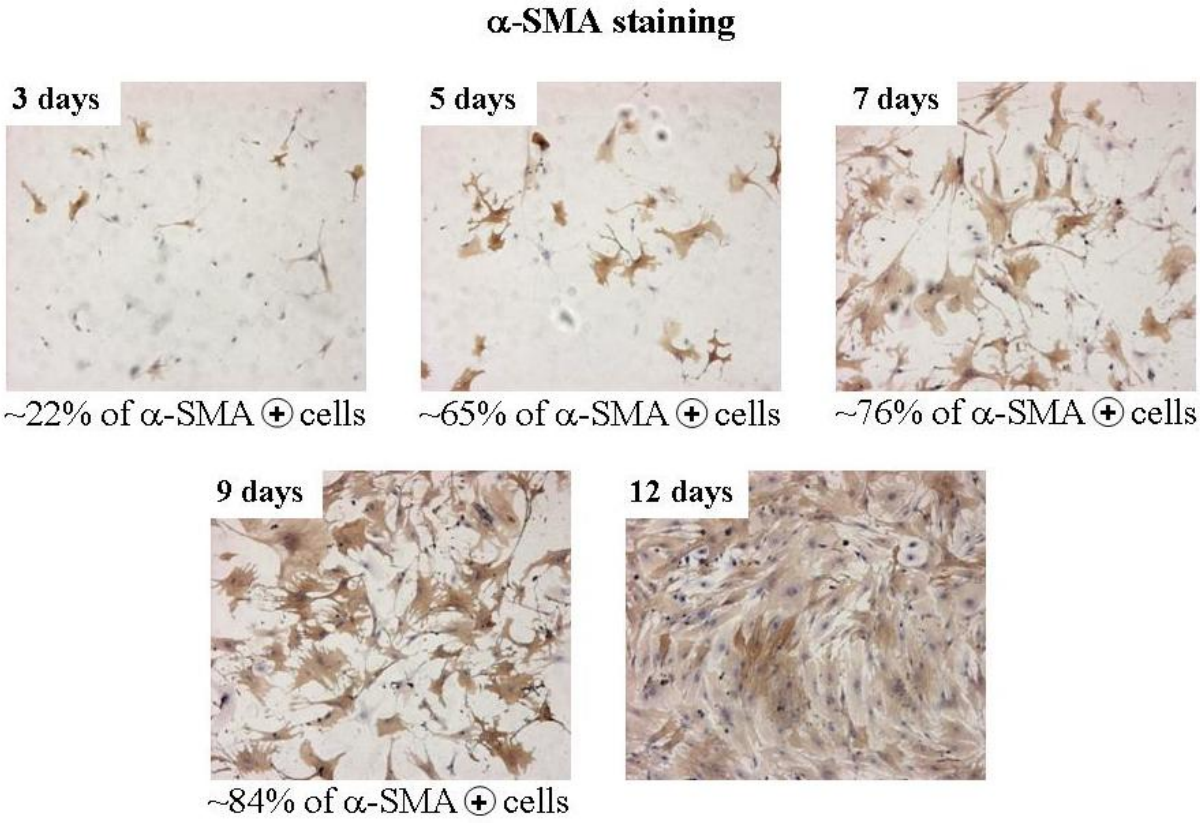

Figure 22: α-SMA immunostaining of cultured mouse HSCs

Primary mouse HSC are fixed in 4% formaldehyde at different time points after isolation and stained with α-SMA. At day 3 after isolation, about 22% of HSCs are α-SMA positive cells. This staining increased significantly during time in culture, confirming the spontaneous trans-differentiation process after plating on plastic dishes.

Another marker to assess the trans-differentiation of HSC is the evaluation of the collagen-α1 (Col-α1) mRNA expression during time in culture. This expression also increased significantly during time in culture (Picture 6).

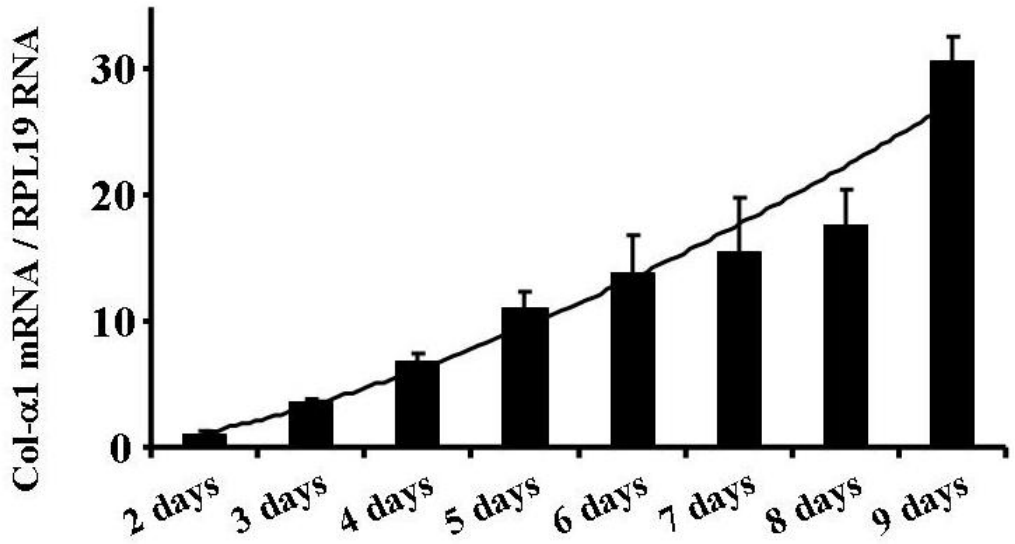

Figure 23: Collagen-α1 mRNA expression in cultured mouse HSCs

Bar graph representing the collagen-α1 gene expression quantitated by real time PCR in primary mouse HSC during time in culture. Individual value represent the ratio of collagen-α1 mRNA to RPL19 mRNA. The value obtained on cDNA derived from 2 days-old HSC has been arbitrarily set at one. Data are mean ± SD (arbitrary units) for n=10 dishes per group, from 3 different cell preparations.

Trypsinisation

After washing the cells with PBS and removed it, 5ml of trypsin-EDTA is added and dishes are incubated 8 min at 37°C. After incubation, 5ml of DMEM supplemented with 20% FBS is added to stop the action of trypsin. Cells are collected, centrifuged, the pellet is resuspended in DMEM supplemented with 5% FBS, and cells are plated and incubated at 37°C.